Cranfield University

Goulielmos-Zois Garifallou

Development of impedimetric immunosensors for the detection of a range of antigens of biological or biomedical significance

Cranfield Health

PhD

Cranfield University

Cranfield Health

PhD

2008

Goulielmos-Zois Garifallou

Development of impedimetric immunosensors for the detection of a range of antigens of biological or biomedical significance

Professor S. P. J. Higson

Abstract

This PhD project was funded by the European Union Framework 6 ELISHA programme as part of the ELISHA programme. The aim of the research was focused towards the development of point-of-care, simple, cost-efficient and reliable impedimetric immunosensors for the rapid detection of important antigens such as ciprofloxacin and digoxin. Through the cooperation of the 9 involved partners a number of protocols have been developed for sensor fabrication and sample testing that allow both rapid and reliable detection of a range of antigens. This work describes in depth, the use of polymers and cyclic voltammetry for electrode surface modification, the use of the avidin-biotin system for antibody immobilisation and finally the use of Electrochemical Impedance Spectroscopy for antigen detection. We report here the successful development of electrochemical impedimetric carbon based immunosensors for the detection of free-form and chelated ciprofloxacin (both in laboratory buffer and milk), digoxin and green fluorescent protein. It was observed during this work that unavailability of sufficient quantities of the monoclonal antibodies could lead to early sensor saturation and hence a less extended antigen detection range, while very low quantities of immobilised antibodies could also give rise to erroneous results. The immunosensors towards ciprofloxacin detected the respective antigen when this was present between 1 ng ml^{-1} and 10 μg ml^{-1} in PBS buffer and 0.1 ng ml^{-1} to 10 μg ml^{-1} when the antigen was added to milk samples. The developed digoxin immunosensors could detect digoxin between the concentrations of 0.1 ng ml^{-1} and 10 μg ml^{-1}. Lower detection limits where observed for the sensors targeting GFP which could detect their respective antigen at concentrations as low as 100 pg ml^{-1}. The tested concentration range of the latter sensors was extended up to 100 ng ml^{-1}.

Acknowledgements

I would like to thank my supervisor, Professor S. P. J. Higson for his invaluable help and support towards the successful completion of this PhD project. I also wish to thank Dr. Stuart Colyer and Dr. Frank Davis for their help during the practical stages of this PhD programme. Finally, I would like to thank Mr. George Tsekenis for our close collaboration within this PhD project.

List of contents

Appendice 1: Published work

Garifallou, G. Z., Tsekenis, G., Davis, F., Higson, S. P. J., Millner, P. A., Pinacho, D. G., Sanchez-Baeza, F., Marco, M. P., Girona, J., Gibson, T. D., 2007. Labeless Immunosensor Assay for Fluoroquinolone Antibiotics Based Upon an AC Impedance Protocol, *Analytical Letters*, **40**, 1412-1422

Tsekenis, G., Garifallou, G. Z., Davis, F., Millner, P., Gibson, T., Higson, S. P. J., 2008**.** Labeless Immunosensor Assay for Myelin Basic Protein based upon an AC Impedance Protocol, *Analytical Chemistry*, **80 (6)**, 2058-2062

Tsekenis, G., Garifallou, G. Z., Davis, F., Millner, P. A., Pinacho, D. G., Sanchez-Baeza, F., Marco, M. P., Gibson, T. M. and Higson, S. P. J., 2008. Detection of Fluoroquinolone Antibiotics in Milk via a Labelless Immunoassay based upon an AC Impedance Protocol, *Analytical Chemistry*, **80 (23)**, 9233-9239

Barton, A. C., Collyer, S. D., Davis, F., Garifallou, G. Z., Tsekenis, G., Tully, E., O'Kennedy, R., Gibson, T. D., Millner, P. A., Higson, S. P. J., 2009. Labeless AC impedimetric antibody-based sensors with pgml(-1) sensitivities for point-of-care biomedical applications, *Biosensors & Bioelectronics*, **24 (5)**, 1090-1095

List of tables and figures

Figure 5.9: Bode plot-total impedance vs frequency. Total impedance response for polyaniline doped with IgG (non specific antibody) after exposure to various concentrations of ciprofloxacin (in 10 mM ferri/ferrocyanide). Range of frequencies from 1Hz to 10Hz.

Figure 5.10: Z'' v Z' - Nyquist plot. Impedance responses of anti-ciprofloxacin loaded carbon based sensors upon exposure to various ciprofloxacin concentrations (in PBS, 10 mM ferri/ferrocyanide).

Figure 5.11: Bode plot. Impedance responses of anti-ciprofloxacin loaded carbon based sensors upon exposure to various ciprofloxacin concentrations (in PBS, 10 mM ferri/ferrocyanide).

Figure 5.12: Calibration curve of per cent (%) impedance response against $\log_{10}$ ciprofloxacin concentrations (1 ng ml^{-1} to 10000 ng ml^{-1}) for anti-ciprofloxacin doped polyaniline coated carbon electrodes at 1Hz (in 10 mM ferri/ferrocyanide).

Figure 5.13: Calibration curve of per cent (%) impedance response against $\log_{10}$ ciprofloxacin concentrations (1 ng ml^{-1} to 10000 ng ml^{-1}) for polyclonal IgG doped polyaniline coated carbon electrodes at 1Hz (in 10 mM ferri/ferrocyanide).

Figure 5.14: Corrected calibration curve of per cent (%) impedance response against $\log_{10}$ ciprofloxacin concentrations (1 ng ml^{-1} to 10000 ng ml^{-1}) for anti-ciprofloxacin doped polyaniline coated carbon electrodes at 1Hz (in 10 mM ferri/ferrocyanide).

Figure 5.15**:** Corrected calibration curve of per cent (%) impedance response against $\log_{10}$ ciprofloxacin concentrations (1 ng ml^{-1} to 10000 ng ml^{-1}) for anti-ciprofloxacin doped polyaniline coated carbon electrodes at 1Hz (in 10 mM ferri/ferrocyanide). 1-100 ng ml^{-1} concentration range.

Figure 5.16: Z'' vs Z' Nyquist plot. Impedance responses of anti-ciprofloxacin loaded carbon based sensors upon exposure to various ciprofloxacin concentrations (in milk).

Figure 5.17: Total impedance vs frequency, Bode plot. impedance responses of anti-ciprofloxacin loaded carbon based sensors upon exposure to various ciprofloxacin concentrations (in milk).

Figure 5.18 Calibration curve of per cent (%) impedance response against $\log_{10}$ ciprofloxacin concentrations (0.1ng ml^{-1} to 10000 ng ml^{-1}) for anti-ciprofloxacin doped polyaniline coated carbon electrodes at 1Hz (in milk).

Figure 5.19: Calibration curve of per cent (%) impedance response against $\log_{10}$ciprofloxacin concentrations (0.1ng ml^{-1} to 10000 ng ml^{-1}) for polyclonal IgG doped polyaniline coated carbon electrodes at 1Hz (in milk).

Figure 7.4: Calibration curve of per cent (%) impedance response against GFP concentrations (0.1ng ml^{-1} to 100 ng ml^{-1}) for polyclonal IgG doped polyaniline coated carbon electrodes at 1Hz (in PBS, 10 mM ferri/ferrocyanide).

Figure 7.5: Corrected calibration curve of per cent (%) impedance response against GFP concentrations (0.1ng ml^{-1} to 100 ng ml^{-1}) for anti-GFP doped polyaniline coated carbon electrodes at 1Hz (in PBS, 10 mM ferri/ferrocyanide).

Commonly used abbreviations

AC Impedance	Alternating Current Impedance
CV	Cyclic Voltammogram
FCA	Ferocene Carboxylic acid
GFP	Green Fluorescent Protein
PBS	Phosphate Buffered Saline
PSA	Prostate Specific Antigen
PCR	Polymerase Chain Reaction
DC	Direct Current

Section 1

Introduction Literature Review and Experimental Methods

Chapter 1
Context of Research Programme and Rationale for this Research

1.1 Aims and Objectives

This PhD research programme focused towards the development of a label-free, inexpensive, fast and reliable prototype immunosensor format for point-of-care applications.

The research undertaken in this PhD programme was funded as part of the ELISHA contract funded by the European Union 6th Framework ELISHA programme and includes Cranfield University alongside 8 other European Union partners as detailed below:

1) University of Leeds, UK, as co-ordinator
2) Cranfield University, UK
3) Ecole Centrale de Lyon & Centrale Lyon Innovation, France
4) Technische Universität München , Germany
5) NMRC-Tyndall National Institute, Ireland
6) CSIC- Spanish National Research Council, Spain
7) Uniscan Instruments Ltd, UK
8) University of Grenoble, France, and,
9) Technology Translators Ltd, UK

The specific objectives of this research project within the responsibilities for Cranfield University as partner 2 within the project were to:

1) Identify optimal protocols and procedures for reproducible sensor fabrication.
2) Test a range of materials i.e. carbon, gold, platinum for electrode fabrication as well as different polymers for use within sensor fabrication.
3) Investigate the effects of different fabrication protocols with regards to sensor loading and sensitivity.
4) Extend the range of analytes that had previously been analysed using the same approach.
5) Characterise the sensors i.e. detection limits, stability and reusability using analytes important to industry as well as within medicine.

1.2 The ELISHA consortium

The acronym ELISHA stands for "Electronic Immuno-Interfaces and Surface Nano-biotechnology: A Heterodoxical approach". The hypothesis upon which this project was initiated was a novel concept based on previous breakthroughs in affinity sensing, and hence the term 'heterodoxical'.

When exposed to their respective antigens and upon AC impedance interrogation, antibody loaded polymer based sensors provide a measurable signal that is dependant on antigen concentration.

Within and from this research, the European Union aims to 'promote real breakthroughs, based on scientific and technical excellence' (ELISHA Annex, 2003). Each of the 9 partners have shown excellence in their respective fields whether it be biology, biochemistry, electronics or commercial exploitation of scientific discoveries. The academic and industrial partners have collaborated closely to bring this project to successful completion.

The approaches used within ELISHA include multidisciplinary research covering the following areas:

- *Molecular Electronics*: the electronics that will allow 'sensing' of the Antibody/Antigen interaction occurring at the nano-scale level on the project specific electrode surface (due to irreproducibility issues with the project specific electrodes, the carbon electrodes depicted in figure 3.4, section 3.4.2 where alternatively used).

- *Molecular Interfaces*: the interaction between biological molecules and non-biological surfaces.

- *Understanding materials phenomena*: furthering the understanding of multifunctional materials and creating new methods for processing these.

- *Nano-biotechnologies and the general public*: the integration of nano-biotechnology, new materials and new production technologies in modern medicine, the food industry and environmental processes

The primary focus of the consortium was towards the production of nanostructured immunosensors that will ultimately form the basis for a commercially viable sensing device. This will in turn have a major impact in rapid and reliable analyte detection. Main areas of concern are cancer markers, fluoroquinolone antibiotics and prion peptides. All targeted substances/molecules have a major impact in the medical and food industry as well as in environmental control applications. As a result innovations arising towards this scope will promote major strategic and financial benefits.

In order to successfully meet the aims of this project, three main objectives must first be met:

1) To gain a deeper understanding and thus provide further knowledge of a newly observed signal transduction mechanism occurring in nanostructured affinity-based reagent biosensors.
2) To produce model prototypes of electronic and label-free immunosensors and through further development of these, proceed to the manufacture of low-cost, simple and reliable affinity-based biosensors for medical and environmental analyses along with other potentially related purposes, and,
3) The development of electronics specific and dedicated to this project.

The project was structured into 9 workpackages each with a lead project partner as shown in table 1.1 below. All other partners contributed to two or more workpackages working in conjunction with others within the consortium.

Workpackage number and description	Responsible partner	Other partners involved
1) Affinity reagent production and testing	Partner 1	Partner 6
2) Electrochemical Transducer production	Partner 5	Partner 2
3) Production of matrix precursosrs	Partner 8	Partners 1 & 9
4) Fabrication of nano-structured immunosensors	Partner 2	Partners 1, 3, 5, 6, 8 & 9
5) Investigations into immobilisation strategies and matrix construction	Partner 3	Partners 1, 2, 4, 5, 6, 8 & 9
6) Sensor address systems and interrogation electronics	Partner 7	Partners 1, 2, 3, 6, 8 & 9
7) Signal generation and non-specific binding optimisation	Partner 1	Partners 2, 3, 4, 6, 8 & 9
8) Evaluation of affinity sensor systems including signal processing	Partner 2	Partners 1, 3, 5, 6, 7, & 9
9) Laboratory prototype system	Partner 7	Partners 1, 2, 5 & 9

Table 1.1: The ELISHA workpackages and associated partners.

A brief description of each workpackage, as included in the ELISHA technical Annex, follows.

Workpackage 1: To produce hapten derivatives for antibody production; to supply purified antibodies and recombinant antibody reagents for sensor production; to provide modified recombinant antibodies for specific immobilisation protocols enabling simple sensor manufacture.

Workpackage 2: To produce metal (gold and platinum) transducers, using silicon or plastics as the substrates, with corresponding mounting connectors; to produce a range of metal transducers with different geometries; to produce microelectrode transducers.

Workpackage 3: To produce a range of electropolymerisable monomers or electrodepositable materials having specific chemical characteristics to enable entrapment or covalent immobilisation of bioactive antibodies and fragments.

Workpackage 4: To identify the correct techniques and conditions to enable reproducible manufacture of immunosensors based on the antibodies, recombinant antibodies and Fab fragments; to investigate the effect of different fabrication protocols on the loading and the sensitivity of the immunosensors produced.

Workpackage 5: To investigate the immobilisation events themselves and develop understanding on the chemistry-biochemistry of the immobilisation processes to feedback into W4 for effective fabrication; to characterise the nanostructural properties that produce the micro and nano-environments required for device production; to evaluate different matrices in regards to sensitivity and stability.

Workpackage 6: To design and evaluate novel interrogation techniques for extraction and de-convolution of signals generated from the affinity sensors; to develop purpose designed electronics for integration into 1) test bed evaluation rigs and 2) laboratory prototype sensor system; to iteratively feed back into W3, W4, W5 and W7 to optimise and develop sensors, interfaces and electronics for immunosensors.

Workpackage 7: To determine the origin of signal generation in the immunosensors fabricated and relate this to the matrix used and the method of immobilisation; to determine the parameters defining non-specific signal generation and to reduce the non-specific effects by a number of experimental means.

Workpackage 8: To characterise and determine the performance characteristics of a range of affinity sensors in terms of reproducibility, stability and analytical performance; to evaluate a range of prototype sensor systems towards a number of

different targets in terms of lower limits of detection, selectivity and possible interference effects; to compare analytical performance with standard detection and quantification methods, e.g. ELISA.

Workpackage 9: To develop a laboratory prototype system to prove principle using the nanostructured affinity sensors developed in the project as the detection method.

It should be noted here, that the Enzyme Biotechnology Group acted as the project coordinator and point of contact between the ELISHA consortium and the EU.

Chapter 2

Introduction and literature review

2.1 Biosensor definition and brief history of biosensor development

A biosensor is defined by the International Union of Pure and Applied Chemistry (IUPAC) as:

"A device that uses specific biochemical reactions mediated by isolated enzymes, immunosystems, tissues, organelles or whole cells to detect chemical compounds usually by electrical, thermal or optical signals".

A more simple description of a biosensor is given by *Kissinger* (2005) who states that a biosensor is "a device where a biological recognition element is built in (physically attached or confined) and is the primary selectivity element".

The biosensor concept was generated when a progenitor device was pioneered by Professor L. C. Clark in the format of an oxygen electrode in 1956. This system incorporated a biological membrane, permeable only to oxygen, placed over a platinum electrode, polarised at -700 mV, which acted as an amperometric electrical transducer (Clark L.C., Jnr., 1956). The electrochemical reduction of oxygen at the electrode surface generated an amperometric response which allowed for the determination of oxygen levels in a tissue sample. Realising the need to expand on the number of analytes to be measured and based on his previous experience with the oxygen electrode Clark made a landmark address in the New York Academy of Sciences Symposium in 1962, where he described how "to make sensors (pH, polarographic, potentiometric or conductimetric) more intelligent" by adding "enzyme transducers as membrane enclosed sandwiches". It was then that Clark and Lyons demonstrated the use of oxygen electrodes for the determination of glucose levels within a sample. This device involved the entrapment of glucose oxidase on the sensor by means of a dialysis membrane. The catalytic oxidation reaction between glucose oxidase and glucose involved the electrochemical reduction of oxygen, which could be directly related to the generated signal. The lowering in the levels of oxygen was proportionate to the amount of glucose in the sample as shown by equation 2.1 (Clark & Lyons, 1962).

$$\beta\text{-D-glucose} + O_2 \xrightarrow{\text{-700 mV vs Ag/AgCl}} \textit{gluconolactone} + H_2O_2 \qquad \textit{Eq. 2.1}$$

This gave rise to the term 'enzyme electrodes' a term which was by some mistakenly attributed to Updike and Hicks. They, however, expanded on the experimental detail necessary for the development of functional enzyme electrodes targeting glucose (Updike and Hicks, 1967). Figure 2.1 depicts a Clark-type electrode.

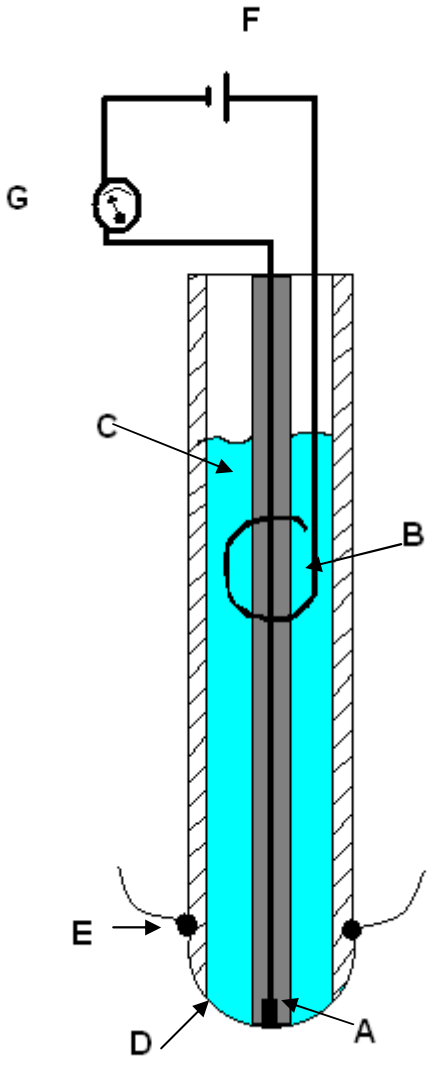

Figure 2.1: The Clark-type electrode; A) Platinum electrode, B) reference Ag/AgCl-electrode, C) half-saturated KCl electrolyte, D) Teflon membrane, E) rubber ring, F) the voltage supply and G) the electronic instrument for the measurements of the current output is shown.

The original Clark oxygen electrode design provided the prototype for various enzyme electrodes. Nowadays the alternative method of hydrogen peroxide detection is more widely used than those sensors employing oxygen concentration measurements. Yellow Springs Instruments Company (Ohio) launched their hydrogen peroxide amperometric biosensor, based on Clark's ideas, in 1975 for whole blood glucose determination. This approach involved the use of a working electrode with reversed polarity which could monitor the enzymic production of hydrogen peroxide.

In 1969, the first potentiometric biosensor was described by Guibault and Montavlo (Guibault & Montavlo, 1969).This was a urea sensor deploying an ammonium-selective liquid membrane electrode with immobilised urease.

In 1974 the first thermal sensors appeared and were termed *thermal enzyme probes* (Cooney *et al,* 1974) or *enzyme thermistors* (Mosbach & Danielsson, 1974). The use of biosensors for biotechnological and environmental purposes was highlighted by the realisation that bacteria could be used as the biological recognition element within microbial based electrodes (Divis, 1975). Lubbers & Opitz, (1975) first used the term 'optode' describing a fibre-optics based sensor for the detection of CO_2 and O_2. These workers subsequently immobilised alcohol oxidase at the end of their fibre optics oxygen electrode for the detection of alcohol (Voelkl *et al.,* 1980).

Clemens *et al*., 1976 described the use of an electrochemical biosensor for glucose in a glucose-controlled insulin infusion system, employing the use of a bedside artificial pancreas. Miles (Elkhart) marketed this system by the name Biostator®. The Biostator® is now no longer commercially available although an alternative amperometric semi-continuous catheter-based blood glucose analyser was introduced by VIA Medical (San Diego). La Roche (Switzerland) additionally, created the Lactate Analyser LA640 in 1975. The integrated biosensor in this system employed the use of hexacyanoferate as a mediator for electron transfer between lactate dehydrogenase and the detecting electrode. While the LA640 was not very commercially successful, it provided initiative for the development of mediated biosensors and lactate analysers for both clinical applications and the sports industry. Schichiri *et al*., 1982 described the first subcutaneous implantation of a needle-type biosensor for glucose which highlighted the possibility of '*in* vivo' sensor use. Two

years later Cass *et al*., 1984 expanded on the use of ferrocene and its derivatives as immobilised mediators for the detection of oxidereductases. These were less expensive biosensor components and formed the basis of the Exactech® glucose meter, a pen-sized blood glucose monitoring device employing screen printed electrodes, launched by MediSense (Cambridge, USA) in 1987. MediSense's sales climbed to $175 million per annum up until the company was acquired by Abbott in 1996. The world market for biosensors is estimated to reach $6.1 billion by 2012 as estimated by Global Industry Analysts, Inc. (www.strategyr.com).Over half of the globally produced biosensors are incorporated into glucose meters for diabetes patients. The biosensors industry comprises of two types of companies which develop either novel biosensor technologies or biosensor-based devices. Some of the companies dominating the development of novel biosensor technologies include AgaMatrix Inc., Cranfield Health, LifeSensors Inc., M-Biotech and Nova Biomedical. Companies dominating the world market for biosensor-based devices include Abbott Point Of Care Inc., Affinity Sensors, Neosensors Limited, Siemens Healthcare Diagnostics Inc, Animas Corporation, LifeScan Inc., Medtronic Diabetes, and Roche Diagnostics Ltd. Boehringer Mannheim and Bayer currently dominate the world market for mediated biosensors which are rapidly being employed as more cost efficient alternatives to reflective photometry technology in home diagnostics for the monitoring of diabetes. It should be noted that the combined sales of Abbot Diagnostics, Boehringer Mannheim and Bayer account for 85% of the global biosensor market. Figure 2.2 below shows the FreeStyle Lite blood glucose monitoring system with an average test response time of 5 s and an average cost $16.95 (www.abbottdiabetescare.com).

Figure 2.2: The FreeStyle Lite blood glucose monitoring system by Abbot Diagnostics.

The original methodology in biosensor design, as discussed earlier, was to immobilise enzymes on the surface of electrochemical sensors assuming that this would enhance the ability of a sensor to detect specific analytes. The use of antibodies in sensing technology to monitor affinity based reactions was researched from the early 1970's onwards, however, the principle of immunoassays was established in 1959 by Berson and Yallow (Berson & Yallow, 1959). Their work developed the widely used radioimmunoassay to examine the properties of insulin-binding antibodies in human serum, using samples obtained from subjects that had been treated with insulin (van der Voort *et al.,* 2005). Since then other immunological techniques have provided a range of simplified alternatives in comparison to techniques such as gas liquid chromatography and mass spectrophotometry (Grant *et al.,* 2005). The idea to develop direct immunosensors by immobilising antibodies on piezoelectric or potentiometric transducers had been explored since the early 1970s. The first 'direct' immunoelectrode (following the actual binding effect) was reported by Janata J. in 1975, however, commercially viable immunosensors were introduced following a paper published by Liedberg *et al*., in 1983 employing surface plasmon resonance technology to detect bio-affinity reactions. Namely, the BIAcore (Pharmacia, Sweeden) launched in 1990, was based on this technology.

Many biosensors are now being developed that can screen a wide range of biomolecular interactions. Advances in computing, electronics, polymer science as well as the biological sciences are accountable for the range of biosensors that are currently used or under development at the time of writing.

Many new biosensors can only be used in a laboratory and can be expensive to fabricate and operate. Following the need for point-of-care measurements most devices are now requiring miniaturisation while their functions are being enhanced or expanded for home use. Similarly, one of the principle aims of sensing technology and nanotechnology is to develop miniaturised biosensors to facilitate ***'real-time, on site'*** testing with the required specificity and sensitivity (Kissinger, 2005).

2.2 The factors determining Biosensor design

Many parameters determine the class, sensitivity, selectivity, longetivity and usability of biosensors. Of these, three key aspects need to be considered in biosensor design. These are 1) the target analyte or process to be measured or monitored respectively, 2) the biological recognition element and finally 3) the transducing element. The target analyte or process is the determining factor in deciding the design steps of a sensor. Which biomolecules or cells have the ability to interact with the desired target must also be considered. A target analyte or microorganism can be detected by a number of recognition elements such as whole cells, enzymes, antibodies or nucleic acids. However, the state of a given sample such as blood, aqueous solution, solid food, entails limitations as to which bio-recognition elements can be used. Antibodies normally have lower tolerances to stresses than enzymes or whole cells, but can provide smaller response times and high selectivity and sensitivity. Microbes can screen for a range of analytes but this also entails limited selectivity. The biological recognition element must effectively interact with the substrate in order to produce a measurable change.

The signal produced during the biological interactions needs to be considered. The changes in mass, temperature, structural changes, changes in the electrical properties of the electrode, or the formed complexes determine what class of transducer can be used. Optical, calorimetric, electrochemical and other types of transduction methods are typically employed according to the nature of the analyte, bio-recognition entity and sample state.

A number of other parameters are important in terms of sensor longetivity, selectivity, sensitivity and response times. One of the most important factors affecting these key

features is the biological recognition entity immobilisation method. Several immobilisation methods exist which can be physically or chemically based. In all cases it is vital that the immobilisation method does not destroy the biological entity or excessively compromise its activity. There are moreover a large number of appropriate polymers, biological membranes and filters or gels which can be used according to the biological entity of preference and the chosen immobilisation method. These substances, whether it be polymers or membranes, require an appropriate metal or plastic support platform. A polymer, for example, must allow for signal transduction between the biological molecules and the metal electrode in electrochemical sensors. Additionally, the signal must not be compromised i.e. decrease in signal due to the interfering polymer, in order to fully measure the occurring changes on the electrode surface. Non-specific interactions are also affected by the immobilisation methods used: these can be decreased or eliminated, but at the possibility of altering the activity of the recognition entity. The following sections provide a brief overview of the different types of substrates that sensing research addresses, the various biological recognition elements that can be used and finally the transduction methods currently available to scientists. Details regarding various immobilisation methods and electrode materials are also provided, however, the materials and methods used for immunosensor design are discussed more extensively later since they form part of this research project. Figure 2.3 depicts the main components of a biosensor.

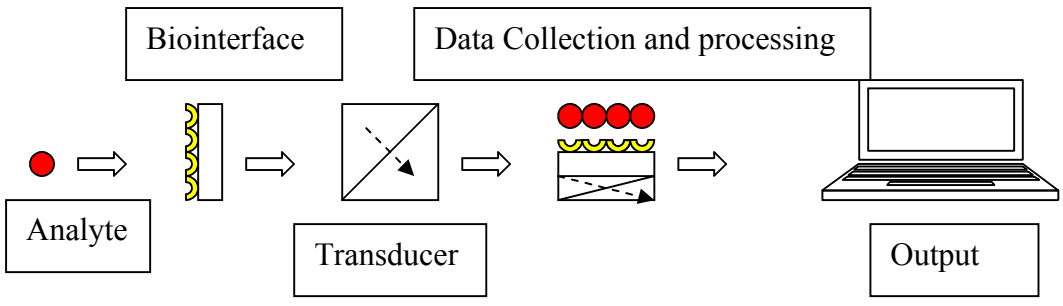

Figure 2.3: The main components of a biosensor.

2.2.1 Biosensor targets

Biosensors were devised as alternatives for expensive and bulky laboratory based analyses for use within quantitative analysis of single analytes found in complex biological and environmental samples. These analytes range from proteins, pathogens or other microorganisms, to the monitoring of biological processes that may be of industrial through to medical interest (Davis *et al*., 1995).

Biosensors for glucose, lactate, urea, alcohol and a range of other analytes, have all been developed (Davis *et al*., 1995). The most successful sensor within the biosensor market globally has, however, been the development of glucose sensors for diabetes. The easy to use self-testing glucose strips coupled with pocket-sized amperometric meters have dominated the $5 billion/year diabetes monitoring market for the past two decades (Newman & Turner, 2005). This project aims to develop similarly successful devices as an alternative to many laborious and cumbersome detection methods.

Food and Water analysis

Initial work within the ELISHA project focused towards the development of immunosensors for the detection of pesticides and herbicide residues which, if found in food may have severe implications for consumer health. Work was also formed towards sensors for fluoroquinolones. Fluoroquinolone antibiotics have been widely used in animal and human medicine for the treatment of urinary tract infections since 1980 (Gendrel *et al.,* 2003). Dairy products and meat may contain residues of fluoroquinolones which have been shown to have potent unwanted biological effects (Hartmann *et al.,* 1999). It is important to note that these compounds, alongside other antibiotics, can also give rise to bacterial resistance. Four fluoroquinolones have now been banned for use in food products (NBPDP, 2002; Batt *et al*., 2006). The EU has provided clear guidelines and established procedures regarding the monitoring of foods for fluoroquinolones, however, with contemporary analytical procedures, these standards for food safety cannot yet be successfully reached.

Pathogenic micro-organisms can give rise to food and water born disease with an estimated 40% of the total annual recorded world deaths being due to infections

caused by food or water born pathogens (Leonard *et al.,* 2003). Approximately 200 million people yearly moreover suffer non-fatal infections due to the same pathogenic micro-organisms (Leonard *et al.,* 2003). *Escherichia coli* is naturally found in the intestine of mammals and other warm blooded animals and aids the body in vitamin synthesis. Some strains of *Escherichia coli* however, such as the O157:H7 strain, are highly pathogenic and can cause acute food poisoning and many more serious complications (Alocilja & Radke, 2003). Alongside *Escherichia coli*, *Listeria monocytogenes and Salmonella* sp. are some of the most commonly encountered pathogens causing disease and can be found in food samples that have undergone insufficient processing or inappropriate storage (Leonard *et al.,* 2003).

Within the food industry continuous and direct monitoring of products is often required to determine the freshness and contamination levels (e.g. genetically modified products, pesticides, fluoroquinolones and infectious micro-organisms) of processed foods. In some cases the monitoring of fermentation processes is also required (Mello & Kubota, 2002).

Biosensors offer a promising alternative to cumbersome and often expensive procedures that are currently being employed for food or raw materials testing. Such procedures may for example include the use of polymerase chain reaction which requires experienced personnel and relatively expensive laboratory equipment and reagents. Tissue culturing is a traditional and rather simple method for pathogen detection, however, the prolonged incubation periods required is the main disadvantage of this method. The common disadvantage of the methods mentioned earlier, however, is that they cannot to date be used for fast 'point-of-care' measurements, as opposed to e.g. handheld devices incorporating biosensors for analyte detection. One of the most important limitations of biosensors within the food or drink industry is that the biological recognition elements can only retain their activity over small temperature and pH ranges. Obviously, during food processing, maintaining the conditions of temperature and pH within a limited range can be difficult in many, if not all, cases. The simplest example of extreme conditions would, for example, be the production of alcohol which can lead to the denaturation of biological molecules and so the performance of the sensor. This and other limitations however, can possibly be overcome by continuous effort within the various research

programmes around the world. The use of bacterial cells and yeast, for example, is a promising alternative to many isolated enzymes and antibodies for use in fermentation process monitoring.

Disease detection

- Cancer research has received great scientific attention during the past decades. The availability of cancer markers, such as PSA allows for the development of immunoassays for early detection. It is a known fact that early detection of any type of cancer decreases the chances that the disease will be fatal to the patient. At the time of writing this report, biosensors targeted towards PSA have been successfully developed within our group (Barton *et al.,* 2008). Prostate cancer is one of the most common cancers suffered by the male population accounting for an estimated 11% of all male cancers in the EU and 9% of cancer deaths amongst European men (Aus *et al.,* 2005).

- The human amyloid disorders, 20 of which have been identified so far, include important diseases such as spongiform encephalopathies (in humans these include Creutzfeldt-Jakob disease, Gerstmann-Sträussler-Scheinker syndrome), Alzheimer's disease, and type II diabetes (Dumoulin & Dobson, 2004). Such diseases have been shown to appear sporadically, be inherited or are sometimes transmissible (Dumoulin & Dobson, 2004). Most of this class of diseases are incurable and lead to premature death. In 2000 4.5 million people in the USA were found to be suffering from Alzheimer's disease. As discussed earlier in this work (section 2.1), over half of the produced biosensors globally are incorporated into glucose sensors for diabetes, indicating how widespread the disease is worldwide. *Prion peptides* are the suggested cause of transmissible spongiform encephalopathies (Dumoulin & Dobson, 2004) and have therefore constituted part of the target analytes within the ELISHA consortium. It is suggested that misshaped *prion peptides* carry the disease between individuals and cause brain deterioration. *Prion peptides* can be transferred through the air or via touching but infection may also occur

via ingestion of infected foodstuffs, through blood transfusion or contaminated medical instruments.

- Other diseases ranging from serious and fatal ones to even the simplest and non-life threatening ones are currently being diagnosed by ELISA immunoassays, PCR and other techniques. Early and reliable detection of bacterial and viral infections, hereditary diseases or ones that appear sporadically is the key for more effective treatment. Aside from the relatively high cost of the required equipment and reagents, the techniques named above, also require heavy human input compared to the proposed biosensor format described by this work. The aim is to develop an immunosensor that will allow rapid screening of multiple samples whether it be for prion peptides, different cancer types, fluoroquinolones and a plethora of important targets.

Environmental monitoring

Human activity has since the industrial revolution undoubtedly had a major effect on the environment over the past few centuries. The disposal of deleterious substances in dig sites was common practice in the past decades, however, environmental pollution and most importantly water contamination meant that the welfare of both the flora and fauna in the surrounding areas could be severely impaired. Currently, many industries team up with waste treatment companies that can successfully decontaminate affected sites or process industrial waste. The use of fertilisers for agricultural purposes is controlled and monitored by tight guidelines allowing for the protection of natural forests and lakes. While chemical disposal is controlled, some by-products may still escape and cause pollution, therefore bioremediation is of utmost importance. For efficient bioremediation however, effective analytical tools are required. Measurements need to be taken in the open land or within rivers, the sea or lakes. Rapid detection of pollutants means that measures can be taken to prevent further damage to the environment. An example of such a biosensor for environmental control and bioremediation is the potentiometric microbial electrode which was designed to detect organophosphorous pesticides (Purohit, 2003). The European Network on Sensors for monitoring water Pollution (SENSPOL) aims to enhance the

practical applications of sensors for the rapid detection of environmental pollutants in water, such as phosphororganic pesticides and insecticides.

Bio-defence and forensics

Biological Warfare Agents (BWAs) have been used in a number of destructive terrorist attacks. Examples include t he Rajneeshee cult in Oregon used Salmonella in a number of restaurants in 1984, the Aum Shinrikyo cult in Tokyo used Sarin gas and anthrax. The attacks towards the USA on September 11th were also followed by anthrax mailed to specific targets around the country (Gooding, 2006). Fast detection and characterisation of agents such as these, alongside explosives and illegal drugs, is the only approach that can effectively protect civilian lives or warn the police and other security agencies of the existence of illegal substances.

According to Gooding (2006), two types of sensors are required; the 'detect-to-treat' sensors focusing on rapid identification thus allowing immediate treatment and so called 'detect-to-protect' sensors, capable of providing an immediate warning when exposed to a BWA, thus preventing infection.

Anthrax, for example, is a gram positive bacterium which can be both aerobic and spore forming. Spores are used as BWAs due to their high resistance to environmental stresses such as temperature or moisture and hence suitability for use as weapons. Inhalation of 1,000 to 10,000 spores is required to cause a lethal infection to an individual, resulting from the production of endema toxin and lethal toxin by the bacterium itself. A detect-to-protect sensor would be based on the detection of anthrax spores to prevent infection while a detect-to-treat sensor would be focused towards rapid detection of the toxins for immediate treatment.

Baeummer *et al*., 2004 described a nucleic acid sensor for the detection of BWAs based on fluorescence which could detect extremely low amounts of the targeted anthrax sequence in 4 hours. Antibody based sensors based on the principles of home pregnancy test kits, have also been developed for anthrax, ricin and botulinum toxin. In the case of anthrax detection, the detection limits is 1μg ml^{-1} in solution and 0.25

μg from a surface with the detection time ranging from 15 to 20 minutes (Gooding, 2006).

The use of biosensors for the detection of drug abuse or for the detection of explosives has also been described in the literature, especially during the last decade. Halamek *et al.,* 2004 report the development of a piezoelectric affinity based sensor for cocaine with limits of detection lower than 100 pmol l^{-1}. Smith *et al.,* 2008 have assembled a review about the use of biological molecules and whole cells within biosensors for the detection of explosives.

It is important at this point to note that the production of a generic immunosensor for all the previously discussed applications would be somewhat difficult to accomplish. Theoretically, the structure of antibodies allows for millions of recombinations that could potentially cover a huge range of different analytes, however, the nature of the specimens or the environments in which each analyte may be found in (solid, liquid, gas) pose an important limitation.

2.2.2 The biological recognition entity

Biosensors can be distinguished according to the bio-recognition element used for the detection of the desired target. Biosensors can be based on a catalytic process or bioaffinity reactions depending upon the biological entity used and the desired target. The biological entities used in sensing technology vary from enzymes and antibodies to nucleic acids, and whole cells and even cell organelles. The biological recognition entity must be specific to the target analyte or biomolecule and plays the most important role in terms of specificity, longetivity (e.g. storage) and re-usability. While the bio-recognition element is itself a major factor contributing to sensor design and characteristics, the immobilisation methods and materials used for sensor fabrication, as discussed earlier, impart greatly on sensitivity, selectivity and shelf-life of the final sensors (Pejcic & De Marco, 2006).

Enzyme sensors

Enzyme sensors utilise enzymes immobilised on an electrode surface. Amperometric biosensors constitute the largest sub-group and of these glucose oxidase enzyme electrodes still represent the most widely used class of sensors to date.

Ion selective electrodes can be used for a variety of analyses. They are often used in potentiometry to detect the catalysed liberation of e.g. hydronium or ammonium ions (Pejcic & De Marco, 2006). One of the major problems faced in amperometric enzyme based sensors is the non-specific adsorption occurring on the electrode surface. Interferents can give rise to erroneous responses. Interferents in blood, for example, can include alcohol, drugs or paracetamol. Ascorbate and uric acid, are also common types of enzyme based sensors.

Enzymes often require cofactors in order to display their intended biological activity. Cofactors can be thought of as helper molecules that can bind tightly or loosely to the enzyme in order to 'activate' it. One of the limitations caused by the need for cofactors in enzyme sensors is that these molecules need to be continuously regenerated if the immobilised enzyme is to retain its biological activity. Figure 2.4 below depicts the enzymatic reaction taking place in order to convert a substrate into a detectable (be the electrode) product.

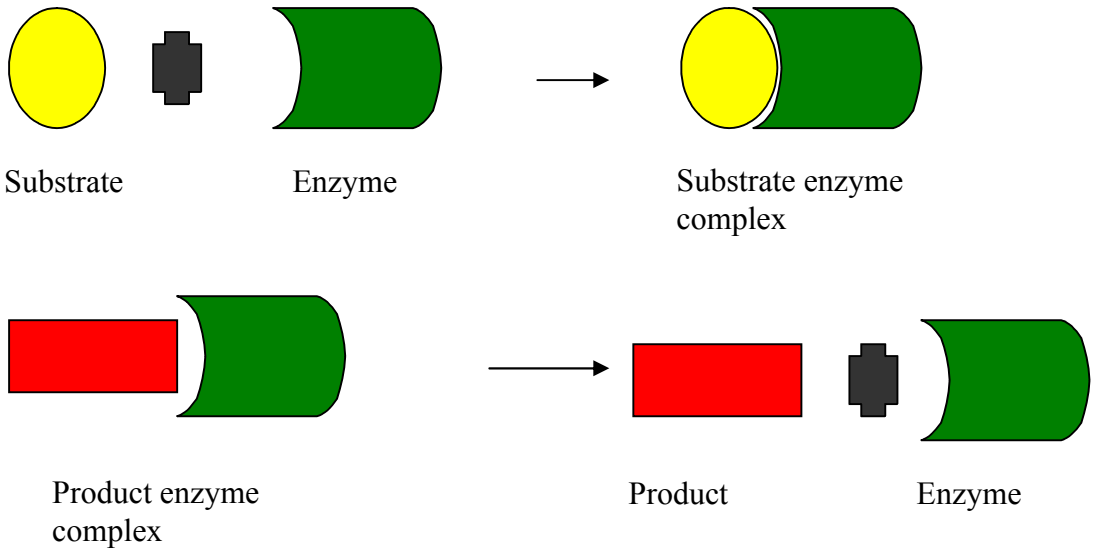

Figure 2.4 Working principle of enzymes.

Immunosensors

Immunosensors are based on the affinity reaction between antibodies and their respective antigens and are widely used for environmental and medical diagnostics. Immunosensors can be sub-divided into *direct* and *indirect* types. *Indirect immunosensors* require a label, such as a fluorescent molecule, for detection. A number of different labels are commercially available, each with different properties. In its simplest form, such an immunosensor would detect an antigen tagged with e.g. a fluorescent probe. In this case, the emitted light, which can be measured, will be proportionate to the concentration of the captured antigen. *Direct immunosensors* do not require a label; the detection is based on chemical, conformational, mass (or other) alterations occurring on the conductive surface upon the antibody/antigen binding effect (Van der Voort *et al*., 2005). The high specificity of antibodies towards their antigens affords improved selectivity. Non-specific adsorption can occur in immunosensing, however, the sensor fabrication protocols aim to limit such interferences or at least account for them. In a similar manner to any biological entity, antibodies are sensitive to environmental conditions such as pH and temperature. Such conditions may alter their binding efficiency or even destroy them completely. Antibodies have been successfully immobilised within conducting polymers in

various works for the development of immunosensors since 1991 (Spencer *et al.,* 1999; Grant *et al.,* 2003; Tsekenis *et al.,* 2008). More recent advances, including work within this research project, have allowed for the site specific immobilisation of antibodies on conductive polymer films.

A major limitation of antibody based sensors is that they suffer from irreversibility. Once an antigen has been attached to its antibody it is very difficult if not impossible to reverse the reaction without damaging the sensing element. In this PhD project we have developed a number of reusable immunosensors, however, once saturation occurs, i.e. all the immobilised antibodies hold the target antigen, the sensors cannot be used any further.

The use of antibodies for affinity based sensors has been described extensively within the literature for the detection of a number of environmental pollutants (Pejcic & De Marco, 2006; Garifallou *et al.,* 2007) This project focuses on the development of a prototype impedimetric immunosensor target towards a range of analytes using an AC impedance interrogation approach.

Nucleic acid sensors

Nucleic acid sensors are based on the affinity based detection of target sequences via the use of immobilised complementary DNA or RNA fragments. Detection is based on the hybridisation event taking place when a complementary target sequence exists within a given sample. During the hybridisation event no new molecules electrons or photons are produced. In a similar manner to antibody based sensors, the formation of double stranded DNA must be recognised by the alterations in the electrical, chemical (or other) properties of the conductive surface (Davis *et al*., 2005). Electrochemical impedance spectroscopy offers huge advantages for this alongside other affinity-based detection methods. Fibre optics have also been used in conjunction with DNA based sensors, however, electrochemical sensors pose a far more cost effective alternative. One of the most important issues in nucleic acid sensor design is the immobilisation of the sequences on the sensor surface. Davis *et al*., 2005 review the successful immobilisation of thiol modified DNA strands on gold electrode surfaces, the

electrostatic immobilisation of DNA onto cationic surfaces and the use of electroconductive polymers such as polypyrrole.

Hahn *et al*., 2004 state that no other event since the introduction of PCR has influenced the clinical analysis of nucleic acids to such an extent. The detection limits facilitated by PCR surpass alternative approaches by far. The development of real time PCR has, moreover, provided a highly simplified and reliable approach for the quantitation of nucleic acids. Nucleic acid sensors have been developed as possible alternatives to molecular biology techniques such as PCR for the detection of, for example genetically modified constituents or organisms in food products (Deisingh & Badrie, 2005). Real-time PCR involves the use of fluorescent molecules called quenchers and reporters. The former molecules normally reduce the light emitted by the latter when these are attached to the DNA probes; when the reporters are removed from the DNA sequence due to the activity of a polymerase molecule they emit radiation at the expected wavelength which can be measured by sophisticated equipment. In this manner it is possible to follow the DNA amplification process in real time. As discussed earlier DNA or RNA sensors have been extensively studied for their uses in bio-defence applications. To date, very few nucleic acid based sensors offer detection limits that can match PCR. It is often seen that a PCR step is carried out before use of the sensor within a sample. Another limitation is that to date artificial oligonucleotide sequences have largely been used within sensor development, and hence, it is not clear how well such devices will perform in real life situations since a plethora of newly formed artificial sequences would be required for the available range of target DNA sequences (Hahn *et al.,* 2004).

Whole cell or organelle biosensors

These sensors are based on immobilised living cells or tissue such as bacteria, plant tissue, or even cell organelles, in order to detect analytes. Biosensors of this type are typically used in biotechnology for fermentation processes or for environmental monitoring. Guibault reported the first biosensor using mitochondria for the measurement of NADH (Guibault, 1976). The main advantages of a sensor of this type are the ability to detect a wide range of substances over a significant pH range and tolerance to temperature variation as well as generally offering longer shelf-lives.

Sensors of this type can easily be regenerated so long as the substances within a sample are not lethal to the cell types used (Lei *et al*., 2006; Mello & Kabuta, 2002). Two of the main limitations associated with microbial biosensors are, however, their slow response time and decreased selectivity due to the plethora of metabolic processes occurring within living cells (Mello & Kabuta, 2002). Molecular biology and the DNA manipulation techniques it provided have revolutionised the use of living cells in sensing technology. It is possible to genetically 'tailor' living cells in order to make them more tolerant to specific environmental conditions e.g. pH, improve the activity of specific enzymes produced by the cells or clone foreign DNA when the requirement for a foreign protein production presents itself. DNA manipulation of bacterial cells also affords the introduction of internal reference systems which can be useful for establishing baseline responses amongst other things.

The immobilisation of cells or organelles plays a major role in the longetivity and stability of microbial sensors, as it does for enzyme based sensors, immunosensors and nucleic acid sensors. The chemical immobilisation approaches include covalent binding and cross linking. Covalent binding is based on the direct reaction between functional groups of the cell wall and the transducer such as amines or carboxylic groups. The process requires the use of reaction conditions that can decrease the biological activity of the cells or organelles. Cross linking employs the use of reagents such as glutaraldehyde to bridge functional groups of the cell membrane of one cell with others. This approach may, however, damage the cells. Of the physical immobilisation methods adsorption is based on ionic, polar, hydrogen bonding and similar interactions that do not damage the cells. Sensor longetivity, however, is not guaranteed due to possibl desorption of cells with time. Entrapment is another physical immobilisation method that employs the use of dialysis membranes, biological polymers or gels (Lei *et al.,* 2006).

Microbial biosensors based on amperometry have been extensively used for the measurement of biodegradable organic pollutants in aqueous solutions. Such sensors are based on biochemical oxygen demand, measuring the cells' oxygen requirements over a period of a few days. Oxygen consumption (respiration) provides information relative to environmental conditions and the stresses under which the microbes live. This information in turn gives indications of the chemical presence within a given

sample. Potentiometric, conductimetric and optical microbial biosensors have also been described in the literature while novel sensors based on barometry (pressure) and other detection methods have also been developed (Lei *et al.,* 2006).

2.2.3 The transduction methods

From the mid 1980s, many types of biosensors have been developed for full commercialisation; some of these have been based on simple and others on more complex-biochemical and electrochemical approaches (Davis, 1986). Biosensors are more often classified according to the mechanism of transduction and four major classes of biosensors include optical, thermal, piezoelectric (mass) and electrochemical based sensors. Ion-selective, impedimetric conductimetric, potentiometric, amperometric, fluorimetric, luminometric, thermometric biosensors and acoustic wave sensors, as well as the more sophisticated fibre optic based biosensors, are only some of the examples to indicate and emphasise the scientific effort underlying the development of such devices (Davis, 1986; Guan *et al.,* 2004; Leonard *et al.,* 2003). The following pages provide an insight of the different transduction methods used in sensing technology.

2.2.3.1 Optical sensors

As discussed earlier the Lubbers and Opitz (1975) were the first to use the term "optode" to describe biosensors employing spectrophotometric techniques. Optical biosensors constitute one of the most important classes of sensors for bioanalysis mainly due to their high sensitivity, selectivity and rapidity of detection. Sensors of this type utilise the light absorbed or emitted as a result of a biochemical reaction. Optical fibres are normally used to guide the light waves to a suitable photomultiplier (Scheper *et al*., 1996). Different interactions used in these sytems make use of bio and chemiluminescence, UV-vis absorption, reflectance and fluorescence and have been successfully used for the detection of pathogenic bacteria, toxins and contaminants. The use of surface plasmon resonance and fluorescence based sensors has more recently been increased due to the increased sensitivity they offer (Lazcka *et al*., 2007).

- Bio-luminescence: the bacterial luminescence *lux* gene has been extensively used for real time process monitoring in either a constitutive or inducible manner. When the toxicity of a certain compound needs to be determined the *lux* gene can be fused to a constitutive promoter and thus be continually expressed. High levels of a toxic compound within the sample will impair or kill cell function and thus a measurable difference in luminescence can be obtained. In the inducible manner, expression of the *lux* gene, can be 'switched on' by the target analyte which may be quantitatively analysed by alterations in luminescence intensity (Lei *et al.,* 2006).

  The exhaustion of nutrients within soil requires monitoring as does the contamination of land with a number of industrial pollutants. Bio-luminescence has been successfully exploited to this end resulting in the development of several sensors for soil monitoring (Lei *et al*., 2006).

- Fluorescence: many fluorescent based detection techniques can be employed for the design of biosensors. Fluorescence based sensors incorporate the use of a fluorescent compound that can be used to either label the analyte pool or the bio-recognition element itself. The difference between fluorescence and bioluminescence is that the former requires fluorescent dyes while the latter technique uses the naturally occurring light emitting proteins for detection. In the case of antibody conjugates, the chosen fluorescent dye is attached to the available antibodies. In the presence of, for example, pathogenic organisms, the antibodies will, normally within 30 minutes, attach themselves to the existent pathogens and can be detected via their conjugated fluorophores when exposed to the correct wavelength. Upon absorption of light fluorophores of this type emit radiation at a lower wavelength to the excitation wavelength. This fluorescence radiation can then be monitored and used in conjunction with standard techniques such as real-time PCR for the detection of more than one type of microorganisms. This technique is, however, frequently both extensive in time and extremely expensive due to the requisition of an overnight microbial culture as well as the cost of real-time PCR equipment (Lazcka *et al.,* 2007). Fluorescence resonance energy transfer (FRET) sensors

employ the use of two different types of fluorophores, one of which acts as a donor and the other acting as a receptor. The formation of the antibody/antigen complex causes structural changes to the antibody. Such structural changes reduce the distance between the donor and receptor fluorophores thus irradiating at known wavelengths. This technique has been shown to reach detection limits of 2 μg/ml in food samples (Lazcka *et al*., 2007).

- Surface plasmon resonance: surface plasmon resonance (SPR) sensors detect changes in the refractive index caused structural alterations i.e. the formation of antigen/antibody complex upon binding, on the surface of a thin metal platform. A thin gold layer is applied on a glass plate which is subsequently irradiated by a p-polarised light from a laser via a hemispherical prism. The reflectivity is measured as a function of the angle of incidence and the resulting curve shows a peak that is called the SPR minimum Adsoprtion phenomena as well as antibody-antigen interaction kinetics may be measured using SPR, however, the technique requires specialised personnel and equipment. This technique has been successfully utilised for the detection of pathogenic bacteria via the antibody/antigen reaction method (Lazcka *et al.,* 2007).

2.2.3.2 Thermal biosensors

Thermal or calorimetric biosensors can utilise absorption or evolution of heat during enzyme/substrate interactions or the temperature variations within an enzyme-containing solution upon addition of the target analyte (Meadows, 1996). The changes in temperature are detected using a thermistor or transistor and normally involve the use of a control biosensor or control system where no target substance is added. Thermistors are essentially ceramic semiconductors with very high negative temperature resistance coefficient. Sintering mixtures of manganese, iron, cobalt, nickel and uranium oxides are used to fabricate thermistors of this type which reflect any temperature changes as changes in resistance (Ramanathan & Danielson, 2001).

During a biochemical reaction, the total heat absorbed or evolved, is proportional to the molar enthalpy and to the number of produced molecules. Total heat is also

dependent on the heat capacity of the system and generally the heat capacity of organic solvents is two to three times lower than that of aqueous solvents. For this reason the use of organic solvents affords higher sensitivity to calorimetric measurements. Thermal sensors have been successfully used for the determination of cholesterol concentration in blood serum; the reactions of oxidation and decomposition produce heat that can be easily detected. Various thermal sensors have also been extensively used by the food and biotechnology industries (Meadows, 1996; Ramanathan & Danielson, 2001).

2.2.3.3 Piezoelectric biosensors

Mass or piezoelectric biosensors employ the use of a quartz crystal which displays an altered vibrational frequency when substances are adsorbed onto its surface. Due to the nature of the effects being detected such devices are also called acoustic wave sensors. The applied pressure deforms the crystal lattice forming a dipole moment in its molecular structure. While many types of crystals exhibit this piezoelectric effect, quartz crystals have been found to possess many favourable electrical and chemical alongside mechanical properties (Meadows, 1996; Bunde *et al*., 1998).

Non-specific adsorption has been a major issue with this type of sensors and they have consequently been mostly used for gas phase analyses. Such devices have, however, displayed extremely low detection limits reaching femtogram levels for drug vapours for forensic applications. AT-cut shear mode quartz crystals have been successfully used for viscometric purposes and interfacial processes.

One of the variants of this type of sensing systems is the mass-amplified quartz crystal microbalance immunoassay. This technique incorporates the use of sol particles ranging in diameter preferably from 5-100 nm. The technique involves the use of antibodies to capture analytes at the crystal surface. Sol particles are antibody modified and can thus bind to the immobilised analyte molecules causing a vastly altered vibrational frequency (Bunde *et al*., 1998).

While successfully employed within the sensing industry and medical diagnostics, the above mentioned transduction methods generally require trained personnel and the use of expensive or complex equipment. The following section focuses on electrochemical biosensors, which are rather simple to use but extremely effective and do not generally require complex instrumentation for measurements to be carried out.

2.2.3.4 Electrochemical biosensors

Electrochemical biosensors have received the major share of the attention in biosensor development (Turner *et al.,* 1986). Electrochemical biosensors employ a biological recognition element and a transducer that converts the occurring biological reactions to an electrical signal (Wang, 2006). The detection methods may be amperometric (current), potentiometric (potential) or impedimetric (impedance) in nature; other methods are available, however the three mentioned above predominate. Some of the overwhelming advantages of electrochemical sensing technology are the low cost of equipment, simplicity of use, rapidity of result acquisition and the ability to work with turbid samples. Sensitivity i.e. how the minimum quantity of target analyte that can be detected in a sample, is probably the most important aspect to consider in regards with a sensing device. As Wang (2006) report, the sensitivity of currently available electrical bioassays allows them to rival the most advanced optical devices. These characteristics frequently make them favourable for use in medical diagnostics, environmental and industrial monitoring and defence purposes (Lazcka *et al.,* 2007).

Surface structure and reactivity are two of the main areas of concern for the development of successful electrochemical sensors. Materials science is extremely important for sensor design. The electrodes as well as the covering layers (recognition element) are required to have unique properties providing selectivity and sensitivity. These aspects are discussed extensively later, however since this project is based on the use of electrochemical immunosensors, a review of the detection methods is provided below.

Amperometric biosensors

The first biosensor, as described in section 2.1, was amperometric in nature. Amperometric biosensors exploit the exchange of electrons between the analyte or biomolecule of interest and the sensing electrode. Upon application of a polarising potential, the electroactive chemical or biological species is oxidised or reduced; these reaction result in an electric current, which can be monitored. This current can be related to the concentration of the analyte (Mello & Kubota, 2002; Wang, 2006). Such amperometric biosensors - those selectively detecting the presence of electroactive species- are collectively called 'first generation' biosensors. 'Second generation biosensors' or 'mediated biosensors' are those employing mediator molecules such as ferrocene carboxylic acid or ferri-ferrocyanide. These compounds are small in size and can mediate the exchange of electrons between the analyte and the sensing electrode in a reversible manner. There are also a number of amperometric sensors that belong to a third generation. Third generation biosensors employ direct electron transfer to and from the electrode to the enzyme and finally to the target analyte. In such examples the electrons themselves act as secondary substrates for the occurring enzymatic reactions and result in the production of a catalytic current, making this a catalytic process in nature (Mello & Kubota, 2002).

The main disadvantage of amperometric biosensors lies in their selectivity which is limited by the redox potential of the present electro-active species, hence the measured current may be the result of the oxidation and reduction of more than one species within a given sample (Mello & Kubota, 2002). In order to reduce or eliminate such interferences it is possible to use permselective membranes and other types of "molecular filters" that allow passage towards the electrode surface to specific analytes but prohibit passage to others.

Amperometric biosensors used for glucose detection have attracted great interest due to the increase of diabetes within the population of developed countries. Glucose oxidase has been extensively used, due to its robustness, for the development of novel fabrication techniques and materials testing. Previous reports have described glucose sensors with response times of 33 s and sensitivity as low as 3.05 μA/ mM glucose (Hervás Pérez *et al*., 2006). Some of the self-testing kits discussed earlier (section

2.2.1) have response times between 5-10 s and only require 0.5-10 µl fingerstick blood samples. Other amperometric sensors have been developed for pesticide detection using cholinesterases, lysine detection using lysine oxidase and sulphite ions using sulphite oxidase. Further work to develop prototypes with higher sensitivity and lower response times is ongoing and amperometry continues to play a major role within biosensor research (Hervás Pérez *et al*., 2006).

Potentiometric biosensors

The first ever potentiometry based sensor was described by Guilbault and Montalvo in 1969. The sensor was directed towards the detection of urea using the enzyme urease, which was immobilised in an ammonium-selective liquid membrane (Guilbault & Montalvo,1969).

Potentiometric biosensors are the least common within the electrochemical sensor class (Lazcka *et al*., 2007). Such sensors employ the use of a membrane (e.g. inorganic crystal, glass, plasticised polymer) or alternatively a surface sensitive to the target species. The sensor produces a potential that is proportional to the logarithms of the concentration of the target molecule. Essentially, potentiometric devices can detect alterations in pH and the concentration of ions within a solution using an ion-selective electrode, and hence the term ion-selective electrodes (ISEs) is often used for potentiometric devices (Mello & Kubota, 2002; Pejcic & de Marco, 2006). Since potentiometric biosensors measure the changes in concentration (or activity) of ions in a solution it is expected that they yield Nernstian responses upon changes in the ionic strength of the solution. Consequently, a decade change in the concentration of the measured ions corresponds to a potential change of 59.1 mV at room temperature. Extensive research in this field has shown that the membrane properties must not vary as a result of sample concentration changes, for the responses to be Nernstian (Bakker & Meyerhoff, 2000). The main advantage of potentiometric biosensors is that they can be used for a broad range of concentrations. Their simplicity, low cost of production, availability for continuous monitoring, stability and long lifetimes have contributed in making them a popular analytical sensor class (Pejcic & de Marco, 2006; Lazcka *et al*., 2007). Equation 2.2 shows the principle of the penicillin

biosensor based on the breaking down of the internal penicillin structure by the enzyme penicillinase.

$$penicillin \xrightarrow{penicillinase} penicillicacid + H^{+} \qquad Eq.\ 2.2$$

The use of transistors that can amplify the generated signal is common in potentiometry and such devices are collectively called ISFETs (ion-selective field effect transistors). In this case the biological reactions are detected using a semiconductor's field-effect. In ISFETs, the generated electric field creates regions of excess charge in a semiconductor substrate that can increase or decrease the local conductivity. ISFETs provide the possibility for miniaturisation in potentiometric sensor design, however, they constitute a concept which brings with it certain disadvantages. Some of these disadvantages include the incompatibility with various immobilisation methods due mainly to ISFET fabrication technology, poor detection limits, poor reproducibility and device instability (Lazcka *et al*., 2007). Figure 2.5 below depicts the principle of ISFET's.

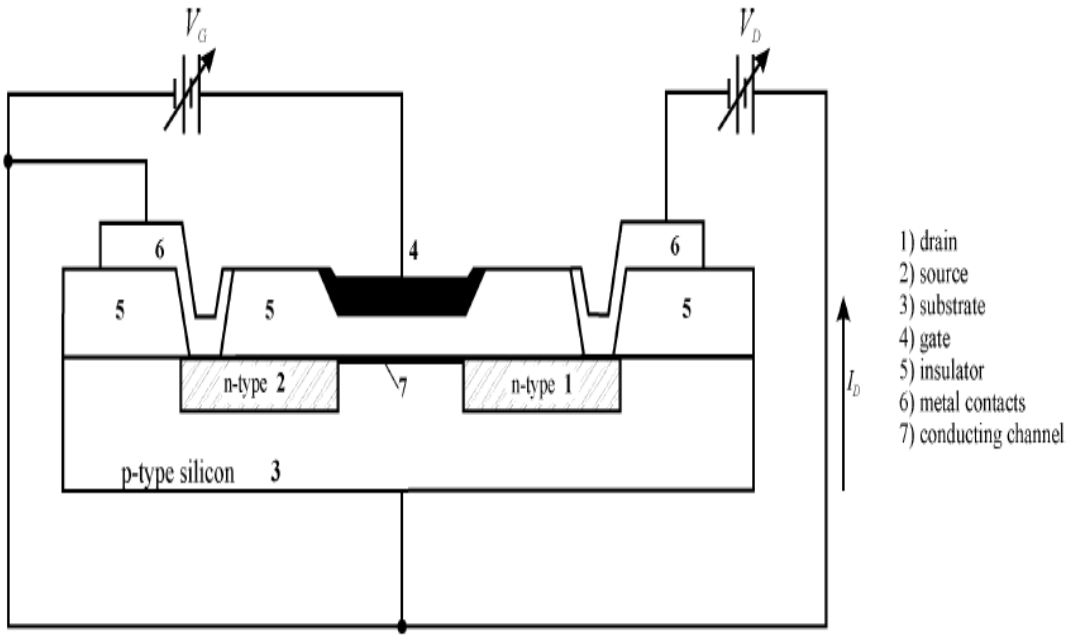

Figure 2.5 Schematic representation of an ISFET.

A p-type silicon substrate with source and drain diffusions is separated by a channel covered with SiO_2 as insulator and a metal gate. The polarity and magnitude of the gate voltage difference (V_G) that is applied between the substrate and the gate are such that a n-type inversion layer is formed between the drain and source diffusions. The effective electrical resistance of the surface inversion layer and the voltage difference (V_D) between source and drain determine the magnitude of the drain current (I_D).

One of the major limitations of potentiometric devices is the leaching of membrane components into the sample. However, attempts to minimise leaching have introduced the use of electroactive ingredients within polymeric membranes. Clinical blood analysers have employed this technique successfully (Pejcic & de Marco, 2006).

Conductimetric sensors

Conductance is the direct opposite of resistance i.e. the ability of a material to pass electrons. Conductimetric biosensors are based on alterations of the conductivity of a medium or substrate resulting from biochemical reactions. Enzyme based conductimetric sensors rely on the increase of conductivity upon substrate binding. Whole cell based conductimetric sensors have also been reported in which the present microorganisms metabolise uncharged substrates to intermediates e.g. carbohydrates to lactic acid. The occurring bioprocesses cause a change in ionic species. The quantifiable amount of charged intermediates is proportional to the growth rates of the existing microorganisms. Since conductimetric measurements monitor changes in the medium they do not show high specificity and can have poor signal to noise ratio, however, they are extremely sensitive (Lei *et al*., 2006; Mello & Kubota, 2002).

Impedimetric sensors

Impedance is very similar to resistance as they both regard the opposition to the flow of electrical current. However, impedance is actually the resistance of a component at a given frequency. Impedance can only exist when there is AC current or fluctuating DC current. Electrochemical Impedance Spectroscopy (EIS) is slightly more complex than most other electrochemical based transducing approaches. This approach

involves the application on the electrode, of small amplitude alternating excitation potential over a range of frequencies, using the resulting current to calculate the impedance of the system. The current and potential possess a phase difference that depends on the nature of the examined system. The angle by which the sine curve of the voltage lags or leads the sine curve of the current is called the phase angle (ϕ).The amplitude of the produced current and voltage and the phase angle between them determine the impedance of the system. Impedance is currently used for the detection of food pathogens, bacteria and sanitation microbiology and was accepted as a first action method by the Association of Official Analytical Chemists (AOAC). Impedance is a non-destructive and low cost technique based on changes of the conductance and capacitance of an electrochemical system. Any process that can affect the conductivity of an electrochemical transducer can be monitored by EIS. The applications of impedance in industry and research range from testing of batteries and semi-conductors to thin film technology and corrosion monitoring (Mello & Kubota, 2002; Pejcic & de Marco, 2006).

An immense amount of impedance studies have been carried out especially within polymer science and the development of metal coatings to monitor electrochemical properties and corrosion respectively. EIS has more recently been used for the development of impedimetric sensors. The use of impedance for protein immobilisation and antibody/antigen interactions was a breakthrough in sensing science, proving that impedance could potentially be used for direct monitoring of affinity based biosensors (Mirsky *et al*., 1997). Essentially EIS can be used for each of the biosensor assembly stages as well as to monitor changes during analyte addition at different concentrations (Fernandez-Sanchez *et al*., 2005). Numerous groups report the use of impedance for monitoring of antibody and DNA based sensors from the late 1990s onwards. Sargent & Sadik, 1999 report the use of antibody doped polypyrrole for the fabrication of sensors and subsequent EIS measurements upon antigen additions. Farace *et al*., 2002 highlight the use of reagentless biosensing using EIS while Davis *et al*., 2005 report the development of DNA based impedimetric biosensors. More recently work within our group involved the use of EIS for the detection of ciprofloxacin at various concentrations (Garifallou *et al*., 2007). Since the use of EIS represents the focus of this PhD project, specifics of this technique will be discussed in detail later.

2.3 European Union Interest in Sensing Technology

This project combines the fields of advanced nanotechnologies and biotechnology in order to provide 'state of the art' low-cost and reliable solutions for the detection of a wide range of diseases as well as food and environmental pollutants. Within and from this research, the European Union aims to 'promote real breakthroughs, based on scientific and technical excellence' (ELISHA Annex, 2003).

The ultimate goal of the co-operating partners is to further enhance knowledge of mechanisms that can be employed towards the development of fast, reliable and cost effective biosensor prototypes. This will in turn have a major impact in rapid and reliable disease detection. Main areas of concern are cancer markers, fluoroquinolone antibiotics and prion peptides.

All targeted substances/molecules have a major impact in the medical and food industry as well as in environmental control and care. As a result innovations arising towards this scope will promote major strategic and financial benefits

2.4 Nanobiotechnology and Biosensors

Nanotechnology aims to improve biosensor sensitivity and performance by the use of nano-materials in the fundamental design of the device. Nano-materials have promoted the introduction of several novel signal transduction technologies to be used for sensing, whilst allowing the development of portable devices for real-time *in vivo* and point of care measurements. Nano-materials are typically defined as those whose dimensions vary from 1 to 100 nm and are affected by the quantum size effect and surface effects, thus displaying a unique set of desirable physical and chemical properties for sensing technology (Jianrong *et al.,* 2004).

Of the numerous nanomaterials available, nanoparticles have been most extensively described. Functional nanoparticles, electronic, magnetic, optical or possessing other properties, can be bound to biological molecules to aid the detection and amplification the produced signals. In acoustic wave sensors and specifically the widely used mass-

amplified quartz crystal microbalance, antibody modified sol particles have been successfully employed for detection of analytes. The sol particles cause a vast change to the vibrational frequency of the quartz crystal due to their large mass. In this technique, analytes are first bound on the electrode surface by immobilised antibodies and a subsequent binding occurs upon addition of modified sol particles.

Gold nanoparticles have been used for fluorescence based detection in optical sensors. This method involves the attachment of thiol and a fluorophore at the respective ends of oligonucleotides which are subsequently bound to gold nanoparticles and form arch like structures. Upon hybridisation with the target sequences, conformational changes restored fluorescence to the quenched fluorophore. Single base detections have been reported by Maxwell *et al*., 2002 using this method.

Magnetic biosensors are based on magnetic nanoparticles that can be prepared in single domain, superparamagnetic or other forms and bound to biorecognition molecules in order to separate or enrich the target analytes. Safarik & Safarikova, (1999) describe the use of magnetic field gradients to separate and manipulate magnetically labelled cells. Figure 2.6 depicts the different biomolecules that can be attached on the surface of nanoparticles for use in various sensing applications.

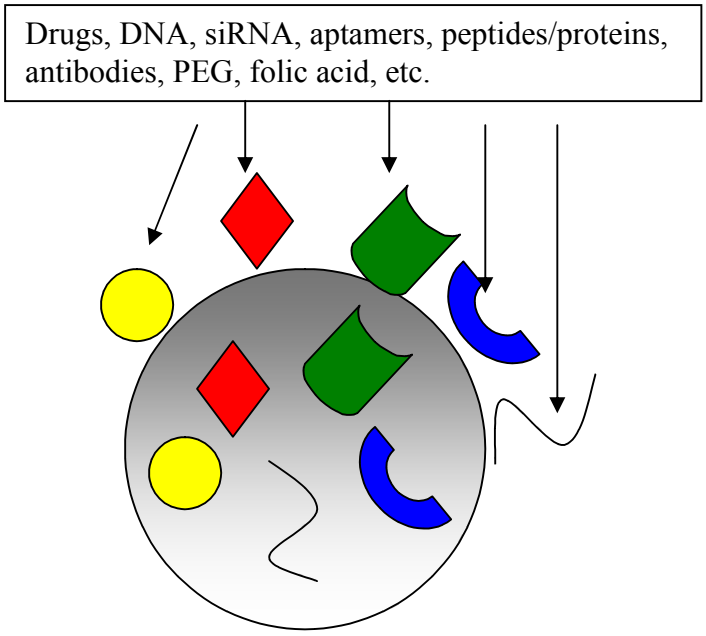

Figure 2.6: Schematic representation of a nanoparticle and the various biomolecules that can be attached to its surface for use in sensing technology.

Electrochemistry based sensing is another field employing nanoparticles for improved sensor performance. It should be noted that metal nanoparticles do not compromise the bio-functionality of any recognition molecules they may be attached to. Cai *et al*., 2001 describe the use of gold nanoparticles in a DNA sensor format to enhance the amount of nucleic acid immobilised onto the electrode surface thus lowering the detection limit. Affinity assays can also be performed by monitoring the electrochemical signals of biomolecule bound metal nanoparticles. Numerous scientific reports describe other approaches employing nanoparticles for electrochemistry based approaches and there is great potential for industrial and medical applications. Miniaturisation of the sensing apparatus and high sensitivity are the main benefits of nanoparticle use within sensing technology. Carbon and gold nanotubes, nanowires and nanofibres have also received increased attention over the past decade for their potential applications within the sensing industry.

2.5 Antibodies and their use in Sensing Technology

As discussed earlier the immunoassay concept was introduced by Berson and Yallow, (1959), while the idea of immunosensors was introduced by Jamata *et al*., (1975). Immunoassay development continues to be a vibrant area of research due to the many advantages offered by the use of antibodies in antigen detection, namely high specificity and sensitivity.

Antibodies are molecules produced by the immune system as a response to the presence of antigens. Antibodies bind their target analytes hence stopping infection of the host organism. The structure of antibody molecules, shown for IgG1 in figure 2.7, is extremely important to their binding capacity (Killard *et al.,* 1995).

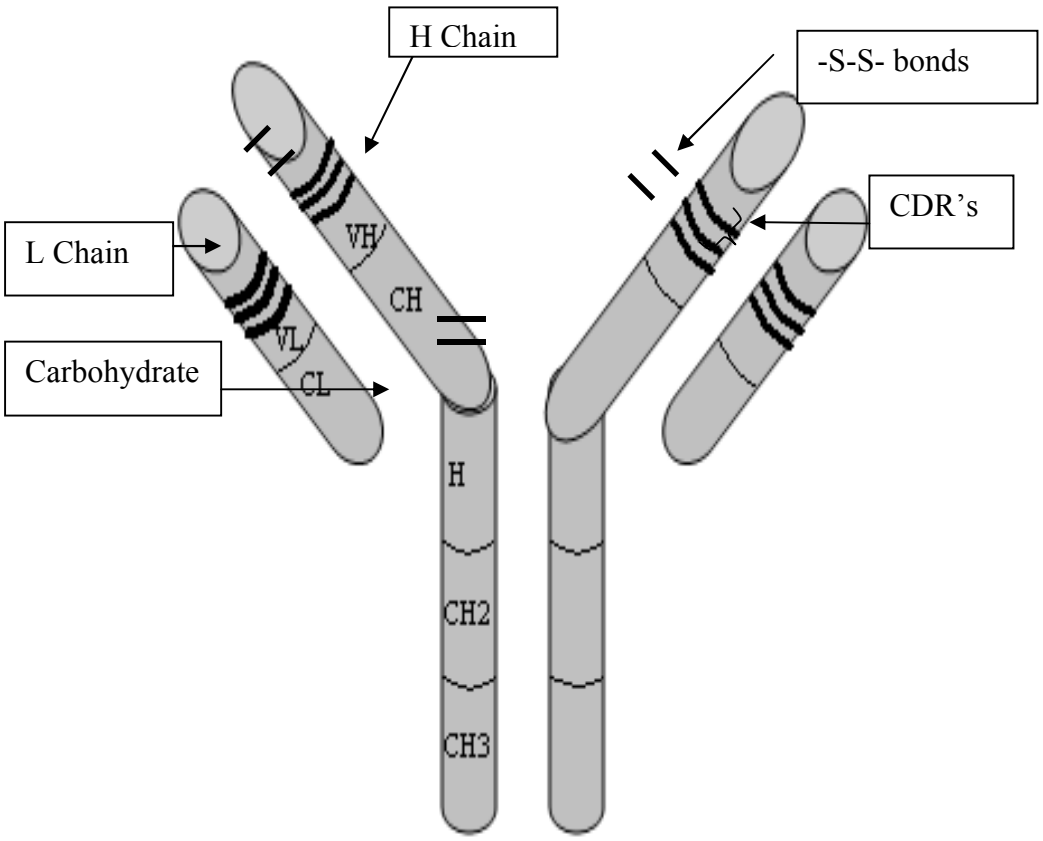

Figure 2.7: Basic structure of the human IgG1 antibody (Killard *et al*., 1995).

Structurally, each antibody or antibody class is unique, however, a typical example is that of the immunglobin G subclass (IgG). Four polypeptide chains constitute one

IgG1 molecule, two heavy (H) and two light (L) chains composed of 450 and 212 amino acid residues respectively. Disulfide bonds (-S-S-) exist that link the H chains with each, the same bonds also link each H chain with a L chain. The L and H chains are divided into constant and variable domains based on the variability of the amino acid sequences found within each chain. The L chains consist of one constant (V_L) and one variable domain (V_L) while the heave chains consist of three constant (C_{H1}, C_{H2}, C_{H3}) and one variable domain (V_H). Two of these domains on both the L and H chains posses intrachain disulphide bonds which contribute to their globular structure. The V_L and V_H domains associate with each other as do the C_L and C_{H1} domains, while C_{H2} regions pair with each other as do the C_{H3} regions. An additional domain exists between CH1 and CH2 that offers flexibility to the two antibody arms and is called the hinge region. V_H and V_L, are the regions most important for the determination of the binding of proteins. Variability in the amino acid sequence of these regions results in different antibody molecules with altered binding abilities. More specifically V_H and V_L each contain three hypervariable regions named '*complementarity determining regions*' (*CDRs*) that essentially form the binding site for the antigen. Thus changes in these regions result in the formation of different antibody molecules with different specificity and affinity for analytes, without altering the basic antibody structure. This system affords an estimated 10^8 different specificities, and hence, a vast number of antibodies targeting specific molecules (Killard *et al.,* 1995).

B lymphocytes are the cells responsible for antibody production in the animal body. During an immune response these cells produce different epitopes i.e. antibody molecules that each target different sites on the antigen surface. This immune response is not reproducible as different antibodies may be formed if subsequent immunisations occur with the same antigen. This population of antibodies is termed *polyclonal* but is of no great use to sensing technology, thus techniques have been developed to produce *monoclonal* antibodies with known specificities and affinities (Killard *et al.,* 1995). As for the population of polyclonal antibodies, monoclonal ones are similarly produced by *B lymphocytes*, which however, have a short *in vitro* life span. This limitation can be overcome by the fusion of *B lymphocytes* producing the desired antibody with tumorigenic myeloma cells offering the former 'immortality'. Animals are normally used for the production of monoclonal antibodies mostly mice,

goats and rabbits. The procedure involves infection of the animal with the antigen to force the animal's organism into producing the desired monoclonal. As Killard *et al.,* (1995) report, in the case of mice, the spleen of the infected animal is removed and the antibody producing *B lymphocytes* (splenocites) harvested. These are subsequently fused to non-antibody producing myeloma cells by means of polyethelene glycol. Upon cell division chromosome mixing can possibly result in the development of 'immortal' antibody producing hybrids. The remaining unfused splenocytes die due to their limited life span after a short while and incubation in HAT medium (hypoxanthine, aminopterin and thymidine) is used to prevent growth of myeloma cells. What remains is a population of fused cells which are allowed to grow in different wells and are periodically checked for antibody production by means of an appropriate immunoassay. Some of these wells contain hybrids deriving from a single parent cell and produce a single type of antibody, a monoclonal. Different procedures can subsequently be used for large scale production either via culture flasks and bioreactors or by injecting the hybrids to mice which develop hybridoma tumours.

A crucial part in antibody research has been played by antibody engineering and molecular biology. Some monoclonal antibodies present a great example of engineered molecules with increased affinity and specificity for their target antigen. The next step of such technologies is the expression of antibody fragments that can be fused with reporter genes (Killard *et al.,* 1995).

Many antibodies are commercially available at the industrial level. It is important however to note that the use of the desired antibody must be teamed with the choice of an appropriate transducer for the derived immunosensor to be successful. Immunosensors are known for their ease of use, low detection limits and high selectivity. There are two main parameters to consider while aiming developing a fit for use sensor:

a) the intrinsic specificity of the biological material; in complex samples specificity may be compromised,
b) the ability of a transducer to detect the binding process and produce a readable signal, normally of electrical nature (Killard *et al.,* 1995).

The transduced signal whether it be electrochemical, based on fibre-optics or derived in any other form is frequently proportional to the concentration of analyte in the tested sample (Miller & Anderson, 1989). The need for *in vivo* measurements in order to e.g. monitor the metabolism and/or drug intake for patients in clinical units, necessitates the development of devices that can remain stable for a prolonged period of time within an organism (Miller & Anderson, 1989). The main problem for *in vivo* use of immunosensors is the stability of the antibody over a period of time. Biological functionality may be lost or compromised due to environmental factors i.e. blood constituents or simply due to the antibody's limited life. Matrix interferences (such as chemical and physical interferences from the range of constituents in e.g. blood) and drift problems must be addressed before immunosensor implantation is feasible and reliable (Luppa *et al*., 2001). The reversibility of the binding reaction is another problem requiring a solution before *real-time in vivo* monitoring is realised. In its own nature, the antibody/antigen reaction is a non-reversible process. However, regeneration of the immunosensor surface may be possible. One proposed solution is the application of a highly concentrated antigenic solution with weak affinity for the antibody of interest but it should be noted that surrogate antigens are not always available. Another solution is to engineer antibodies or antibody fragments with high tolerance to chemical treatments that can help dissociate the complex on the sensor surface without compromising biorecognition functionality. Jung *et al*., (1999) report the use of phage display for selection of high stability antibody fragments. Phage display involves the insertion of DNA fragments (e.g. those responsible for producing the antibody of interest) into phage DNA which is then used to transfect bacterial cells, normally *Escherichia coli*. The inserted DNA regions ensure the expression of the antibody fragments on the coating protein of the phage particles. The phage are allowed to replicate and the ones displaying antibodies or antibody fragments that may be useful can be retained by the use of wells with immobilised target DNA or proteins. Such libraries are nowadays successfully used for the production of a plethora of antibody fragments for use in immunoassays.

Despite the overwhelming amount of scientific literature describing successful immunosensor prototypes, their use in medical diagnostics, while not negligible, is not widespread. Problems arising during immunosensor development, range from the immobilisation method to antibody orientation on the transducing surface. The

immobilisation method and fabrication reagents may compromise antibody functionality.

2.6 Polymers in Sensing

Traditionally the use of polymers in sensing technology was primarily focused towards the entrapment, by different methods, of biorecongition elements on the electrode surface. The advantages in polymer science, however, have produced materials that apart from bioelement immobilisation can also play a major role in the electrical and chemical properties of the sensor. Some polymers can offer permselectivity while others can act as mediators for the occurring enzymatic reactions (Davis *et al*., 1995). According to Adhikari & Majumdar, (2004), polymers have played a major role in the development of state-of-the-art biosensors over the past three decades. Whether in conducting or non-conducting forms, polymers possess chemical and physical properties that provide great versatility in terms of sensor fabrication; different substances can be chemically manipulated in various ways, so as to obtain different characteristics and behaviour (Adhikari & Majumdar, 2004). Electrode coating by polymers is a commonly used technique. Polymeric coatings can insulate an electrode or enhance its electroconductivity and also prevent degradation of the electrode surface or the active molecules trapped on the sensor. The properties of conventional gold, carbon and platinum electrodes have previously been enhanced by polymer deposition (Gerard *et al.,* 2002). Alternatively the chosen polymer may play a role in the sensing mechanisms involved (Adhikari & Majumdar, 2004).

The most attractive polymers for use within sensing technology are those that can be electropolymerised or electrodeposited. Electropolymerisation can be carried out *galavanostatically*, *potentiostatically* or by *potential cycling*. These methods are detailed and discussed later as they are used extensively in this research programme. Where biomolecule entrapment is concerned the electrodeposition process involves the electrochemical oxidation of a chosen monomer via the use of an electrolyte that contains the desired biomolecule to form a thin membrane, a polymer film, on the electrode surface. Immobilisation of biomolecules on a polymer film requires different procedures, however, the polymer electrodeposition on the electrode surface is similar in both cases. The advantages of electrodeposition are that the

polymerisation reactions can be performed at room temperature and can be entirely controlled e.g. via allowing greater control over the thickness of the polymer film and greater reproducibility (Gerard *et al.,* 2002; Yuqing *et al.,* 2004). Film thickness is important when considering signal transduction i.e. a very thick polymer film may become a limiting factor as to how much charge reaches the electrode surface. Another advantage of depositing polymers via electropolymerisation is that this approach is not limited by the surface area or geometry of the electrode and can thus be applied to electrodes with more complex geometries (Yuqing *et al.,* 2004). With regards to polyaniline, electrodeposition and especially potential cycling leads to the formation of a highly homogenous film. Details relating to the electrochemical deposition of o-phenylenediamine and polyaniline (the two polymers used in this project) are included in the results section of this work.

Older technologies required entrapment of enzymes within the polymer film, thus a mixture of monomer and enzyme were used to coat the sensor via electrodeposition. It is nowadays common practice to directly immobilise enzymes and other biomolecules onto a deposited polymer film. Novel biocompatible polymers have offered the possibility of these new immobilisation procedures alongside enhanced properties making them favourable for use in biosensing.

2.6.1 Conducting polymers

Conducting polymers were introduced in the 1970s as novel organic materials with electrical and optical properties very similar to those of metals and semiconductors. Guimard *et al*., (2007) report that polypyrrole was known since the 1960s. However, very little was understood regarding its electroconductive properties. The existence of a conductive polymer was realised in 1977 when researchers noticed a 10 million fold increase in the conductivity of iodine doped polyacetylene. Polyacetylene, while extensively studied is a non-cyclic polyene sensitive to air and is difficult to study or work with due to its inherent instability. Polyheterocycles, one of which is polyaniline, started being produced in the 1980s and emerged as polymers with high stability, ease of processing and great conductivity. A vast range of conducting polymers with diverse chemical structures is currently available each offering different favourable characteristics. Many of the monomers used are compatible with

aqueous solutions at neutral pH which allows their use with biological components such as in biosensors. Additionally, the polymerisation conditions define the chemical and electrical properties of the formed polymer film offering more flexibility in the choice of an appropriate material (Bartlett & Birkin, 1993). Conducting polymers enhance the sensitivity, versatility and reaction kinetics of biosensors used in the diagnostics and medical industries (Gerard *et al.,* 2002). They can efficiently transfer electrical charge derived from a biological/chemical reaction and are frequently biocompatible in neutral aqueous solutions (Gerard *et al.,* 2002). For this reason they can be used for biomolecule immobilisation or entrapment for biosensor fabrication (Adhikari & Majumdar, 2004; Gerard *et al.,* 2002). The most extensively used monomers for biomolecule entrapment within a polymer film have been polyporrole and its derivatives. Such substances can be polymerised under mildly oxidative conditions rendering them favourable for use with bioelements. Other popular monomers, however, require specific non-biocompatible conditions to form a conducting polymer film. Aniline for example requires acidic conditions to form a highly conductive polymer (Wallace *et al*., 1999). For this reason such monomers have not been extensively used for entrapment purposes as the potential for biomolecule denaturation is a possibility. Currently used immobilisation methods, however, surpass this limitation. Biomolecules nowadays are frequently immobilised on the surface of the polymer film rather than within it, thus, the electrodeposition conditions do not affect any of the biological molecules involved in e.g. sensor fabrication.

Conducting polymers owe their unusual but very favourable properties such as conductivity and high electron affinity to the π-electron backbone of their molecular structure (Gerard *et al.,* 2002; Saxena & Malhotra, 2003). Some of the most widely used conducting polymers include polyaniline (used in this project), polyazulene and polythiophene and have also found use as electrode materials for rechargeable batteries; polyaniline, for example, is being as an anti-static coating material by Hitachi-Maxell for a 4Mb floppy-disk (Gerard *et al.,* 2002). Figure 2.8 depicts the chemical structure of aniline.

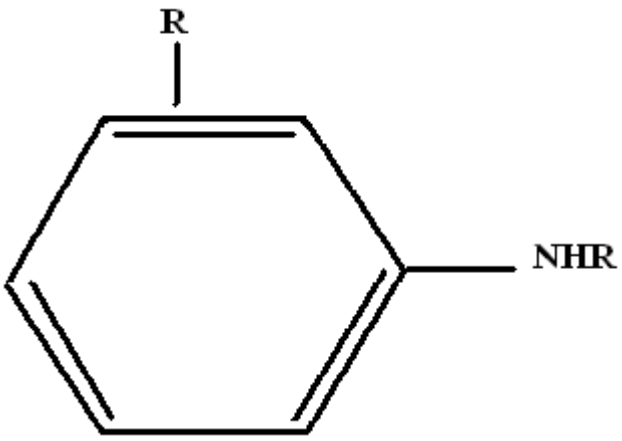

Figure 2.8: The chemical structure of aniline. Aniline consists of a phenyl group attached to an amino group.

2.6.2 Non-conducting polymers

While conducting polymers have offered great benefits to the continuous research for higher quality biosensors, they also have some disadvantages. One of these disadvantages is that conducting polymers can be affected by other components that are present in a sample and this can give rise to erroneous readings (Guerrieri *et al.,* 1998). Guerrieri *et al.,* 1998 also report that significant advancements have been achieved using non-conducting polymers.

As would be expected, electrodeposition of a non-conducting polymer film onto any electrode surface is a self-limiting process (Law & Higson, 2005), thus non-conducting polymer films are often very thin contrary to conducting polymer films. The insulating nature of non-conducting polymer electrodeposition, results in films that may range from 10 to 100 nm in thickness and are virtually defect free. The thickness of any polymer film can affect sensor magnitude of response as well as response times (Myler *at al*., 1997). This allows for rapid diffusion of substrates and products to and from the biorecognition element thus offering faster result acquisition. Alongside rapidity, non-conducting polymer films also offer permselectivity by preventing interfering species from reaching the electrode surface and contaminating it, thus improving sensor selectivity (Yuqing *et al.,* 2004). Non-conducting polymers have also been shown to provide great reproducibility (Guerrieri *et al.,* 1998; Yuqing *et al.,* 2004). Yuqing *et al*., (2004) report the use of poly 1,3-diaminobenzene in order to eliminate interference from ascorbate, urea and other oxidisable species. As

Guerrieri *et al.,* (1998) report, rapid and interference free amperometric biosensors have been developed for glucose and lactate using non-conducting polymers. Some of the most important non-conducting polymers include derivatives of phenol and those of the phenylenediamines e.g. *o*-phenylenediamine the structure of which is shown in figure 2.9 (Yuqing *et al.,* 2004). Phenylenediamines in particular provide thin dense films and are inert to reactive chemical species such as O_2H_2 and have thus been of particular interest for their O_2 and O_2H_2 selectivity. Myler *et al*., (1997) describe the development of enzyme electrodes for the detection of glucose in whole blood, based on ultra thin *o*-phenylenediamine composite membranes (Figure 2.10). According to the authors, the resulting sensors displayed increased biocompatibility and excellent diffusion limiting properties while the determinations from this work showed close correlation to hospital laboratory analysis. Yuqing *et al*., (2004) report the attempt to develop an implantable glucose biosensor using phenylenediamines. The described sensors functioned extremely well in buffer, urine, plasma and serum, they did not, however, perform as well in blood samples (Daly *et al*., 2000). As the authors state, the electrodes tested in whole blood showed decreased reproducibility and in some occasions reduced detectable signal as well as high background signal, which is expected due to the number of constituents (some of which may interfere with the sensing process) present in blood.

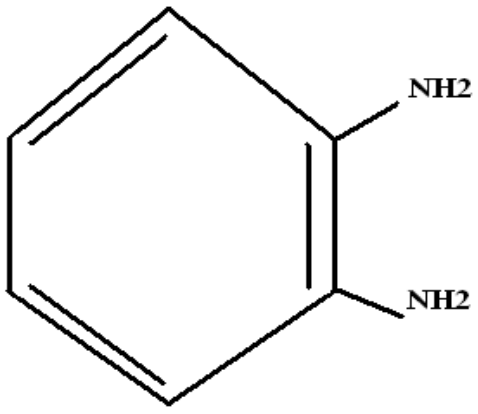

Figure 2.9: The chemical structure of *o*-phenylenediamine.

Figure 2.10 Electron micrograph of an o-phenylenediamine insulated electrode (Barton *et al*., 2004).

2.6.3 Non conducting polymers and their use in this research project.

The use of non-conducting polymers within this research programme is far more specific however. Here it is aimed to produce *impedimetric microelectrodes* by the use of both conducting and non-conducting polymers, namely poly-*o*-phenylenediamine and polyaniline. The process is described by Barton *et al.,* (2004) and involves the insulation of gold-coated glass slides with the non-conductive poly-*o*-phenylenediamine followed by *sonication* of those modified electrodes to produce cavities on the polymer surface. Immediately afterwards aniline is electrodeposited on the surface of the electrode forming mushroom-like formations that rise from the sonication cavities. Otherwise, aniline can first be electrodeposited onto the bare gold electrodes followed by deposition of *o*-phenylenediamine and subsequent sonochemical ablation.

2.7 Electrochemistry and electrochemical methods

Electrochemistry is the science that studies and explains the relationship between chemical and/or biological changes and electrical potentials or currents. It is a powerful analytical tool and closely associated with this project since the use of electrochemistry is important for both sensor fabrication and analysis of results collected from the final biosensor formats.

In 1793, Alessandro Volta discovered that by placing two metals on opposite sides of a wet tissue one could produce electricity (Lower, 1994). Only a few years onwards Nicholson and Carlisle indicated that water can be decomposed to its basic elements, hydrogen and oxygen by the application of electricity; this is called *electrolysis*. Following this important discovery it was realised that all atoms are electrified, metals being electropositive alongside hydrogen and all the non-metals being electronegative. Over one century after this theory was proposed Michael Faraday proved that the quantity of a product of electrolysis depends on the amount of applied electric charge passed (Lower, 1994). This can be summarised by equation 2.3 below.

$$m = \left(\frac{Q}{F}\right)\left(\frac{M}{z}\right) \qquad \textit{Eq. 2.3}$$

Where:

m is the mass of the substance altered at an electrode

Q is the total electric charge passed through the substance

F = 96 485 C mol^{-1} is the Faraday constant

M is the molar mass of the substance

z is the valence number of ions of the substance (electrons transferred per ion)

There is an abundance of literature regarding electrochemistry and the different phenomena this science studies, thus very few concepts will now be briefly described. The concepts of mass transport and the electrical double layer are considered in the following pages, alongside voltammetry and AC impedance, two of the techniques used extensively within this PhD research project.

2.7.1 Mass Transport

For a species in a solution to sufficiently undergo redox reactions, the working electrode must constantly be provided with fresh reactants. This introduces the concept of mass transport, i.e. how the species in a solution reach and leave an electrode surface.

There are three modes of mass transport: *Migration, Convection and Diffusion*.

Migration arises from the movement of ions in the solution in the presence of an electric field. For movement of ions towards an electrode, the electrode in question must be polarised. Since migration effects are difficult to measure it is desirable to introduce in the solution an electrolyte such as KCl which suppresses migration effects while increasing conductivity of the solution (Monk, 2001).

Convection involves the physical movement of the solution. It occurs by physically moving the solution; this may occur via stirring, agitation or even movement due to localised changes that occur due to heating of the solution.

Diffusion occurs due to the continual consumption of reactant in the solution to produce the product. This causes changes in the concentration of species throughout the solution while *entropy forces* naturally attempt to minimise the changes of the *concentration gradient*. *Fick's Laws* describe the effects of diffusion in a solution with an electroactive species. *Fick's first law* states that the diffusive flux moves from regions of high concentration to regions of lower concentration with a magnitude that is proportional to the concentration gradient. *Fick's second law* states that the time rate of concentration change is related to the second derivative of the concentration gradient through the diffusion coefficient. Diffusion will always exist in a solution containing electrolytes even if migration or convection are not present (Monk, 2001).

2.7.2 The electrical double layer

Whether it be under potentiostatic control or equilibrium, the molecules and ions in a solution always interact with the electrode surface. The region where these

interactions take place is called the *Electrical Double Layer*. The events taking place in this region are non-faradaic, i.e. no exchange of electrons occurs. Ions and other particles constantly adsorb and desorb from the electrode surface. When the cell is in equilibrium, adsorption and desorption occur at the same rates. When an electrode is polarised this equilibrium is disturbed (Monk, 2001).

Various models have been created to explain these interactions; two of the earliest are schematically represented and discussed, while the newer models involve numerical modelling to better approach those interactions.

The Helmholtz model (1850s)

Helmholtz assumed that any excess charges on the metal surface of an electrode immersed in solution are neutralised by a layer of ions with opposite charge present in the solution itself. This redistribution of charges which is caused by electrostatic forces renders the electrode surface neutral. In essence, the interface between the solution and the electrode surface acts like a capacitor storing charge and there is a potential drop that is proportional to the distance from the electrode. As the Helmholtz model suggests, the electrical double layer is an electrically neutral interface. This is described in the schematic of figure 2.11.

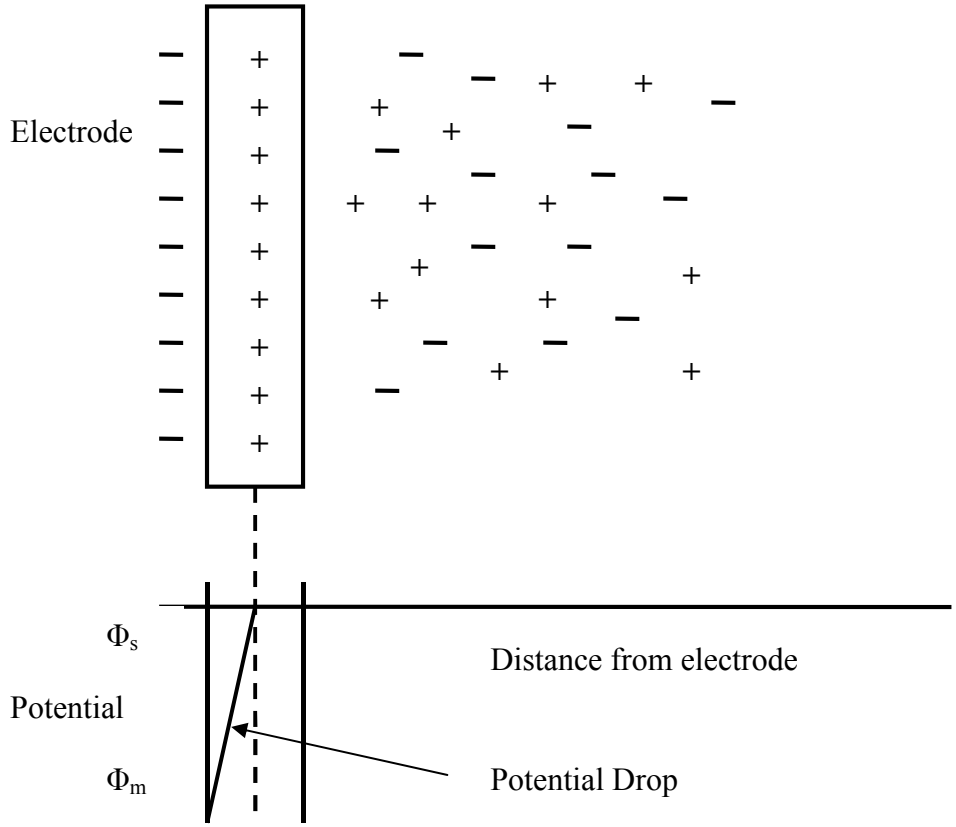

Figure 2.11: The Helmholtz Model (http://www.cheng.cam.ac.uk/research/groups/electrochem/teaching.html).

The Stern Model (1924)

The Stern model takes into account the fact that ions are capable of movement within the solution while also accounting for diffusion and adsorption effects, as discussed earlier. Finally according to the Stern Model the attracted ions can be adsorbed onto the electrode surface while diffusion drives other attracted ions closer to this area. This region is called the *diffuse layer* (as shown in figure 2.12).

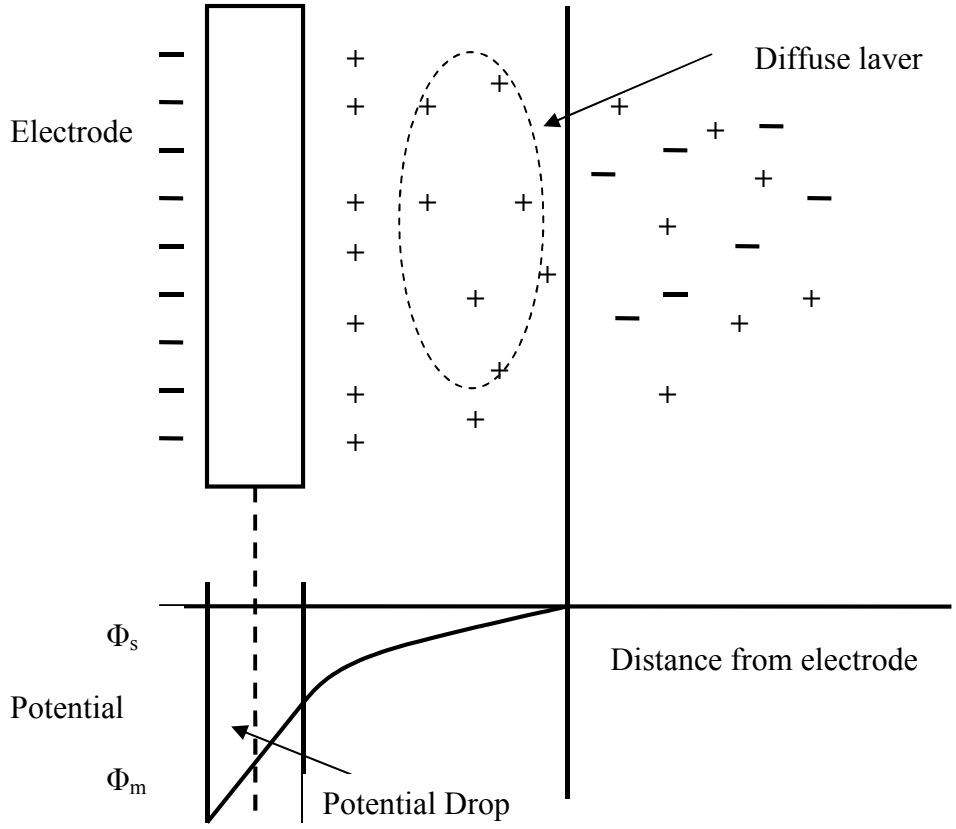

Figure 2.12: The Stern Model (http://www.cheng.cam.ac.uk/research/groups/electrochem/teaching.html).

2.7.3 Voltammetry

Voltammetry is a technique widely used in electroanalytical chemistry, that allows the study of potential-current relationships in electrochemical cells. In voltammetry the varying potential results in differences in the current thus providing information about the analyte of interest. The measurements involve a polarised working electrode and the method of polarisation determines the type of voltammetric technique being employed. Importantly it is the difference between the potentials of two electrodes that can be measured rather than the absolute potential of one electrode. For this reason it often is required that a *reference electrode* is present for voltammetric experiments alongside a *working electrode* and a *counter electrode*. The reason for using this three electrode system will now be discussed.

The potential difference (E) observed between a reference and a working electrode will be equal to the sum of potential drops of two interfaces, namely the working electrode-solution and reference electrode-solution interfaces, as shown be equation 2.4 below.

$$E = (\varphi m - \varphi s) + iR + (\varphi s - \varphi ref) \qquad Eq.\ 2.4$$

R is resistance of the solution and *i*R is the voltage drop in the solution due to current passing through the two electrodes.

The potential drop of the reference electrode-solution interface is fixed when small currents pass through the two electrodes e.g. in the case of microelectrodes and *i*R is negligible, hence any changes in the potential are reflected by (φm - φs) and no counter electrode is required. The use of larger currents however, e.g. when large electrodes are used, means that a) *i*R ceases to be negligible and b) the chemical composition of the reference electrode may be altered so the potential drop of the reference electrode-solution no longer retains a fixed value. For this reason a counter electrode is introduced in the system.The power source for any voltammetric experiments is a *potentiostat*.

A wide range of voltammetric techniques exist many of which are based on linear sweep voltammetry. Linear sweep voltammetry measures the current at a working electrode when the potential between the working and reference electrodes is swept in a linear manner over time. Cyclic sweep voltammetry is an extension of linear sweep voltammetry. In this method, when the potential reaches a pre-defined value, the potential scan is reversed and the same potential range is scanned in the opposite direction. Cyclic voltammetry has been extensively used within this PhD research program for electrode testing and polymer deposition.

Cyclic Voltammetry

Cyclic voltammetry is best suited method for the fast acquisition of kinetic and thermodynamic processes such as, for example information relating to electron transfer reactions within an electrochemical cell. It is often the first step in electrochemistry to determine analyte redox potentials in a laboratory environment.

It is now important to introduce the Nernst equation which is used to predict the relations between voltage and concentration of reactants at non standard conditions. 1 molar solute concentrations, gas pressures of 1 atmosphere and typically a temperature of 25^{o}C are defined as standard conditions. At such conditions, the potential of an electrochemical cell can be calculated from the standard electrode potentials. The Nernst equation, shown below (Eq. 2.5), is used to calculate the equilibrium electromotive force (reduction potential) of an electrochemical cell by taking into account the standard electrode potential and the activities of the electroactive species within the cell.

$$E = E^{0} - \frac{RT}{nF} \ln \frac{[O]}{[R]} \qquad Eq.2.5$$

E^{0} is the standard electrode potential.
R is the universal gas constant (8.314510 J K^{-1} mol^{-1}).
T is the absolute temperature.

O and R are the concentrations of the reacting species. The Nernst equation ideally uses the activity coefficients of these components however at low concentrations these coefficients can be replaced by concentrations instead.
F is the Faraday constant.
n is the number of electrons transferred in the cell reaction or half cell reaction.
At room temperature, the constant *RT/F* can be replaced by 25.679 mV.

Under ideal conditions, when the reaction in the solution is reversible the peak separation will be 59 mV. A voltammogram from a cyclic sweep is depicted in figure 2.13 below.

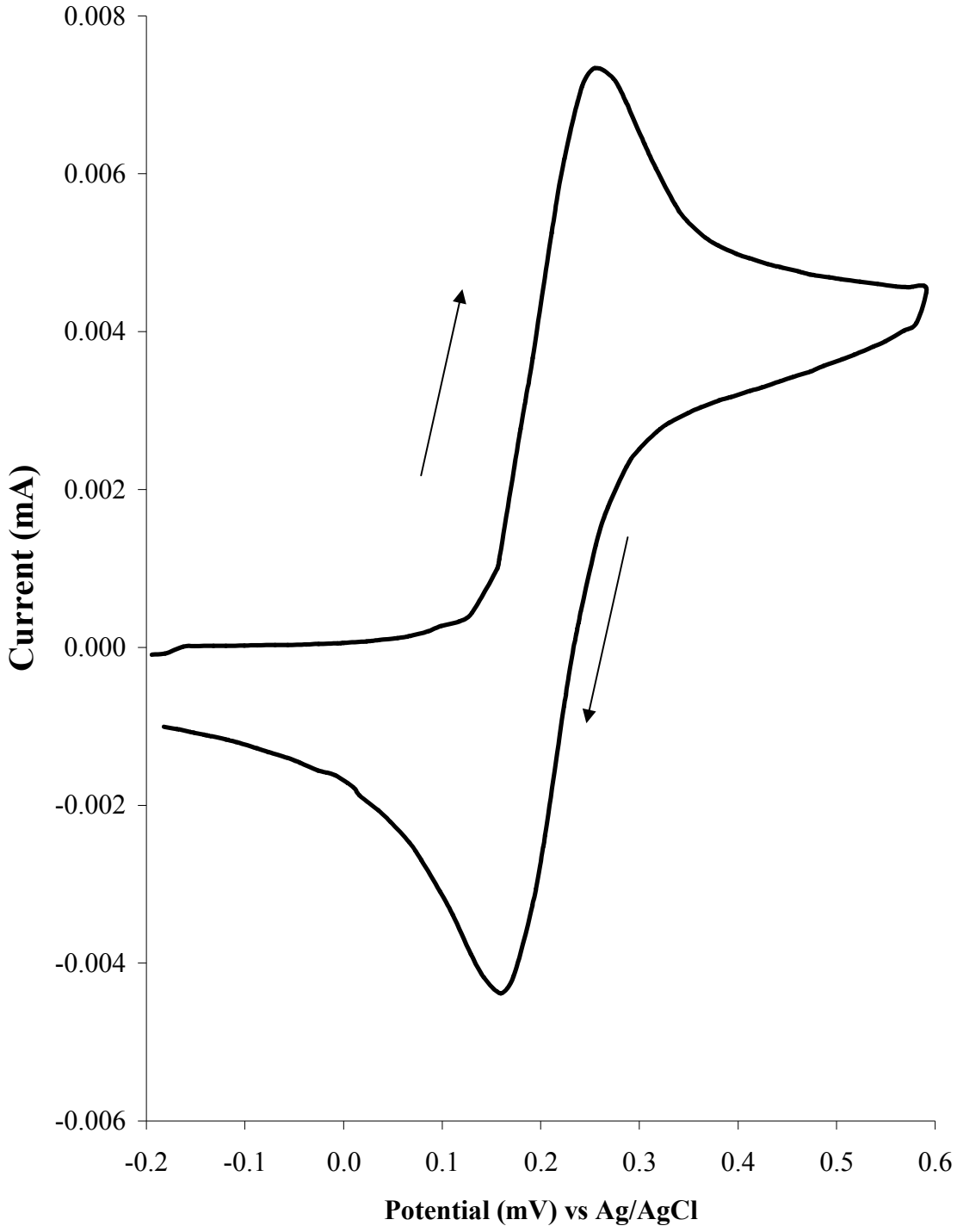

Figure 2.13: A typical Cyclic Voltammogram; Au working electrode using Ferrocenecarboxylic acid in PBS at a scan rate of 50 mV s^{-1}.

In cyclic voltammetry and for any typical redox reaction, species O will be reduced to species R during the cathodic scan until a reduction peak is created where no further conversion occurs. At this point species R will have formed a diffusion layer around

the electrode inhibiting species O to reach the electrode surface. This results in loss of equilibrium and the subsequent decrease in passing current. When the predetermined potential limit of the cathodic scan is reached, a reverse scan is initiated during which species R is oxidised to species O. The availability of species R due to the previously formed diffusion layer causes a current increase while at higher potentials the conversion rate from species R to species O increases. When all of species R within the diffusion layer has been oxidised, a current decrease is observed. In the above figure, ferrocenecarboxylic acid acts as a redox couple. When the reaction is completely reversible the two peaks that reflect the oxidation (forward peak) and reduction (reverse peak) of the species will have the same peak current height.

In an ideal environment the difference between the two peaks in such a reaction should be 59mV. This can be seen by the Nernst equation when this is expressed in base 10 logarithms rather than natural logarithms.

$$E = E^0 - \frac{0.05915}{n} \log \frac{[O]}{[R]} \qquad \textit{Eq. 2.6}$$

Cyclic voltammetry may be used to test the reactivity of species in a solution while in this research project it is also mainly used for electrodeposition of polymers on the electrode surface to fabricate biosensors (Barton *et al.,* 2004). Additionally cyclic voltammetry may be used for antibody entrapment within a polymer film for use in biosensors (John *et al.,* 1991; Sadik & Wallace, 1993).

2.7.4 AC Impedance

Impedance (**Z**) of a given circuit quantifies the opposition to a sinusoidal alternating current. During impedimetric analysis a perturbing voltage is applied across an electochemical cell, over a frequency range, thus minimal changes occur in the concentration of the solution while a current is still generated. An AC impedance voltage is applied in a cyclic *sinusoidal* manner due to which the current alternates. The current that is generated from this system is frequency (**ω**) dependent and will be out of phase by a time factor (**θ**). Two components of impedance are measured; the

real component (resistive) is indicated by **Z'** and the imaginary component (capacitive) **Z"** (Monk, 2001). An impedimetric approach may be modelled by a system made of resistors and capacitors.

In any impedimetric process the applied oscillating sinusoidal potential will be:

$$E = \Delta E \sin \omega t \qquad \textit{Eq. 2.7}$$

Where ω is the angular frequency equal to $2\pi f$ where f is in Hertz.
E is the instantaneous value.
ΔE is the maximum amplitude.

The applied potential described in equation 2.7 can be represented on a polar diagram as the rotating vector E, as depicted in figure 2.14.

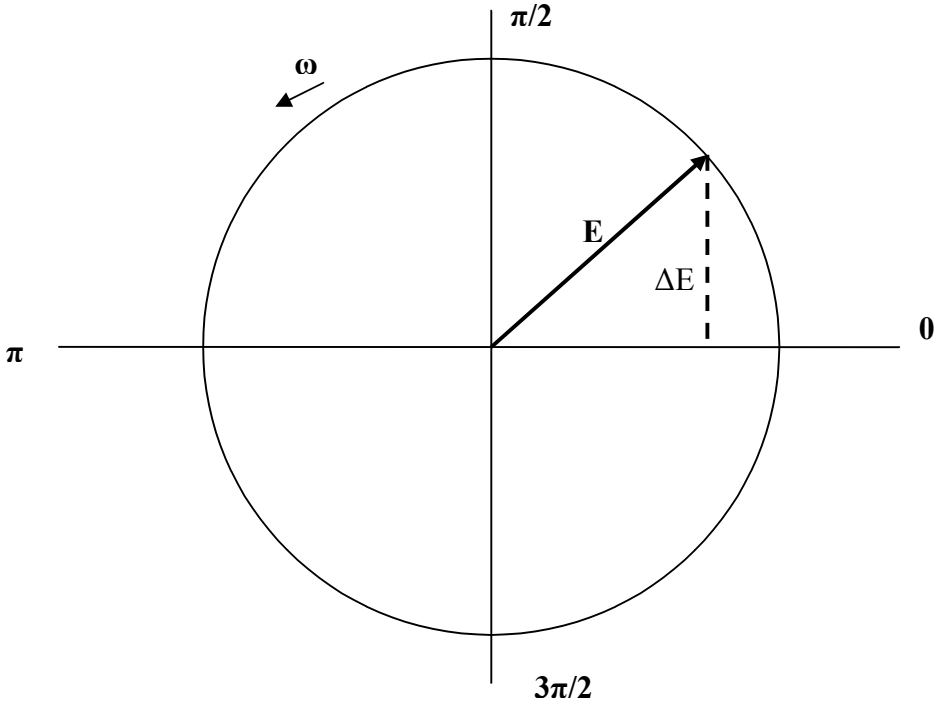

Figure 2.14: Representation of sinusoidal potential in the complex plane.

This applied potential causes a current flow determined by the equation

$$i = \Delta i \sin(\omega t + \phi) \qquad \textit{Eq. 2.8}$$

hence the resulting current will be of different phase (lagging or leading) and amplitude to the applied voltage. However, it will in most cases retain the same frequency and be of sinusoidal nature.

Upon application of a voltage E, the response of the elements within a simple circuit, can be determined by Ohm's law, when only simple resistance exists.

$$i = \frac{E}{R} \qquad \textit{Eq. 2.9}$$

In a polar diagram the rotating vectors, potential (E) and current (i), of a circuit with pure resistance, are separated by the phase angle φ. In this case, however, the phase angle is zero. This is shown in figure 2.15.

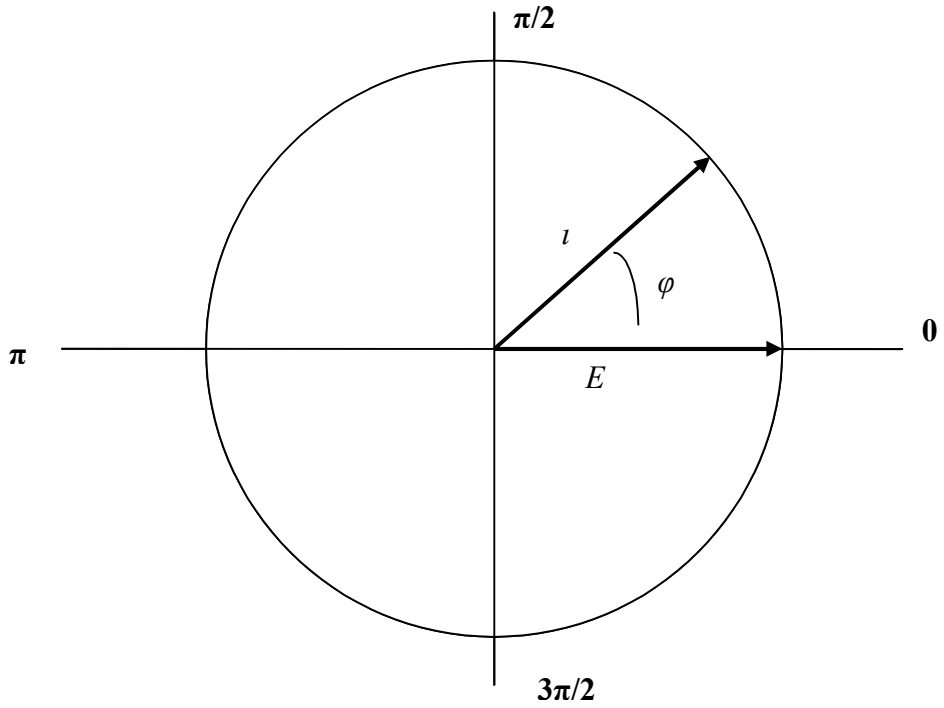

Figure 2.15: Representation of current and potential in the complex plane.

Earlier within this work, the electrical double layer was introduced. Within this region ions of the constituents within a cell can be accumulated or depleted. This ability of the system to store charge introduces the concept of capacitance. In simple terms capacitance is the measure of stored electric charge upon the application of a potential and is determined by the equation:

$$C = \frac{q}{E} \qquad \textit{Eq. 2.10}$$

q is the stored charge among the capacitor elements

E is the applied potential

For a capacitive system, the relationship between current and potential can be given by the following equation, derived from equations 2.7 and 2.9:

$$i = \omega C \Delta E \cos \omega t \qquad \textit{Eq. 2.11}$$

Where capacitance is concerned, $1/\omega C$ can be replaced by X_c (capacitance reactance) resulting in the equation below:

$$i = \frac{\Delta E}{X_C} \sin(\omega t + \pi / 2) \qquad \textit{Eq. 2.12}$$

This equation is similar to Ohm's law for resistive systems but with *R* replaced by X_c and a current that leads the voltage in terms of phase, since the phase angle is $\pi/2$. The introduction of $j = (\sqrt{-1})$ is now necessary, which describes the sinusoidal response of a system. Then equation 2.7 becomes

$$E = -jX_C i \qquad \textit{Eq. 2.13}$$

In a phasor notation, *E* is the sum of every voltage drop across the different elements, within a system of resistors and capacitors connected in series.

$$E = E_R + E_C = i(R - jX_C) \Rightarrow E = iZ \qquad \textit{Eq. 2.14}$$

Where Z is the impedance. The current is no more in phase or 90^o out of phase with the voltage. Then the phase angle is determined by the following equation:

$$\tan \phi = \frac{X_C}{R} = \frac{1}{\omega RC} \qquad \textit{Eq.2.15}$$

Total impedance can be further analysed into two more components the real and imaginery component symbolized by **Z'** and **Z''** respectively, **Z'** being the resistive

and **Z''** being the capacitive component. Figure 2.16 describes the relationship between the real and imaginery components and the total impedance of a system.

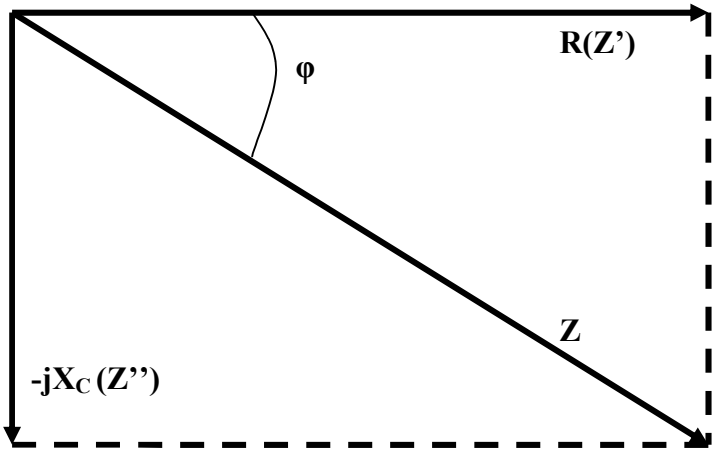

Figure 2.16: Representation of Total impedance Z and the real (Z') and imaginery (Z'') components.

For series circuits the overall impedance is the vector sum of the reactance of the separate components. The overall impedance for parallel combinations is the reciprocal of the sum of the reciprocal impedances of each of the components. **1/Z** being the reciprocal impedance is defined as the admittance **Y**, which is used to describe impedance combinations.

Some general considerations regarding impedance measurements need to be taken into account for AC impedance to be successfully used in diagnostics. Normally, a large frequency range must be used. The system that will be interrogated i.e. electrode material, polymers used, bioelements used determine which impedance spectra will be covered during the interrogation. Within this project the chosen frequency range is between 1 Hz and 10000 Hz. Additionally, electrochemical processes are by nature non-linear while the most developed impedance theories are linear. In order to overcome this limitation, the exciting signal must be kept small enough to allow for an approximation to linearity, generally this means that a peak-to-peak current of 10 mV should ideally be used. One more important aspect to consider is electrode positioning. The working and counter electrodes must be symmetrically arranged to allow uniformity in current distribution, while the reference electrode should have as low resistance as is physically possible.

Electrode impedance is normally described by equivalent electrical circuits the, simplest of which is the Randles circuit as shown in figure 2.17.

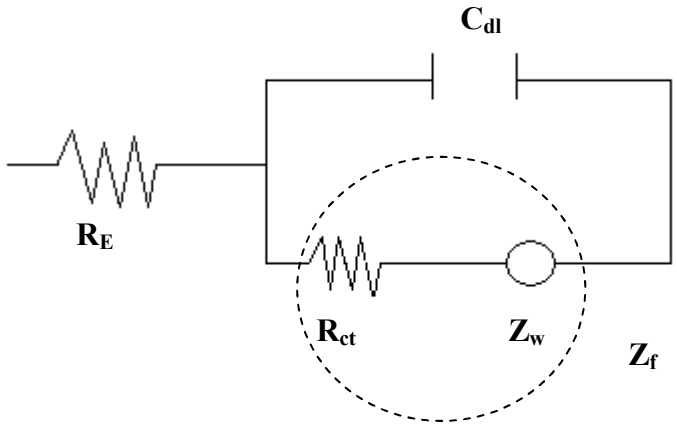

Figure 2.17: The Randles circuit.

$\mathbf{R_E}$ is the electrolyte resistance between the working and reference electrodes.
$\mathbf{C_{dl}}$ is the double layer capacitance.
$\mathbf{R_{ct}}$ is the charge transfer resistance.
$\mathbf{Z_w}$ is the Warburg impedance reflecting the effect of mass transport of the electroactive species on the system.
$\mathbf{Z_f}$ is is the combination of $\mathbf{R_{ct}}$ and $\mathbf{Z_w}$

The last two elements can normally be combined ($\mathbf{Z_f}$) to reflect Faradaic impedance caused by the charge transfer process between the working electrode and the electrolyte. For diffusion limited processes $\mathbf{Z_w}$ is dominant while for charge transfer controlled processes $\mathbf{Z_f}$ equals $\mathbf{R_{ct}}$. Impedance data is normally displayed in a Nyquist plot where the Z'' component is plotted against the Z' component. A typical Nyquist plot, based on a Randles circuit, could be presented as in figure 2.18 below (Fernandez-Sanchez *et al*., 2005).

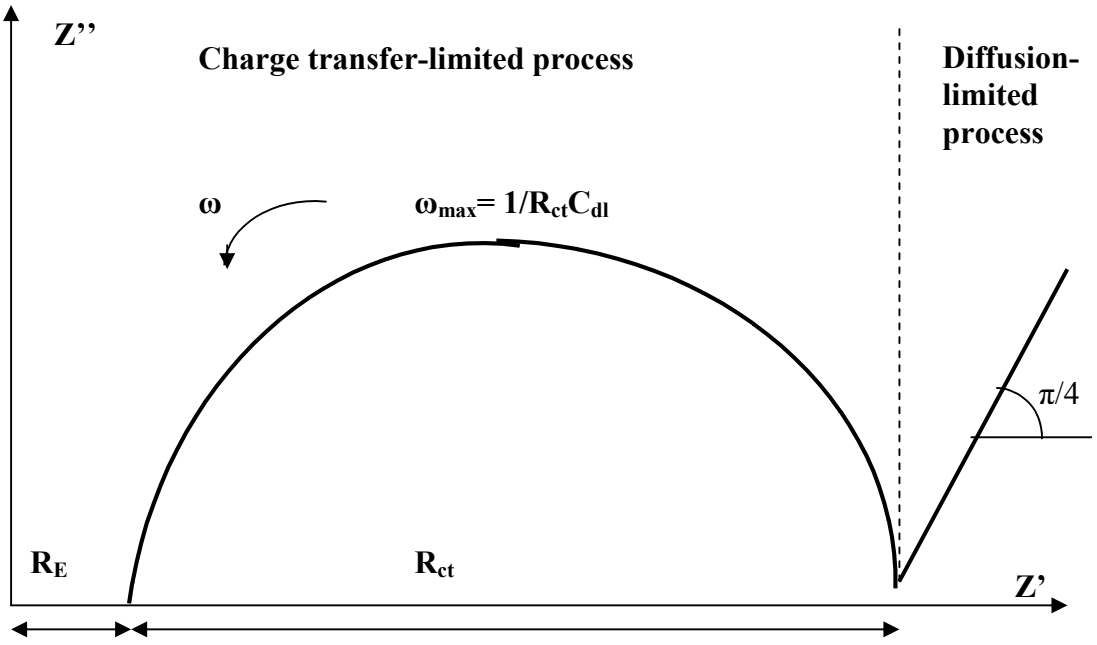

Figure 2.18: Typical Nyquist plot based on a Randles equivalent circuit.

At high frequencies the solution resistance does not allow for any electrolysis to occur while as the frequency is lowered the faradaic (charge transfer) component of the working electrode impedance gives the semicircular shape. At the lowest end of the frequency range the process becomes diffusion limited due to the changes in ion localisation within the solution, driven by the perturbing potential. At this point the component with the major contribution is the imaginary or capacitive component.

AC Impedance allows the detection of minor changes on the surface of the electrode in question by detecting changes to the opposition of flowing current. The technique is non destructive since the perturbation used is near zero current thus not affecting any kinetic information on the surface of interest. Impedance techniques are nowadays extensively used for corrosion studies on polymer coated or metal transducers. The technique can relay information regarding the biological or chemical processes that cause sensor degradation. Lazcka *et al*., (2007) report the use of EIS for determination of total biomass in a sample while extensive examples of DNA and antibody modified electrochemical impedance based biosensors are described in the scientific literature (Davis *et al*., 2005). One of the main advantages of EIS over potentiometry and amperometry is that the technique does not require any type of label. Expensive labels or those harmful to human health such as radioisotopes can be

avoided using this powerful tool for chemical analysis. Additionally the technique offers rapidity and simplicity. However, Lazcka *et al*., (2007) further report that the detection limits of EIS are still poor. Additionally, the understanding of the phenomena occurring on EIS of immunosensors, and the subsequent creation of a measurable signal, is not as of yet well studied and understood. Furthermore, electrode size and separation distance may play a role in the detection limits achieved, however, this aspect has not yet been examined either.

Extensive work within the sensing industry included the use of EIS for sensor development. A large number of studies incorporated EIS to gain an understanding of the biomelecular interactions of conductive and semi conductive surfaces. Enzyme and whole cell based sensors have also been characterised by EIS, while its use for cell culture monitoring has also been reported (Pejcic & de Marco, 2006). Finally, EIS has been used to provide details concerning the immobilisation of biomolecules on the sensor surface by determining the changes in impedance of modified electrodes. In this project minor changes on the sensing surface occur when antigen is attached to an antibody covered electrode, hence the system functions as a biosensor. Several groups have reported successful detection of various types of antigens or other molecules by the use of AC Impedance (Farace *et al.,* 2002; Ouerghi *et al.,* 2002). Davis *et al.,* (2005) have reported the use of impedimetric DNA sensors for differentiation among different species of fish. Impedimetric experiments allow the experimentalist to monitor such changes and effectively make the detection of disease, pollutants, chemicals in various samples, feasible.

Figures 2.19 and 2.20 contain representative Nyquist (Z' vs Z") and Bode (total impedance vs frequency) plots. These were obtained from data acquired during this research project. It can be seen that increasing concentrations of polyclonal (non-specific) IgG result in changes of impedance whether it be the faradaic or capacitive components or total impedance. These figures are further discussed in the Results and Discussion section.

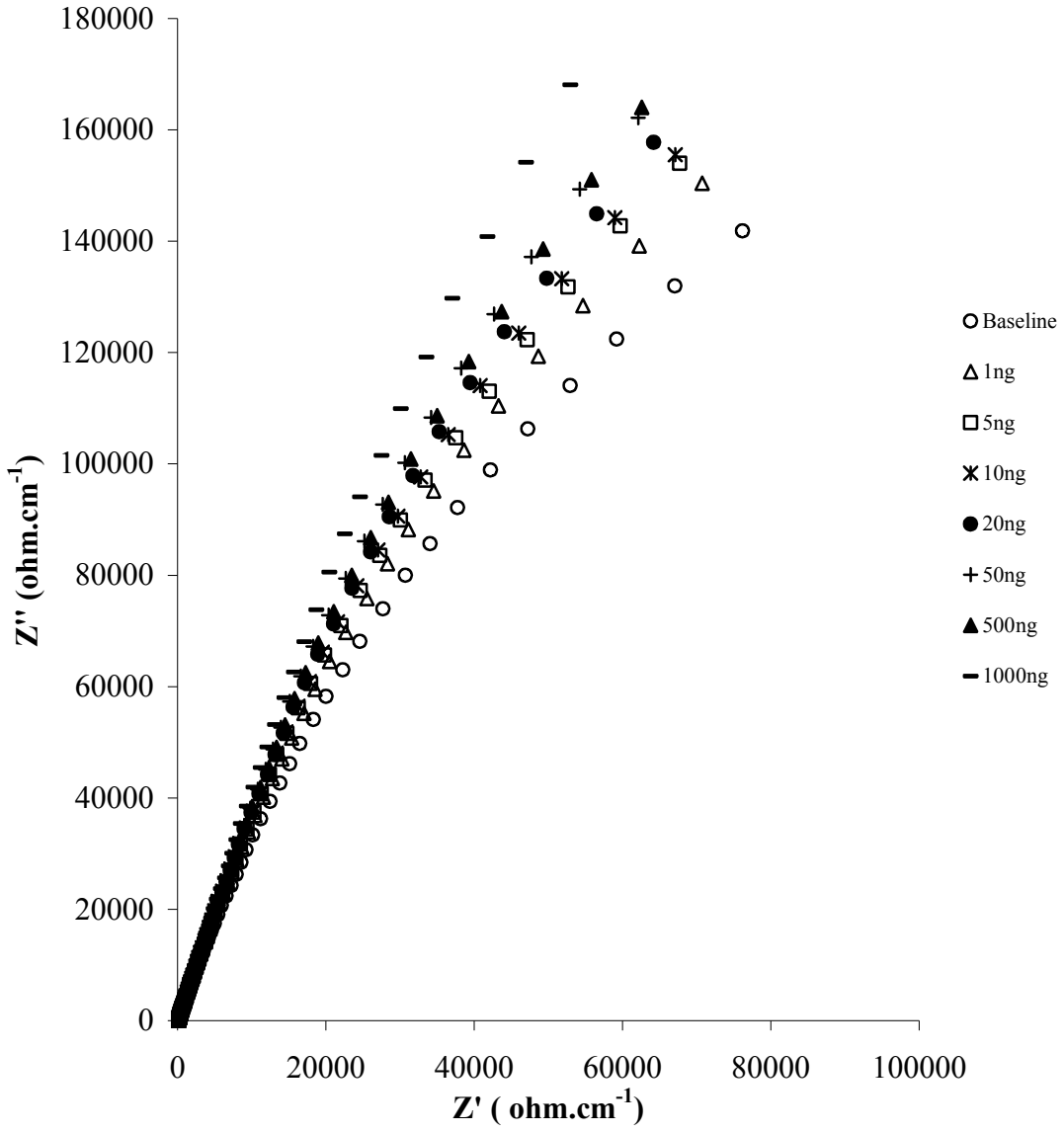

Figure 2.19: Z' v Z'' - Nyquist plot; Impedance responses of polyclonal IgG loaded carbon based sensors upon exposure to various antigen concentrations (in PBS).

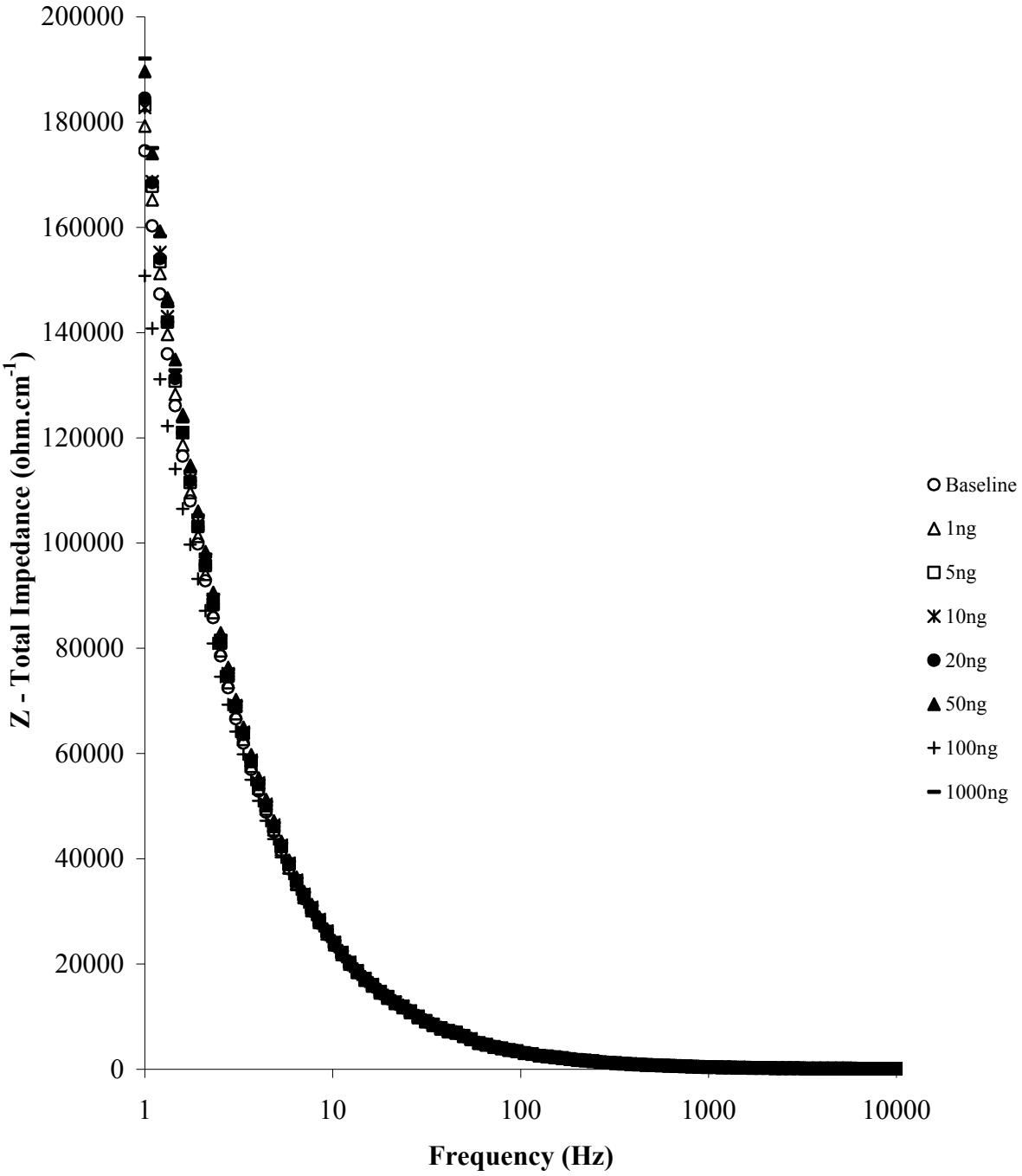

Figure 2.20: A typical Bode plot, total impedance vs $\log_{10}$ frequency; total impedance responses of polyclonal IgG loaded carbon based sensors upon exposure to various antigen concentrations (in PBS).

2.8 Antibody Immobilisation

In any biosensing device, the main component affecting specificity is the biological sensing moiety. The immobilisation method used in each case depends upon the type of the biorecogniton element and the transducer to be used. Bioelement immobilisation is of pivotal importance to sensor fabrication because it affects parameters such as the sensor detection limits, sensitivity, reusability as well as reliability. Some of the most widely used methods include encapsulation, cross linking, adsorption, covalent bonding and entrapment (Mello & Kubota, 2002).

Reports from the early 1990s (John *et al.,* 1991; Cooper & Hall., 1992; Sadik & Wallace., 1993) suggest that physical entrapment was then viewed as the preferred method for biomolecule immobilisation resulting in successful sensing devices for a variety of target substances. This immobilisation method normally involves the addition of both antibody and monomer to be used in an aqueous solution protocol followed by an electropolymerisation protocol. In this manner the antibody molecules are entrapped within the polymer structure thus imparting it with molecular recognition. The polymer of choice may simply provide support for biomolecule immobilisation or subsequently be involved in the occurring reactions i.e. as a mediator. While this method and newer improved variations are supported by a large number of researchers, others support that possible antibody leakage, long term instability and poor reproducibility are three of its drawbacks and choose alternative immobilisation approaches (Korri-Youssoufi *et al.,* 2001). Nevertheless, as it has already been stated in this work, conducting polymers offered favourable biocompatibility allowing for a range of different approaches to be developed based on the characteristics of available polymer substrates. Alongside physical entrapment, passive adsorption, electrochemical micro-assembly and other techniques, most of which in essence involved dipping of electrodes into antibody containing solutions, have been developed (Bender & Sadik, 1998).

Adsorption on the active surface of the sensor is possibly the simplest method for antibody immobilisation as the only requirement is that the polymeric or metal support surface to be incubated in a solution in the presence of the biorecognition element (Bilitewski, 2006). Adsorption is based on van der Waals forces between the

biorecogntion molecules and the supporting surface. The method often includes the use of an analyte permeable membrane, covering the transducer, on which the antibodies or enzymes are adsorbed (Mello & Kubota, 2002). However, as Lazcka *et al*., (2007) report, adsorption may also occur on an unmodified electrode surface such as gold. The method while fast and extremely simple suffers irreproducibility issues since the biomolecule antibody attachment is random and the orientation of the binding sites is not even minimally controlled. It is thus possible that the antibody binding site becomes inaccessible to the antigen and hence this could compromise sensor sensitivity. Additionally, desorption of the attached biomolecules may occur upon changes to pH, ionic strength or temperature (Anzai *et al.,* 1993; Mello & Kubota, 2002).

Covalent immobilisation is also a very commonly used method for protein attachment on a membrane matrix or even an unmodified electrode surface. This method is based on the interactions between terminal functional groups (normally from the amino acid side chain and non important for catalytic activity) and reactive groups on the support surface. Carbodiimide or succinimide derivatives are used for the activation of such functional groups which can then readily react with aldehyde, epoxide, carboxylic or amino groups. Chemical treatment of the support surface whether it be polymer based or an unmodified substrate, is required for the generation of functional groups. Upon deposition of the protein solution on the support surface, only a small incubation period at room temperature is required (Bilitewski, 2006; Mello & Kubota, 2002). Similarly to physical adsorption described earlier, this method suffers from random orientation; additionally, the chemical pretreatment may lead to slight distortions on the protein structures, thus rendering a large amount of molecules inactive.

A more recent alternative to all of the above immobilisation methods is the use of bioaffinity binding which offers, above all else, oriented immobilisation of the biorecognition molecules. This method is based on the biochemical properties of the chosen recognition entities as they utilise biochemical affinity reactions. Bilitewski, (2006) describes three techniques, namely, immobilisation via protein A or protein G, immobilisation via biotin-binding proteins or immobilisation of recombinant proteins via tags. Of the three methods mentioned, the one incorporating the use of biotin

binding properties will be now discussed, as it has been chosen for antibody immobilisation within this research project.

Anzai *et al.,* (1993) have reported the use of the avidin-biotin system for biomolecule immobilisation on conducting polymers. Avidin is a glycoprotein with a molecular weight of 68 kDa and a very high affinity constant for biotin binding ($\mathbf{K_a}= 10^{15}$ M^{-1}). Each avidin molecule has four biotin binding sites (Anzai *et al.,* 1998). Biotin is a vitamin with a molecular weight of 244 Da, found in every living cell with the highest concentrations being found in the liver, kidney and pancreas. Many proteins bind to biotin, while biotinylated antibodies have successfully been prepared (Dakshinamurti *et al.,* 1986). Due to the strong interactions between biotin and avidin, this is a very useful system for exploitation in protein immobilisation on sensors. Bilitewski, (2006) indicates that the biotin-avidin system was found to be more efficient than direct chemical or physicochemical immobilisation procedures. The same author reports that sensors fabricated using the avidin-streptavidin system can be regenerated by denaturation of streptavidin at very harsh conditions and subsequent reloading of the sensing surface with fresh proteins. Several groups have reported the fabrication of successful amperometric and impedimetric biosensors using the avidin-biotin complex (Ouerghi *et al.,* 2002; Ding *et al.,* 2005), and hence the use of this system is also preferred in this project. In this research project neutravidin is used rather than avidin. Neutravidin is a deglycosylated form of avidin with a near neutral isoelectric point of 6.3; it has many key characteristics that give provide low non-specific binding which is very important when it comes to sensitive immunological measurements. Figure 2.21 describes the immunosensor format when the biotin/avidin system is used. The protocol for sensor fabrication can be found in Materials and Methods chapter.

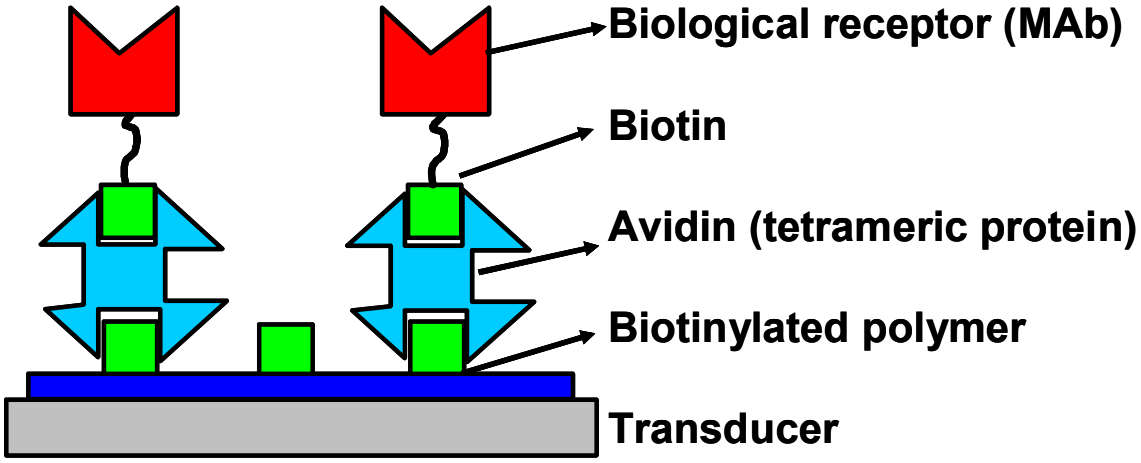

Figure 2.21: Covalent attachment of bioreceptor to a biotinylated polymer modified with a tetrameric protein (ELISHA 2nd year report).

2.9 Sonication and Microelectrodes

Sonication is a process that involves the use of sound waves to lyse whole cells, speed up biological interactions and more recently create cavities on different surfaces (Law *et al.,* 2003). This latter procedure can only be carried out in liquids e.g. in a water bath and involves the creation of bubbles that rapidly collapse onto target surfaces.

The use of sonication in this research programme is limited to the fabrication of microelectrodes. Law & Higson, (2005) report the use of a custom made sonic bath in which electrodes covered by the insulating polymer poly-*o*-phenylenediamine were immersed and sonicated in order to produce cavities on the polymer surface. These cavities provide passage to the electrode surface through very small openings that can act as microelectrodes. To further enhance the conductivity of the cavities aniline can be electrodeposited forming mushroom like formations that rise form the sonication cavities (Barton *et al.,* 2004; Myler *et al.,* 2004). Barton *et al.,* (2004) report the use of this technique for the production of microelectrode arrays on the surface of planar electrodes. It is suggested by the authors that one microelectrode would give a limited response due to size limitations while an array would provide a similar if not greater response to a normal sized electrode (due to the cumulative signal production of the existing microelectrodes) as well as offering stir independence.

As discussed in section 2.7.1, diffusion is one mode of mass transport to and from the electrode in an electrolyte solution. While a solution is unstirred diffusion control is normally the prevalent mode of mass transport; if this same solution was to be stirred then the diffusional gradients in the solution would change (Higson, 2003). A planar normal sized electrode can be affected by this and provide inaccurate data. However, microelectrodes are small enough to experience *hemispherical solute diffusional profiles* (Barton *et al.,* 2004). Any molecule can move towards or away from the electrode in a 180^{o} two dimensional arc much like the shape of a hemisphere thus rendering it stir-independent (Higson, 2003). Additionally ready made microelectrodes (P10 described in the Materials and Methods section) have already been prepared for this project without the use of sonication and are described in the Materials and Methods section.

The custom made sonic tank (Ultrawave Ltd., Cardiff, UK) contains sonic transducers that induce the formation of cavitational bubbles. Figure 2.22 shows the energy distribution within the old sonic tank; 'hot' spots (nodes) and 'weak' spots (anti-nodes) are clearly visible. For this reason rotating the sensors during the sonochemical ablation step was necessary when using this tank. The new tank as can be seen in figure 2.23 contains 108 transducers as opposed to 12 in the previous design. The increased number of transducers allows for a better distribution of the ultrasound energy within the bath area and so homogeneity for the final sensors.

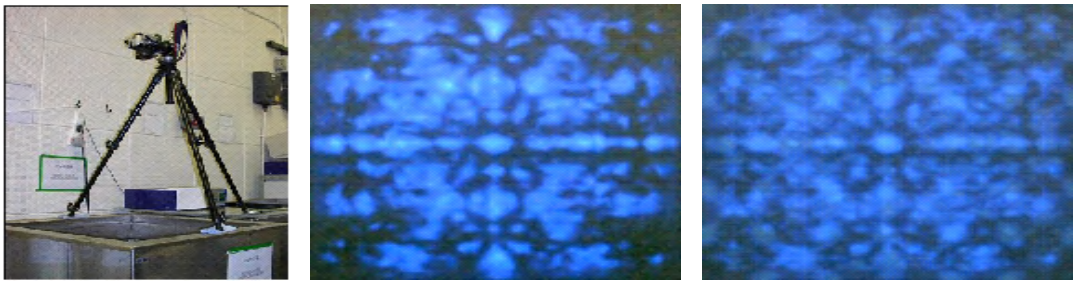

Sonoluminescence tank profiling with no baffling

Sonoluminescence tank profiling with the addition of baffling in the tank to disrupt standing waves

Figure 2.22: The first custom made sonic bath and Sonoluminescence Profiling of the tank (ELISHA 2nd year report).

Figure 2.23: The new sonic bath (ELISHA 2nd year report).

Chapter 3
Materials and Methods

3.1 Buffers and Solutions

Sodium di-hydrogen orthophosphate (AnalaR), di-sodium hydrogen orthophosphate and sodium chloride (AnalaR) were obtained from BDH (Poole, Dorset, UK) and used for the preparation of 10X Phosphate Buffered Saline (PBS) at pH 7.4 stock solution using 0.13 mM NaH_2PO_4, 0.528 mM Na_2HPO_4 and 0.51 mM NaCl. 1mM or 5 mM ferrocenecarboxylic acid from Sigma-Aldrich (Gillingham, Dorset, UK) was diluted in PBS for cyclic voltammetry.

5 mM *o*-phenylenediamine (Acros organics, Geel, Belgium) was dissolved in PBS for electrode polymerisation. 1 dm^3 of aniline buffer was prepared using 0.5 M KCL (Fisher Scientific UK Ltd, Loughborough, UK)and 0.3 M HCL (AnalaR, Poole, Dorset, UK) at pH 1 to for 0.2 M aniline (Sigma-Aldrich, Gillingham, Dorset, UK)solutions.

All buffers were prepared with H_2O obtained from a Purelab UHQ Deioniser (Elga, High Wycombe, UK).

3.2 Antibody/antigen preparation and biotinylation

Anti-Prostate specific antigen and prostate specific antigen were purchased from Europa Bioproducts Ltd (Cambridge, UK). Ciprofloxacin polyclonal antiserum (As 171) was provided by AMRg and was raised against 1-(3-mercaptopropyl)-6-fluoro-7-(piperanicyl)-1,4-dihydro-4-oxo-quinoline-3-carboxylic acid coupled to HCH. The preparation of the immunogen and of the antibodies will be described elsewhere (Pinacho *et al.,* 2007). Polyclonal IgG from rabbit, goat, murine and human whole serum were purchased from Sigma-Aldrich (Gillingham, Dorset, UK). Digoxin and anti-digoxin where purchased from Sigma-Aldrich (Gillingham, Dorset, UK). GFP was purchased from Millipore/Upstate (Hampshire, UK) and monoclonal anti-GFP was purchased from Sigma-Aldrich (Gillingham, Dorset, UK).

The biotynilation kit BK101 and Biotin 3-sulfo-N-hydroxysuccinimide ester sodium salt (water soluble biotin) were purchased from Sigma-Aldrich (Gillingham, Dorset,

UK). Immunopure NeutrAvidin protein was purchased from Perbio Sciences UK Ltd (Nothumberland, UK). Bovine serum albumin was obtained from Sigma-Aldrich (Gillingham, Dorset, UK). For antibody biotynilation the procedure outlined in the BK101 kit was followed (See section 2.8 for details). Biotinylated antibodies and their respective antigens were kept in aliquots of 200 µl at a concentration of 1 mg ml^{-1}. When lower antibody concentrations could only be obtained, these were concentrated. Concentration and purification of antibodies is described later in this chapter.

3.3 Equipment

For any process involving voltammetric procedures a potentiometer supplied by Sycopel Scientific (Tyne & Wear, UK) was used. The GillCac impedance kit (ACM Instruments, UK) was used for all impedimetric measurements. The custom made sonication tank was built by Ultrawave Ltd (Cardiff, UK).

3.4 Electrodes

3.4.1 Project specific electrodes

Project specific electrodes, designed and fabricated by Tyndall National Institute (Ireland), were given the labels of P3, P4, P5 and P10 (microarray-type) type electrodes, schematics of which are shown in figures 3.1, 3.2 and 3.3.

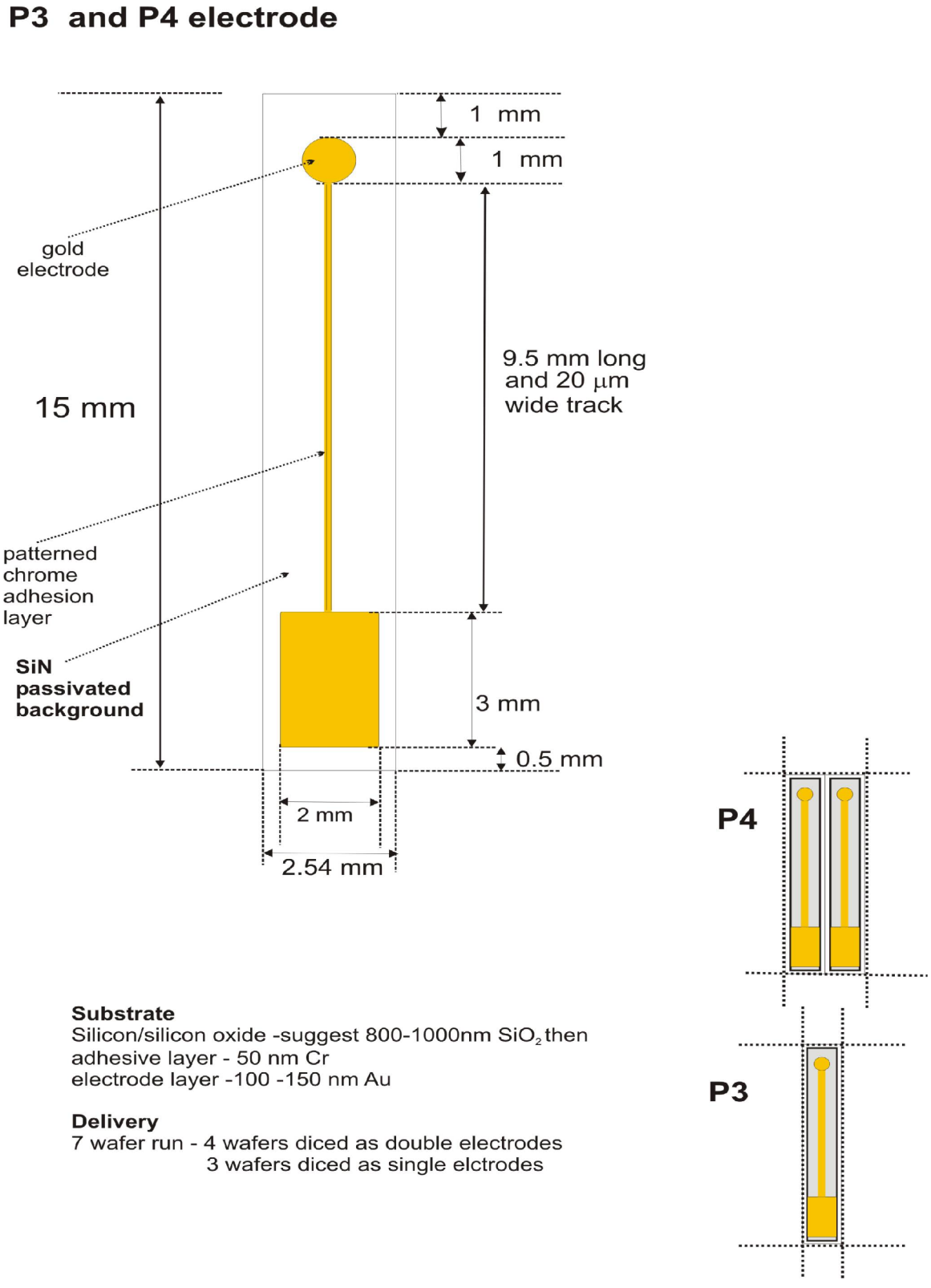

Figure 3.1: P3 and P4 electrodes.

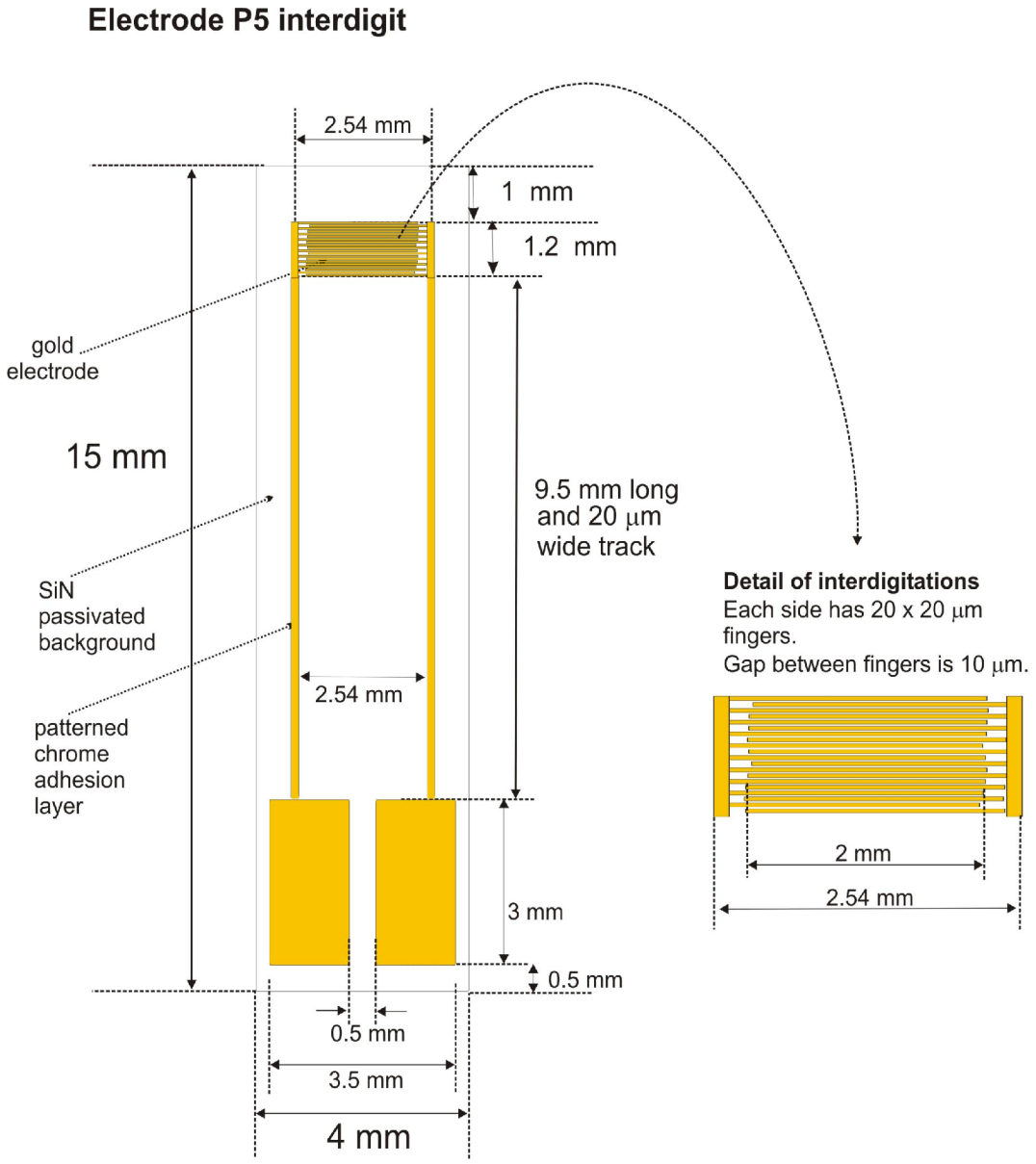

Substrate
Silicon/silicon oxide -suggest 800-1000nm SiO_2 then
adhesive layer - 50 nm Cr
electrode layer -100 -150 nm Au

Delivery
7 wafer run - wafers diced as single electrodes,
15 x 4 mm

Figure 3.2: P5 electrodes.

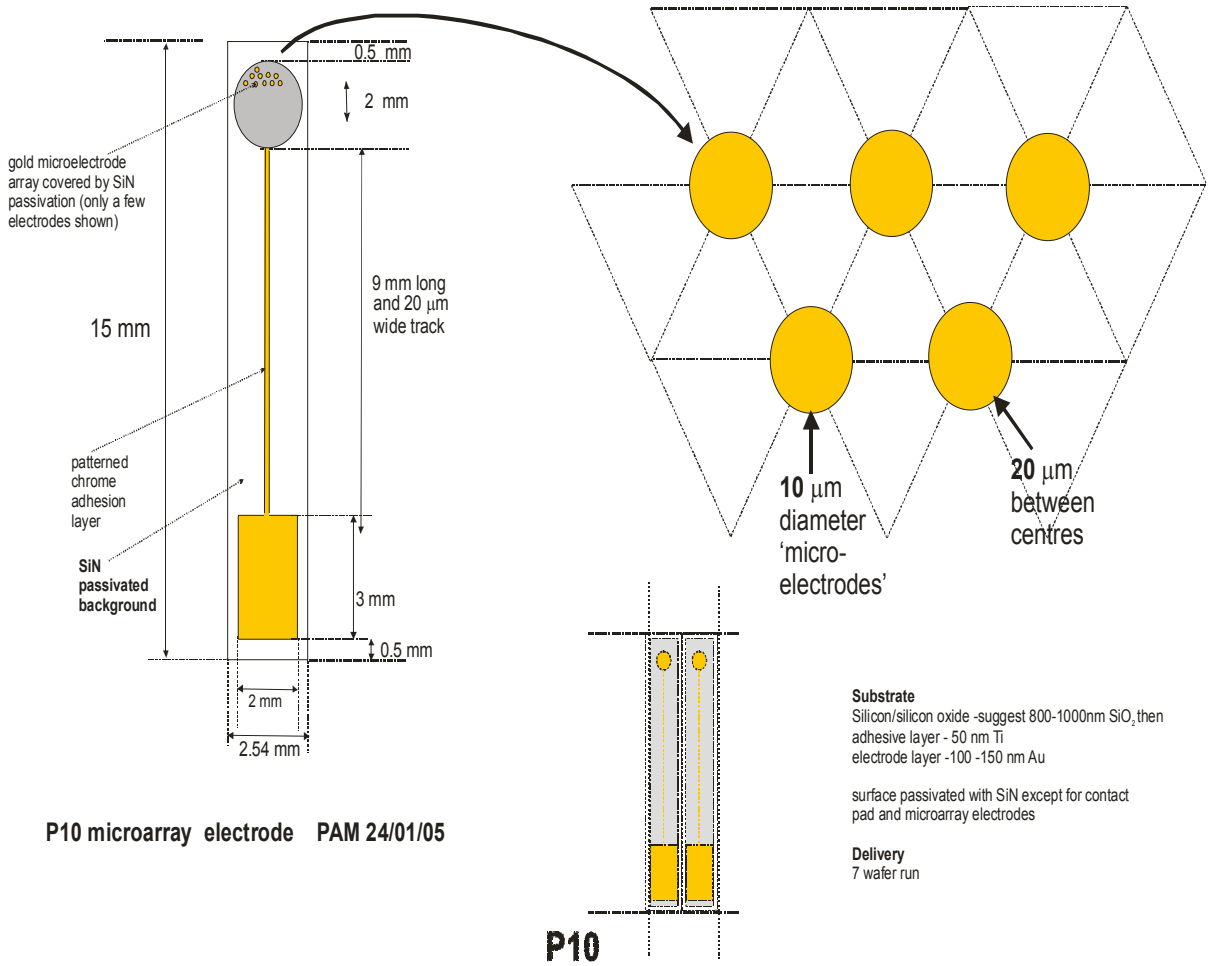

Figure 3.3: P10 electrodes.

3.4.2 In-house carbon electrodes

The screen printed carbon electrodes designed by Microarray Ltd., Manchester, UK and fabricated by Parlex Corp. Ltd., Isle of Wight, UK, where mainly used for the impedimetric work carried out within this PhD research project.

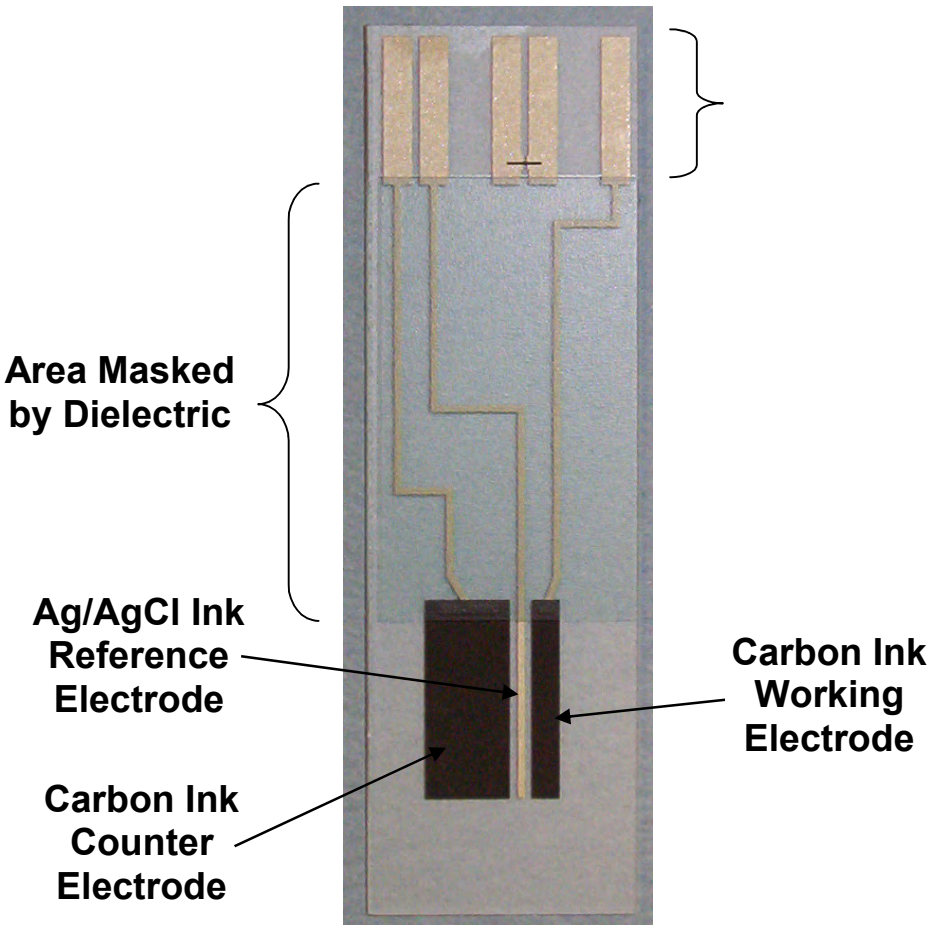

Figure 3.4: Typical in-house screen-printed carbon electrodes (Parlex Corp Ltd, Isle of Wight, UK). Surface area of working electrode is 0.2178cm^2.

3.5 Cyclic Voltammetry

3.5.1 FCA tests and polymer deposition

Ferrocenecarboxylic acid (FCA) tests were normally performed by cyclic sweeps between -0.2 V and +0.6 V unless otherwise stated. *o*-phenylenediamine was electrodeposited by 100 cyclic sweeps between 0 V and +0.9 V (vs Ag/AgCl) initially and between 0 V and +0.8 V in later work. Aniline was electrodeposited by 20 (or until the voltammograms matched for each electrode) cyclic sweeps between -0.2 V and +0.8 V (vs Ag/AgCl) and by finally running a linear sweep from -0.2 V to +0.8 V (vs Ag/AgCl). This ensured conversion of aniline to its emeraldine form (green).

3.6 Sonication

A custom made sonic tank with internal dimensions of 750 x 750 x 600mm andworking volume 750 x 750 x 500 mm (Ultrawave Ltd., Cardiff, UK). Sonochemical ablation of polymer coated electrodes was performed using a number of different parameters. The energy at which the sonication tank operates (total output 25 kW) determines the intensity of sonochemical ablation applied on the sensors. Normally the energy level was between 50 % and 100% and time of ablation did not exceed 60 seconds. The electrode sheets were fixed in the middle of the tank and sonicated for the chosen time.

3.7 Sensor fabrication

30 µl volume of biotin-sulfo-NHS (Sigma-Aldrich, Gillingham, Dorset, UK) at 10 mg ml^{-1} was placed on the polymer coated working electrode surface for 24 hours. After 24 hours, the sensors were rinsed with deionised water and 30 µl of neutravidin at 10 µg ml^{-1} placed on the working electrode for 1 hour. After rinsing biotinylated antibody was added at a concentration of 1 mg/ml. Finally, non-specific interactions were blocked by 10^{-6} M bovine serum albumin; the sensors were then left in PBS buffer overnight prior to use.

3.8 AC impedance

Antigen solutions for ac impedance were prepared by diluting the required concentration of antigen in 30ml of PBS pH 7.4 unless otherwise stated. The sensors were first interrogated without antigen addition. Following this each sensor was exposed to the required antigen concentration for 30 minutes, rinsed well with deionised water and then subjected to impedance interrogation.

Impedance parameters:
Previous work within our group established the optimum test settings for the type of work carried out towards sensor development. A frequency range from 10000Hz to 1Hz (5mV a.c.) was used and 100 readings were taken per test. As discussed in section 5.2 the faradaic charge transfer process dominates the impedance of the system at the lower frequency range between 1 Hz and 1.5 Hz, for this reason the impedance values obtained at 1 Hz where further used to construct calibration curves. The working electrode surface area (for carbon sensors) was 0.2178cm^2. Potassium hexacyanoferrate and potassium ferricyanide were purchased from Sigma-Aldrich (Gillingham, Dorset, UK) to prepare a 10 mM ferri/ferrocyanide ratio 1:1 in PBS pH 7.4 buffer to be used as a redox couple for impedimetric measurements.

3.9 Antibody purification and concentration

When monoclonal antibodies where provided in whole antiserum, these were purified using a 5 ml protein G-column (Pharmacia). The process involved the collection of two eluents the first of which samples contained unwanted substances while the second contained the polyclonal or monoclonal IgG sample to be further used for sensor fabrication. The IgG fraction was eluted using glicine buffer (pH 2.7) and dialyzed overnight. Samples were then aliquoted and stored at -20 °C or subjected to biotinylation. This work was carried out by partner 1, University of Leeds.

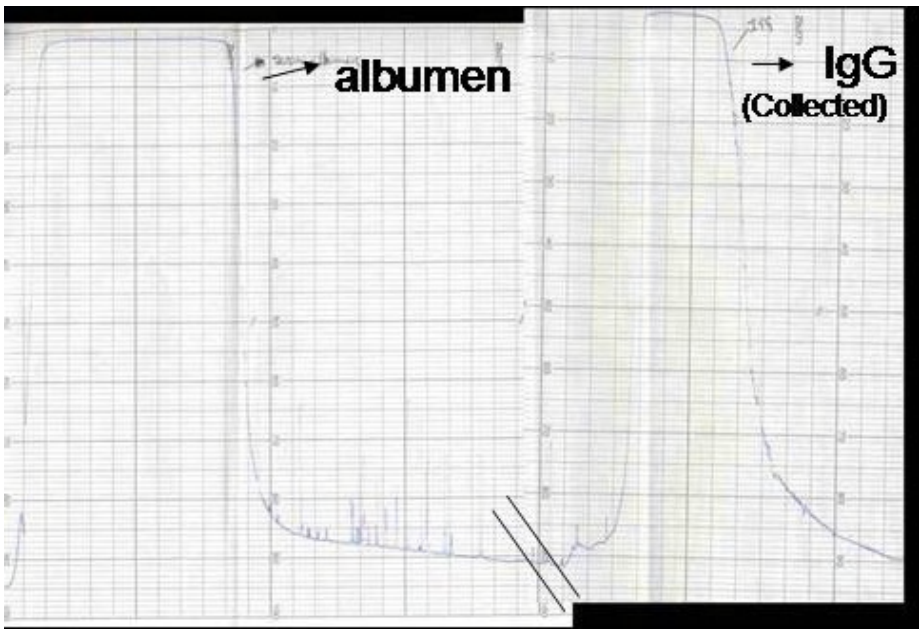

Figure 3.5: Absorbance trace recorded at 280 nm from a sample of rabbit sera following IgG separation, showing both absorbance peaks of sera albumen, and IgG fraction.

For antibody concentration, a Centriprep centrifugal filter unit fitted with an Ultracel YM-30 membrane containing glycerol, to prevent drying, was used. This procedure also ensured the removal of sodium azide from the antibody solution. The unit was purchased by Millipore, Hertfordshire, UK. The procedure involved three subsequent centrifugations in a cold room (4ºC), each for 20 minutes at 30,000 rpm.

Section 2

Results and discussion

Introduction

One of the aims of this research project is to develop fast and reliable immunosensors targeting a range of analytes including, for example, fluoroquinolone antibiotics, digoxin and prostate specific antigen. The experimental procedures include polymer deposition on gold and carbon electrodes, antibody immobilisation on transducer surfaces and impedimetric interrogation of the fabricated sensors.

A set of experimental procedures were undertaken in order to fabricate and subsequently interrogate impedimetric immunosensors using different antibody/antigen pairs. Several conditions affect the development of appropriate, fast and reliable immunosensors, including the polymer used, the electrodeposition conditions, antibody attachment to the polymer and ultimately the interrogation method and parameters. The conditions of polymer electrodeposition and electrode interrogation using voltammetry were extensively evaluated in order to obtain the optimum set of parameters for highly reproducible and reliable sensors.

Chapter 4

Characterisation of gold and platinum electrodes and electrochemical methods

Introduction

One of the first objectives was to apply protocols previously developed by our group to the newly acquired sensors specific to ELISHA. Initially our work involved the electrodeposition of *o*-phenylenediamine and aniline on electrodes provided by the Tyndell National Institute (Ireland), and subsequent sonochemical ablation for the planar gold electrodes. The electrodeposition conditions had previously been used with success by our group on different carbon electrode formats (Law *et al*., 2000; Barton *et al*., 2004). The choice of electrodeposition by means of cyclic voltammetry was made so that the oxidation and reduction peaks indicating the deposition of each polymer layer would be clearly seen and hence the process could be followed. The objective was therefore to determine whether these predetermined conditions could be successfully applied to gold and platinum planar electrodes and microelectrodes as described in the materials and methods chapter.

4.2 *O*-phenylenediamine electrodeposition

The insulating nature of *o*-phenylenediamine (Law & Higson, 2005) is clearly seen in figure 4.1 which displays cycles 1, 5 and 100 of a one hundred cycle sequence of voltammetric deposition of *o*-phenylenediamine between 0 mV and 900 mV. In order to confirm the electroconductivity of each gold electrode, potential sweeps were also performed before and after polymerisation, in the presence of 1mM ferrocenecarboxylic acid (*FCA*). Cyclic voltammetry with added FCA was performed using different potential sweeps, however, it was finally decided to set the potential limits to -0.2 and + 0.6 V in order to minimise the compromising of results due to the double layer charging effects. FCA has a Nernstian (reversible) behaviour. As expected in typical cyclic voltammograms an anodic peak is seen at oxidising potentials when the reduced FCA is converted to ferrocinium ion species (Fernandez & Carrero, 2005). When the potential sweep is reversed ferricinium is converted to FCA thus causing a cathodic peak of similar magnitude to the previously observed anodic peak.

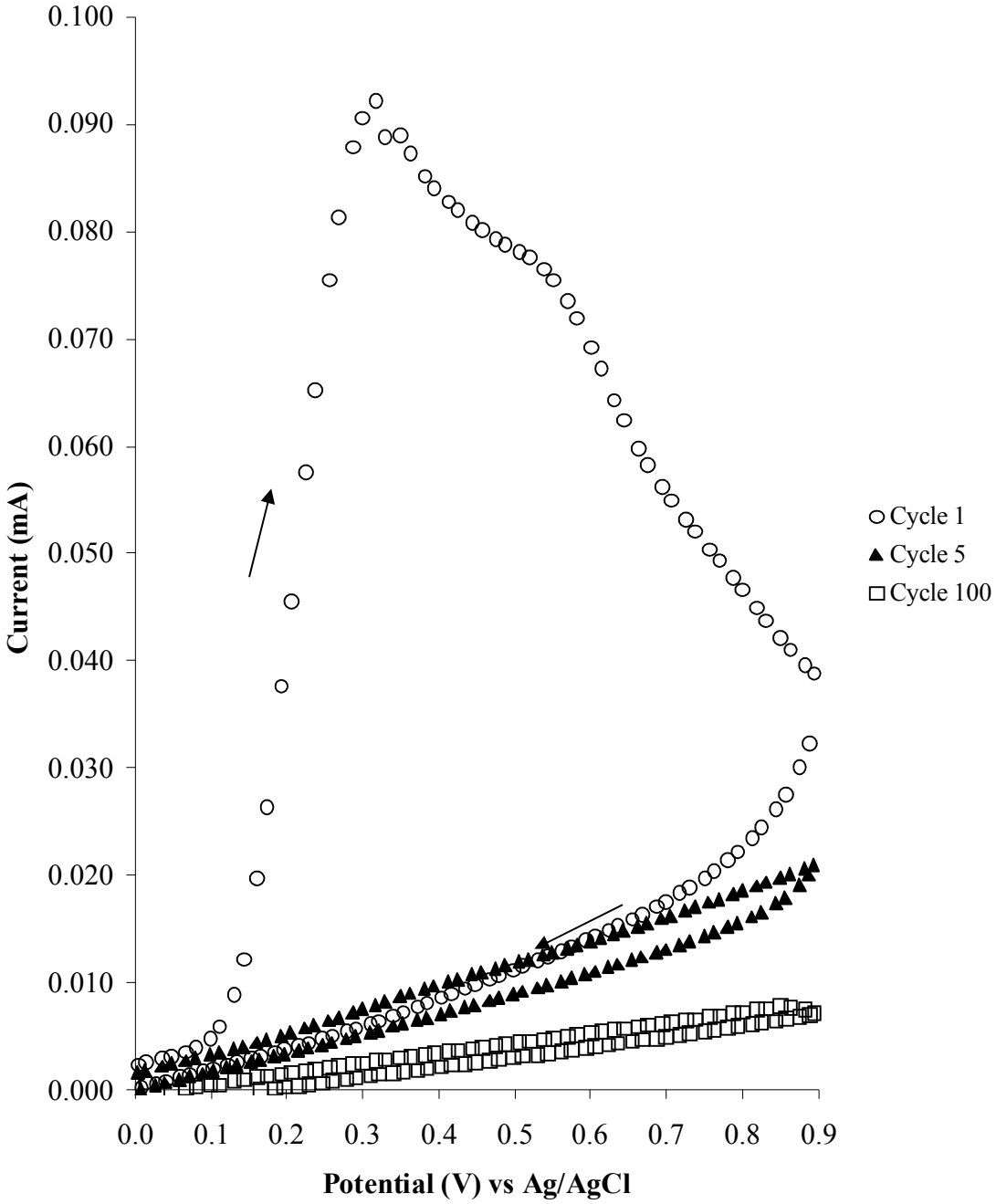

Figure 4.1: *O*-phenylenediamine electrodeposition (-0.2 to 0.9 V) on a P4 Au electrode showing cycles 1, 5 and 100.

As clearly seen in figure 4.1, the predetermined *o*-phenylenedimaine electrodeposition conditions were successfully used for gold planar electrodes, which had previously been tested for their electroconductivity by being imposed to cyclic voltammetric sweeps. As expected during the first electrodeposition cycle, a large peak was observed with the current reaching the range of 90 μA. Subsequent cycles cause the

electrode surface to become less conductive until at 100 cycles of polymerisation a baseline current is achieved as a result of electrode insulation. As Pritchard *et al*., (2004) report, the resulting insulating film has an approximate thickness of 50 nm. Additionally, it should be noted that *o*-phenylenediamine films are colourless when at a reduced form but red when oxidised (Martinusz *et al*., 1994). Martinusz *et al*., (1994) have made some important observations regarding the electrochemical polymerisation of *o*-phenylenediamine. The authors suggest that *o*-phenynelenediamine polymerisation is not autocatalytic and occurs at low potentials during the reverse cyclic voltammetry scan. Additionally, film formation can be explained by two electron transfer processes which include the redox reaction of 1, 4-diazine groups, followed by a protonation-deprotonation reaction and possibly a dimerisation reaction.

Figure 4.2 depicts near perfect insulation that was achieved using the discussed *o*-phenylenediamine electrodeposition conditions.

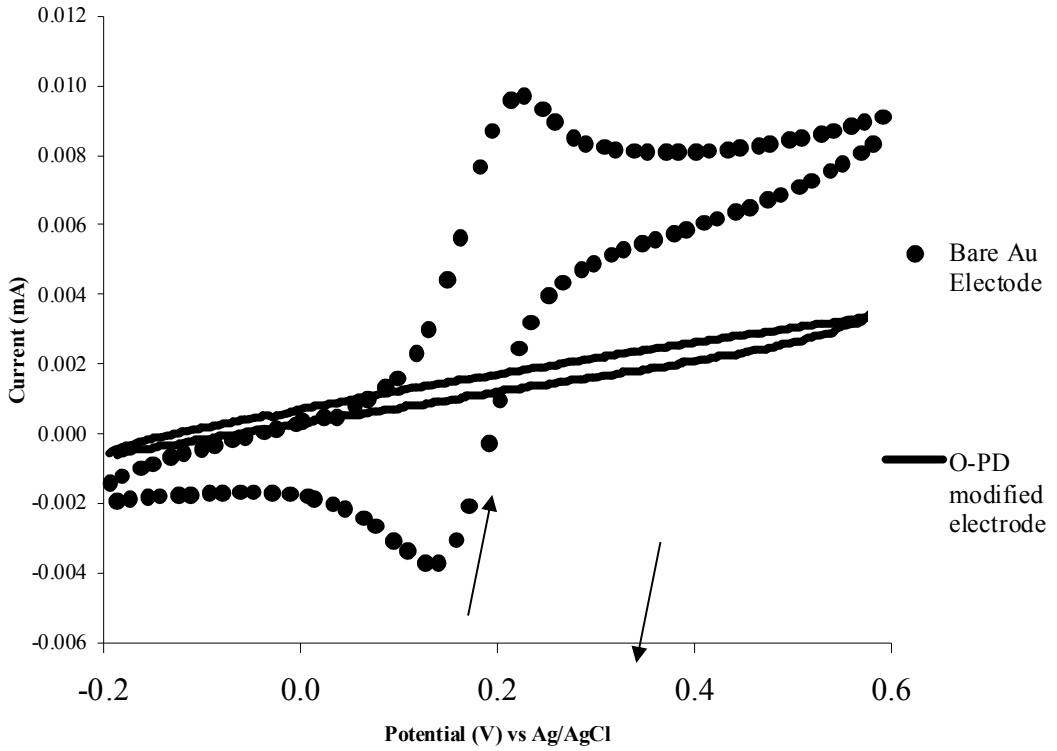

Figure 4.2: Cyclic voltammetric interrogation (-0.2 to 0.6 V) of a P4 Au electrode before electrodeposition and after electrodeposition of o-phenylenediamine (O-PD) (100 cycles).

The peak separation for the unmodified electrode does not resemble the expected 59 mV value obtained for an ideal diffusion controlled reaction, but rather a larger peak separation of 87 mV. The effects of electrode fabrication, solution constituents and environmental conditions do indeed affect the kinetics of the occurring electrochemical reactions, however, this observation in conjunction with others gave rise to subsequent investigations that will be discussed in the following sections.

4.3 Aniline electrodeposition

In three electrode cells (working-counter-Reference), similar to the ones being used in our work, monomers of the chosen conductive polymers undergo reactions that eventually cause them to become insoluble and precipitate on the electrode surface. As Gardner and Bartlett, (1995) report the movement of counter-ion into and out of the polymer film results in visible current peaks during cyclic voltammetric sweeps. It is readily understood within the literature that the shape of the resulting voltammograms and peak currents will be determined by the individual monomer used and the electrode surface (gold, platinum, carbon).

In this work, 0.2 M poly-aniline pH 1 was deposited onto P4 electrode surfaces by 25 continuous potential sweeps between -0.2 V and +0.8 V. Previous works have indicated that optimal conditions for polyanaliline deposition include a potential between -0.2 V and 0.7 to 1.2 V along with acidic solution pH. HCl is very often used for the successful electropolymerisation of aniline (Genies *et al*., 1989). The buffer recipe used to dissolve aniline is described in Materials and Methods, section 3.1 and ensured electroconductivity of the final polymer as polyaniline is not electroconductive if prepared at neutral or basic pH (Pritchard *et al.,* 2004). The pH range used varied from pH 3.7 down to pH 1 and it was found that electroconductive aniline was best when obtained at pH 1. The oxidised form of a polyaniline film has a blue-green colour and is normally referred to as emeraldine. It should be noted that the surface area of the deposited film increases as a power of the volume. Genies *et al*., 1989 have extensively reviewed the properties of aniline and the effects of different deposition methods on the properties of the resulting film. It should initially be noted that the observed peaks during cyclic voltammetric work vary greatly depending upon the electrode material used e.g. gold, carbon or platinum. The

reaction rate of electrodeposition has been shown to be proportional to the temperature between 0°C and 60°C and thus environmental conditions along with solution temperature can also affect the deposition process hence the shape of the voltammograms.

There has within the literature been some debate between different research groups as to the number of electrons required for aniline polymerisation. It is generally accepted that two electrons are required along with a number of supplementary electrons necessary for polymer oxidation, however, the mechanism of polymerisation has not yet been fully understood. Acidic conditions are required for PANI deposition. However, the rate of deposition depends on the concentration of anions and not the pH. It has been suggested that aniline oxidation is catalysed by the fully oxidised form of polyaniline, pernigraniline, and that the reaction is self catalysing. An intermediate was shown to arise through aniline oxidation, *p*-aminophenylamine (PADPA), which has attracted extensive research itself for the possibility of novel polymer discovery.

Polymerisation of the aniline polymer gives rise to five distinct oxidation states. Given the generic structure depicted in figure 4.3 these five oxidation states can be analysed.

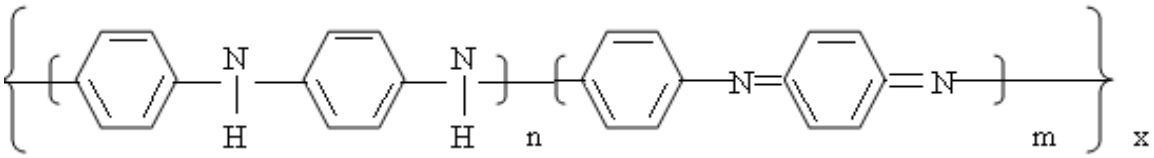

Figure 4.3: Generic structure of polyaniline.

With x equal to half the degree of polymerisation:

1) Leucoemeraldine n=1, m=0 is the fully reduced state and is easily oxidised.
2) Pernigraniline with n=0 and m=1 (imine groups instead of amine) is the fully oxididised state but can be easily degraded.
3) Emeraldine with n=m=0.5 is either neutral or partially reduced or oxidised and is the most stable form.

Figures 4.4 and 4.5 display the voltammograms obtained from electrochemical deposition of aniline on P4 Au electrodes. Figure 4.4 depicts electrodeposition of aniline under non-conductive conditions (buffer pH 3.7), while figure 4.5 depicts the electrodeposition of the polymer under strongly acidic conditions (buffer pH 1).

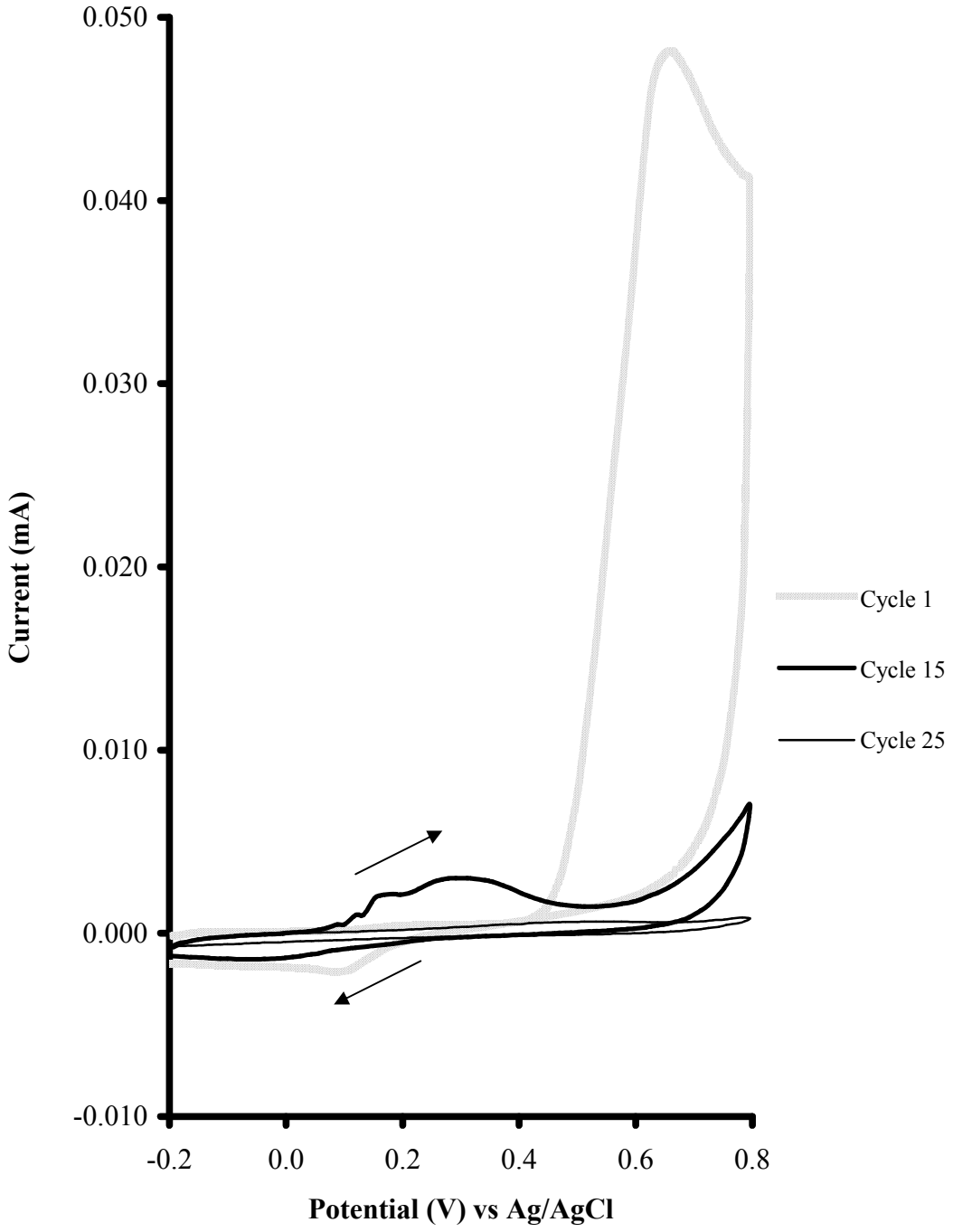

Figure 4.4: Electrochemical deposition (-0.2 V to 0.8 V) of aniline on a P3 Au electrode under non-conductive conditions (pH 2.8).

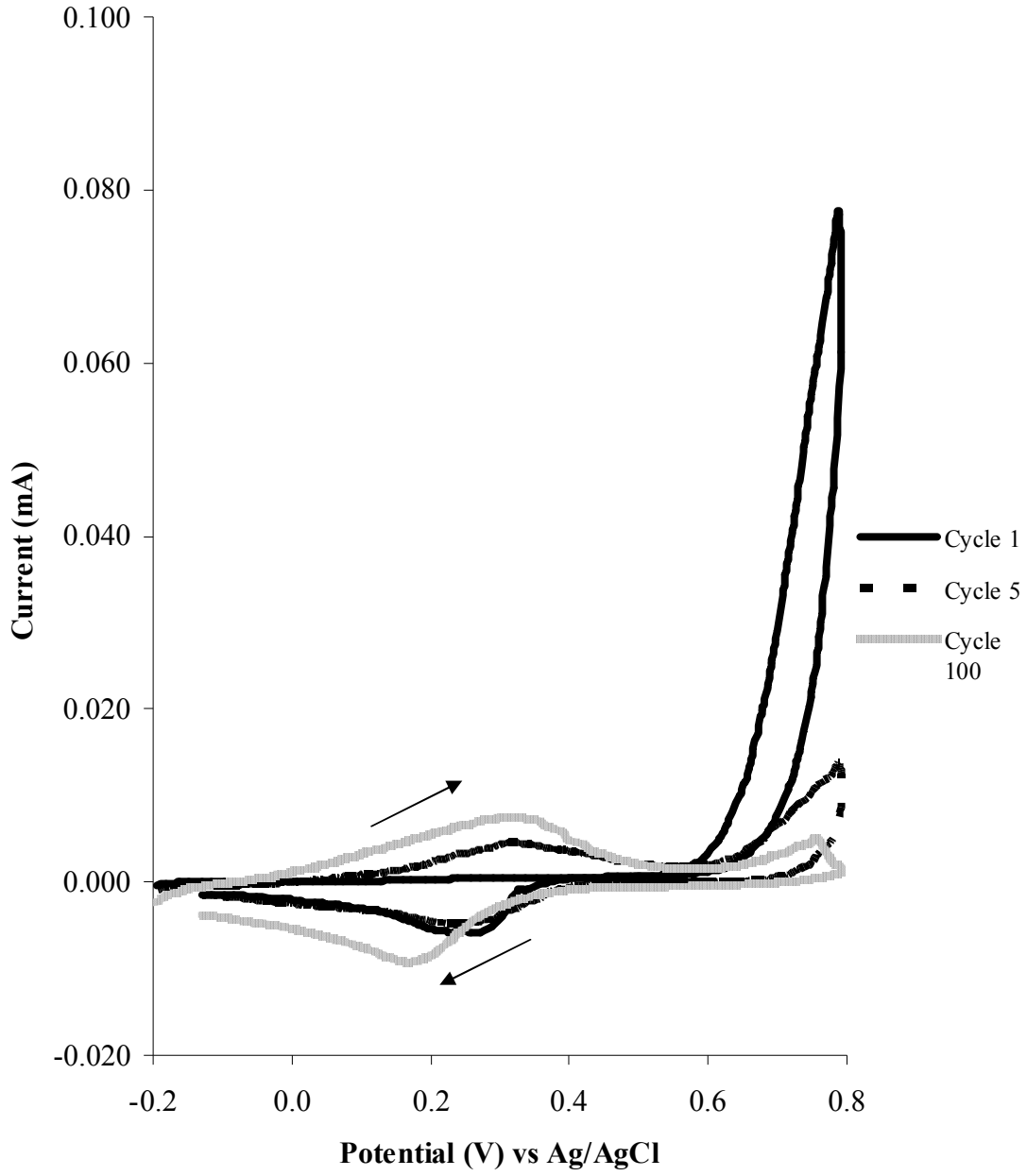

Figure 4.5: Cycles 1, 5 and 100 of aniline pH 1 electrodeposition on P4 electrodes under conductive conditions (pH 1).

It can be seen that with every deposition cycle, the peak current observed increases (figure 4.5). This is due to the increase of the conductive surface area from accumulation of polyaniline layers on the electrode surface with each potential sweep. It should be noted here that gold and most metals are superior conductors to any of the known conductive polymers. While initially the conductivity of coated electrodes is seen to increase, it must be understood that a high number of consecutive potential sweeps (e.g. 100) will become a limiting factor and the cumulative conductivity through the polymer will start decreasing. This can be explained as the polymer film becomes thicker with each sweep. In agreement with results obtained by Sasaki *et al*., (1986), our observations from aniline electrodeposition on P3 electrodes indicate an initial peak which is non reversible. This peak that occurs only in the first cyclic sweep corresponds to the diffusion limited oxidation of the monomer and partial deposition.

Cyclic sweeps using an FCA doped solution of PBS buffer (pH 7.4) was used to investigate the electroconductivity of each P4 electrode after polyaniline deposition. Figure 4.6 compares the voltammograms before and following polymerisation with both 200 mM aniline (25 cycles) and 5 mM *o*-phenylenediamine (100 cycles).

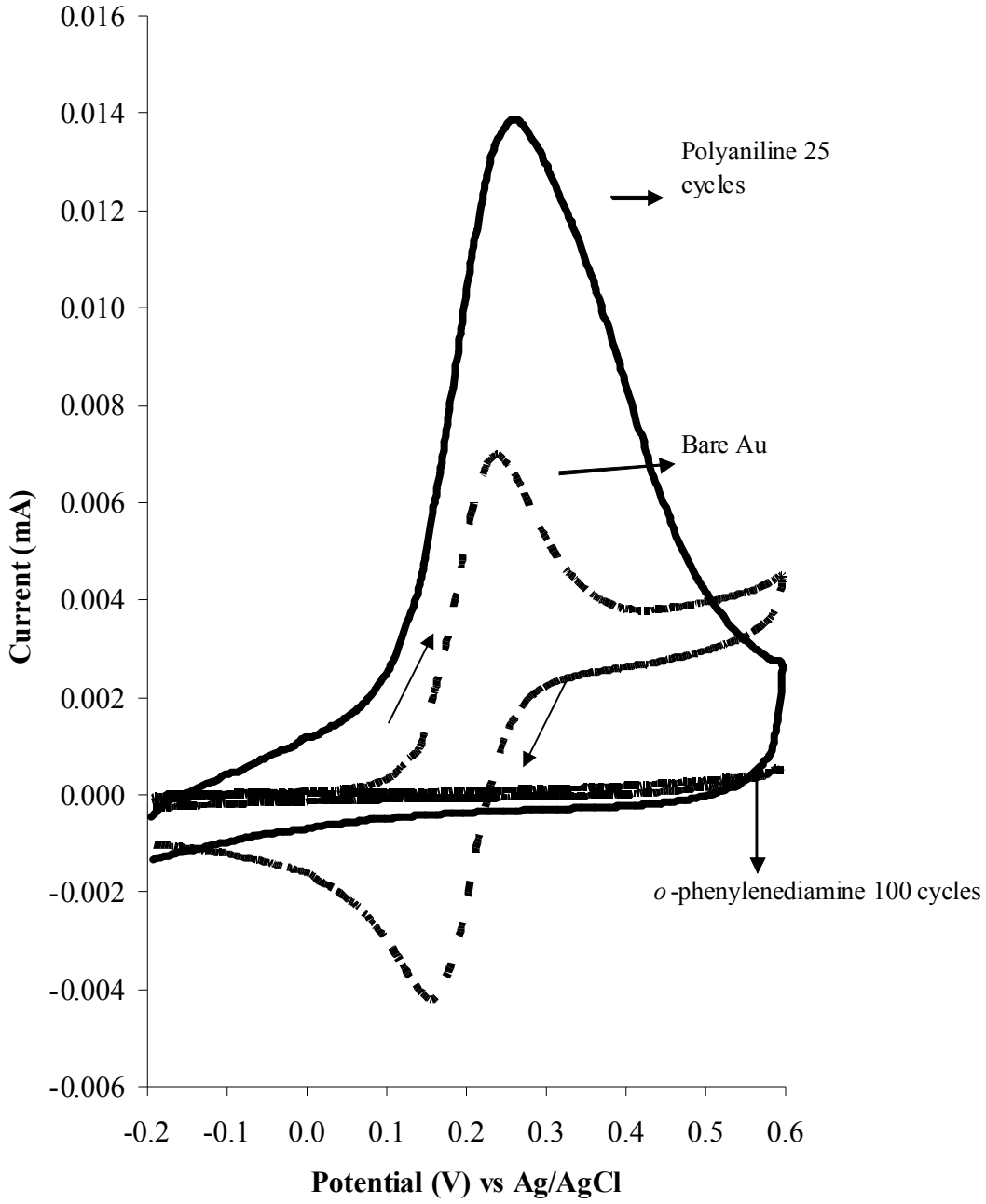

Figure 4.6: 1 mM FCA before deposition and after deposition of aniline and *o*-phenylenediamine, potential sweep between -0.2 and +0.6 V.

As intended and expected, the polyaniline modified electrode displays the highest current peaks in comparison to the bare electrode and the *o*-phenylenediamine coated

electrode. Having made these observations, we verified that the polymer deposition protocols previously developed with our group could be successfully applied to work involved in the ELISHA project.

4.4 Sonochemical ablation

Sonochemical ablation of the polymer coated electrodes was performed following the electrodeposition of the insulating polydiaminobenzene film. Either single electrodes or electrode coated sheets (depending on the nature of the experiment) where immersed in the sonication tank, which was filled with water, and fixed at a set location. The procedure has been previously described by our group (Barton *et a*l., 2004). It was observed that *o*-phenylenediamine results in a defect-free film of approximately 30-40 nm in thickness using the described electrodeposition conditions. An extensive set of different parameters with regards to sonication power level, time of ablation and electrode positioning within the tank, were tested in order to determine the optimum conditions for microelectrode array construction.

The sonochemical ablation of polymer coated electrodes for the formation of microelectrodes has previously been described by a number of papers within our group (Myler *et al*., 2004; Barton *et al*., 2004, Grant *et al*., 2005). As it is suggested by Barton *et al*., (2004) ultrasound passing through water (or another solvent) creates thermal agitation alongside localised hotspots, resulting in the creation of superheated vapour bubbles. At standard temperature conditions (25^{o}C) these bubbles can be cooled by the solvent and implode into high velocity microjets, rendering them capable of shattering a range of solids. This mechanism was exploited in this work towards the creation of microelectrode arrays on a diaminobenzene coated electrode. Upon implosion, the bubbles cause cavities on the deposited film surface thus exposing the underlying conductive surface. Cavity distribution is random due to the fact that sonochemical ablation is a chaotic process. The resulting pores range in diameter from a few hundred nm to 3 μm. The smaller cavities are thought to act as nucleation sites for the creation of more bubbles thus aiding their own expansion as more microjets can reach the polymer surface (Barton *et al*., 2004).

It should be noted that the largest cavities of a 3 μm diameter no longer act as nucleation sites. It is also noted that some pores may initially form close to each other and upon further expansion unite forming a 'dumb-bell cavity' as depicted in figure 4.7. Due to the presence of two different sizes of electrodes on the surface, these are called bi-modal. Barton *et al*., (2004) report that sigmoidal voltammograms were observed upon cyclic sweep testing, however, the diffusion layer effects present a major interfering factor. Diffusion layer charging effects are typically much smaller in the case of microelectrode arrays over normal size electrodes, however, it is suggested that the large pore density on the electrode surface may cumulatively give rise to diffusion layer charging. Barton *et al.,* (2004) continue by describing the electrochemical deposition of GOx doped aniline for the formation of mushroom-like protrusions on the electrode surface and subsequent amperometric and impedimetric analysis to determine sensor responses to a range of glucose concentrations.

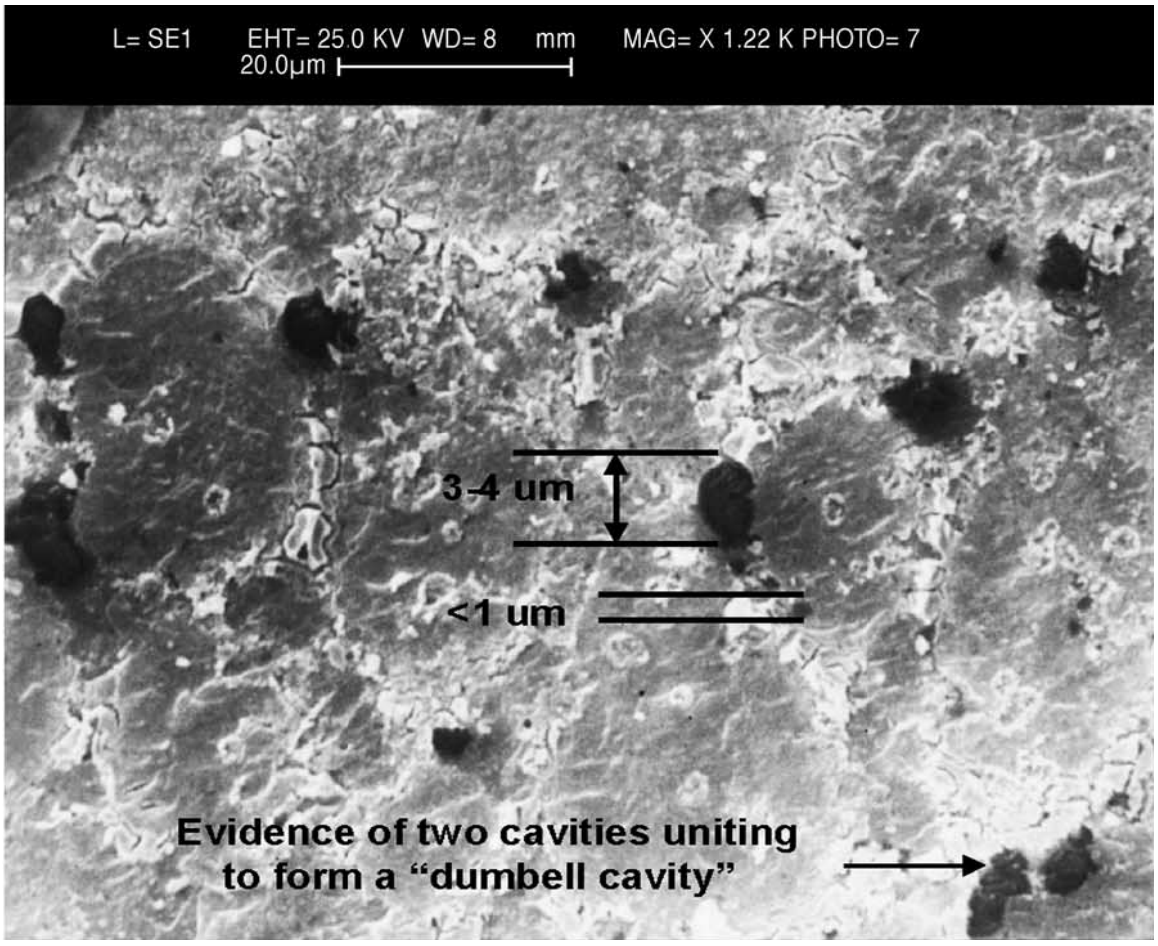

Figure 4.7: Formation of cavities following sonochemical ablation of *o*-phenylenediamine covered sensors.

Figure 4.8 below depicts the voltammetric responses of bare, insulated and finally sonochemically ablated gold electrodes, as described by Barton *et al*., (2004).

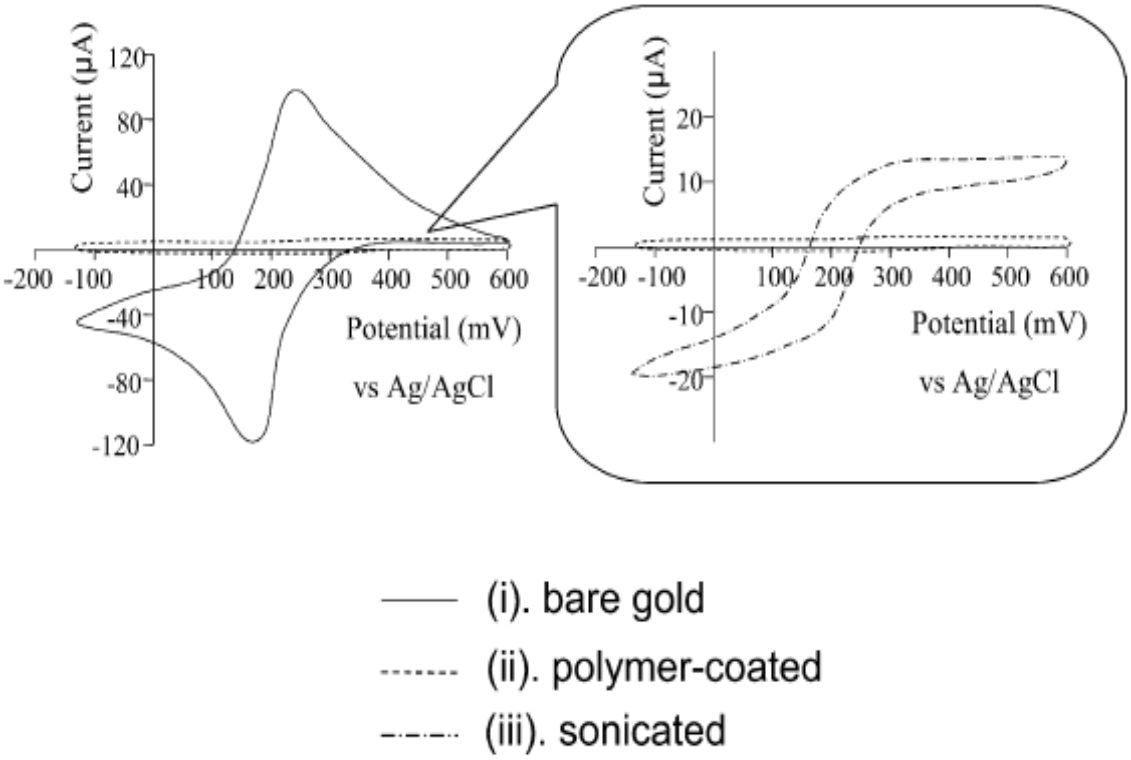

Figure 4.8: Cyclic voltammetry testing for a bare, an insulating polymer coated and a sonochemically ablated electrode.

The same microelectrode array fabrication procedures were followed in our work, however reproducibility issues indicated the necessity for further testing of the project specific electrodes provided by Tyndall National Institute (Ireland). Having evaluated a set of different conditions, it was found that usage of very high acoustic power stripped off the insulating polymer and damaged the Au surface; a similar effect was also seen to occur if the time allowed for sonochemical ablation was too great. After some empirical experiments it was decided to use 50% power (maximum operational frequency of 20 kW) for times between 15 seconds and 60 seconds. In order to test the formation of sonication cavities, the electrodes were subsequently subjected to cyclic voltammetry using 1 mM FCA as described in previous experimentation within the project. Figure 4.9 displays the results obtained following sonochemical ablation of polymer coated electrodes.

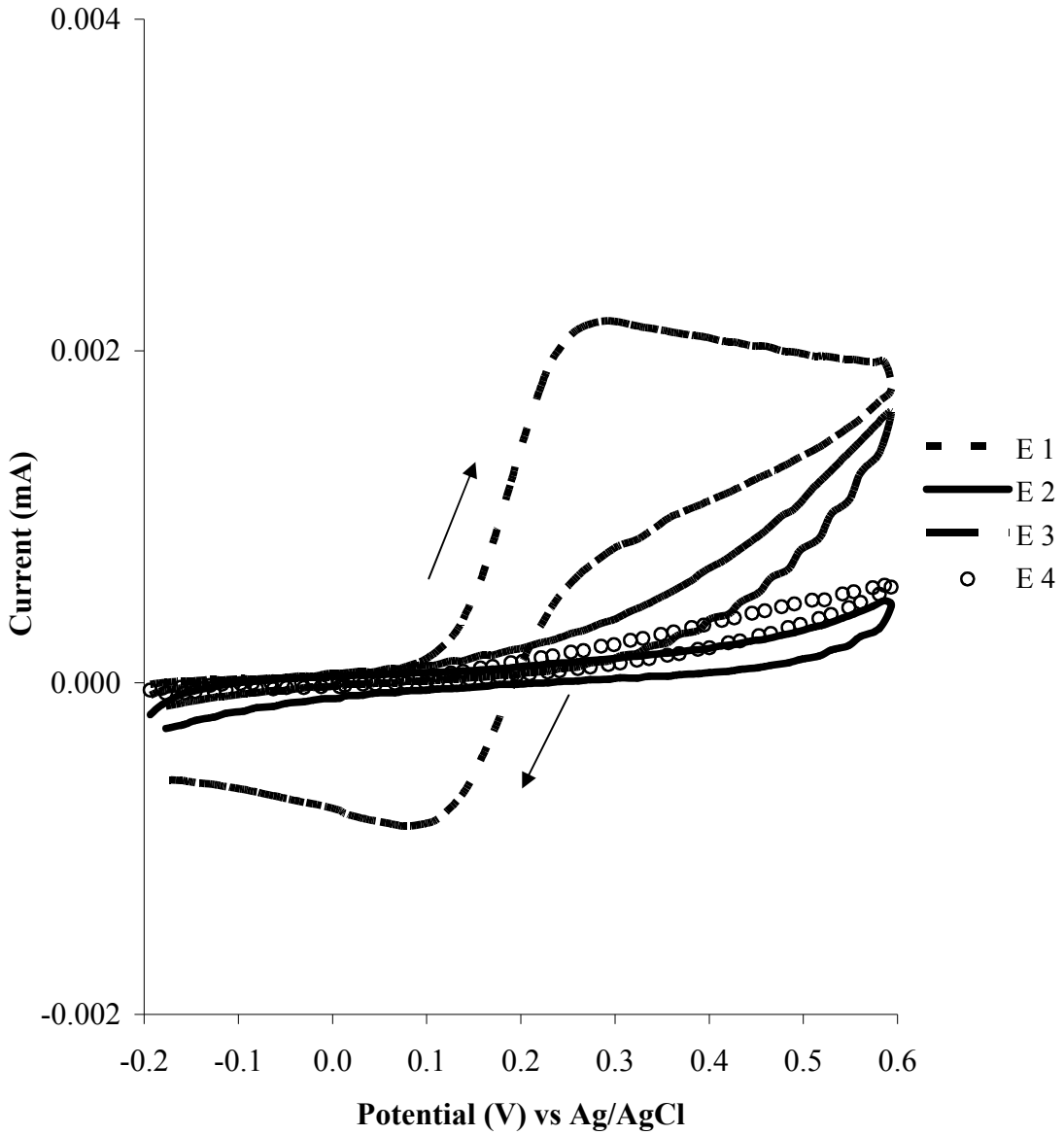

Figure 4.9: Cyclic voltammetric sweeps of sonochemically ablated electrodes by rotation, at 50% power for 30 seconds in FCA.

While electrode 1 (figure 4.9) displays almost perfect microelectrode behaviour (almost sigmoidal shape of the voltammogram), the rest electrodes seem to have become insulated. Some reasons that may result in irreproducibility are discussed here. As already mentioned sonochemical ablation does not allow for perfectly even distribution of energy i.e. the cavitation bubbles are not distributed evenly within the bath area. Additionally, the project specific electrodes are very small in size and this

minimises the averaging effect afforded by the use of larger electrodes. As discussed earlier high power or sonochemical ablation for an extended time may damage the polymer and the electrode surface, however, since one electrode was not damaged it was realised that the problem might be associated with the electrode fabrication process.

4.5 FCA tests on non-modified electrodes

In order to examine whether there was a fault in the electrode fabrication process, a set of voltammetric tests was performed on all types of project specific electrodes (including platinum) to ensure that there was reproducibility among electrodes when the conductive surfaces were not coated. The behaviour of each electrode was to be tested in solutions containing 1 mM ferrocenecarboxylic acid (FCA). It should be noted that those tests were performed at various scan rates (10 mV s^{-1}, 25 mV s^{-1} and 50 mV s^{-1}). The scan rate affects the shape of a resulting voltammogram due to the presence of the diffusion layer. At a slow scan rate the diffusion layer grows by a substantial amount thus the flux of electrons reaching the electrode surface is limited hence the passing current observed on a given voltammogram will be low. At increasing scan rates, the measurements are recorded faster, thus the observed current will be higher. Alternative scan rates were used in this work in order to extensively analyse the reproducibility in the voltammetric measurements among the project specific microelectrodes. The chosen potential range was from -200 mV to 600 mV. Where the format used was that of dual electrodes (e.g. P4 and P5), the second electrode was connected as a counter. A typical voltammetric sweep is depicted in figure 4.10.

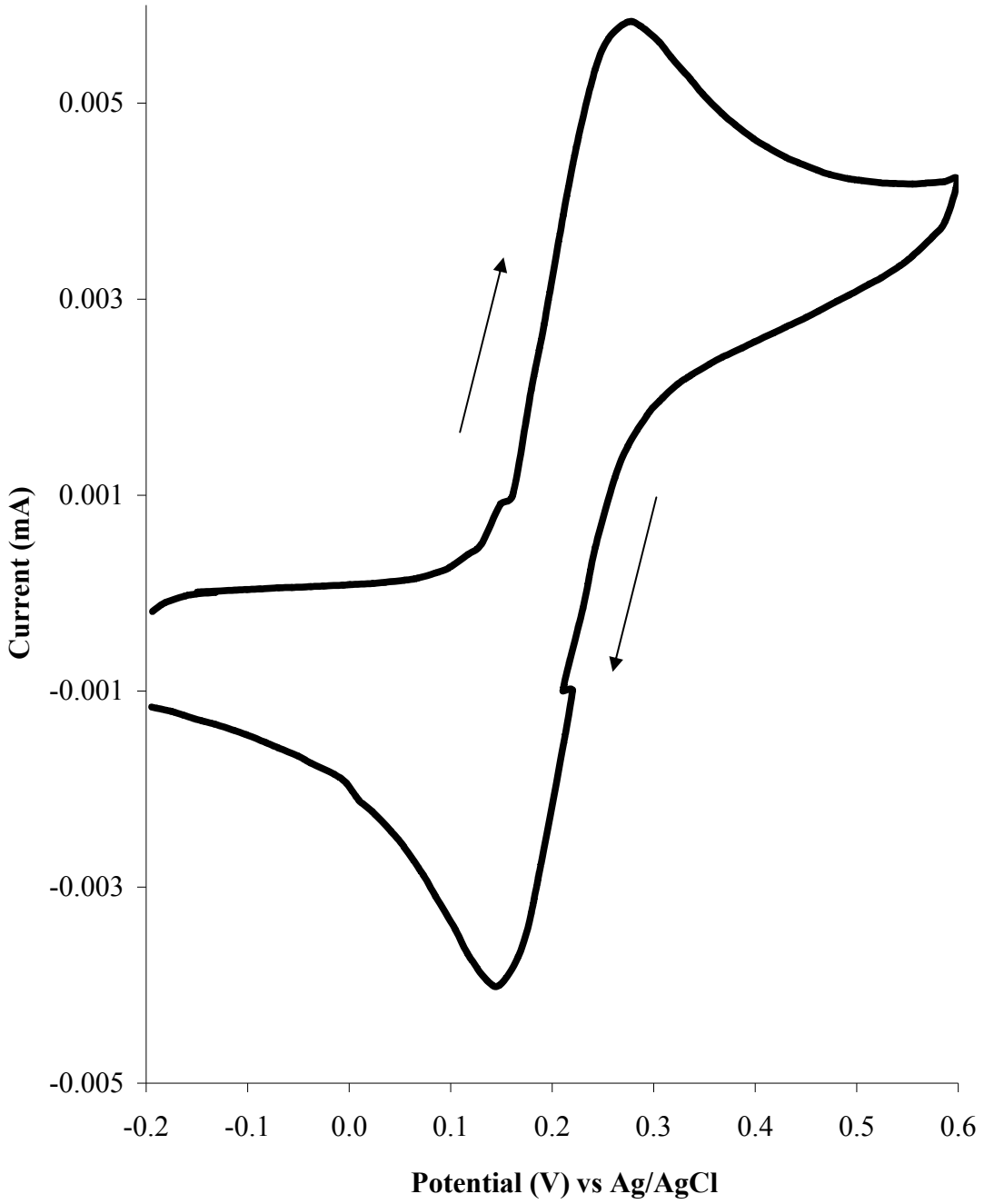

Figure 4.10: Cyclic sweep between -0.2 and 0.6 V for a bare P4 electrode in FCA at 50 mV s^{-1}.

The voltammogram in figure 4.10 displays a cyclic sweep of 1 mM FCA between the potential range of -0.2 V and 0.6 V at a scan rate of 50 mV/s. The two expected peaks occur during the anodic scan at 274 mV with an observed current of 5.82 μA and for the cathodic scan at 148 mV with an observed current of 4 μA. The distance between the peaks is 126 mV, more than double of the 59 mV typically expected peak separation distance. Additionally, while well defined, the peaks were not similar in magnitude to each other suggesting either the existence of a non completely reversible redox reaction or a disturbance during the scans. In order to sufficiently test the reason for this, the potential range for the cyclic sweep was increased between -1 V and 1 V as seen in figure 4.11.

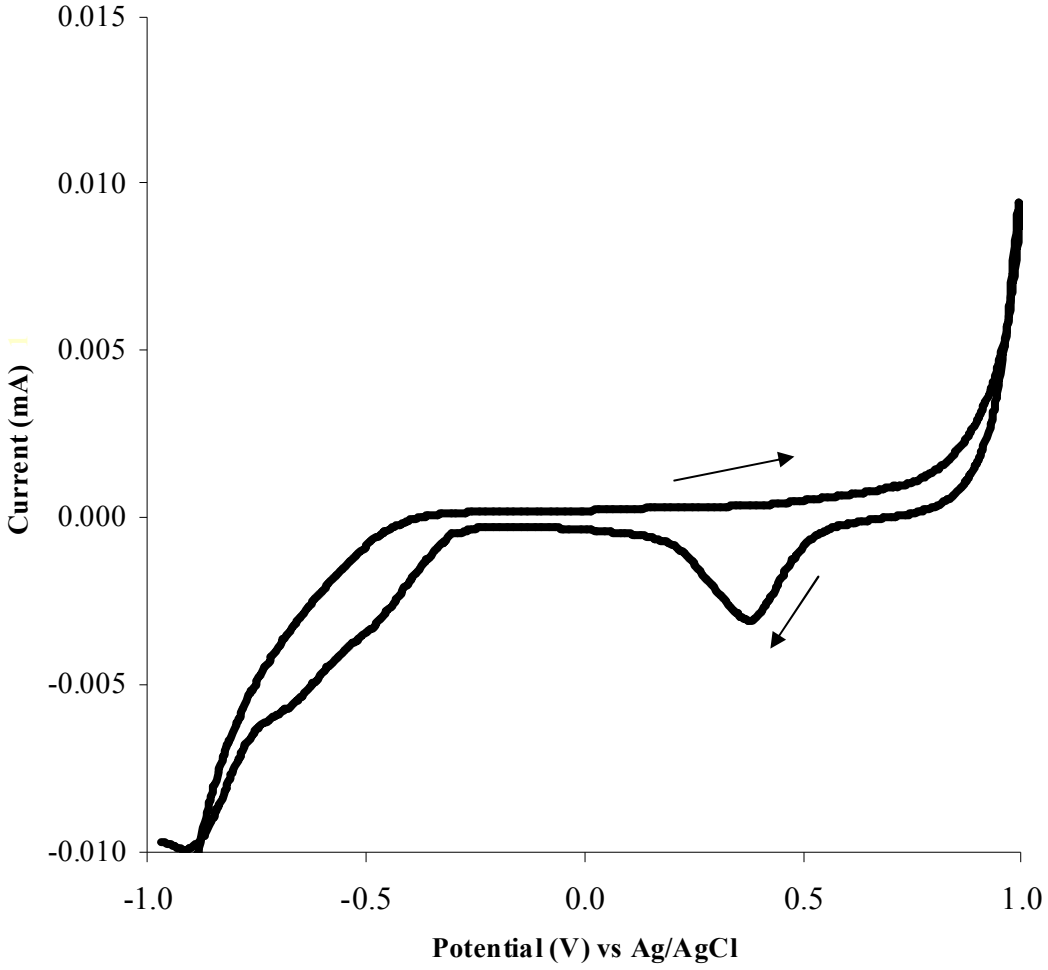

Figure 4.11: Cyclic sweep between -1 V and 1 V for a bare P4 gold electrode in plain PBS at 50 mV s^{-1}.

Fresh solutions were prepared while the electrodes were only interrogated by voltammetric scans in plain PBS buffer. The absence of a redox couple allowed measurements to be made purely on the characteristics of the electrode itself. The voltammogram in figure 4.11 displays one cycle of a cyclic sweep on a bare gold electrode (P3 and P4) between -1000 mV and 1000 mV. The cathodic peak occurs at 375 mV with an observed current of 3.09 μA. The appearance of a reduction peak under these conditions leads to the conclusion that a pollutant may be present in either the solution used or the electrode materials that interferes with the normal oxidation/reduction behaviour of FCA. The P3 and P4 electrodes were subsequently sent to the manufacturer for testing and re-evaluation while our work continued with voltammetric testing of gold and platinum P5 and P10 electrodes. These findings were then compared to the screen-printed carbon three electrode system described by Law & Higson (2005). As expected due to the absence of analyte, the normal oxidation-reduction peaks were not observed while the extra reduction peak was still present when using the P4 electrodes.

In subsequent experiments, the scan rate of voltammetric sweeps was varied between 10 mV s^{-1}, 25 mV s^{-1} and 50 mV s^{-1}. The scan rate affects the shape of a resulting voltammogram due to the presence of the diffusion layer. At a slow scan rate, the diffusion layer grows by a substantial amount, hence the current observed within a given voltammogram will be low. At increasing scan rates, the measurements are recorded faster, thus the observed current will be higher. Alternative scan rates were used in this work in order to extensively analyse the reproducibility in the voltammetric measurements among the project specific microelectrodes. The chosen potential range was from -200 mV to 600 mV. Two characteristic voltammogram of the obtained results can be seen in figure 4.12.

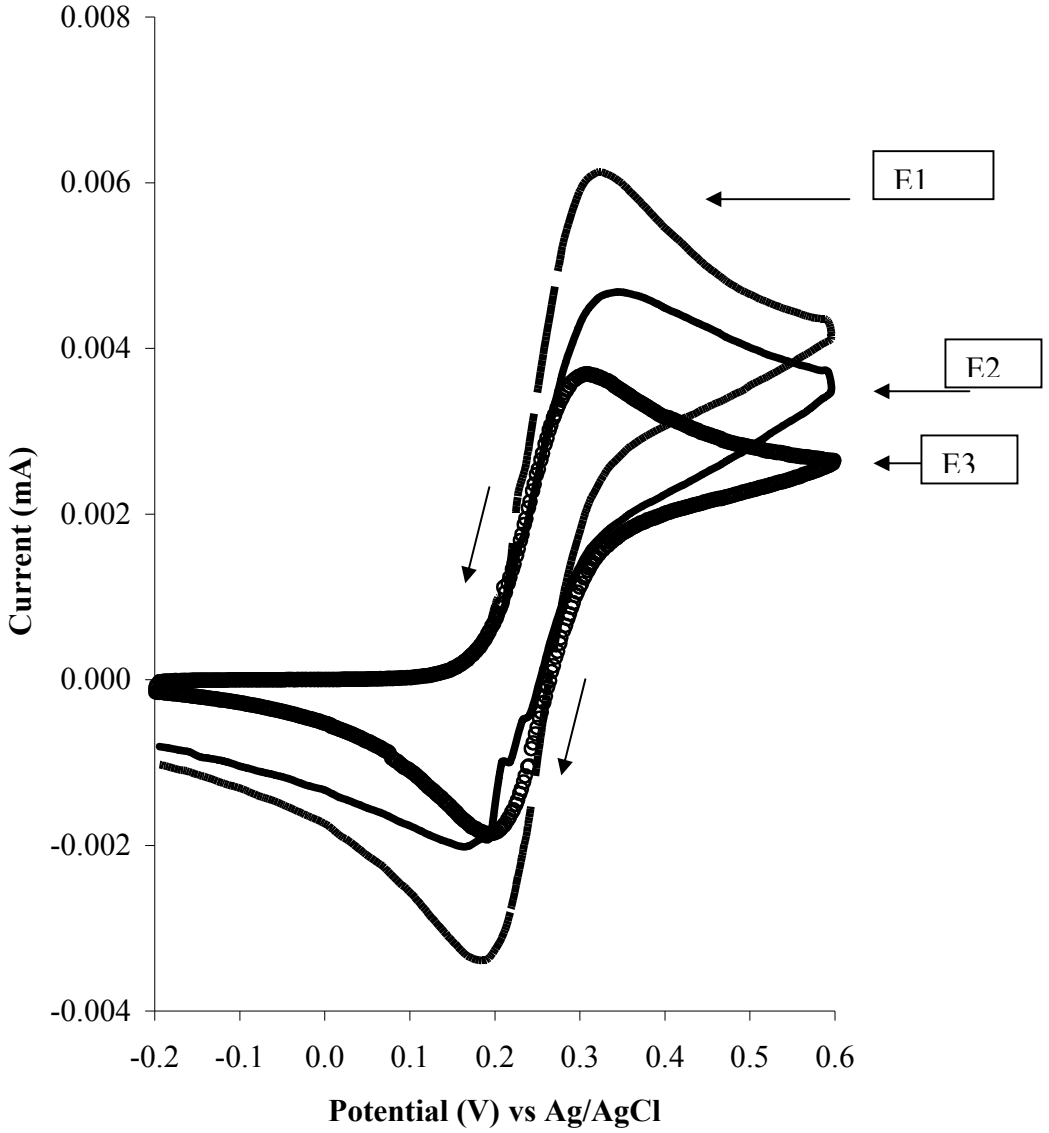

Figure 4.12: Cyclic sweeps between -0.2 V and 0.6 V in 1mM FCA for P10 Au electrodes at different scan rates. E1: 50 mV/s, E2 25 mV/s and E3 10 mV/s.

It was found that all gold electrodes (P3, P4, P5 and P10) displayed highly irreproducible behaviour from one another. Irreproducibility was found for the platinum electrodes; however, it was not as high as that found for the gold electrodes. P5 (intedigitated) and P10 (microarrays) should be expected to behave like microelectrodes due to their design. While typical microelectrode voltammograms were obtained for some gold and most platinum electrodes, the irreproducibility of these voltammograms still was very significant. Cyclic voltammetry is typically not as sensitive a technique as ac impedance. It was expected that small differences between electrodes during cyclic voltammetry would be extremely pronounced if impedimetric experiments were to take place. Figures 4.13 and 4.14 display cyclic voltammograms

from P5 gold and platinum electrodes respectively, in 1 mM FCA at a scan rate of 10 mV s^{-1}.

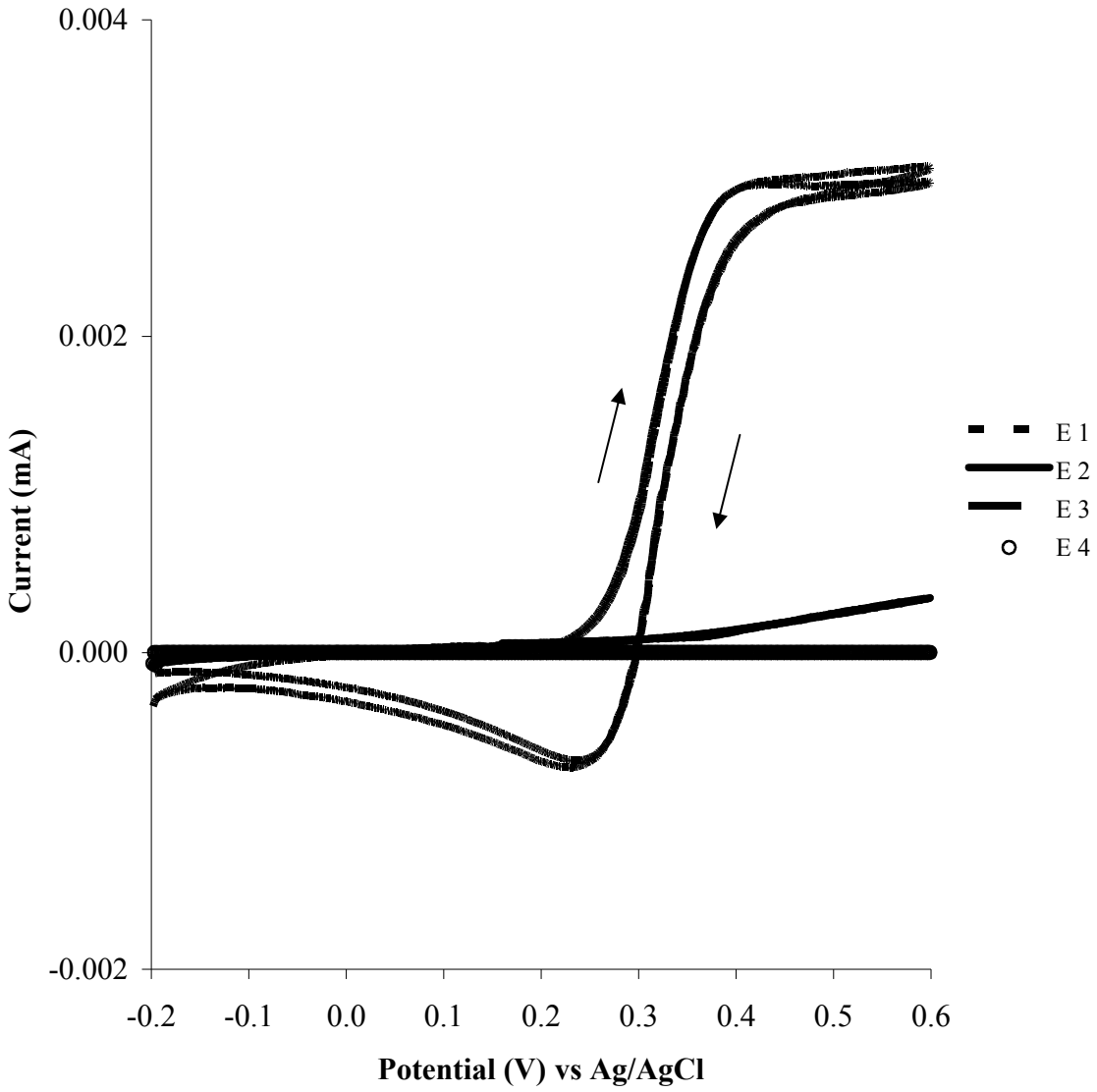

Figure 4.13: Cyclic sweeps between -0.2 V and 0.6 V in 1 mM FCA for 4 different P5 Au electrodes at 10mV s^{-1}.

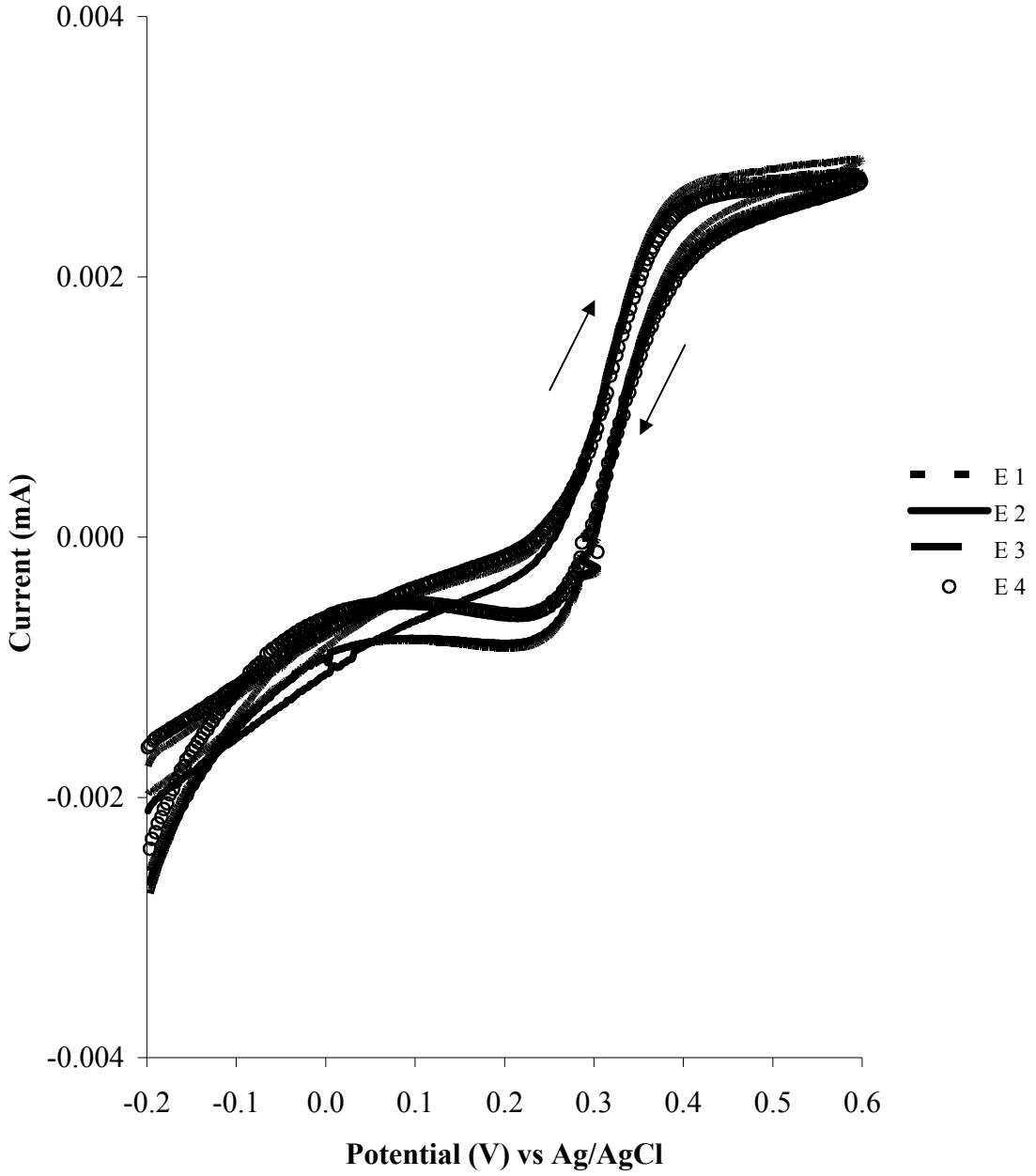

Figure 4.14: Cyclic sweeps between -0.2 V and 0.6 V in 1 mM FCA for 4 different P5 Pt electrodes at 10mV s^{-1}.

4.6 Screen printed carbon electrodes

Due to the unexpected and irreproducible behaviour of the gold and platinum electrodes, it was decided to select alternative designs of electrodes for subsequent impedimetric sensor fabrication. Within our group two sensor formats have been extensively used and characterised as described by Barton *et al*., (2004) and Law &

Higson (2005). The screen printed carbon sensors described by Barton *et al*., (2004) were chosen in this context for all subsequent work within this project. The authors report that the reproducibility of the sensors after extensive trails was found to be 5% variability. Figure 4.15 depicts the electrodeposition of aniline on a planar carbon electrode of this type.

No peaks appear during the first cyclic sweep while current peaks start to appear between -200 and +350 mV vs Ag/AgCl, indicating the reduction/oxidation of surface bound polyaniline. The first of these peaks appears at 212 mV vs Ag/AgCl with a current reaching 110 μA, while the second peak appears at -39 mV and reaches 103 μA. As already discussed, conductivity increases from each subsequent scan due to the increasing thickness of polyaniline on the electrode surface.

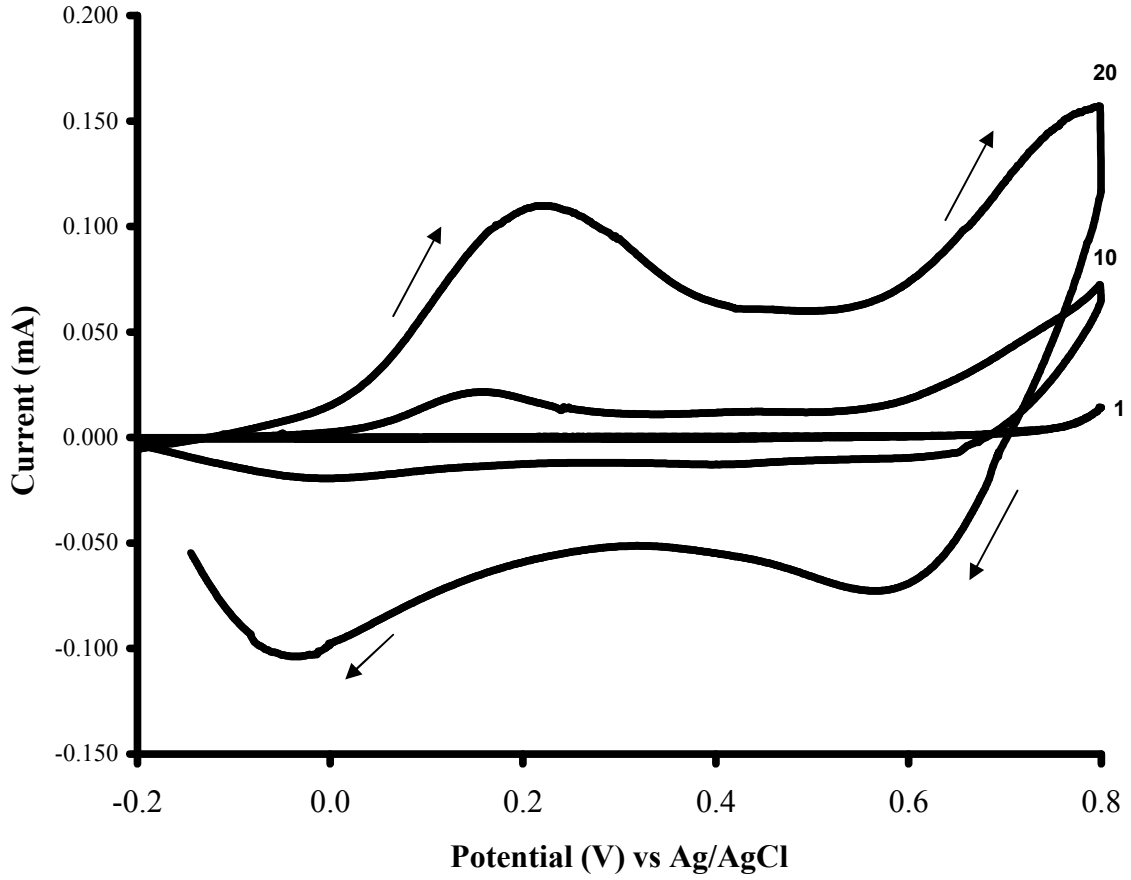

Figure 4.15: Polyaniline electrodeposition (-0.2 to 0.8 V) on a screen printed carbon electrode 1, 10 and 20 cycles shown.

4.7 AC impedance

Impedimetric experiments using the project specific electrodes were carried out to confirm the findings being achieved via cyclic voltammetry. Impedance changes are measured in ohms (Ω). While performing impedimetric experiments on bare electrodes, great discrepancies were observed among them with impedance values displaying differences as high as 700 Ω from one electrode to the other. The changes in percentage impedance response from baseline that occur due to antibody binding are normally low (results shown in the following chapters). It is clear in this context that using different sensors (replicates) would result in differences rising due to sensor irreproducibility, rather than antigen-antibody binding and thus any results using these electrode templates could not be considered to be valid. For this reason the project specific electrodes were not used further during this research programme but instead in-house carbon screen printed electrodes (Microarray Ltd, Manchester, UK) were used in addition to a commercial screen-printed carbon three electrode format (WE-REF-CE).

Chapter 5
Development of immunosensors for the detection of Ciprofloxacin

5.1 Development of immunosensors for the detection of Ciprofloxacin using non-highly concentrated and non-purified antigen

Introduction

Ciprofloxacin belongs to a group of antibiotics known as the fluoroquinolones as stated earlier. Due to problems arising from antibiotic resistance, the EU has established guidelines regarding the use of such substances by humans and for animals (Bishai, 2002; Bogialli *et al*., 2008). AC impedance analysis is a promising tool for the detection of anti-fluoroquinolones in food products (Mello & Kubota 2002).

Quinolones are a group of antibiotics with great antibacterial activity and broad spectrum of action but are also associated with the emergence of bacterial resistance and some adverse biological effects that in some cases have been severe (Blondeau, 2004). Nalidixic acid, the first quinolone to be described, was produced by the modification of a compound isolated during the production of chloroquinolone in 1962 (Pinachoa *et al*., 2008). Quinolones onstitute a relatively new class of antibiotics and are synthesised from a 3-quinolone carboxylic acid. They have a broad antibacterial spectrum against both gram negative and gram positive bacteria. Their mode of action is based on the inhibition of DNA gyrase and DNA topoisomerase, both of which are involved in DNA replication, recombination, decatenation and repair. Some quinolones, such as danofloxacin and enrofloxacin were specifically developed for the treatment of enteric and respiratory infections in cattle (Bogialli *et al*., 2008). Due to limited activity and early development of bacterial resistance to quinolones a new group of antibiotics was developed by the addition of a fluorine in carbon six position (C6) to the initial quinolone structure. Fluoroquinolones have been seen to have excellent tissue penetration as well as strong interactions with outer membrane protein.

The first fluoroquinolone to be approved for clinical medicine was ciprofloxacin in the mid 1980s. In general quinolones can be classified into three generations. The first generation includes nalidixic acid and oxolimic acid alongside others, which have been found to have limited activity against *E. coli* and other gram negative bacteria.

Additionally, they display poor oral bioavailability and limited distribution into systemic tissues. The second generation fluoroquinolones includes ciprofloxacin and danofloxacin. These compounds, developed in the 1980s, displayed increased activity against gram negative *Enterobacteriaceae* as well as some activity against gram positive bacteria such as *P. aeruginosa*. They further displayed improved oral bioavailablility. The third generation quinolones displayed similar activity to second generation drugs but showed enchanced antibactiral activity against gram positive bacteria. They also displayed better oral bioavailability alongside lower toxicity and longer serum half-life (Martinez *et al*., 2006; Ball, 2000).

A continuous effort for the development of novel fluoroquinolones has resulted in the discovery of many new compounds some of which complete their clinical trials in 2010. This initiative for novel antibiotic development results mainly from the rapid emergence of bacterial resistance. Specifically in the case of fluoroquinolones, with concentration dependant antibacterial activity, emergence of bacterial resistance is mostly associated with suboptimal dosing.

Falagas *et al.,* (2007), examine literature reports regarding the dosage to humans of various fluoroquinolone antibiotics. They aim to determine, in their review, the effectivity and safety of low versus high daily dosages. Safety is an important matter in the case of any drug. Fluroquinolones display somewhat high toxicity with adverse effects that range from moderate to extremely severe. Phototoxicity for example, results from the additional fluorine in lonefloxacin and chlorine in clinafloxacin. Adverse effects in the central nervous system have been associated with the unsubstituted 7-piperazine derivatives. More severe reactions include haemolytic ureamic syndrome associated with temafloxacin and unpredictable hepatic reactions resulting from the use of trovafloxacin. Trovafloxacin has been withdrawn from the market and banned from use for this very reason.

Ciprofloxacin has a broad spectrum of activity against particularly gram negative and some gram positive bacteria. It has been extensively used for the treatment of urinary and respiratory tract infections for decades, however, there have been reports of failure when used for the treatment of pneumonococal infections. Ball, 2000 reports that gemifloxacin appears to be the most effective compound for use against *S.*

pneumoniae infections also showing the least potent adverse biological reactions. Hartmann *et al.,* (1999) studied the concentration of ciprofloxacin in hospital wastewaters using high performance liquid chromatography (HPLC) and made correlations with DNA damaging effects. The levels of detected ciprofloxacin ranged from 0.7 ng- 124.5 ng ml^{-1} and genotoxicity was observed from levels as low as 5.2 ng ml^{-1}. The therapeutic range of ciprofloxacin lies between 0.57-2.3 μg ml^{-1} in serum and 1.26-4.03 μg ml^{-1} in tissue (Licitra *et al.,* 1987).

The importance of fluoroquinolones in the medical industry and the potent biological effects of some of these drugs on human health and environmental welfare have made it a necessity to develop methods for their fast detection and reliable determination of their concentration in e.g. in food products. Torriero *et al.,* (2006) describe a horseradish peroxidise sensor for the detection of ciprofloxacin based on the inhibition of catechol oxidation, however, exisiting piperazine compounds may interfere with the detection process.

In this chapter, the development of an impedimetric biosensor for ciprofloxacin is described. Screen printed carbon electrodes where coated with polyaniline and subsequently loaded with biotynilation reagent. By the exploitation of biotin-neutraviding interactions, biotynilated antibodies were attached to the modified sensor surface and the resulting sensor interrogated through an impedance protocol after exposure to various concentrations of ciprofloxacin in PBS buffer 7.4, 10 mM Ferri/ferocyanide. Control sensors were also fabricated containing polyclonal IgG antibodies to account for non-specific interactions. Work on the development of ciprofloxacin sensors was undertaken with the collaboration of Mr. G. Tsekenis. Figure 5.1 below depicts the structure of ciprofloxacin.

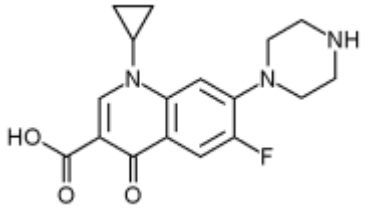

Figure 5.1: Structure of ciprofloxacin.

Results and discussion

The procedures described in chapter 3 were followed in this work for the fabrication of ciprofloxacin immunosensors using screen printed carbon electrodes. For this set of experiments the polyclonal IgG on each sensor surface was kept at a concentration of 1 mg ml^{-1}. The biotynilation procedure resulted in a significant loss of anti-ciprofloxacin antibody thus the obtained concentration was 0.25 mg/ml. Additionally, no further purification or concentration steps were performed for this initial phase of sensor development. The consequences of this are discussed along with the interpretation and analysis of data. As supported by Tully *et al.,* (2007), the polyclonal IgG response is expected to be much lower than the specific antibody responses, since a polyclonal immune response contains a plethora of antibodies targeted to various antigens, while the monoclonal antibodies target only one specific antigen.

Additional investigations were carried out to determine the optimum impedance conditions with regards to solution use and impedance parameters. During this work, the cell offset was set to -0.4 V, 0 V and +0.4 V and two different solutions were used for impedimetric measurements; a PBS buffer pH 7.4, and a 10 mM ferri/ferrocyanide PBS solution. Data interpretation indicated that the greatest result resolution was achieved at an offset of + 0.4 V and would be the best choice of offset potential for subsequent work. It was also observed that the presence of a redox couple for impedimetric measurements limits the imaginary component of impedance, while in plain PBS buffer, the Z" component normally dominates impedance. Previous work within our group (Grant *et al.,* 2005) indicated that the Z' component of impedance is far more reproducible for data interpretation. For this reason 10 mM ferri/ferrocyanide enriched PBS buffer (pH 7.4) was used in all subsequent work to a) minimise the capacitive effects, and, b) to enhance the resolution of results based on charge transfer effects, however, some experimentation using plain PBS buffer has also been undertaken for comparison of results.

The chosen concentration range (1-1000 ng ml^{-1}) covered four orders of magnitude, thus providing basic information regarding sensor characteristics such as reusability (how many times the sensor can be reused for measurements) and detection (What is

the lowest and highest concentrations the sensor can effectively detect and quantify) limits. The chosen range was to be further extended in subsequent work. Unfortunately, as we will discuss in chapter 6, early sensor saturation resulted in non-reliable measurements for the specific antibody loaded sensors. As reported by Defega & Kwak, (2008), while working with DNA based sensors, an equilibrium state is observed where no more hybridisation occurs. Similarly, saturation of antibody loaded sensors means that no more specific binding can occur on the sensor surface.

Figure 5.2 is the Nyquist plot for the specific anti-fluoroquinolone antibody to varying concentrations of ciprofloxacin in PBS pH 7.4 in the presence of 10 mM ferri/ferrocyanide. It should be noted that impedance increases as the frequency decreases, with maximum impedance values being obtained at 1 Hz. An initial observation of this figure suggests sensor saturation upon addition of antigen at 1 μg ml^{-1}. This can be deduced by a small drop in faradaic impedance from 500 ng ml^{-1} to 1 μg ml^{-1}. Another interesting observation is that the capacitive impedance at 20 ng ml^{-1} was higher than that observed for 50 ng ml^{-1}. Aside from these two occasions for both the faradaic and imaginary component, impedance generally is seen to increase upon exposure to higher antigen concentrations as shown in figure 5.2. This increase is, however, relatively small, a fact which in combination with non-specific antibody responses indicates that these measurements could be not be relied upon. Upon saturation, any further changes in impedance are assumed to be caused due to non-specific binding (antigen loosely absorbed on the sensor surface) and can thus, as already stated, be erroneous (Garifallou *et al*., 2007).

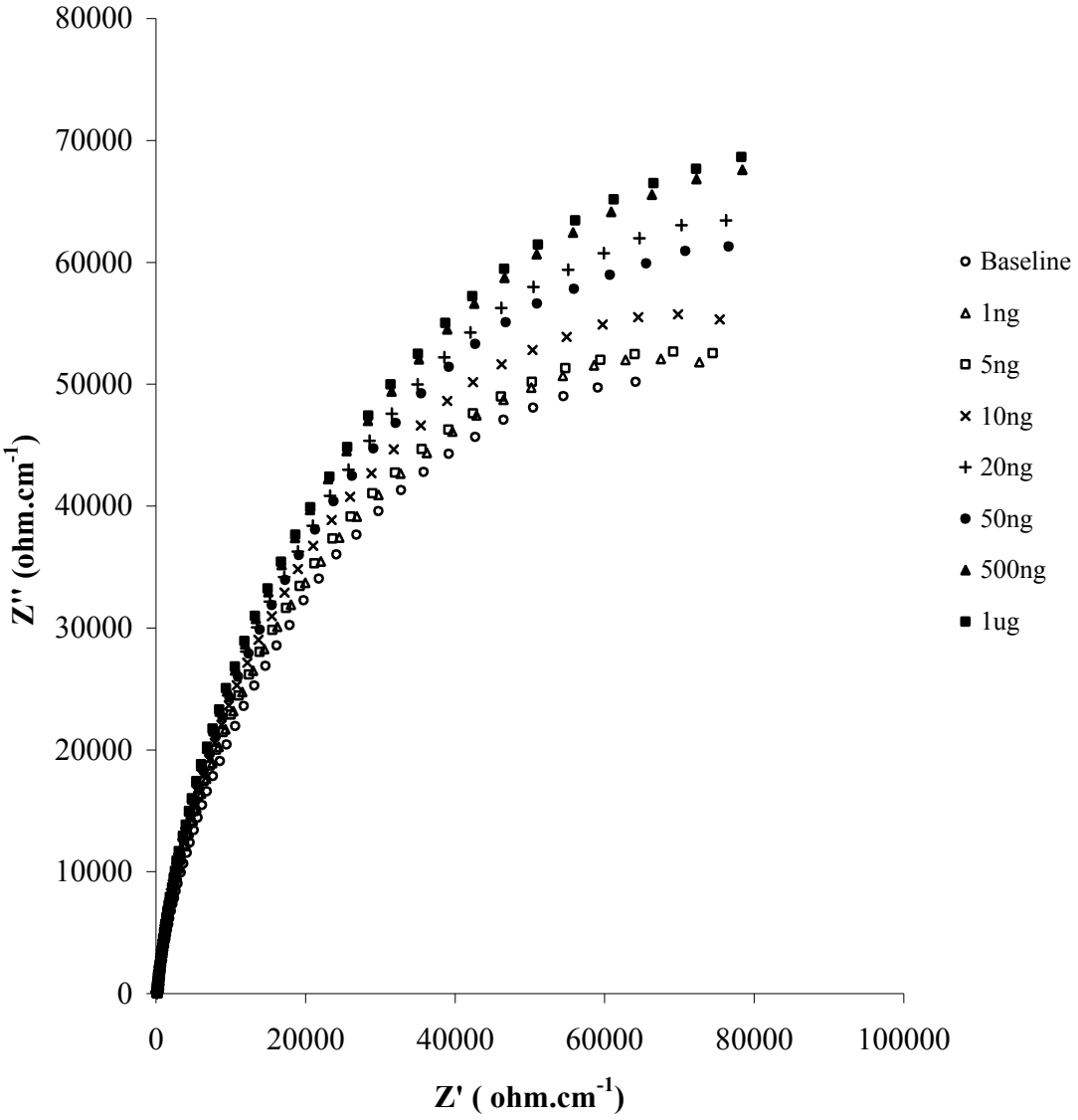

Figure 5.2: Z'' v Z', Nyquist plot. Impedance responses of anti-ciprofloxacin loaded carbon based sensors upon exposure to a range of ciprofloxacin concentrations (in PBS, 10 mM ferri/ferrocyanide).

As already stated, the polyclonal IgG concentration on the sensors was higher than the concentration of anti-ciprofloxacin. It was thus assumed that the ciprofloxacin sensors were becoming saturated due to a low antibody concentration on the surface. Sensor saturation renders the production of a calibration curve impossible not only due to non reliable measurements being made but also due to the variations among the interrogated sensors, which inevitably lead to increased standard errors. It was

assumed that after concentration and purification of the specific antibody, the responses would become greater due to larger quantities of antigen being immobilised at the sensor surface. The concentration of anti-ciprofloxacin was increased from 0.25 mg ml^{-1} to 1 mg ml^{-1}. The following impedance plots provide details about the responses of IgG loaded sensors and a further insight into the differences between plain PBS buffer and a 10 mM ferri/ferocyanide solution for impedance interrogation.

Figures 5.3 and 5.4 depict the Nyquist plots (faradaic vs capacitive impedance components) for polyclonal IgG response to varying concentrations of ciprofloxacin, using ferri/ferocyanide (figure 5.3) and in plain PBS (figure 5.4). In the presence of a redox couple it can be seen that both the Z' (real) and Z" (imaginary) components increase with increasing antigen concentrations (figure 5.2). Changes in the Z' component of impedance indicate the occurrence of a charge-transfer mechanism on the electrode surface upon exposure to antigen, as suggested by Tully *et al*., (2007). Increased amounts of antigen result in an increase of both the capacitive and faradaic components. Contrary to observations for the specific sensors, the non specific loaded electrodes, do not show signs of saturation. The production of calibration curves for both specific and non specific response was required for direct comparison, and an explanation of how these calibration curves where produced is provided within this section.

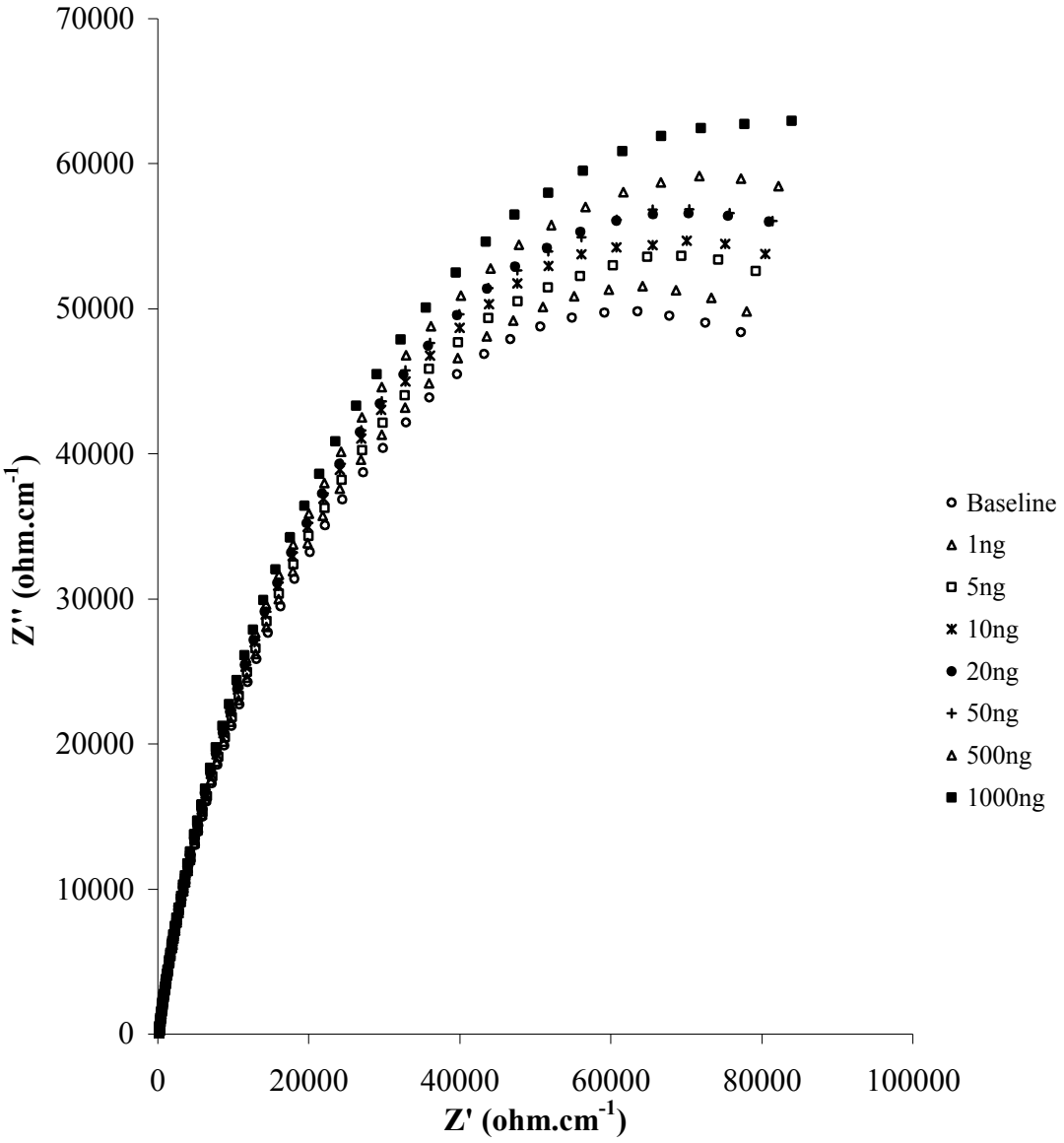

Figure 5.3: Z'' v Z' - Nyquist plot. Impedance responses of polyclonal IgG loaded carbon based sensors upon exposure to various ciprofloxacin concentrations (in PBS, 10 mM ferri/ferrocyanide).

As seen in figure 5.4, below, the use of plain PBS buffer results in an increase of the capacitive component of impedance upon antigen exposure while the faradaic component is seen to decrease with increasing concentrations. It is important to note that the presence of a redox couple such as ferri/ferrocyanide facilitates charge transfer and decreases the capacitive charging effects occurring on the electrode surface. As discussed earlier in this chapter, it is the faradaic events that are of interest in this work, thus, further work using plain PBS buffer were not undertaken.

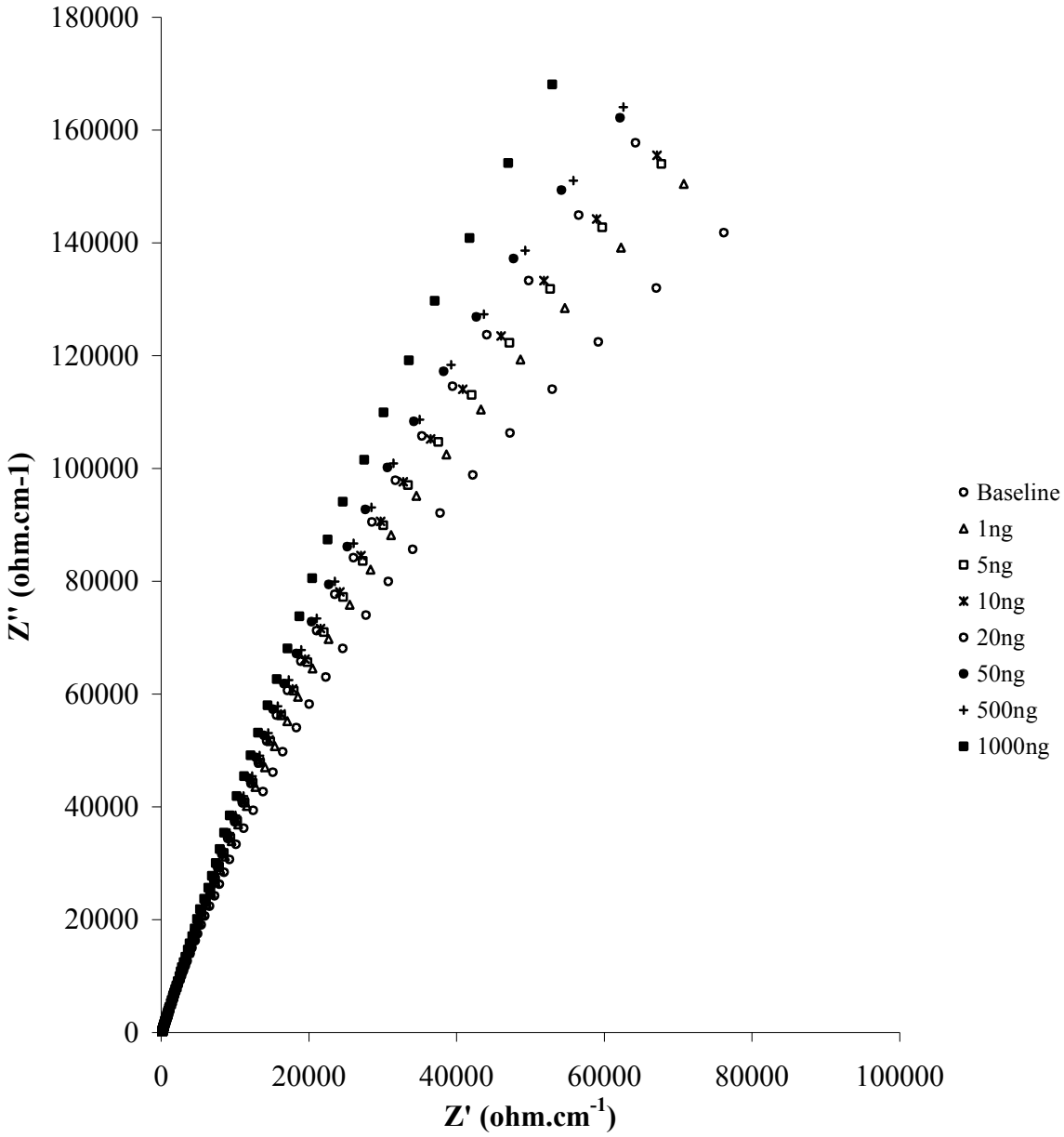

Figure 5.4: Z'' v Z' - Nyquist plot. Impedance responses of polyclonal IgG loaded carbon based sensors upon exposure to various ciprofloxacin concentrations (in PBS).

The high impedance values obtained at 1 Hz (as discussed in section 3.8) allowed the creation of two calibration curves (figures 5.5 and 5.6 for specific and non-specific response respectively) for the range of concentrations that was investigated. The Z' component values at 1 HZ upon antigen addition can be compared to the baseline response at 1 Hz thus showing the percentage increase in Z' from baseline at various

concentrations. This procedure is followed for both specific and non-specific sensor responses and subsequently the non-specific response is subtracted from the specific response. In this manner, any non-specific interactions that may be occurring on the monoclonal antibody loaded sensors can be accounted for.

The above results were further analysed in order to produce percentage impedance change plots for both IgG and anti-cirpofloxacin sensors. The equations used for this analysis are shown below, where,

$$\% \text{ Impedance change} = \left(Z_0^{'} - Z^{'}\right) / Z_0^{'} * 100 \qquad \textit{Eq. 5.1}$$

$Z^{'}_0$ is the baseline faradaic component of impedance at 1 Hz and $Z^{'}$ is the sample faradaic component of impedance at 1 Hz.

As we will see later in this chapter, impedance may fall or rise with increasing antigen concentrations, and this depends on the antigen/antibody pair being used; this phenomenon will be discussed later. For this reason any values obtained by equation 5.1 above are converted to absolute values for use in the calibration curve plots.

The standard errors (for three replicate sensors) are individually calculated for non-specific and specific responses using the standard deviation equation. However, in order to obtain standard errors for corrected calibration curves, a different approach is required. In these plots the values used for the 'corrected impedance' curve are the result of subtraction of non-specific responses from their respective specific responses as follows, where,

(% specific change at 1 ng ml-1)- (% non-specific response at 1ng ml-1)
=% corrected change *Eq. 5.2*

For the calculation of standard errors for specific plots:
=SQRT [(STDev for specific change at 1ng ml-1)^2+
(STDev for non-specific change at 1ng ml-1)^2] *Eq. 5.3*

Figures 5.5 and 5.6 depict the change in impedance from baseline upon the addition of ciprofloxacin concentrations ranging from 1-1000 ng. A near linear correlation (R^2=0.97) was found to exist between change in impedance and $\log_{10}$ ciprofloxacin concentration. It is obvious that the IgG response was much greater (6.57% change at 1000 ng) than the specific response while the accounted errors where also much lower. A maximum 4.6% impedance change form baseline was observed, however, the extremely high standard errors clearly indicate that these results are not reliable. An additional trend can be seen in figure 5.5. A usual calibration curve would contain a linear phase within its curve, which reaches a plateau towards the higher end of concentrations, representing sensor saturation. Such behaviour was seen in subsequent work that was undertaken following this initial set of impedimetric experiments. In this case the IgG sensors were not saturated thus no plateau is visible. It is clear from these calibration profiles, that the fabricated immunosensors would not meet the requirements for use as a practical sensing device.

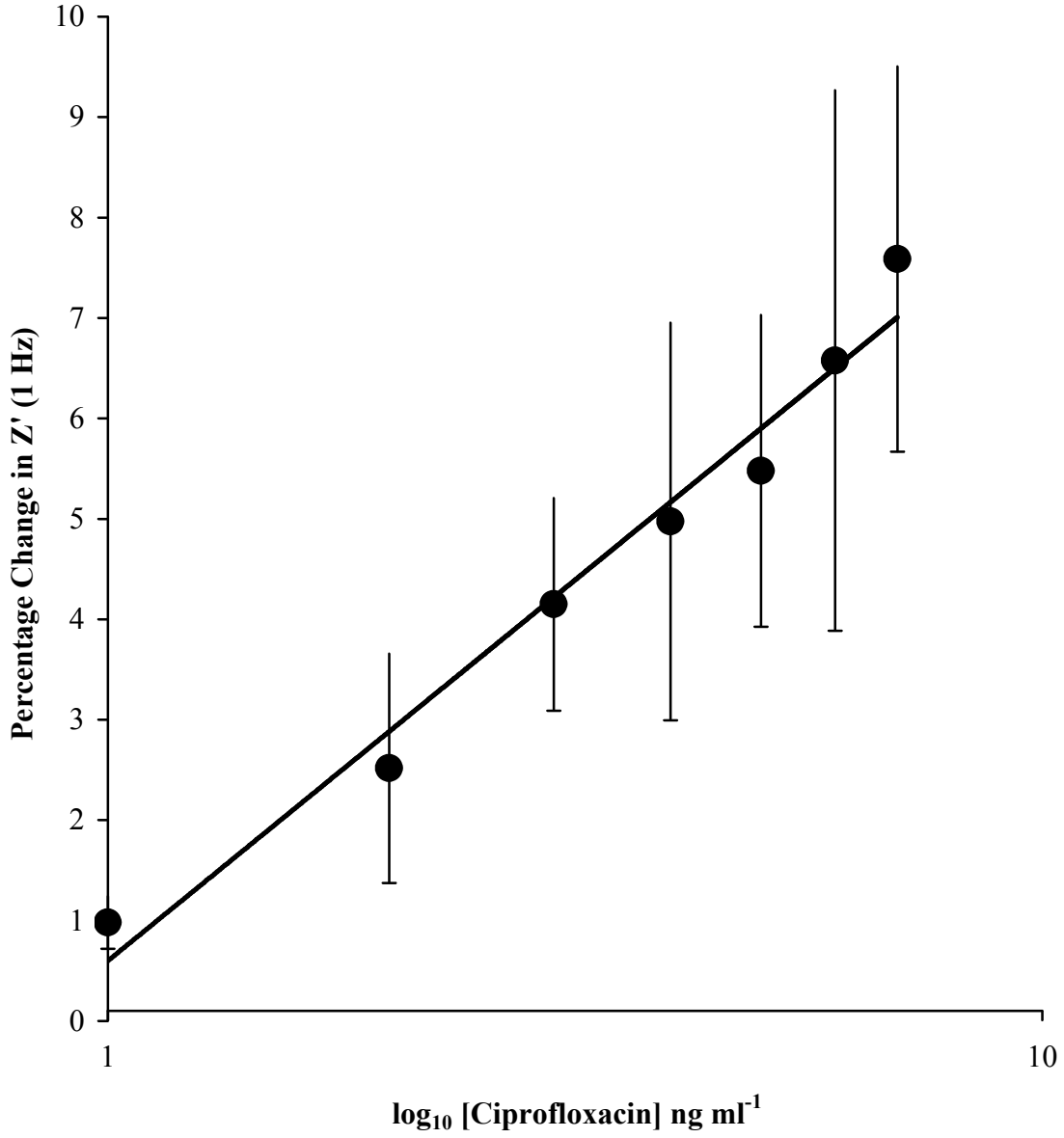

Figure 5.5: Calibration curve of per cent (%) impedance response against log_{10} ciprofloxacin concentrations (1 ng ml^{-1}-1000 ng ml^{-1}) for IgG doped polyaniline coated carbon electrodes at 1Hz (in 10 mM ferri/ferrocyanide).

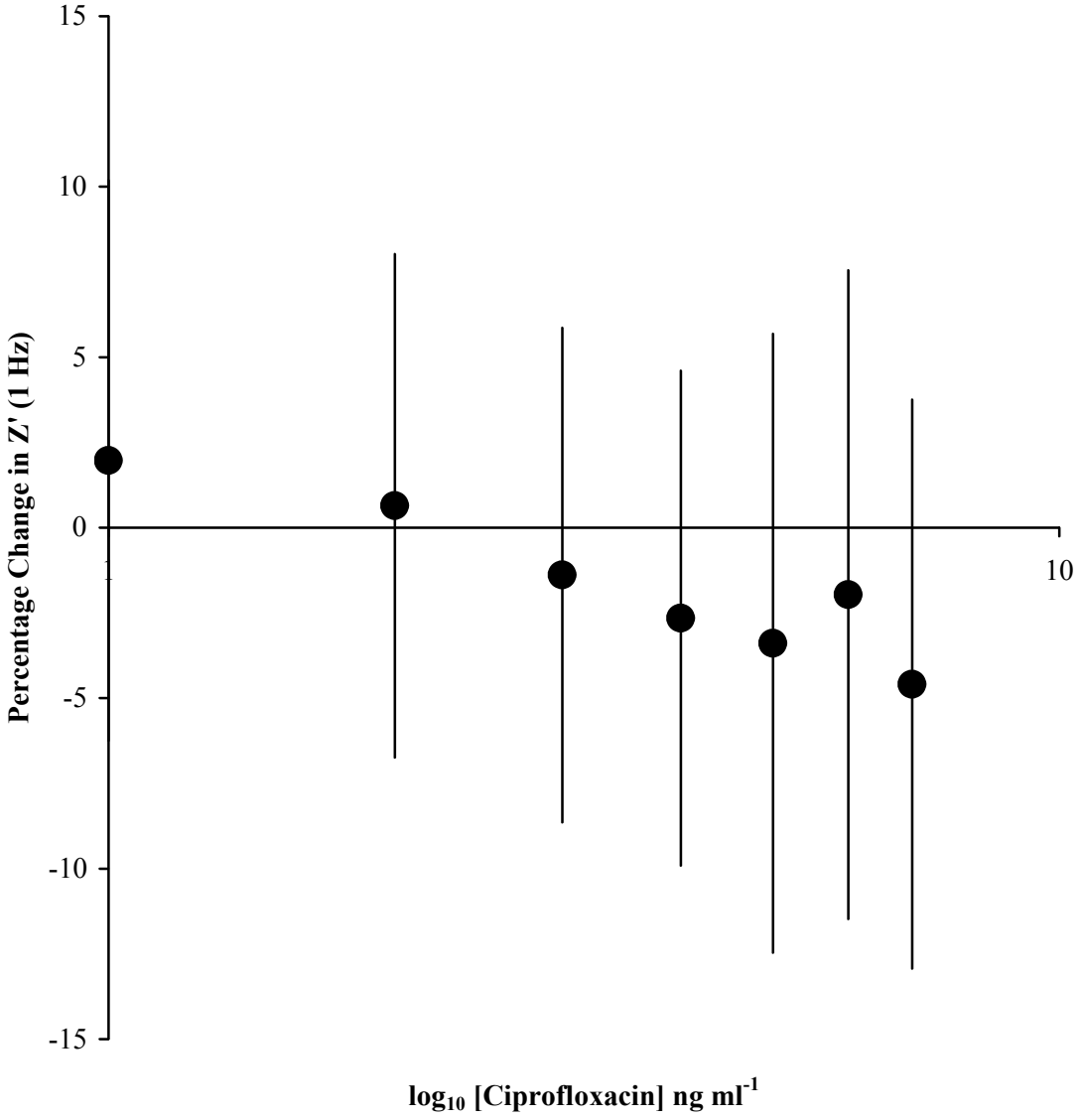

Figure 5.6: Calibration curve of per cent (%) impedance response against log_{10} ciprofloxacin concentrations (1 ng ml^{-1}-1000 ng ml^{-1}) for anti-ciprofloxacin doped polyaniline coated carbon electrodes at 1Hz (in 10 mM ferri/ferrocyanide).

Figure 5.7 represents the corrected calibration curve which resulted following subtraction of the non-specific response from the specific response.

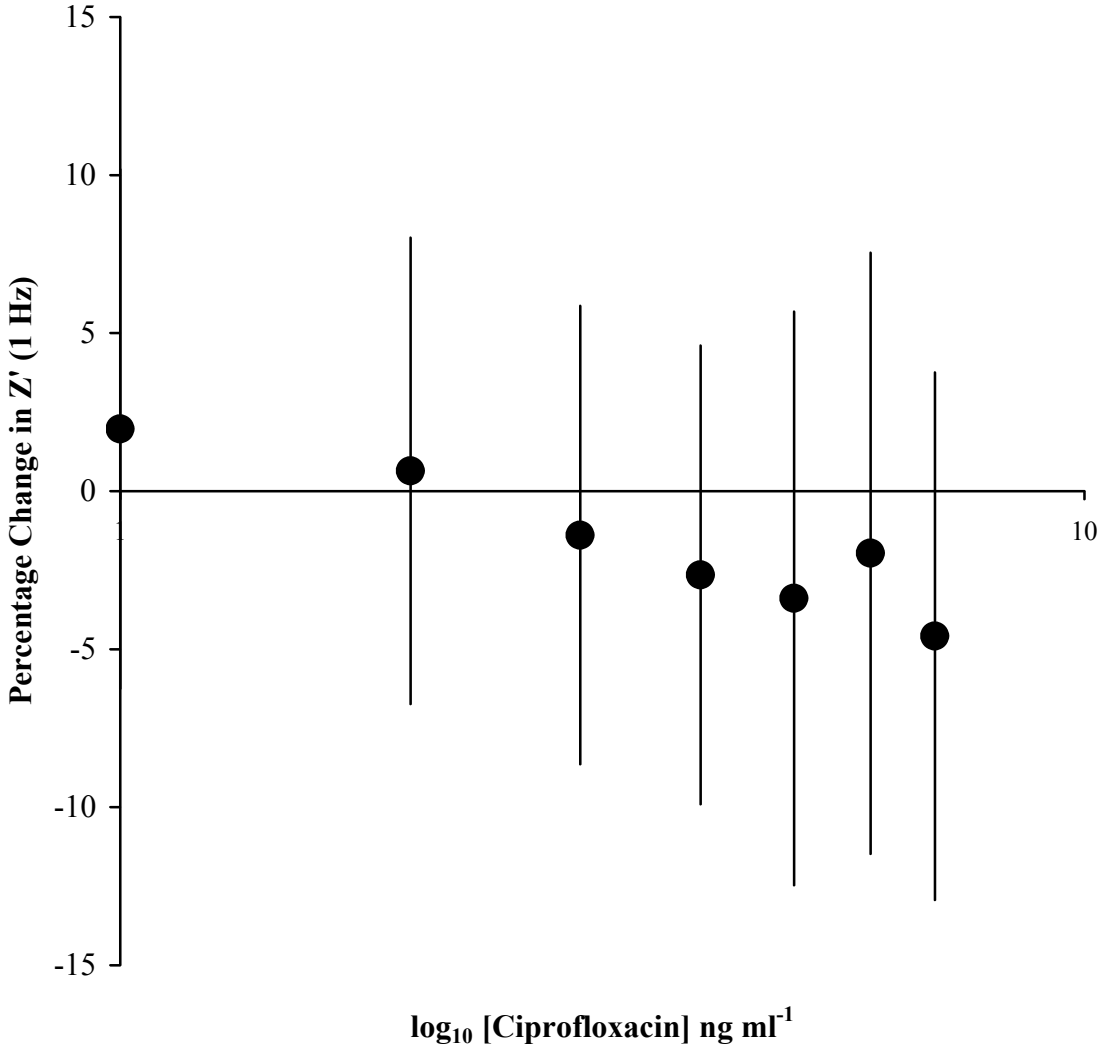

Figure 5.7: Corrected calibration curve of per cent (%) impedance response against log_{10}ciprofloxacin concentrations (1 ng ml^{-1}-1000 ng ml^{-1}) for anti-ciprofloxacin doped polyaniline coated carbon electrodes at 1Hz (in 10 mM ferri/ferrocyanide).

Figure 5.8 below includes a typical Bode plot obtained for polyclonal IgG sensors at various antigen concentrations in 10 mM ferri/ferrocyanide.

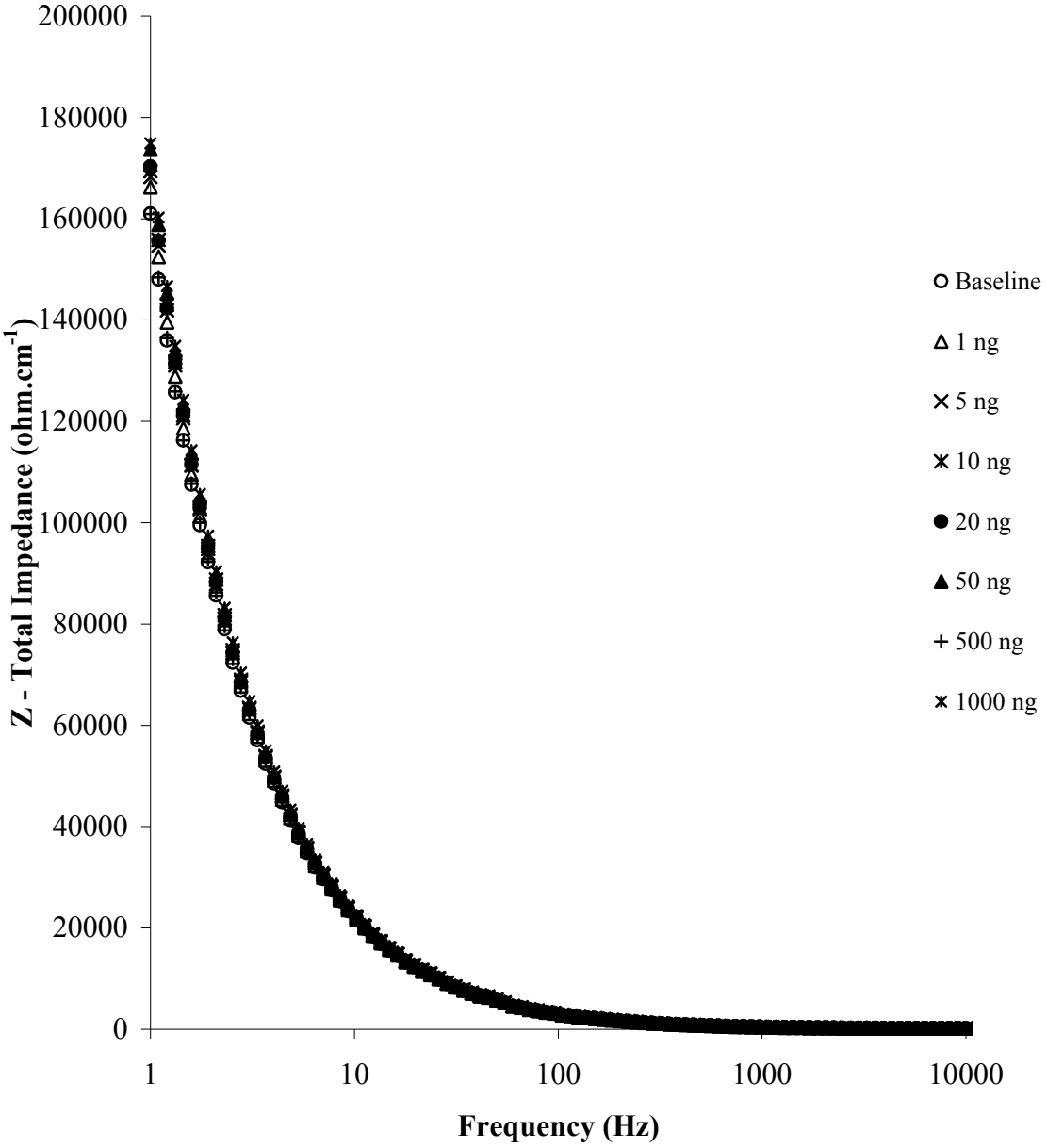

Figure 5.8: Bode plot- Z vs frequency. Total impedance response for polyaniline doped with IgG (non specific antibody) after exposure to various concentrations of ciprofloxacin (in 10 mM ferri/ferrocyanide).

Figure 5.9 is a variation of figure 5.8 focusing in the frequency range between 10Hz and 1Hz and a smaller spectrum of impedance values to allow for better resolution.

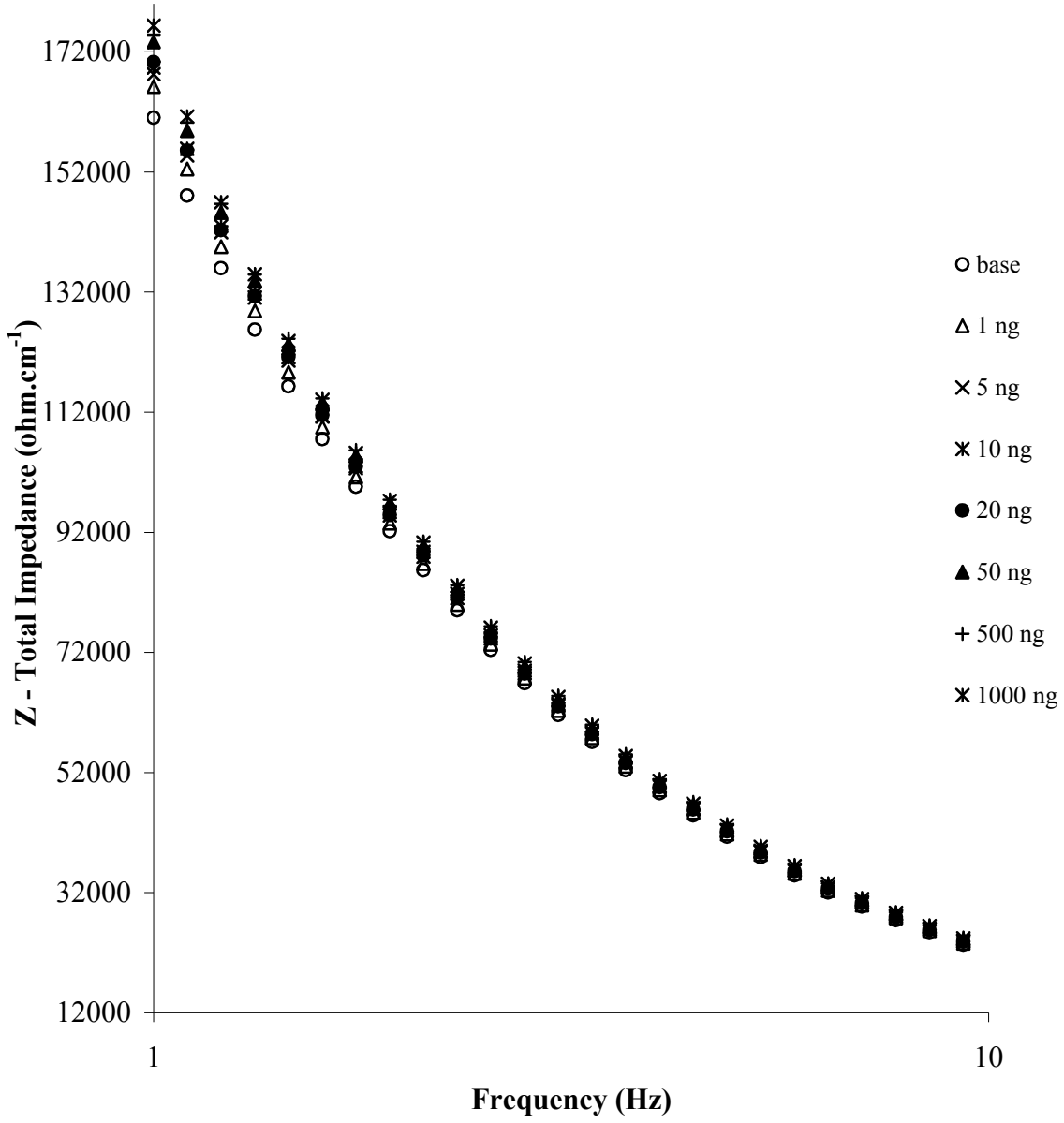

Figure 5.9: Bode plot-total impedance vs frequency. Total impedance response for polyaniline doped with IgG (non specific antibody) after exposure to various concentrations of ciprofloxacin (in 10 mM ferri/ferrocyanide). Range of frequencies from 1Hz to 10Hz.

Conclusions

One of the most important matters to consider by this set of experiments is that in general increasing antigen concentrations caused an increase in impedance. The

Nyquist plots (figures 5.3 and 5.4) show near semicircle curves corresponding to the occurring charge transfer mechanism. In this case the semicircle diameter increases upon material binding on the sensor surface, whether this material be antigen binding to antibody or target DNA being hybridised to the immobilised complementary sequence (Trully *et al*., 2007; Defega & Kwak, 2008). Partners within the ELISHA consortium (Ionesku *et al*., 2007) also report increasing impedance upon exposure to higher antigen concentrations, which this far, is in accordance with our results. Further work indicated that whether an impedance increase or decrease is observed (with exposure to various antigen concentrations) is determined by the nature of the antigen/antibody combination as well as any possible purification and concentration procedures. This subject will be covered within the following section.

Another important issue within these initial investigations have been the observations of rather large error bars arising from irreproducibility amongst replicate sensors during ac impedance testing. The procedures described within this work have been heavily manual from electrode coating with polymers to antigen addition for impedance testing in the final stages of each experiment. Naturally, extreme care has been taken to minimise possible human errors, however, further automation would ensure that his important factor were minimised even more. It should be noted here that human error was not the contributing factor for the observed error bars. Work carried out later (as shown in the following sections) indicated that using set concentrations of antibody for sensor immobilisation was vital for reproducibility among replicate sensors. Sensor saturation upon antigen addition was thought to be resulting in these large error bars and it was thus decided to try using antibody concentration post biotinylation of 1 mg ml^{-1}. As will be seen, later within this chapter, when antibodies are used at this concentration, sensor saturation does not occur early during testing, and hence more extended ranges of antigen concentrations can be used.

5.2 Development of immunosensors for the detection of Ciprofloxacin using purified and concentrated anti-Ciprofloxacin

Introduction

The experimental procedure described in section 5.1 was repeated using purified and concentrated anti-ciprofloxacin. The concentration of immobilised polyclonal and monoclonal antibodies on the sensor surface was 1 mg ml^{-1}. Figures 5.10 and 5.11 are the average Nyquist and Bode plots from three replicate sensors with immobilised anti-fluoroquinolone when exposed to different concentrations of the antigen. Baseline impedance of these newly fabricated sensors, containing purified monoclonal antibody, was dramatically lower than the previously described sensors containing non-purified anti-fluoroquinolone. It is important here to note that while impedance was previously found to increase upon exposure to increasing concentrations of antigen; in this instance the obtained results indicated impedance decrease with increasing antigen concentrations.

Previous work within this group showed that the binding event for different antigen/antibody pairs may increase or decrease the impedance of the systems. It is argued here that this is the result of two competing processes; non-specific adsorption (non-purified antibody) leads to increases in impedance-especially in regards with the capacitive component of the system (**Z"**). Specific antigen/antibody binding in the case of ciprofloxacin leads to a lowering of impedance. Other work within our group has indicated that not all specific binding leads to impedance increase (Tsekenis *et al.,* 2008). Impedimetric interrogation of electrodes containing anti-myelin basic protein antibody displayed increases in impedance with increasing antigen concentrations. Impedance responses heavily depend upon the very nature of the antibody/antigen complex of choice. Myelin basic protein is a mixture of materials varying in molecular weights from 14-24 kDa. It is likely that this specific protein is insulating in nature thus causing impedance increase upon binding contrary to ciprofloxacin binding which causes impedance to decrease. We believe that all antibody/antigen pairs lead to impedance decrease, however, the larger antigens appear to have a competing insulating effect on the sensor, which in some instances, may be the dominant factor in impedance change.

Upon the antibody/antigen binding event H_2 bonds are formed which stabilise this interaction while the binding specificity between the two biomolecules is affected by some weak interactions such as van der Waals and electrostatic forces alongside hydrophobic interactions. Such events may also cause variation of impedimetric responses among different antibody antigen pairs. While the reasons underlying these two events cannot as yet be answered with certainty, this give may rise to new projects when this project has been completed and a prototype sensing device has been fully developed.

It should be noted that while the observed impedance changes may be positive or negative, the percentage impedance change from baseline values is always reported as absolute values allowing for comparison of different sets of sensors.

Results and Discussion

Figures 5.10 and 5.11 contain the Nyquist and Bode plots obtained for anti-ciprofloxacin doped sensors upon exposure to ciprofloxacin and following impedance interrogation. A steady decrease is obvious in the real component of impedance with increasing antigen concentrations indicating that the binding event enhances charge transfer rather than hindering it. As seen by the Nyquist plot (figure 5.10), there is a 9 kΩ (Z' component) difference between the baseline response and the response at antigen concentration of 10 μg ml^{-1} at 1 Hz (real component). Impedance changes are higher in the lower range of concentrations but decreases, however, at much higher antigen concentrations, indicating sensor saturation. Degefa & Kwak, (2008), report that their DNA based sensors reached 'hybridisation equilibrium' after 1 hour and resulting in a plateau value for any further impedance measurements, which is in accordance with the data obtained here. As discussed in section 5.1 the Z' component was found to be far more reliable, as evidenced by the magnitutde of error bars, than the Z'' and this is obvious in the present work. The observed impedance changes suggest that the real component of impedance is the main contributor to total impedance and hence the values obtained at 1 Hz will be further used for the production of a calibration curve. While there is a constant increase of the real component of impedance, the imaginery component reaches its maximum value at a

midrange frequency (normally below 100 Hz) and then displays a drop with a minimum value at 1 Hz. As suggested by Barton *et al.,* (2009) this type of impedance spectrum indicates a surface-modified electrode system for which the electron transfer is slow and impedance is controlled by the interfacial electron transfer.

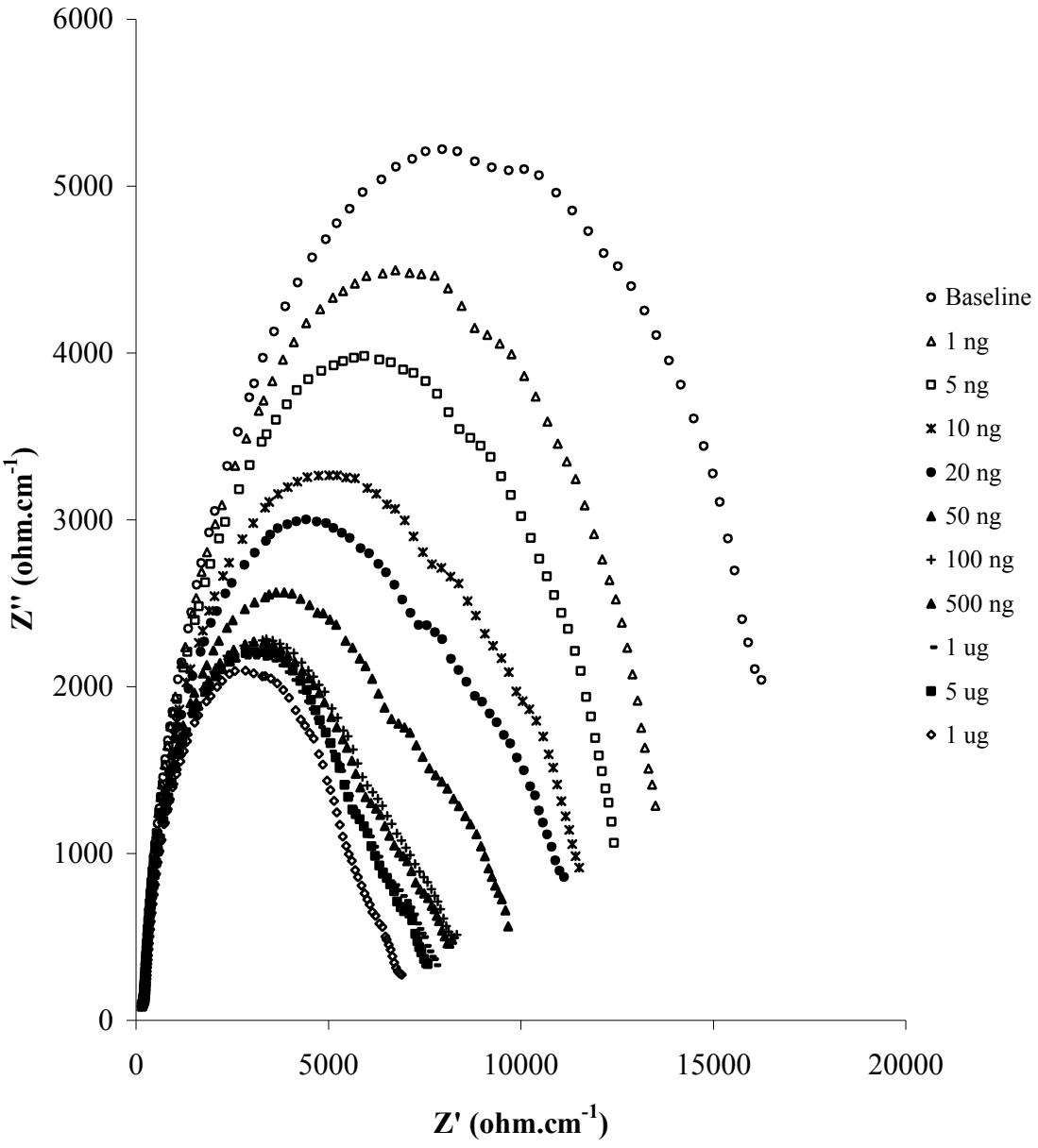

Figure 5.10: Z'' v Z' - Nyquist plot. Impedance responses of anti-ciprofloxacin loaded carbon based sensors upon exposure to various ciprofloxacin concentrations 1ng ml^{-1} to 10µg ml^{-1} (in PBS, 10 mM ferri/ferrocyanide).

A Bode plot was also recorded depicting the total impedance change against $\log_{10}$ of the frequency range. Observation of the bode plot in figure 5.11 indicates the presence of faradaic charge transfer (Z_f) in the range of frequencies between1 Hz- 1.5 Hz while the double layer capacitance (C_{dl}) dominates impedance above 1.5 Hz and up to 1 kHz. The electrolyte resistance (R_e) dominates the interrogation above 1 kHz.

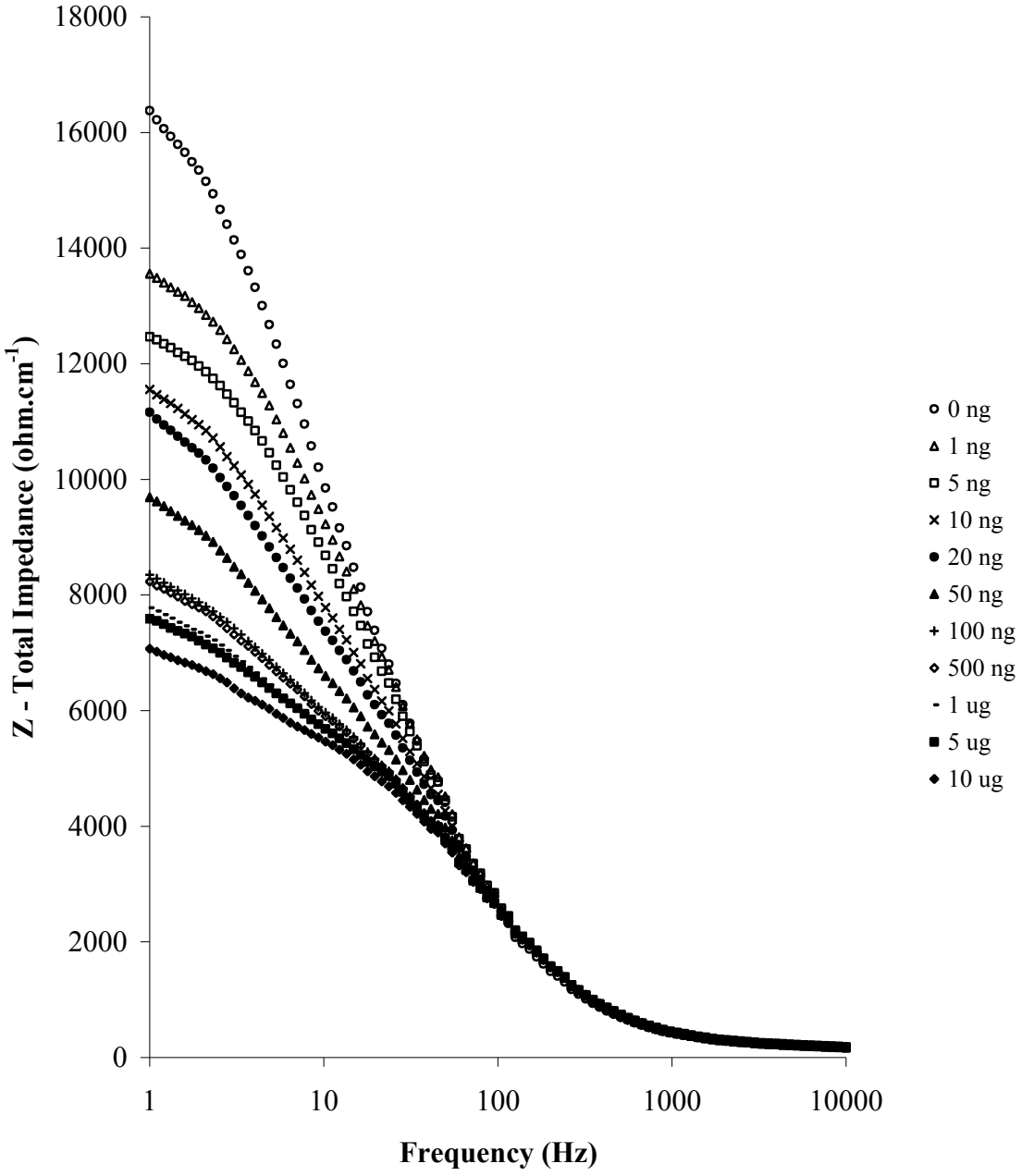

Figure 5.11: Bode plot. Impedance responses of anti-ciprofloxacin loaded carbon based sensors upon exposure to various ciprofloxacin concentrations (in PBS, 10 mM ferri/ferrocyanide).

Figures 5.12, 5.13 and 5.14 respectively depict the percent impedance change from baseline for specific and non specific sensors and finally a calibration profile for the newly fabricated anti-ciprofloxacin biosensors. It can be seen that the specific responses were much greater than non–specific responses and also displayed little variation among the 3 replicate sensors. As depicted in figure 5.14 there was a 57% increase in impedance from baseline at the highest antigen concentration of 10ug ml^{-1}. It is further apparent that the specific sensors started saturating towards the higher end of concentrations thus a plateau is becoming visible towards higher concentrations in this plot. The highest response observed for non-specific sensors was approximately 8% change from baseline while higher variation was also observed among the three non-specific replicates.

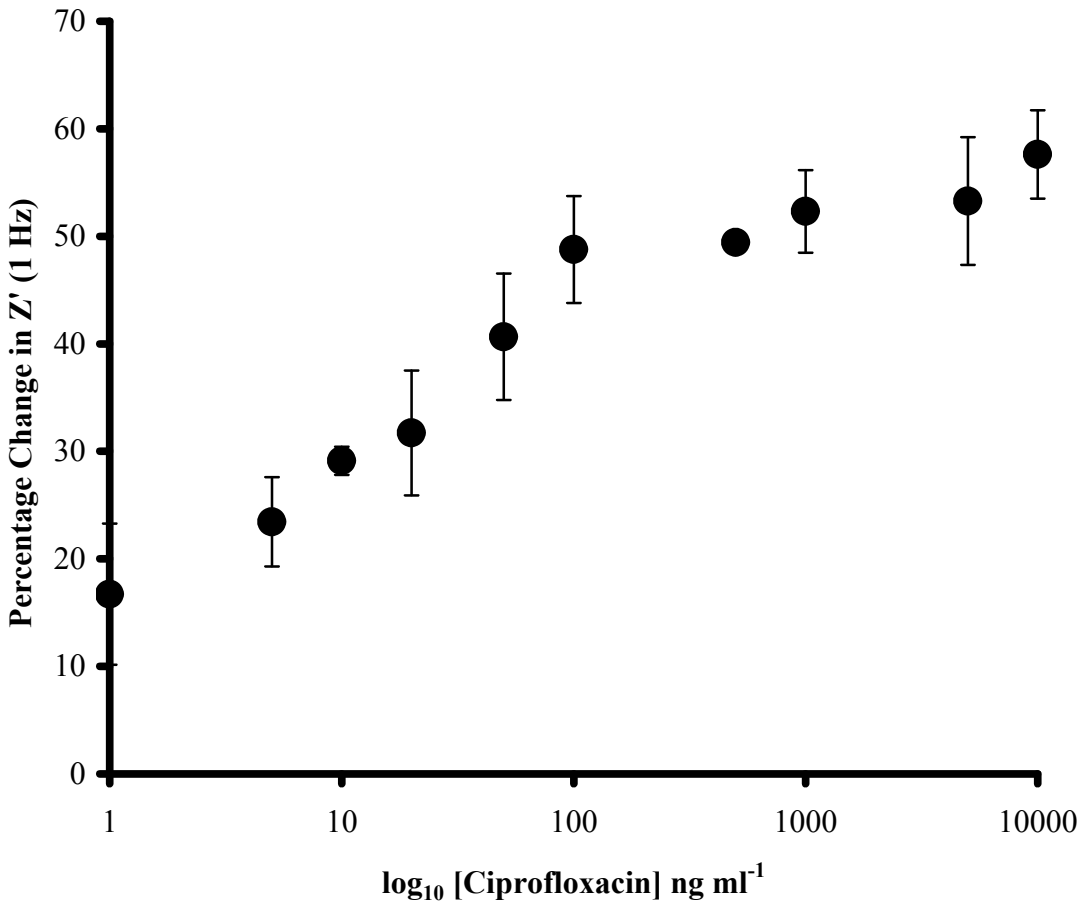

Figure 5.12: Calibration curve of per cent (%) impedance response against log_{10} ciprofloxacin concentrations (1 ng ml^{-1} to 10000 ng ml^{-1}) for anti-ciprofloxacin doped polyaniline coated carbon electrodes at 1Hz (in 10 mM ferri/ferrocyanide).

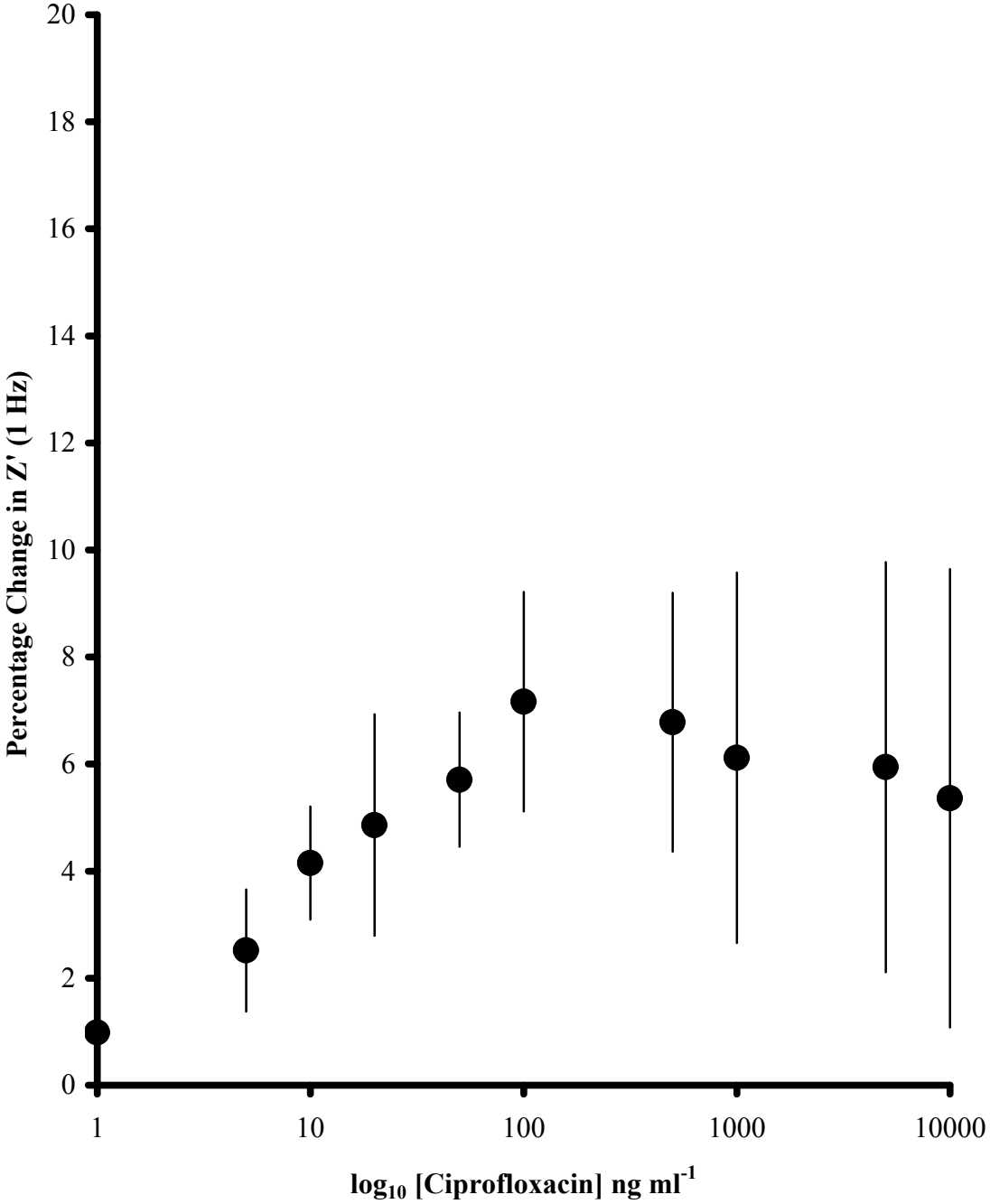

Figure 5.13: Calibration curve of per cent (%) impedance response against log_{10} ciprofloxacin concentrations (1 ng ml^{-1} to 10000 ng ml^{-1}) for polyclonal IgG doped polyaniline coated carbon electrodes at 1Hz (in 10 mM ferri/ferrocyanide).

As depicted in figure 5.14 the responses between 1-100 ng ml^{-1} show a constant increase in impedance change while a plateau is reached upon subsequent measurements at higher antigen concentrations.

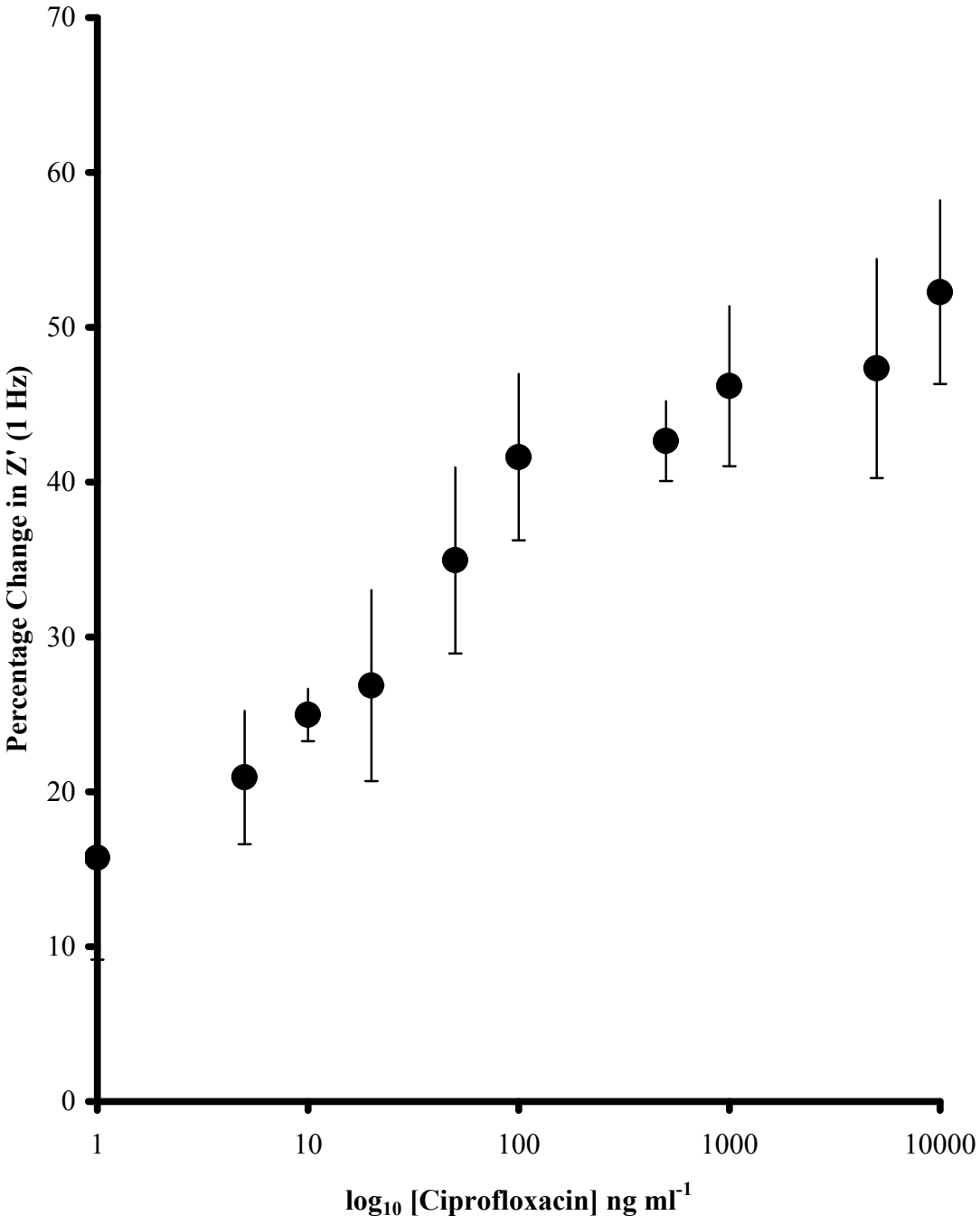

Figure 5.14: Corrected calibration curve of per cent (%) impedance response against log_{10} ciprofloxacin concentrations (1 ng ml^{-1} to 10000 ng ml^{-1}) for anti-ciprofloxacin doped polyaniline coated carbon electrodes at 1Hz (in 10 mM ferri/ferrocyanide).

The Pearson correlation coefficient, R^2=0.94, demonstrated a near linear correlation for the $\log_{10}$ concentration range from 1 to 100 ng ml^{-1} (Figure 5.15) after subtraction of the non-specific response which constituted a minor percentage of the impedance changes recorded.

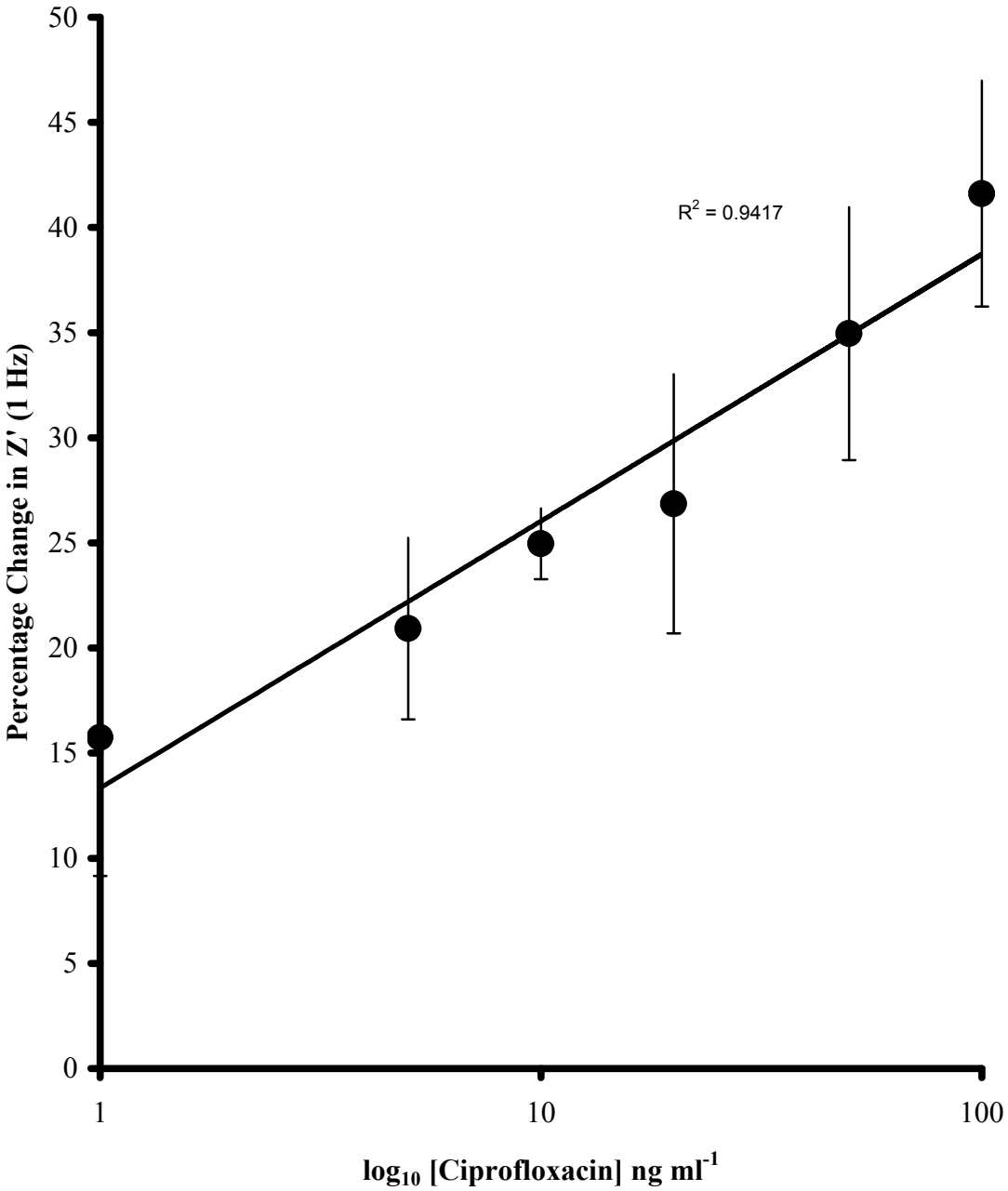

Figure 5.15: Corrected calibration curve of per cent (%) impedance response against $\log_{10}$ ciprofloxacin concentration for anti-ciprofloxacin doped polyaniline coated carbon electrodes at 1Hz (in 10 mM ferri/ferrocyanide). 1-100 ng ml^{-1} concentration range.

Conclusions

The development of an immunosensor targeted towards ciprofloxacin detection was described here. The observed impedance changes indicated that the sensor has an approximate detection limit of 1 ng ml^{-1} and can detect various concentrations of ciprofloxacin up to 10ug ml^{-1}. Sensor responses to antigen exposure were found to be concentration dependant with a linear correlation at least over the lower concentration range between 1-100ng ml^{-1}. It should be noted that the same three replicates were interrogated for each of the antigen concentrations appearing in the figures discussed. We have not to date attempted to refresh the sensors by removing the bound antigen via chemical or other procedures.

It is possible that if the binding reaction could be reversed, the linear correlation range for impedance response and antigen concentration could be extended further to higher concentrations. Nevertheless, the analysed data indicate the fabrication of a successful sensor for the detection of ciprofloxacin in PBS, 10 mM ferri/ferocyanide solution that may form the basis for a commercial device. Published work from impedance interrogation of ciprofloxacin sensors using PBS buffer can be found in appendix I (Garifallou *et al*., 2007).

5.3 Development of immunosensors for Ciprofloxacin detection in milk

Introduction

In the previous section (section 5.2) the development of a biosensor for ciprofloxacin detection in PBS, 10 mM ferri/ferocyanide solution was described. Practical uses of the sensor e.g. in real samples such as milk and food products, had not at the time been investigated by our group. For the device developed to be of any practical value further investigations were required using this time a consumable food product. It was therefore decided to attempt to detect ciprofloxacin at various concentrations in milk. The maximum allowed concentration of ciprofloxacin or enrofloxacin in milk products has been limited to no more than 100 ng ml^{-1} by the European Union.

Other groups have reported the use of liquid chromatography based methods for the detection of fluoroquinolones in milk (Hassouan *et al*., 2007; Rodriguez-Diaz *et al*., 2006). In both works the authors report that the developed immunoassays have a detection limit of 3 ng ml^{-1}. The assay described by Rodriguez-Diaz *et al*., (2006) employed the use of luminescence detection with liquid chromatography, and it was reported to provide a linear range between 8ng and 3.5 μg ml^{-1}. ELISA based assays for fluoroquinolone detection in milk have also been reported but their detection limits are in the range of several ng ml^{-1} (Bucknall *et al*., 2006; Duan & Yuan, 2001). Cao & Mirsky, (2008) described a DNA sensor coupled with a surface plasmon resonance technique that was reported to detect between 3-20 ug ml^{-1} enrofloxacin in milk. Ionescu *et al*., (2007) described a polypyrrole based sensor coupled with an AC impedimetric capable of detecting as low as 10 pg ml^{-1} ciprofloxacin in milk. In this work the lower limit for interrogations was 0.1 ng ml^{-1}. We have previously showed that our sensors can detect ciprofloxacin in PBS at concentrations of 1 ng ml^{-1} and hence we subsequently decided to attempt the detection of lower concentrations.

Results and discussion

As can be observed in figures 5.16 and 5.17, the Nyquist and Bode plots respectively, a steady increase in impedance was shown with exposure to increasing antigen concentrations. The Nyquist plot presented in figure 5.16 displays the Z' and Z''

components of impedance and in agreement with previous observations, Z' is the main contributor to total impedance, and so further analysis will be undertaken using the real component rather than the imaginery component. The difference in impedance between baseline response and response for 10μg ml^{-1} ciprofloxacin is approximately 30 kΩ (Z'), indicating a rather high response hence adequate antigen detection. Interestingly, the increase in impedance was not in line with previously obtained data for ciprofloxacin in PBS pH 7.4, 10 mM ferri/ferocyanide solutions as described in section 5.2, where we discussed the possible reasons for impedance decrease with increasing antigen concentrations. The possible reasons for this are discussed later within this section.

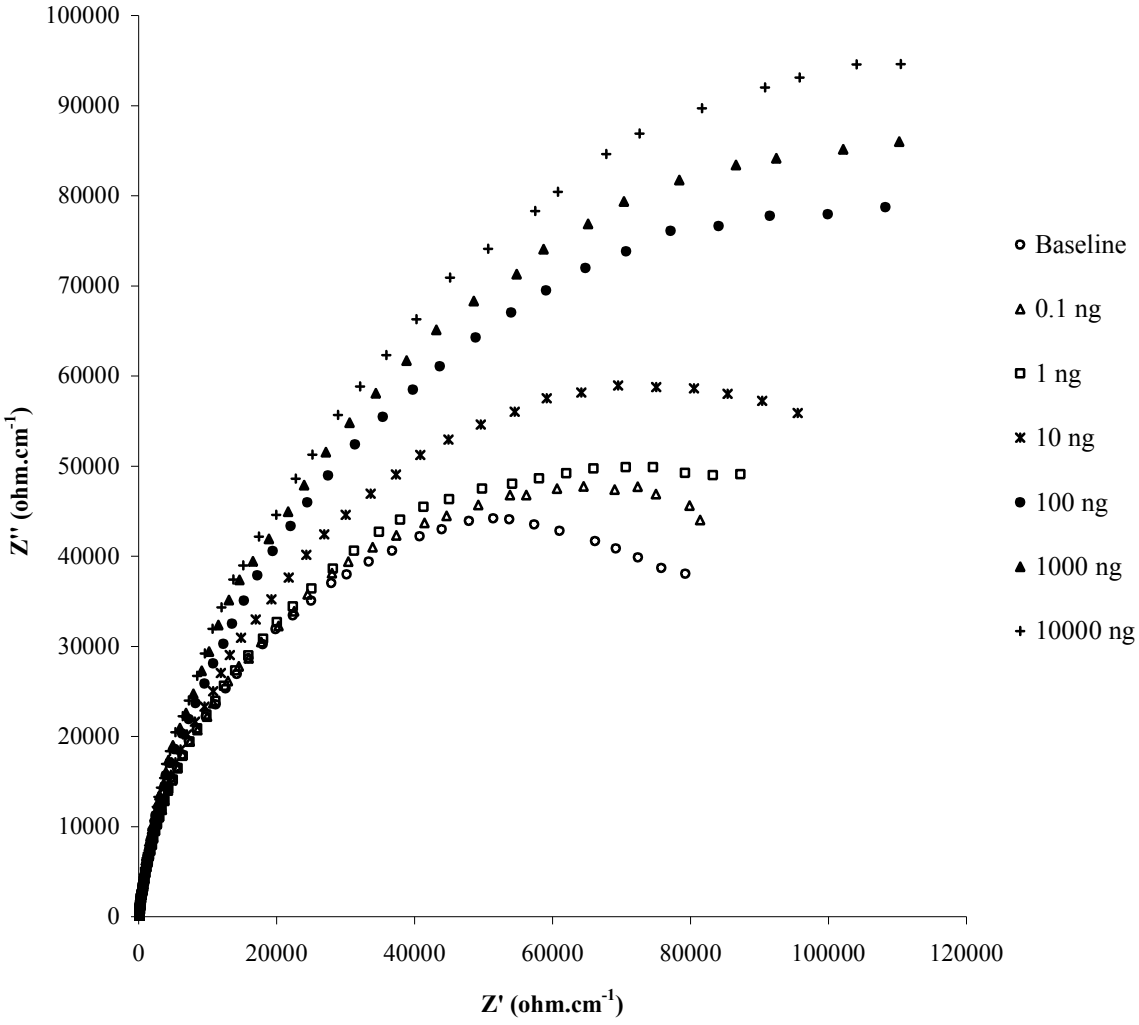

Figure 5.16 Z'' vs Z' Nyquist plot. Impedance responses of anti-ciprofloxacin loaded carbon based sensors upon exposure to various ciprofloxacin concentrations 0.1ng ml^{-1} to 10000 ng ml^{-1} (in milk).

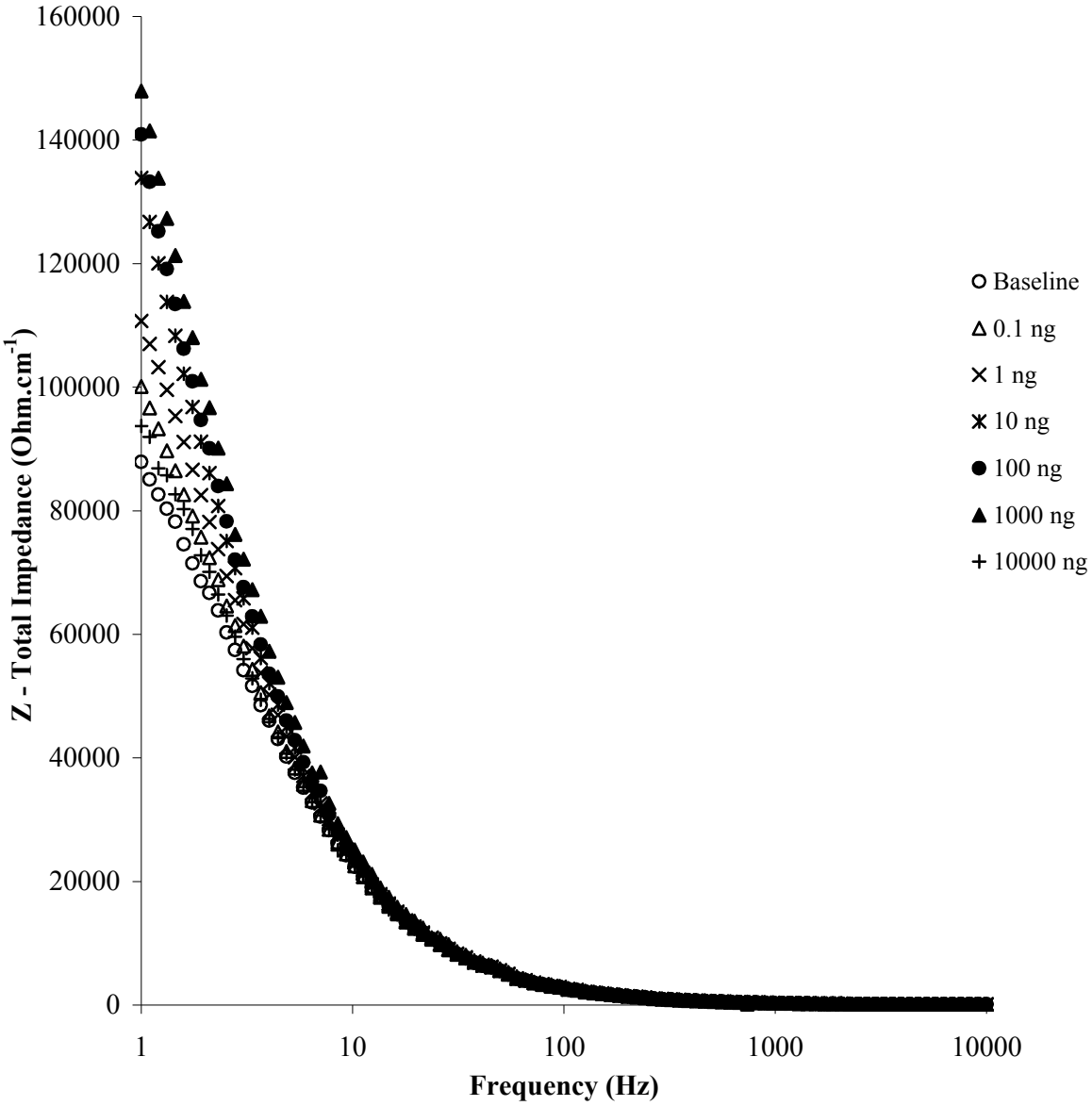

Figure 5.17: Total impedance vs frequency, Bode plot. impedance responses of anti-ciprofloxacin loaded carbon based sensors upon exposure to various ciprofloxacin concentrations (in milk).

Figure 5.18 displays the calibration curve for anti-ciprofloxacin loaded sensors at 1 Hz. As can be easily observed there was a 39% change in impedance from baseline upon exposure to 10 μg ml^{-1} ciprofloxacin.

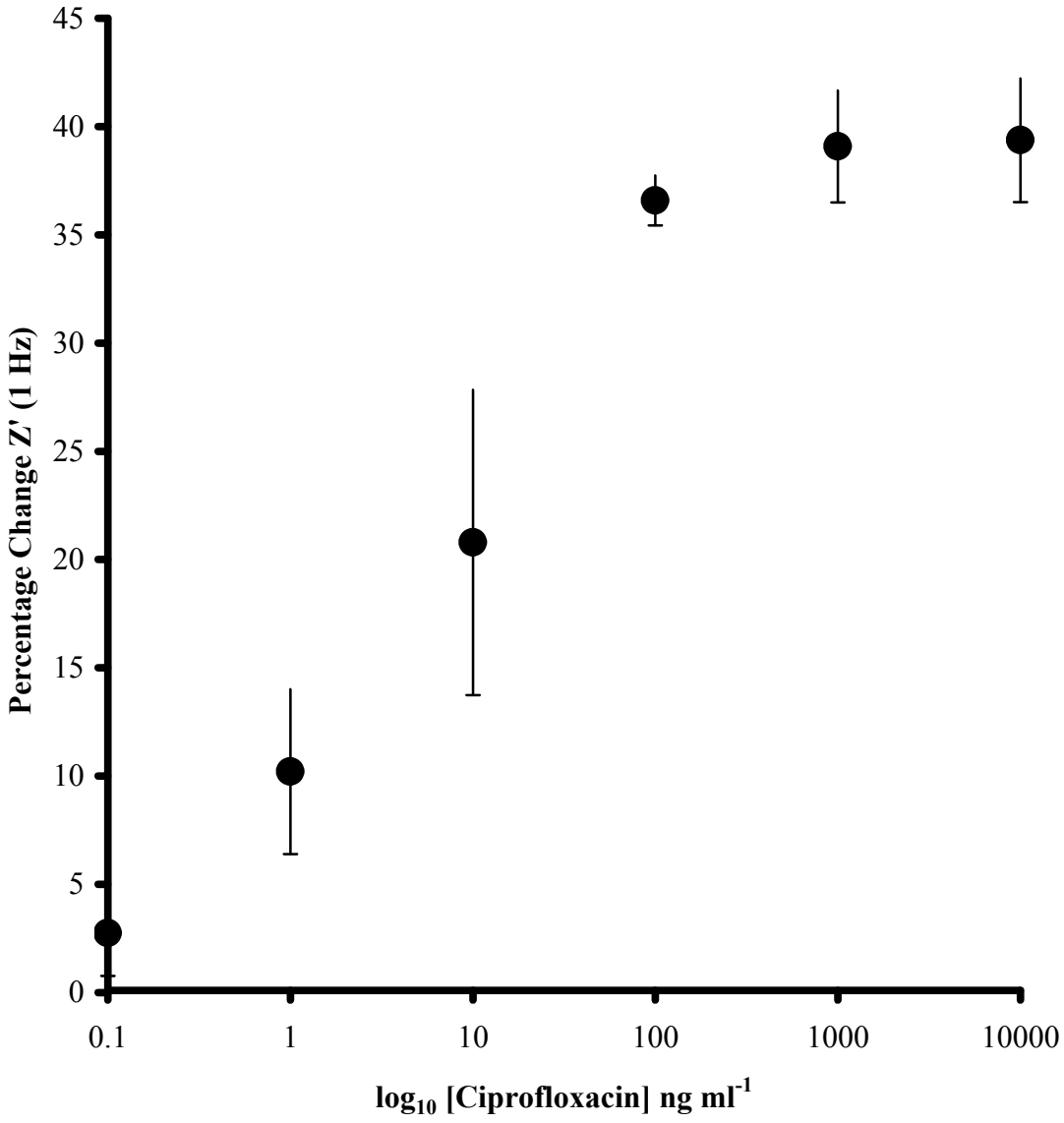

Figure 5.18 Calibration curve of per cent (%) impedance response against log_{10} ciprofloxacin concentrations (0.1ng ml^{-1} to 10000 ng ml^{-1}) for anti-ciprofloxacin doped polyaniline coated carbon electrodes at 1Hz (in milk).

Initially during this work, a set of polyclonal IgG sensors were fabricated to be used as controls similarly to previous work in this project. However, it was evident that the non-specific response in this case was not significantly lower than the specific response reaching a value 28% change to baseline upon exposure to the highest antigen concentration. Figure 5.19 depicts the calibration curve obtained for polyclonal IgG coated sensors. Milk is a complex matrix of various constituents

including proteins, salts and a plethora of other components. It is thus understood that polyclonal IgG is most likely to bind a large amount of these constituents, resulting in high impedance responses upon AC impedance interrogation. Interestingly, the IgG loaded sensors displayed impedance decrease upon exposure to milk. Milk is expected to contain a range of antigens that can be detected by antibodies present in the IgG mixture, and therefore, the high response observed for these control sensors was attributed to the nature of the matrix. Considering the complexity of milk as a sample, it is hard to make any conclusions regarding the reactions taking place on the polyclonal sensor surface and the obtained results from AC impedance interrogation at this stage. For this reason an alternative anti-PSA (since PSA is not found in milk) monoclonal antibody was chosen for the fabrication of new control sensors. As discussed in the materials and methods section, BSA was used to minimise all non-specific binding, as a result the observed responses for the polyclonal sensors were indeed caused by the polyclonal antibodies binding a range of antigens found in milk.

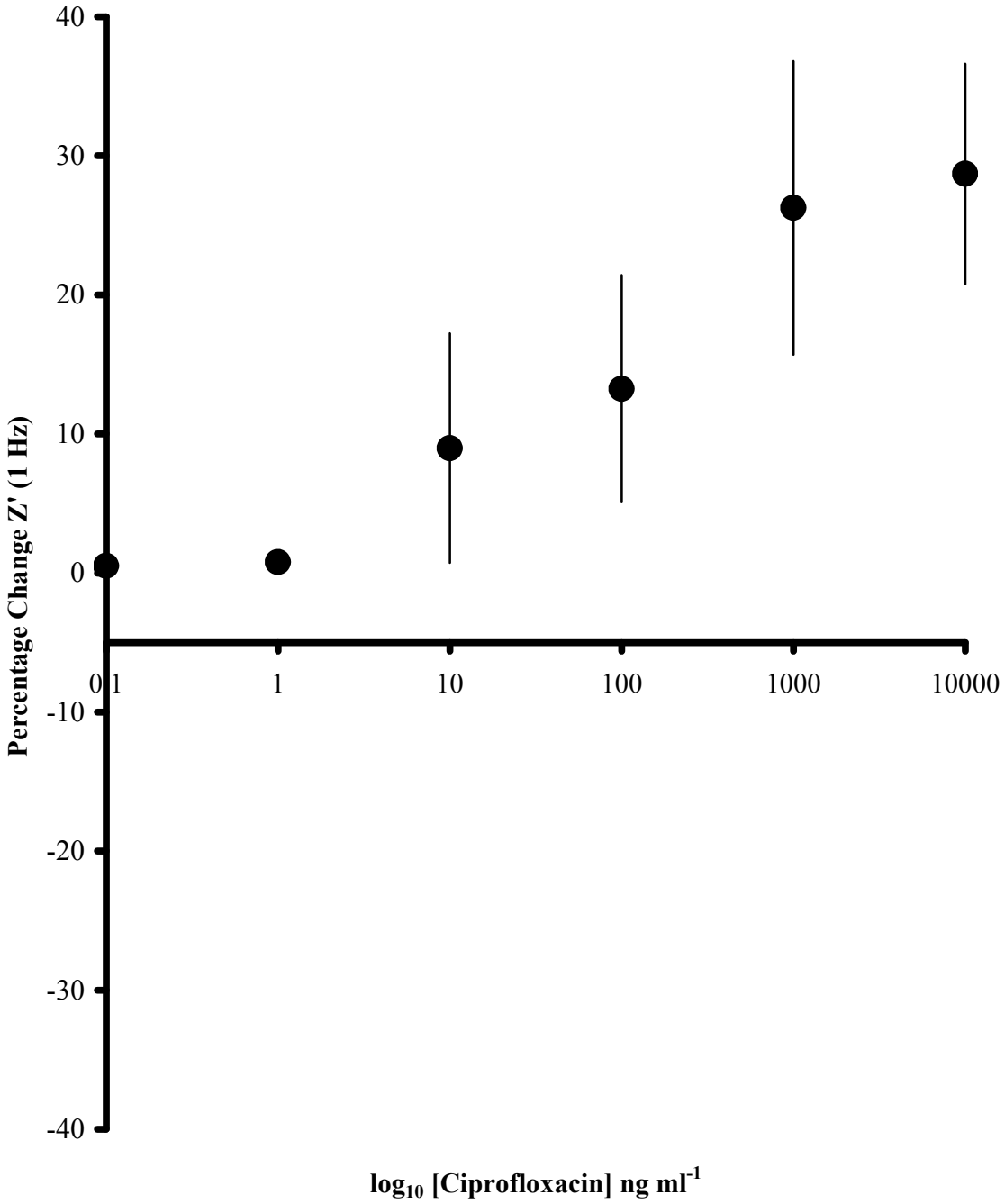

Figure 5.19: Calibration curve of per cent (%) impedance response against log_{10}ciprofloxacin concentrations (0.1ng ml^{-1} to 10000 ng ml^{-1}) for polyclonal IgG doped polyaniline coated carbon electrodes at 1Hz (in milk).

Figure 5.20 depicts the calibration curve obtained for anti-PSA based sensors when these were exposed to the chosen range of ciprofloxacin concentrations in milk. As expected, the non-specific responses obtained were a minimal fraction of the specific

responses reaching 11% change from baseline at 10 μg ml^{-1} ciprofloxacin. As previously, these were subtracted from their respective specific responses in order to produce a corrected calibration curve accounting for any non-specific interactions.

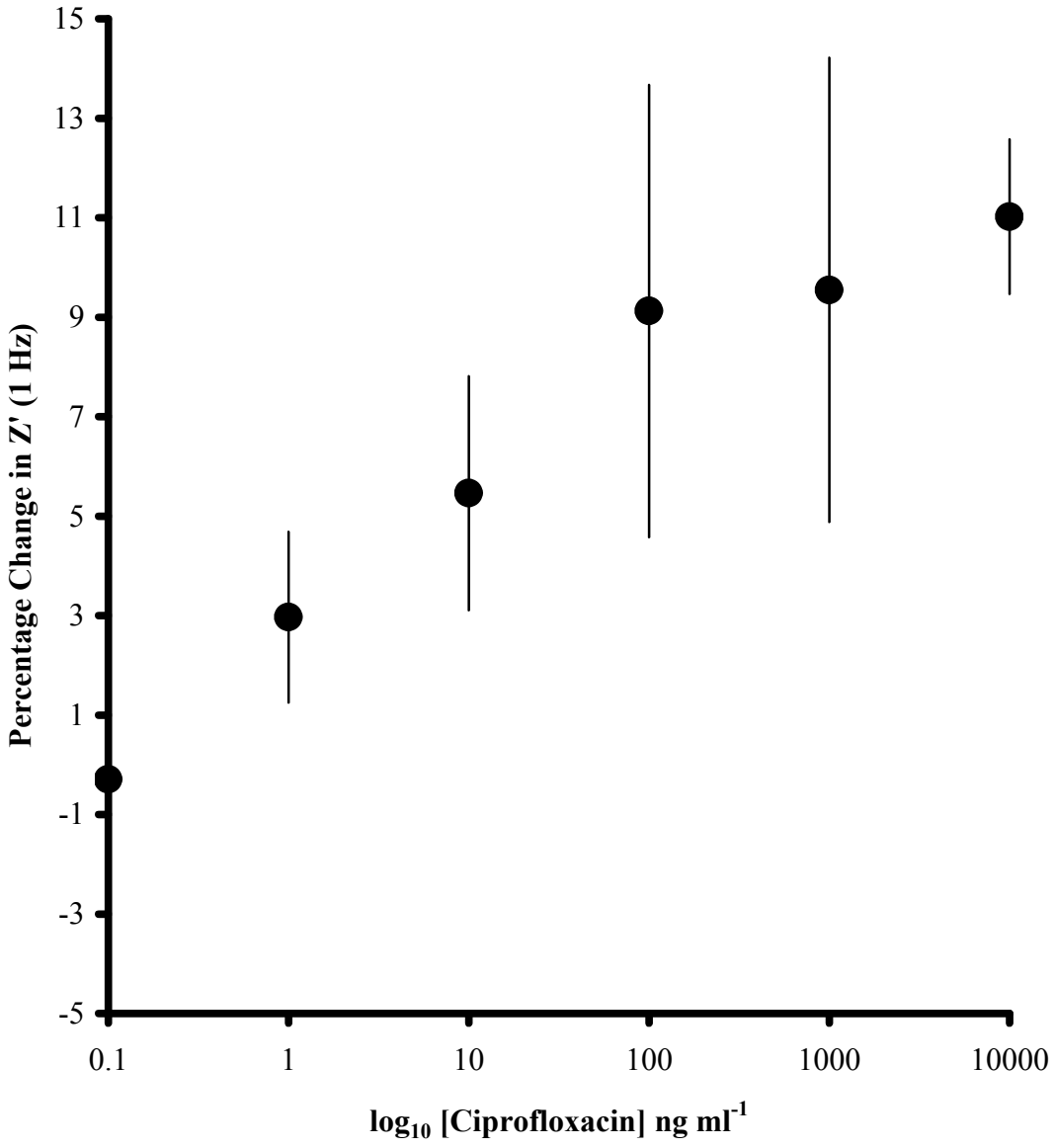

Figure 5.20: Calibration curve of per cent (%) impedance response against log_{10} ciprofloxacin concentrations (0.1ng ml^{-1} to 10000 ng ml^{-1}) for anti-PSA doped polyaniline coated carbon electrodes at 1Hz (in milk).

Figure 5.21 represents the corrected calibration curve obtained upon AC impedance interrogation for the chosen range of antigen concentrations. As previously, these values are those obtained from the real component of impedance at 1 Hz.

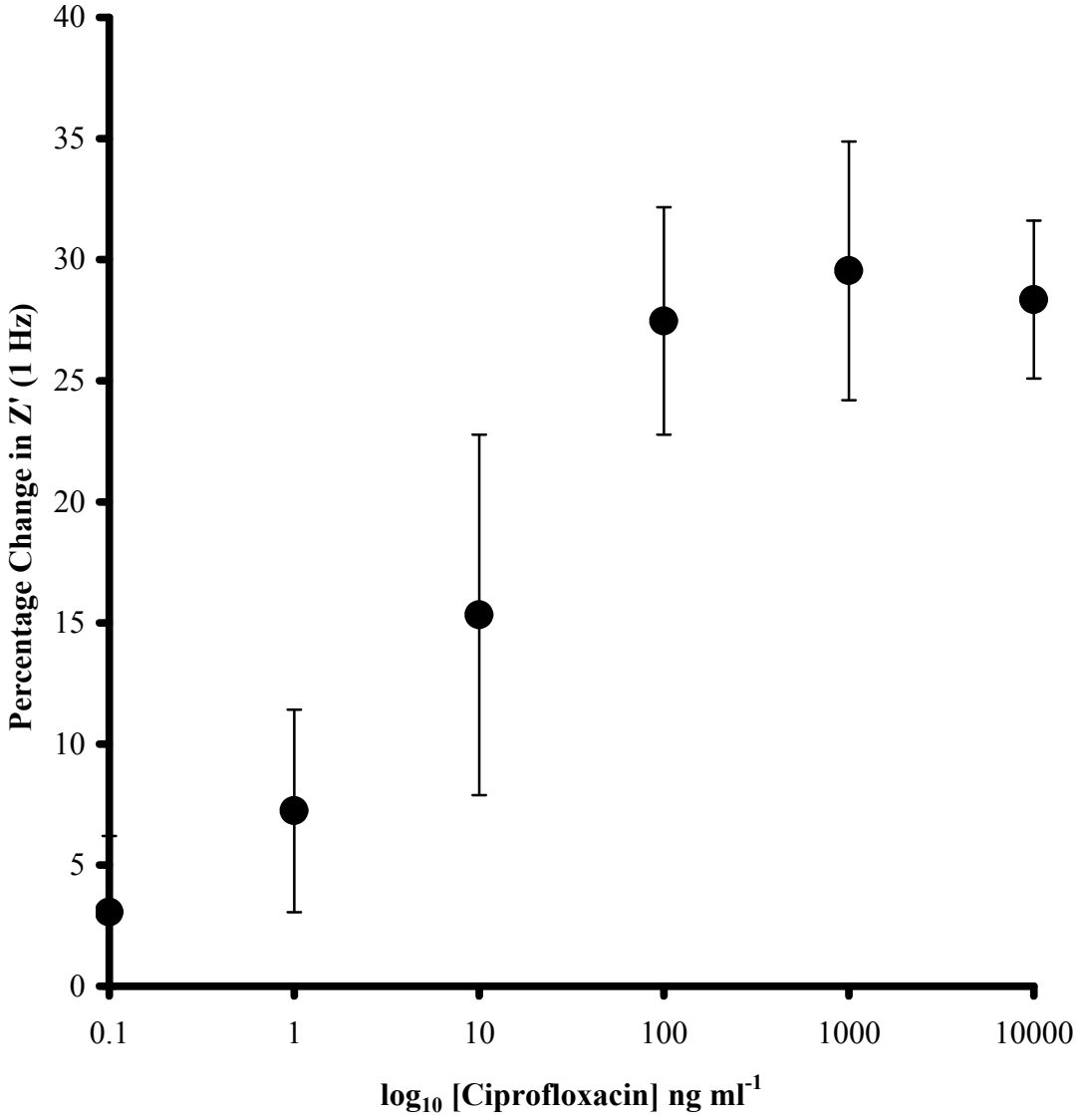

Figure 5.21: Corrected calibration curve of per cent (%) impedance response against log_{10} ciprofloxacin concentrations (0.1ng ml^{-1} to 10000 ng ml^{-1}) for anti-ciprofloxacin doped polyaniline coated carbon electrodes at 1Hz (in milk).

Figure 5.22 displays the corrected calibration curve for the range between 0.1-100 ng ml^{-1} ciprofloxacin concentrations. In accordance with previous work, there is a linear correlation between impedance increase and log_{10} antigen concentration in the lower

range of concentrations and up to 100 ng ml^{-1} (R^2=0.95), whereas higher concentrations tend towards a plateau indicating sensor saturation.

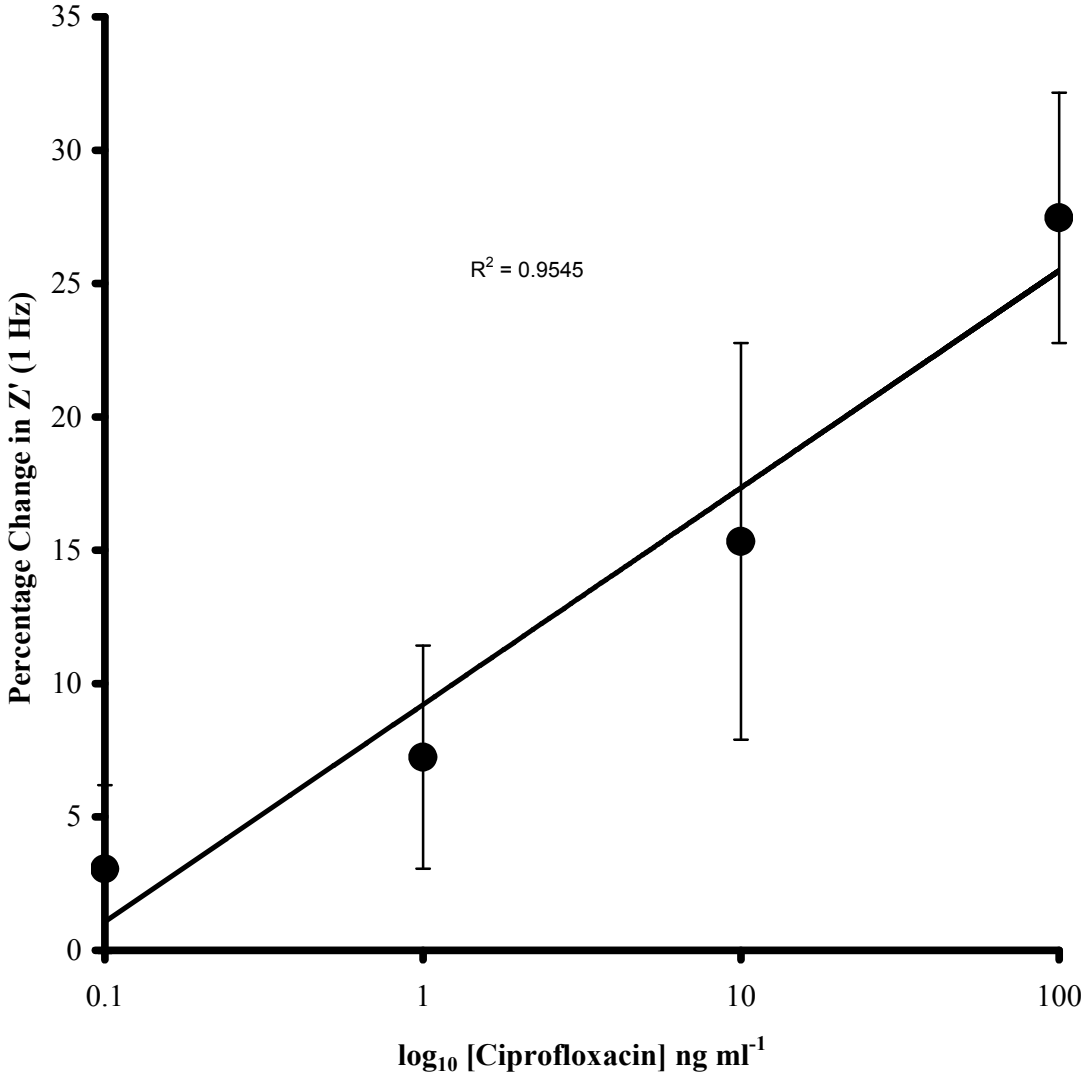

Figure 5.22: Corrected calibration curve of per cent (%) impedance response against log_{10} ciprofloxacin concentrations (0.1ng ml^{-1} to 10000 ng ml^{-1}) for anti-ciprofloxacin doped polyaniline coated carbon electrodes at 1Hz (in milk). 1-100 ng ml^{-1} concentration range.

The matter of increasing impedance upon exposure to antigen has been discussed earlier in this work in regards with non-specific adsorption and also the nature of some large molecular weight antigens. Ciprofloxacin is known to form chelation complexes with the calcium ions present in milk. These complexes give rise to

increasing impedance upon binding rather than decrease which has previously been described for ciprofloxacin samples in PBS buffer and a redox couple. Whether it is the chemical properties of chelation complexes or their size that causes increase in impedance is at this stage unknown.

Conclusions

Ciprofloxacin and other fluoroquinolone antibiotics are reported to form calcium chelate complexes in the presence of calcium ions. These complexes consist of two ciprofloxacin units attached to one calcium ion (Katz & Willner, 2003; Upadhyay *et al*., 2006). It was previously observed within our group that DNA based sensors give rise to such variations in impedance behaviour. Adsorption of complimentary DNA on the sensor surface led to impedance decrease while adsorption of non-complimentary strands led to impedance increase (Davis *et al*., 2004; Davis *et al*., 2007). It is, nevertheless, obvious that the fabricated immunosensors can detect ciprofloxacin in milk and PBS buffer and hence it is evident that the detection of both free and chelated ciprofloxacin is achievable. The obtained results also indicate that our sensors can differentiate between the free and complexed form of ciprofloxacin by means of impedance decrease or increase, respectively, upon exposure to antigen. The development of successful immunosensor for the detection of ciprofloxacin has been described. The fabricated sensors where to found to have detection limits between 0.1 ng and 10 μg ml^{-1} upon interrogation by an AC impedance protocol.

Chapter 6
Development of immunosensors for the detection of digoxin

Introduction

Digitalis or as it is more widely known, Digoxin, is a plant extract from Digitalis lanata (Hollman, 1996). Digoxin is a purified cardiac glycoside used for the treatment of congestive heart failure and cardiac arythmia. It is often used for conditons such as atrial fibrillation, atrial flutter and also heart failure that cannot be controlled by any other medication. Therapeutic preparations based on Digoxin include Lanoxin, Digitek and Lanoxicaps.

The mode of action of digoxin is based on effects on both the heart directly and the parasynthetic nervous system. Any effects on the parasynthetic system are due to the regulation of plasma norepinephrine. The drug can block the antrioventricular node causing a reduced conduction velocity thus essentially decreasing electrical pulses followed by decreases in heart rate; therefore it is invaluable for conditions like arythmia (Chun & Chodosh, 2006; Dawson & Buckley, 2007). Its direct cardiac effect is the increase of the force of contraction via inhibition of the Na^+/K^+ ATPase dependant pump (sodium-potassium pump).This is a transmembrane protein that helps to maintain resting potential, mediates transport and regulates cellular volume. Digoxin can bind to the extracellularly located a-subunit of this protein on myocyte (heart) cells and compete with K^+ ions. This binding effect results in the increase of Na^+ ions in the cellular environment which leads to an increase in Ca^{2+} ions. The reason for this is that the activity of the Na^+/Ca^{2+} pump is slowed down by increased levels of Na^+. Eventually, these events lead to an increase in phases 4 and 0 of the cardiac action potential, which controls the function of the electrical conditions system in the heart. These effects alongside the parasynthetic nervous system effects lead to a decrease in heart rate. The increased amounts of Ca^{2+} are stored in the sarcoplasmic reticulum and released by each action potential resulting in increased contractivity of the heart (Goldstein *et al*., 2006; Chun and Chodosh, 2006).

The adverse effects of digoxin are concentration dependant and normally occur when the serum concentration of the drug exceeds 0.8 ng ml^{-1}. The therapeutic range of digoxin has been referred as between 0.8-2 ng ml^{-1} (Wang & Song, 2005), so adverse effects are inevitable in most cases. Several reports indicate that heart failure patients being treated with high concentrations show higher all-cause mortality rates than

patients being administered the drug at lower concentrations (Wang & Song, 2005). It is widely known, however, that anything surpassing 2 ng ml^{-1} leads to toxicity. Patients with low K^+ levels often suffer adverse effects since, as discussed earlier in this section, digoxin competes with K^+ for binding to Na^+/K^+ transmembrane protein. Some of these unwanted consequences of digoxin use include nausea, vomiting, diarrhea and other disturbances that can occur due to use of medication. Less frequent but more severe adverse effects include acute psychosis, delirium, amnesia and many more. Goldstein *et al*., (2006) report that Na^+/K^+ ATPase activity may be involved in the etiology of mental disorders. Consequently any medication that can affect the transmembrane protein function, such as digoxin, may also play a role in the development of depressive disorders.

Digoxin toxicity results from the paralysis of the sodium-potassium pump giving rise to a condition known as malignant hyperkalaemia. The most effective treatment requires the use of anti-digoxin antibodies for removal of the drug from the system. The severe adverse effects of digoxin present the necessity for reliable assays that can rapidly and effectively determine the serum concentrations of the drug.

Results and discussion

We have previously described successful impedimetric based sensors for the detection of ciprofloxacin in PBS 7.4, 10 mM ferri/ferocyanide, and ciprofloxacin in milk as a real sample. The current work aims to develop biosensors for the detection of digoxin in PBS 7.4, 10 mM ferri/ferocyanide solution. The chosen concentration range reflects the range of clinical significance for digoxin. Due to anti-digoxin being supplied at low concentrations it was not possible to maintain the antibody concentration a 1mg ml^{-1} following the biotynilation procedure. The antibody was further purified and concentrated, however, the maximum concentration reached was 0.5 mg ml^{-1}. The corresponding IgG loaded sensors were treated with 500 mg ml^{-1} IgG antibody in an attempt to maintain uniform sensor fabrication procedure.

Figures 6.1 and 6.2 contain the average Nyquist and Bode plots from 3 replica anti-digoxin loaded sensors and their responses upon antigen exposure and followed by AC impedance interrogation. As in earlier work the real component of impedance

was found to be the major contributor to total impedance. A 4.2kΩ change from baseline was observed following exposure to the highest concentration of digoxin at 10 ng ml^{-1}. As depicted in figure 6.1 the characteristic impedance semicircles were gradually decreasing when the sensors were exposed to higher antigen concentrations. This behaviour was also observed for anti-ciprofloxacin loaded sensors interrogated in PBS 7.4, 10 mM ferr/ferocyanide solution, supporting the assumption that specific binding or bare antigen results in impedance decrease rather than increase. As can be readily observed sensor saturation occurs at 2 ng ml^{-1} since impedance at this concentration appears to increase rather than decrease.

It has already been discussed that upon saturation the sensors may provide erroneous results that are related to non-specific binding. The low concentration of anti-digoxin available for sensor fabrication explains early saturation. Data obtained for IgG control sensors support this assumption. It is apparent, that given higher concentrations of purified biotinylated antibody, the sensors would most likely not show early saturation signs.

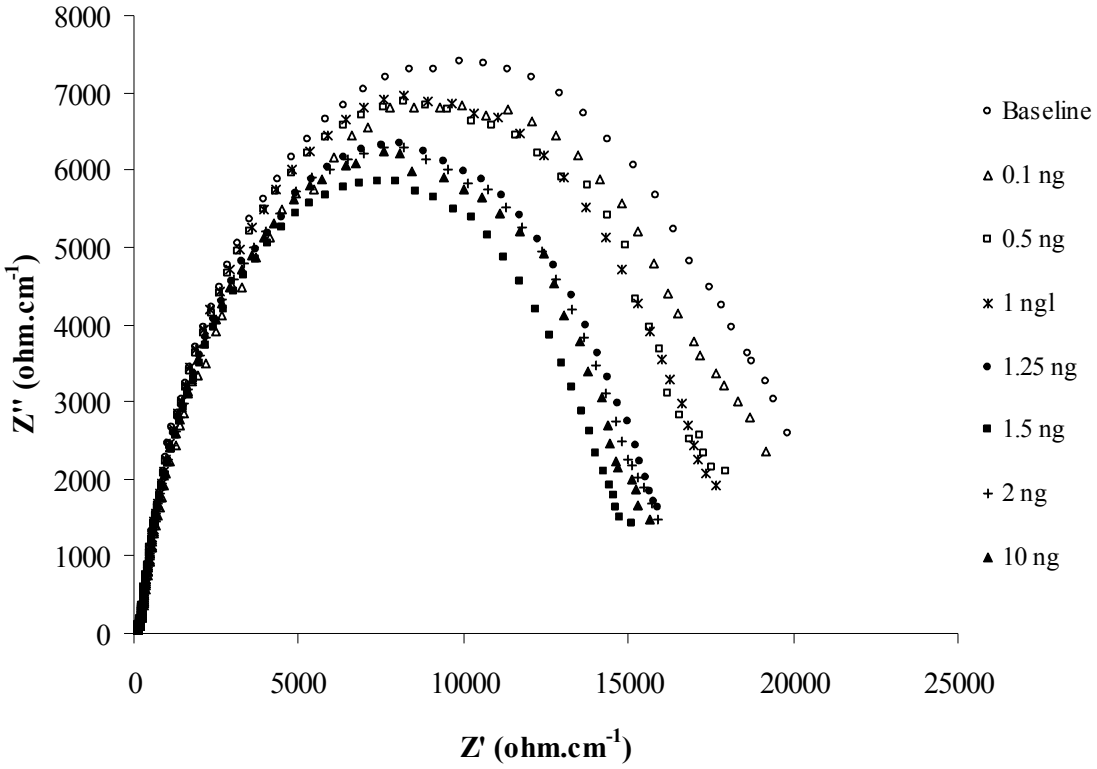

Figure 6.1 Z' vs Z'', Nyquist plot. Impedance responses of anti-digoxin loaded carbon based sensors upon exposure to various digoxin concentrations (in PBS, 10 mM ferri/ferocyanide).

Figure 6.2 depicts the average Bode plot for the chosen concentration range of digoxin. In line with previous work, a drop in impedance is observed upon exposure to higher concentrations of antigen with the highest obtained impedance values obtain at 1 Hz. It can also be seen in the Bode plot that sensor saturation has occurred following addition of antigen at 2 ng ml^{-1}, indicated by the fact that total impedance at this concentration of digoxin is slightly higher than the response obtained for 1.5 ng ml^{-1} but also very similar to the impedance obtained upon addition of digoxin at 10 ng ml^{-1}.

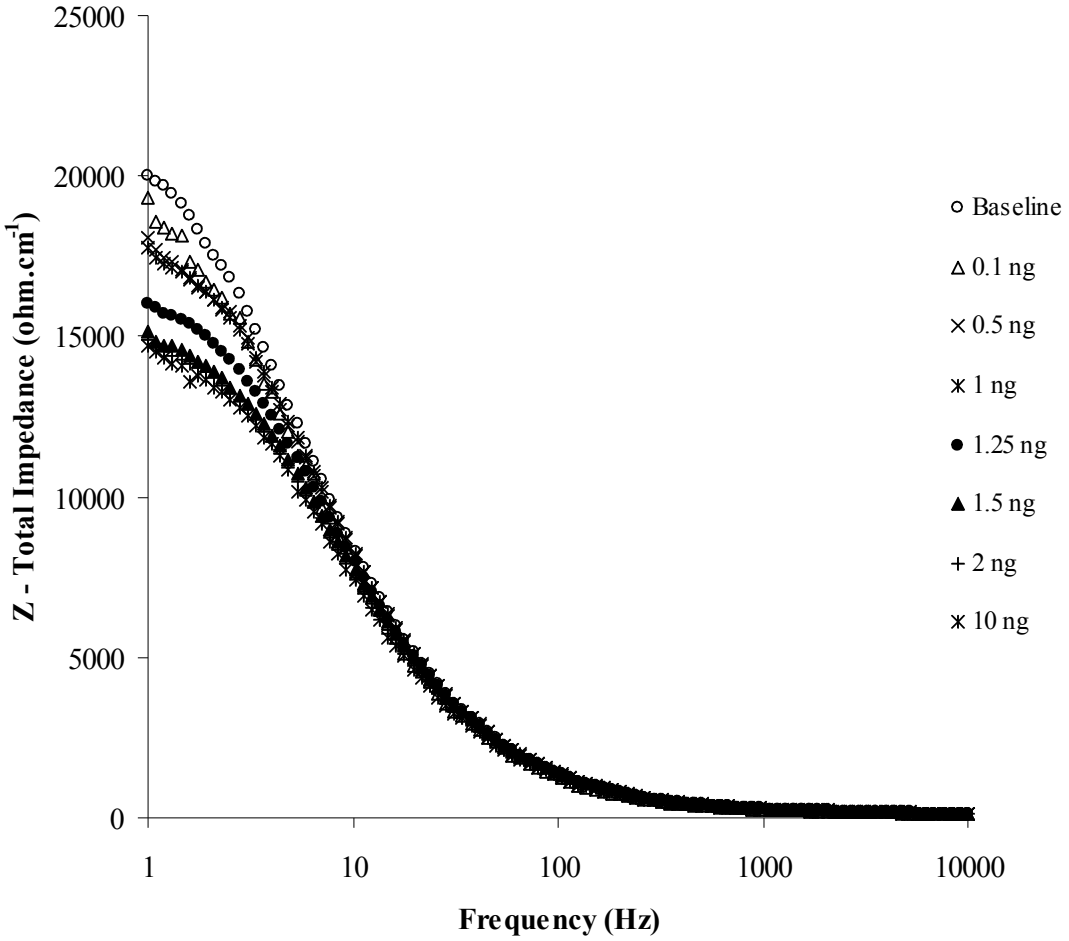

Figure 6.2Total impedance vs frequency, Bode plot. Impedance responses of anti-digoxin loaded carbon based sensors upon exposure to various digoxin concentrations (in PBS, 10 mM ferri/ferocyanide).

Figure 6.3 displays the calibration profile for ac impedimetric responses of anti-digoxin sensors at 1 Hz. A 24.16% increase is obvious at 1.5 ng ml^{-1} antigen with impedance change dropping again at the final concentration as already discussed, due to saturation. A near linear correlation to antigen concentrations is observed between 1-1.5 ng ml^{-1} digoxin with the R^2=0.96. Figure 6.4 displays the percent impedance change upon digoxin exposure for the control sensor fabricated through the same procedures to specific sensors. Non-specific sensor saturation is extremely apparent. This can be explained by the low concentration of biotynilated antibody used to treat the sensor before interrogation with AC impedance. High variation is also observed among the IgG replicas indicating that these standard errors will dominate the corrected calibration curve.

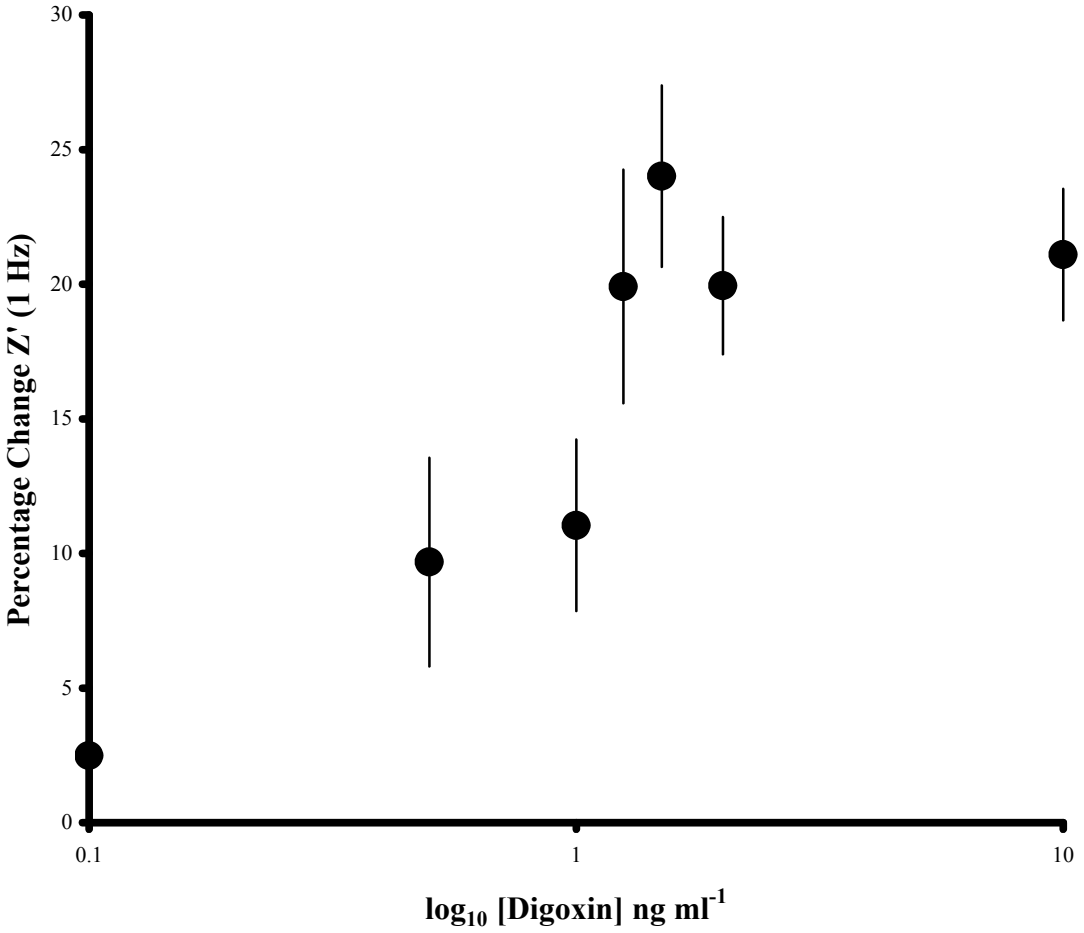

Figure 6.3: Calibration curve of per cent (%) impedance response against log_{10} digoxin concentrations (0.1 ng ml^{-1} to 10 ng ml^{-1}) for anti-digoxin doped polyaniline coated carbon electrodes at 1Hz (in PBS, 10 mM ferri/ferrocyanide).

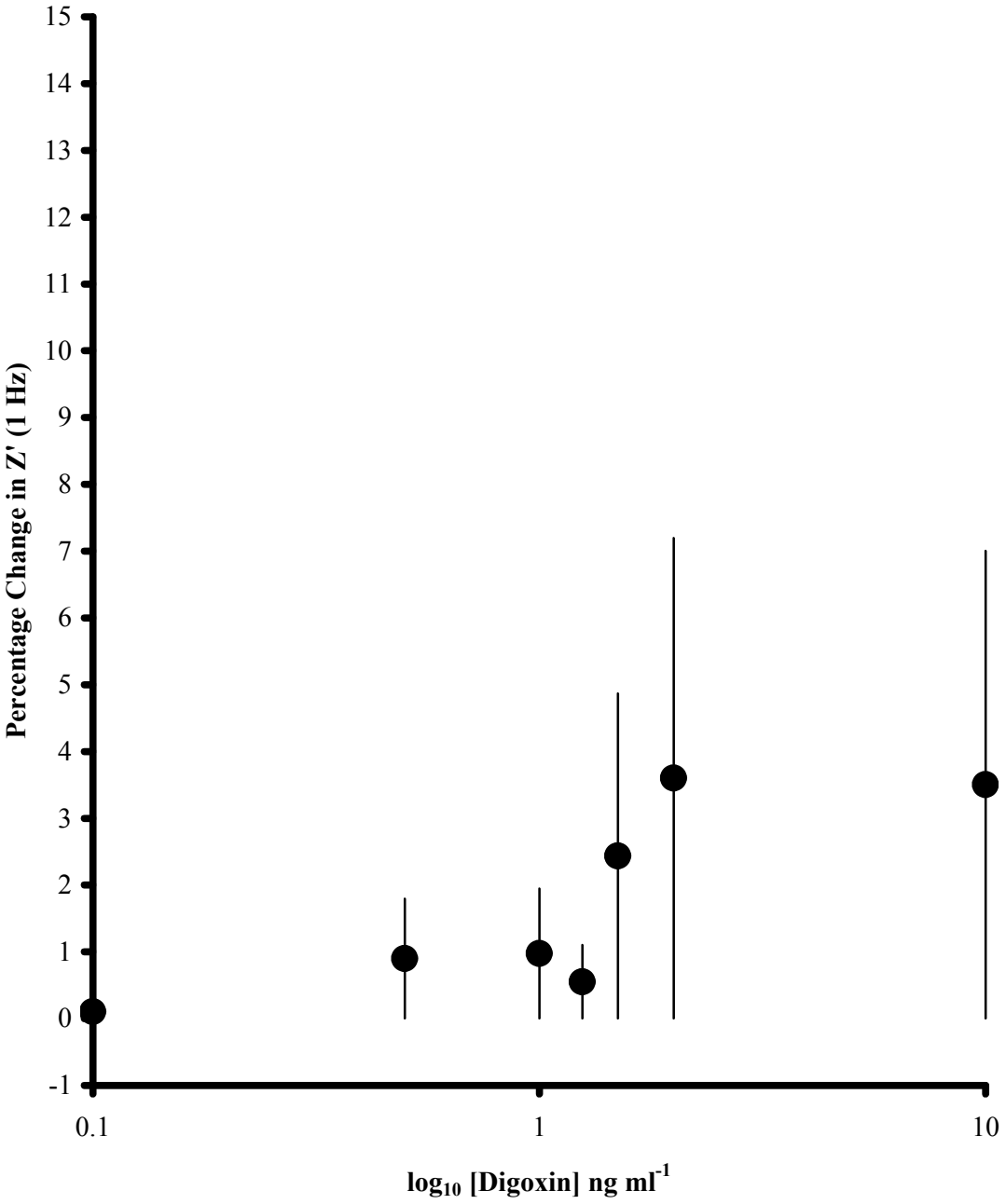

Figure 6.4: Calibration curve of per cent (%) impedance response against log_{10} digoxin concentrations (0.1 ng ml^{-1} to 10 ng ml^{-1}) for polyclonal IgG doped polyaniline coated carbon electrodes at 1Hz (in PBS, 10 mM ferri/ferrocyanide).

Figure 6.5 contains the corrected calibration curve for digoxin over the chosen range of concentrations. The response as already discussed is largely affected by the high variation observed among IgG sensors due to immediate saturation.

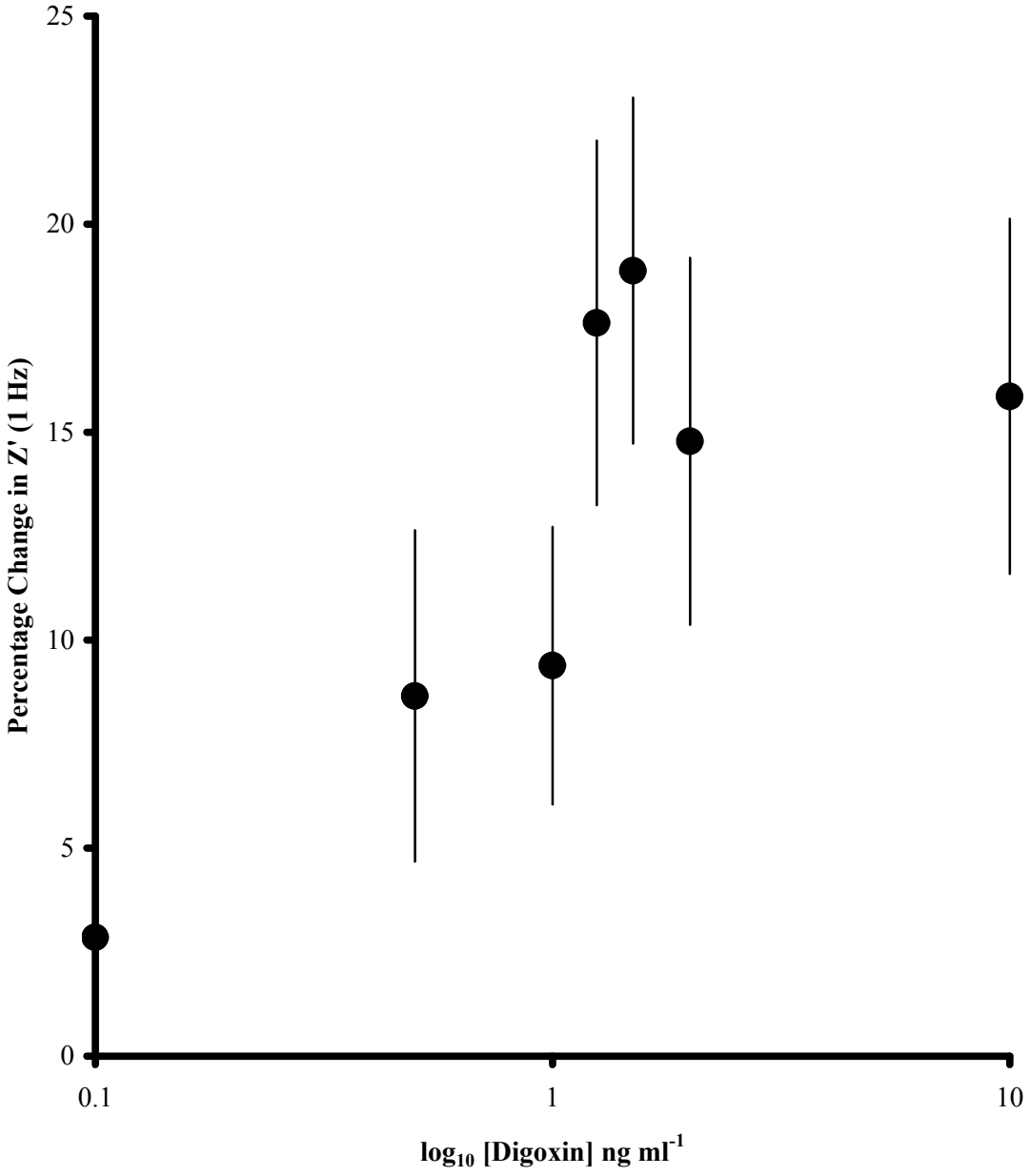

Figure 6.5 Corrected calibration curve of per cent (%) impedance change against digoxin concentrations (0.1 ng ml^{-1} to 10 ng ml^{-1}) for anti-ciprofloxacin doped polyaniline coated carbon electrodes at 1Hz (in PBS, 10 mM ferri/ferrocyanide).

As shown in figure 6.6 the linear correlation to $\log_{10}$ concentration of antigen for the corrected calibration curve between 1-1.5 ng ml^{-1} is R^2=0.89.

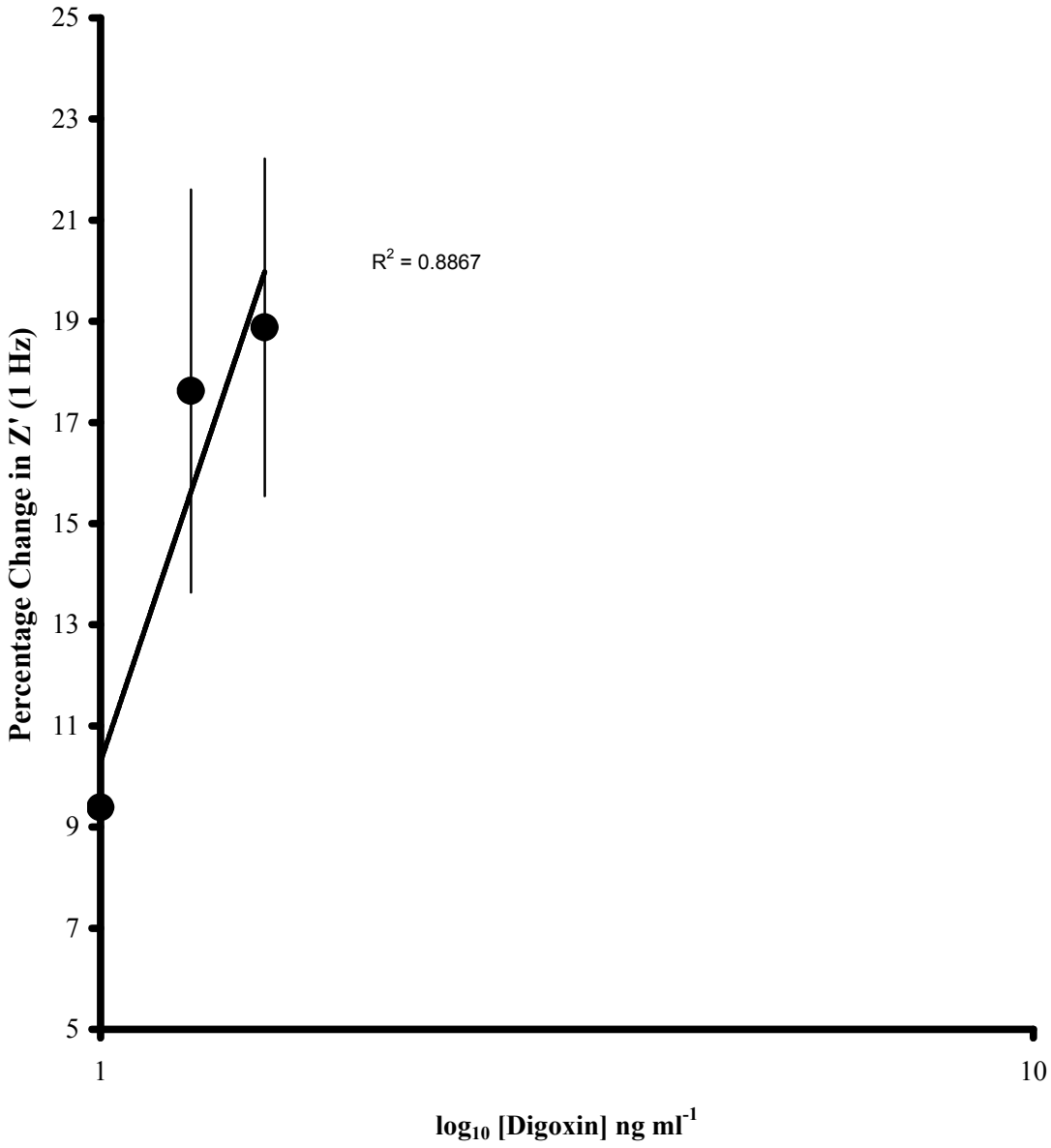

Figure 6.6 Corrected calibration curve of per cent (%) impedance change against $\log_{10}$ digoxin concentrations (0.1 ng ml^{-1} to 10 ng ml^{-1}) for anti-ciprofloxacin doped polyaniline coated carbon electrodes at 1Hz (in PBS, 10 mM ferri/ferrocyanide). 1-1.5 ng ml^{-1} digoxin concentrations.

Conclusions

It is clear that given a higher concentration of purified anti-digoxin, saturation would not be observed so early and a more extended range would be achieved. The

polyclonal IgG response might also display lower variability hence allowing for the production of a calibration curve with smaller error bars that could have been taken as being more reliable. The low molecular weight of digoxin indeed makes it a hard to detect molecule so the observed data, while, indicating early sensor saturation still prove that the developed immunosensors can detect even minute molecules and hence prove the selectivity of the proposed system.

Chapter 7
Development of immunosensors for the detection of Green fluorescent protein

Introduction

The green fluorescent protein was isolated from the jellyfish *Aequorea victoria*. It is a large protein with a molecular weight of 26.9 kDa, comprised of 238 amino acids and upon exposure to blue light fluoresces green. The mechanism responsible for conversion from blue light to green involves the Ca^{2+} sensitive photoprotein, aequorine. According to Errampalli *et al*., (1999) the active chromophore is a tripeptide that maturates in the presence of oxygen. In 1992, molecular biology based techniques were used for the development of a GFP-based reporter system displaying visible fluorescence (Errampalli *et al*., 1999). Wild type GFP absorbs light at 395 nm and emits green light at 510 nm in both bioluminescent organisms or in a purified form present in solution. Cloned GFP cDNA from *A. Victoria* was successfully obtained in 1992 while the cloned gene was further introduced in oprganisms like Drosophila and *E. coli* and shown to cause fluorescence. The GFP gene can be introduced into intact cells or cell organells and be exploited as a reported gene for gene expression and protein localisation.

As a reporter protein, GFP is harmless to the host cells or organisms and can thus be used for *in vivo* as well as *in vitro* monitoring. Detection is simply based on exposure to blue or ultraviolet light and the addition of either substrates or complex culture media is not required. GFP based detection and monitoring systems are characterised by low equipment cost. In contrast, other alternatives such as the *luxAB* gene, require aldehyde substrates for visualisation to be possible. GFP is characterised by high stability to temperature ($65^{o}C$), pH (6-12) and a range of denaturants.

Errampalli *et al*., (1999) report that molecules produced from a single copy of wild type GFP present in the bacterial chromosome did not fluoresce enough to allow detection by fluorescence microscopy. Other workers have reported that a minimum of 10,000 wild type GFP molecules in tissue culture cells were required for microscopy based detection. Fortunately, a mutant GFP strain was isolated, *Psedomonas putida*, which displayed higher solubility and cytoplasmic distribution alongside more fluorescence, thus allowing single cell detection *in situ* (Errampalli *et al*., 1999; Eberl *et al*., 1997).

GFP mutants have been developed that emit blue, red and yellow light, each at different excitation and emission wavelengths. These mutants have made it possible to detect and simultaneously monitor a number of bacterial species co-existing in the same environment. Quantitative studies carried out by Patterson *et al*., (1997), showed that no single GFP variant is well suited for all applications, but rather, each has specific advantages and disadvantages over the others, and thus the appropriate protein can be chosen depending upon the specific application objectives.

GFP is currently used to monitor a variety of environmental and ecological processes. It is used for monitoring of genetically modified organisms introduced into the environment, plant-microbial interactions, biofilm studies and biodegradation monitoring. Similarly, GFP has found use in the sensing industry. Errampalli *et al*., (1999), discuss the development of bioluminescence based sensors based on the reduction of light emission in the presence of pollutants that are toxic to bacterial cells. One aspect considered by the authors, is that GFP fluorescence is not dependent on cellular metabolic activity, thus toxicity assessment may not be reliable. Nevertheless, the protein has been invaluable to science as observed by the vast number of scientific works employing its use.

Results and discussion

In this work, we aim to develop biosensors for the detection and quantification of GFP. As discussed in previous sections of this report, successful sensors for ciprofloxacin, digoxin and myelin basic protein have been developed by our group. The same approaches were used for the fabrication of anti-GFP based sensors in the current work. Following biotynilation, the antibody sample required concentration and removal of sodium azide. This was carried out as described in the materials and methods section. The achieved concentration was 0.3 mg ml^{-1}. Previous works has shown that low antibody concentrations have detrimental effects in the detection range of the sensors, simply due to saturation. Sensors loaded with polyclonal IgG are always matched to specific sensors with regards to the concentration of immobilised antibodies. The problem therein is that IgG loaded sensors become saturated much faster than the specific sensors. This has been shown to result in high variation among the polyclonal IgG loaded replicas, which subsequently affects the variation observed

in the corrected response. For this reason, and since there is no range of clinical significance for GFP, it was decided to initiate measurements from an antigen concentration of 0.1 ng ml^{-1} and increase the concentration by steps of one order of magnitude until saturation signs were observed. The anti-GFP obtained and used for this work was derived from mouse myeloma cells and the murine polyclonal IgG was used for the control sensors. The GFP protein used for this work was of the wild type and produced in *E. coli*. The final aim of this work was to visualise the immobilised protein on the sensor surface using fluorescence microscopy, however, no fluorescence was observed upon microscopic examination. The possible reasons for this are discussed in the end of this chapter.

Figures 7.1 and 7.2 represent the data obtained for anti-GFP loaded sensors upon antigen exposure at a range of GFP concentrations and subsequent impedance interrogation. As can be seen in figure 7.1, a characteristic semicircle region occurs for each of the chosen concentrations indicating the charge transfer process. Gradual increases in impedance are obvious upon addition of higher antigen concentrations. This was not in accordance with previously obtained data for ciprofloxacin and digoxin, where, addition of antigen on specific sensors resulted in impedance drop rather than increase. As discussed earlier, each antibody/antigen pair behaves differently and the nature of the complex heavily affects the resulting impedance changes. It was shown in previous work on myelin basic protein (Tsekenis *et al.,* 2008) that addition of MBP on specific sensors also resulted in impedance increases. Similarly to MBP, GFP is a rather large protein with a molecular weight of 16.9 kDa. Ciprofloxacin and digoxin both have extremely lower molecular weights compared to MBP and GFP, and have both caused impedance decrease upon addition to specific antibody loaded sensors. The results from all previous work and current work suggest that the molecular weight of the antigen may play a role in the resulting impedance of the system. It can be assumed that large molecules generally cause impedance increases while smaller molecules cause impedance decrease upon binding to their respective specific antibodies. Further work would be required to support or reject this theory, however, the results obtained within our work and the limited knowledge of the impedance mechanism itself are only enough to note the occurring phenomenon, but cannot to date, explain it in more depth.

It is clear in figures 7.1 and 7.2, that no saturation of the sensors occurred even at the highest concentration of the chosen range since a rather large change in impedance was observed upon addition of GFP at 100 ng ml^{-1}. A change above 7 kΩ from baseline was observed upon addition of 100 ng ml^{-1} GFP as shown by the real component of impedance. Similarly to previous work, the real component was preferred for the production of calibration curves as it is again the major contributor of impedance in the observed system. The occurring changes in total impedance can be viewed in figure 4.40 which depicts the Bode plot for the specific antibody loaded sensors. An approximate 7 kΩ change from baseline was observed in total impedance upon addition of GFP at 100 ng ml^{-1}. The range tested for this set of sensors was between 0.1-100 ng ml^{-1} GFP. This can be accounted for by an early saturation of the non-specific sensors. As discussed earlier, saturation of the polyclonal antibody loaded sensors results in high variation which eventually has a detrimental effect on the corrected calibration curve. Due to time limitations and unavailability of more concentrated antibodies at the time, this work was not repeated for a more extensive GFP concentration range, however, it is obvious from these results that the detection range for GFP could be extended to lower as well as higher limits.

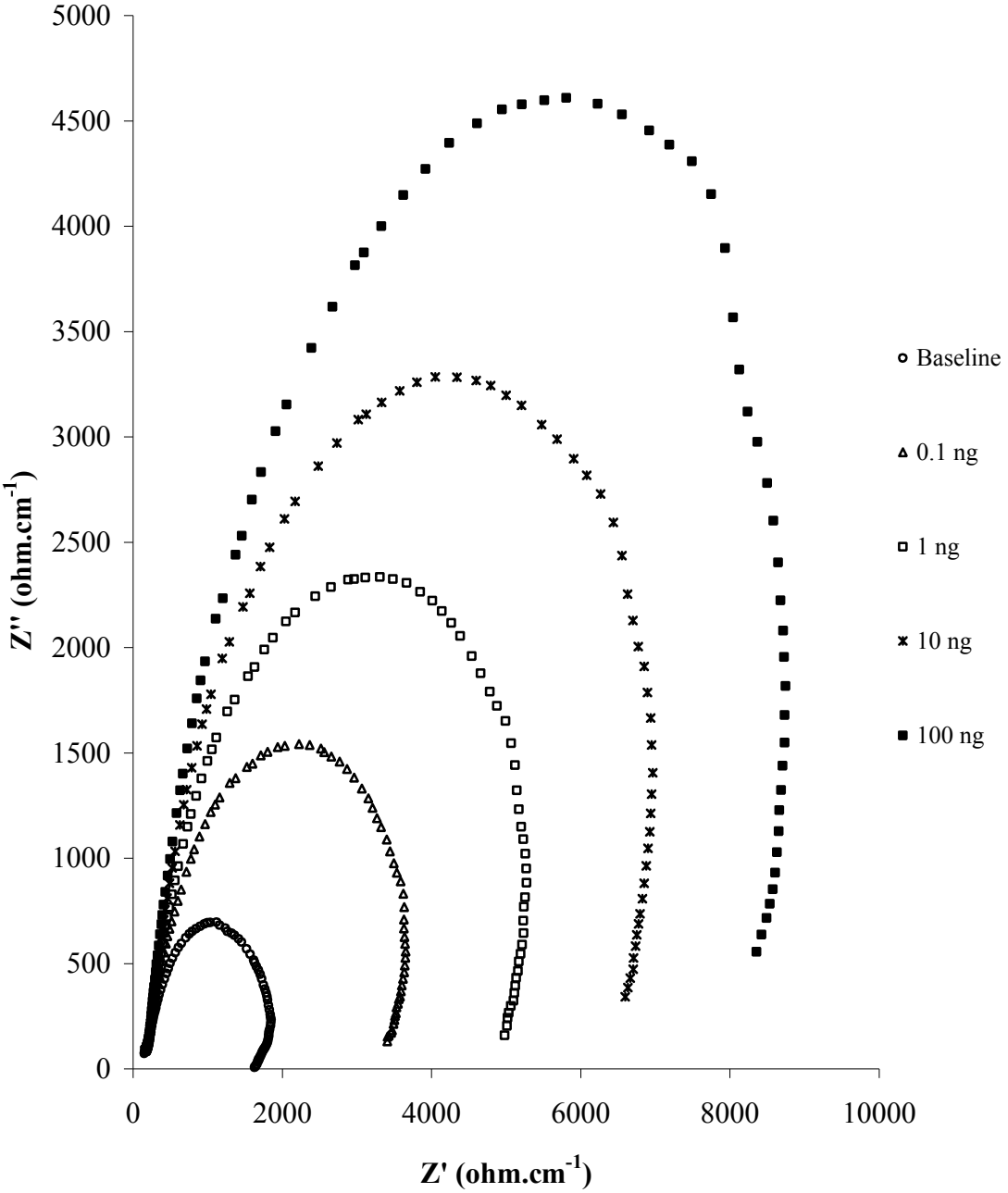

Figure 7.1 Z'' vs Z', Nyquist plot. Impedance responses of anti-GFP loaded carbon based sensors upon exposure to various GFP concentrations (in PBS, 10 mM ferri/ferocyanide).

Total impedance is seen to reach a maximum value above 1 Hz and is then slightly decreased at 1 Hz. This was also obvious from the Nyquist plot (figure 7.1) above. We have in previous work shown that the imaginary component reaches a maximum value before 1 Hz and then displays a rather large decrease at 1 Hz. However, decreases in the real component have not been observed before. It is therefore assumed that the characteristic Nyquist and Bode plot curves can very in shape depending upon the various antigen/ antibody pairs undergoing interrogation via AC impedance. Careful examination of the obtained data indicated that the maximum values for both components for each antigen concentration occur at slightly different frequencies. Therefore, the use of values obtained from the Z' component at 1 Hz were once more chosen for the production of calibration curves.

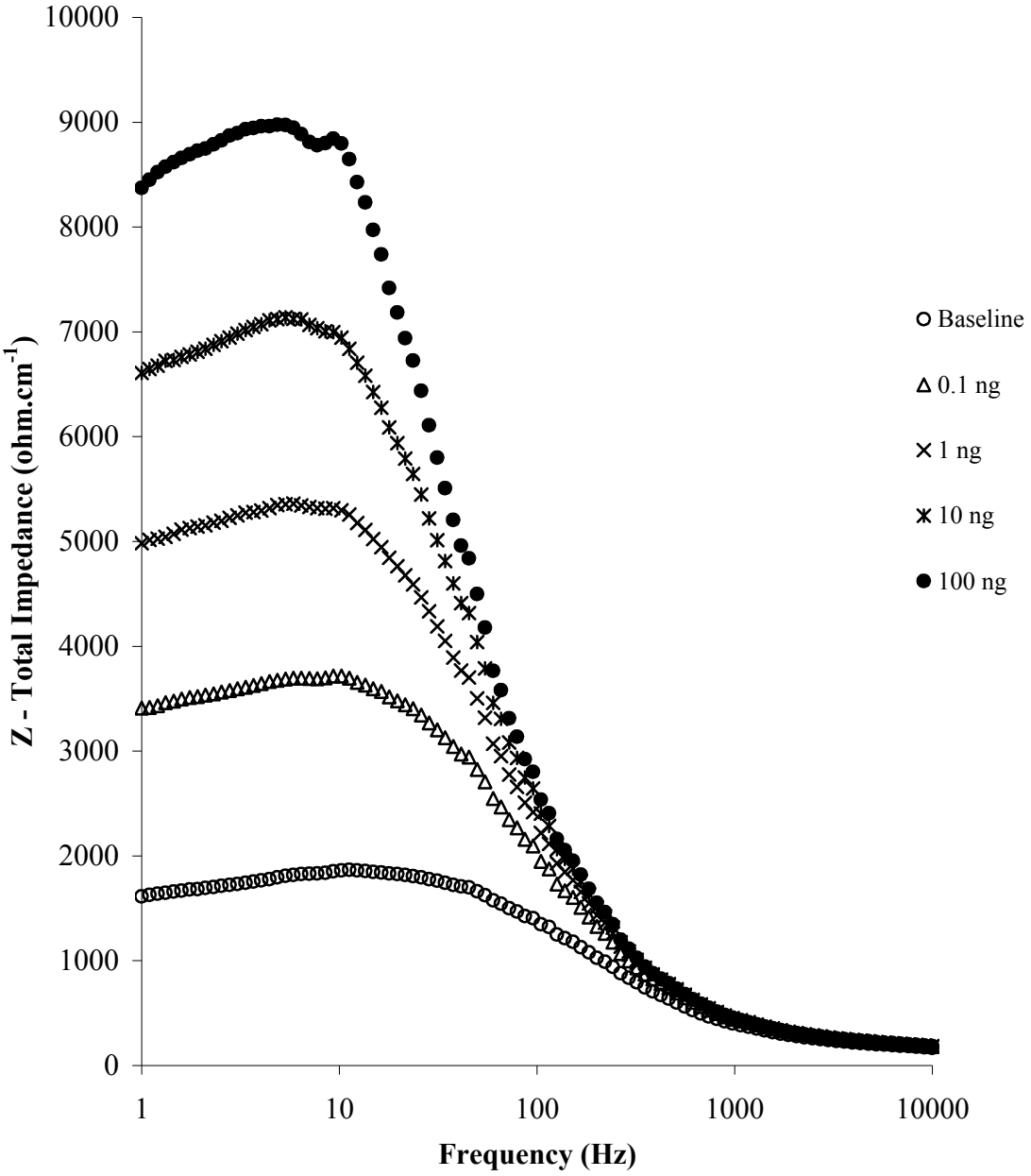

Figure 7.2 Total impedance vs frequency, Bode plot. Impedance responses of anti-GFP loaded carbon based sensors upon exposure to various GFP concentrations (in PBS, 10 mM ferri/ferrocyanide).

Figures 7.3, 7.4 and 7.5 contain the calibration curve for anti-GFP loaded sensors, calibration curve for polyclonal IgG loaded sensors and the corrected calibration curve for anti-GFP based sensors respectively. It is readily seen by the obtained calibration profile in figure 7.3 that the obtained responses where very high ranging

from 111% to 418% change from baseline over the chosen range of GFP concentrations. Relatively high responses were also obtained by the polyclonal IgG loaded sensors but these were not as high as those obtained for the specific antibody interrogations (figure 7.4). It should further be noted that the variation observed among the three specific replicas was not as high as the variation among IgG loaded sensors. High standard errors are thought to occur due to sensor saturation as discussed earlier in this work. Since the IgG standard errors can compromise the corrected calibration curve it was thought best to not extend the concentration range of GFP in order to provide a more reliable calibration plot. Obtaining highly concentrated monoclonal anti-GFP would permit the use of a more extended range of GFP concentrations.

The reasons for these rather different responses of the fabricated anti-GFP sensors are thought to be related to the antibody/antigen pair used. Sensor fabrication still remains a non-automated procedure. The anti-GFP antibody used here was a purified monoclonal antibody with high affinity for GFP fusion proteins as described by the manufacturer. The chosen antigen was a wild type full length GFP protein with a histidine tag. Considering the fact that these products were chosen to provide the best possible results, the high impedance responses could be expected. The antigen size, however, seems to also have an effect in the responses in regards to magnitude. This was assumed due to the high percentage changes form baseline observed for non-specific sensors. As discussed earlier, the impedance mechanism is not to date well understood and the current work is not focused towards collecting background information for the occurring reactions but rather proving that these phenomena can be used for the development of commercially successful sensors.

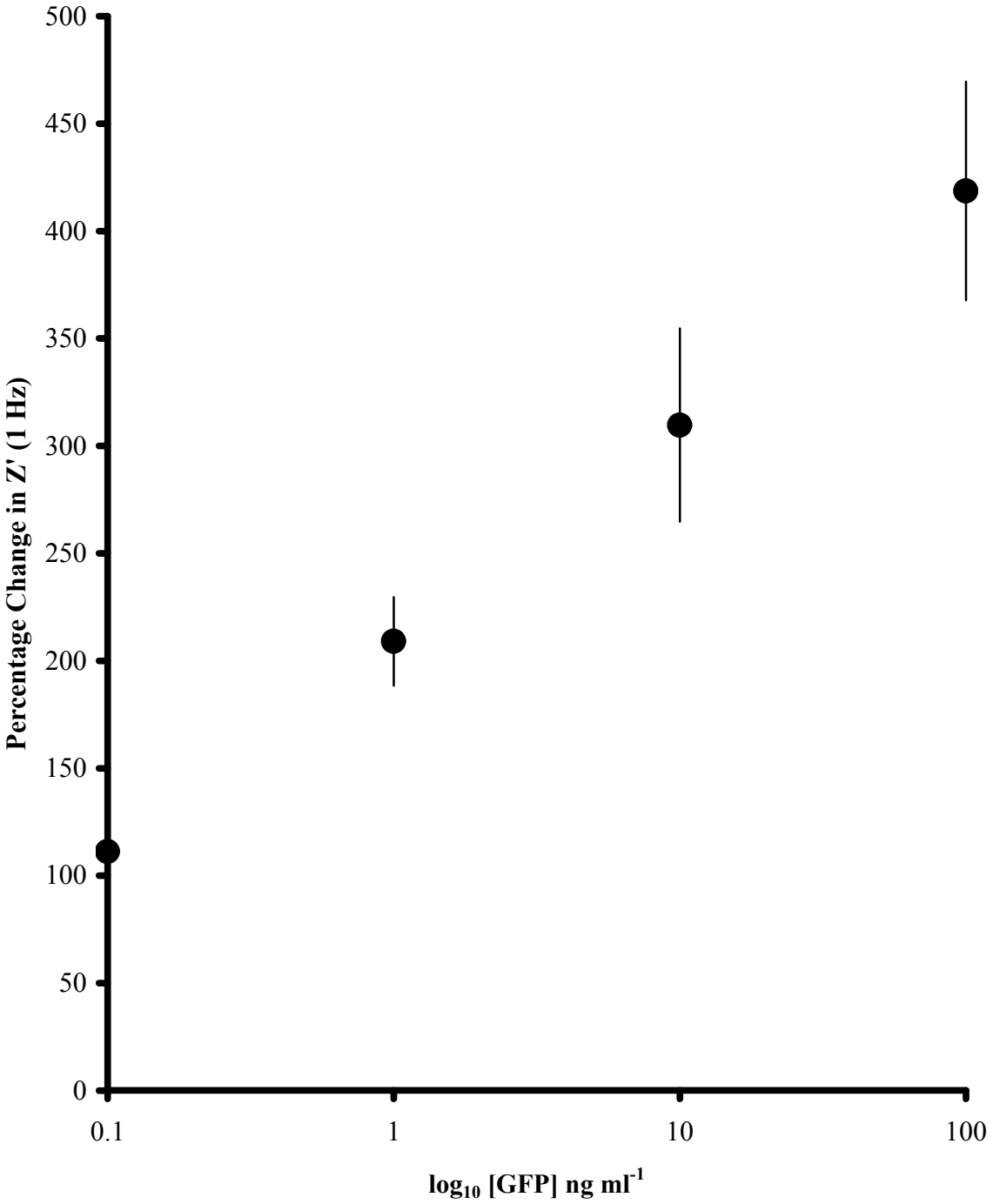

Figure 7.3: Calibration curve of per cent (%) impedance response against GFP concentrations (0.1ng ml^{-1} to 100 ng ml^{-1}) for anti-GFP doped polyaniline coated carbon electrodes at 1Hz (in PBS, 10 mM ferri/ferrocyanide).

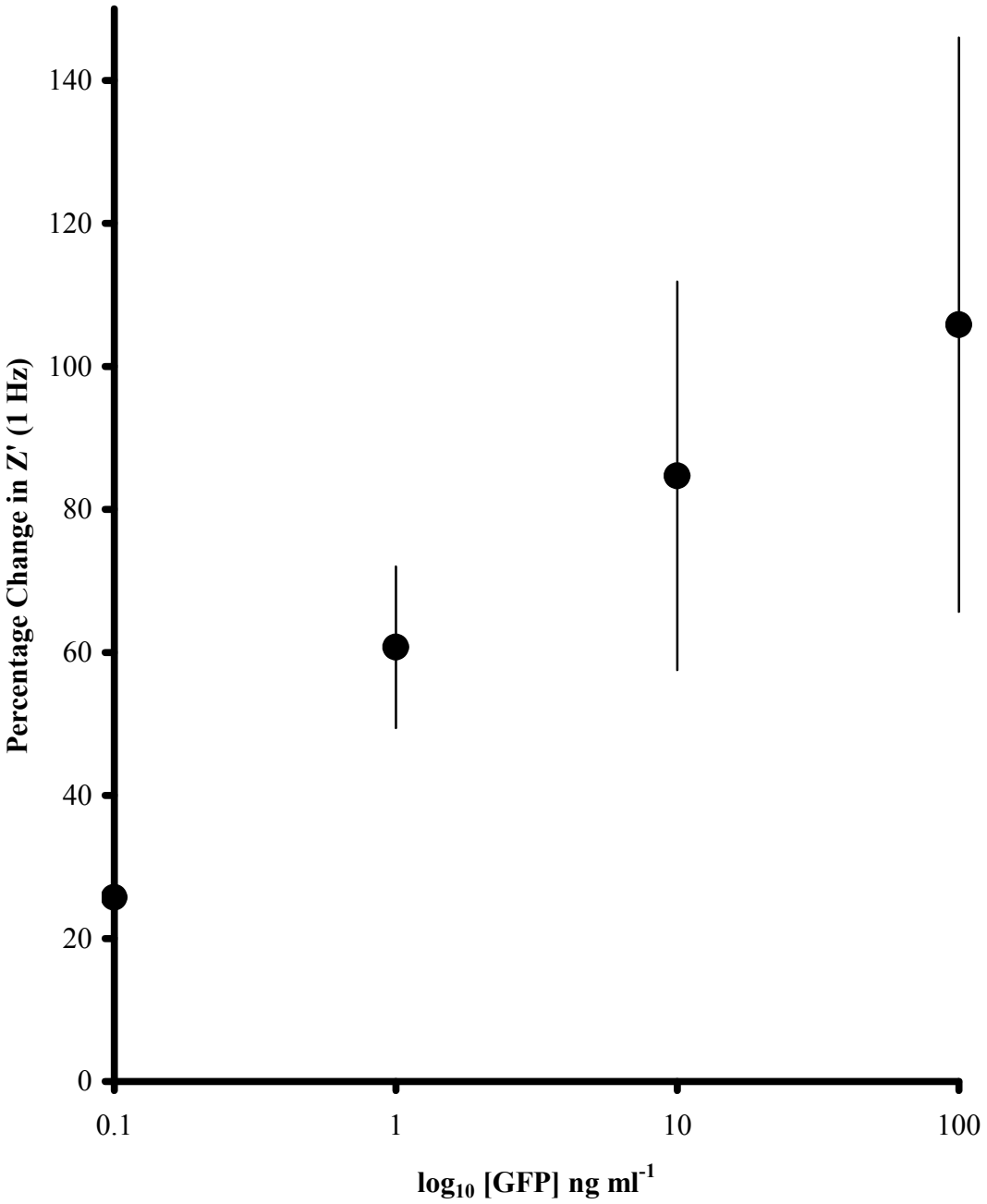

Figure 7.4: Calibration curve of per cent (%) impedance response against GFP concentrations (0.1ng ml^{-1} to 100 ng ml^{-1}) for polyclonal IgG doped polyaniline coated carbon electrodes at 1Hz (in PBS, 10 mM ferri/ferrocyanide).

As observed in figure 7.5 the obtained corrected calibration curve for anti-GFP based sensors displays high impedance responses with almost linear correlation (R^2=0.99) to the $\log_{10}$ antigen concentration over the chosen concentration range (100 pg ml^{-1} to 100 ng ml^{-1}). Even after subtraction of the non specific responses the corrected responses remained extremely high reaching 312% change from baseline for 100ng ml^{-1} GFP. The observed variation for the corrected responses was found to be relatively low, especially considering the high standard errors obtained from non-specific sensors.

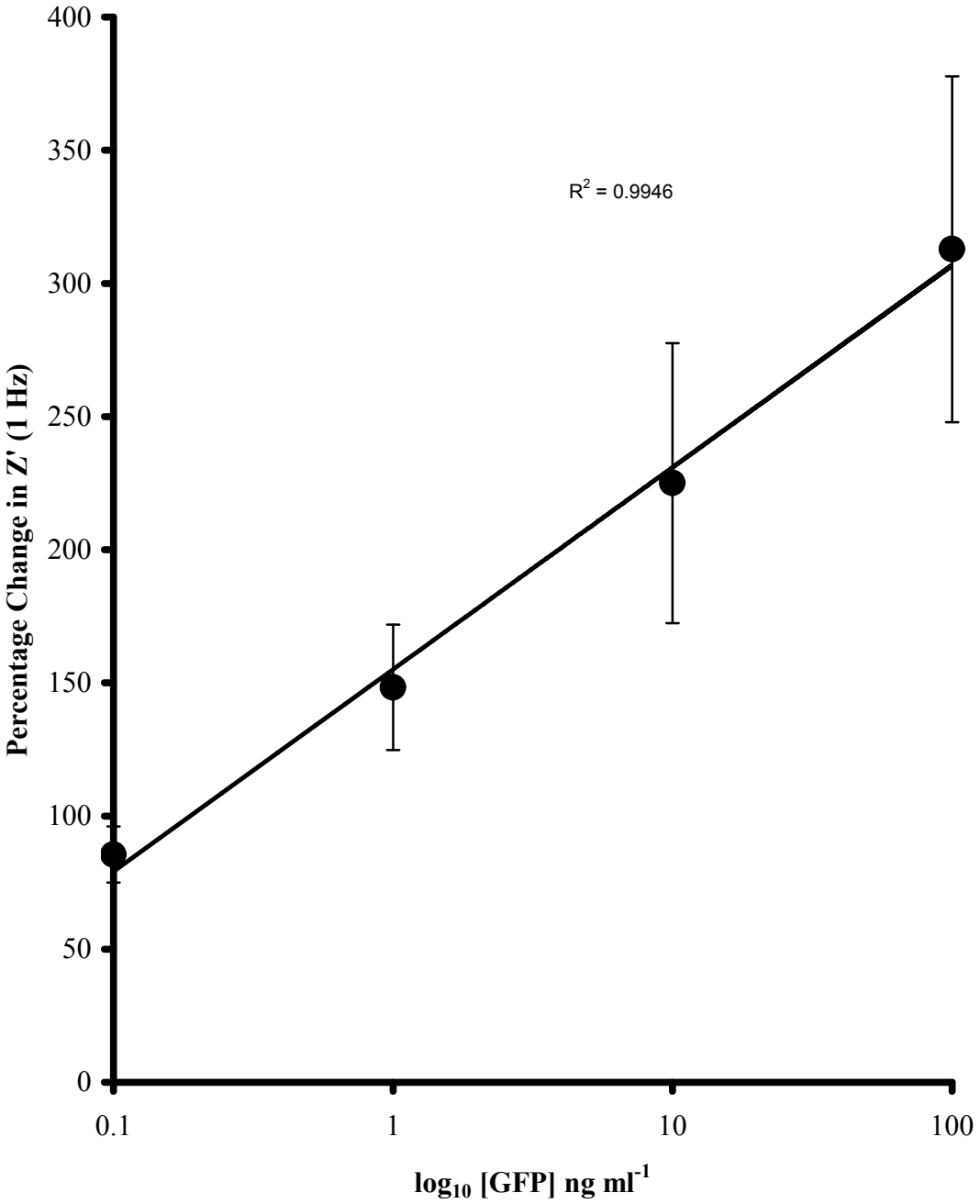

Figure 7.5: Corrected calibration curve of per cent (%) impedance response against GFP concentrations (0.1ng ml^{-1} to 100 ng ml^{-1}) for anti-GFP doped polyaniline coated carbon electrodes at 1Hz (in PBS, 10 mM ferri/ferrocyanide).

Conclusions

Within this work, the development of a successful immunosensor for detection of wild type GFP is reported. The fabricated sensors displayed high responses upon antigen addition at various concentrations, with little variation, and an achieved detection limit of 100 pg ml^{-1}. It is assumed, that given higher concentrations of specific antibody, this range could be extended to lower as well as higher antigen concentrations.

The initial experimentation plan for this work also involved the use of fluorescent microscopy for visualisation of the immobilised GFP on sensor surface. Upon microscopic examination, however, no detectable GFP was found on the sensors surface by means of fluorescence. It is assumed here that the sensor materials blocked a significant amount of the blue irradiation (light source was underneath the sensor) thus no green light was emitted from the top surface where the immobilised protein remained. The small concentration of the immobilised antibody and large size of the antigen have resulted in a small number of protein molecules being attached. As already discussed in the introduction of chapter 4.4, wild type GFP fluorescence is not as strong as that observed by some mutant GFP types. Errampalli *et al.,* (1999) suggest that at least 10,000 GFP molecules are required for fluorescence based visualisation in tissue culture cells. Considering this, the layer of carbon acting as the sensing electrode can be understood to prohibit any irradiation from reaching the sensor top surface and exciting GFP for fluorescence observations. Due to time limitations, such an experiment was not further pursued, however, as already seen, the developed sensors were found to be highly efficient from the ac impedimetric interrogations that were carried out. A paper is in preparation for this work.

Chapter 8

Conclusions and suggestions for future work

Conclusions

While electrodeposition of polymers onto all types of electrodes (including the glass-slide gold electrodes) was found to be an extremely efficient method, the project specific electrodes, both gold and platinum, were deemed unreliable for use in advanced experimentation such as ac impedance spectroscopy. Initially, an extra reduction peak during voltammetric scans was observed while using gold electrodes; this was attributed to a contaminant present within the electrode format and was thought to be a fabrication procedure fault. Later it was realised that the irreproducibility amongst all types of project specific electrodes was severe.

Sonochemical ablation was found to produce typical microelectrode arrays in some cases as described in section 4.2. However, the results were irreproducible amongst electrodes. Irreproducibility of the electrode fabrication procedure was one reason thought to be a cause of this. In addition, the custom made sonication tank used initially in this project did not provide a totally homogenous distribution of cavitation bubbles; this, teamed with the fact that the project specific electrodes are very small in size was another possible complimentary reason for irreproducibility of microelectrode array creation.

AC impedance spectroscopy using typical screen printed carbon electrodes for three different antibody/antigen pairs was met with success. It was shown that sensors containing the specific-monoclonal antibody show higher percent changes from baseline than those containing the non-specific polyclonal IgG or non-purified antibodies. The use of a redox couple such as ferri/ferrocyanide was found to enhance the analytical capabilities of impedimetric measurements and was preferred over plain PBS buffer for subsequent experimentation.

Early investigations using the anti-ciprofloxacin/ciprofloxacin pair lead to two important conclusions regarding the development of successful sensors. It was realised that each antibody of choice must be both purified and concentrated to a minimum of 1 mg ml^{-1} for measurements to be highly reliable, while, lower antibody concentrations meant early sensor saturation. Additionally, the matching polyclonal IgG should be used at the same concentration to the specific antibody for any

comparisons between sensors to be reliable. Purification and concentration works for antibodies where all carried in our partner lab (Leeds University), however, due to the low concentrations at which antibodies are commercially available, it was not always possible to reach the desired concentration of 1 mg ml^{-1}.

Sensors for the detection of ciprofloxacin have been successfully developed and found to detect ciprofloxacin at concentrations as low as 1 ng ml^{-1} in both laboratory PBS samples and in milk products. The maximum concentration used in these works was 10 μg ml^{-1}. As discussed earlier, ciprofloxacin forms chelation complexes with Ca^{2+} from milk indicating the ability of our developed sensors to detect both the free and chelated antigen and differentiate between the two, shown via impedance decrease (free antigen in PBS) and impedance increase (chelated antigen in milk) upon antigen addition.

Succesful sensors for the detection of digoxin have also been developed within this PhD research programme. As discussed earlier, the achieved anti-digoxin concentration was lower than our preferred antigen concentration of 1 mg ml^{-1}, and hence sensor saturation was observed upon antigen addition at low concentrations. The corresponding IgG used for this work was also kept at low concentration, thus resulting in high irreproducibility among IgG coated sensors. A detection limit of 0.1 ng ml^{-1} was achieved, however, due to the extended error bars observed for the corresponding polyclonal IgG, the corrected calibration curve also contained large error bars. In line with previous investigations a decrease in impedance was observed upon antigen addition. It is believed that higher antibody concentrations would produce far more reliable measurements.

Final investigations in this work involved the detection of Green Fluorescent protein (GFP). A detection limit of 100 pg ml^{-1} was achieved with the highest measured GFP concentration being 100 ng ml^{-1}. Interestingly, while the achieved antibody concentration was relatively low, the irreproducibility among sensors was not extreme, however, higher antibody concentration would allow us to measure a more extended range of antigen concentrations. Nevertheless, high responses were achieved upon antigen addition to the developed sensors and the obtained results where deemed reliable.

Three sensors have been reported within this work for the detection of ciprofloxacin, digoxin and GFP. The promising results indicated that the constructed devices may form the basis for development of a commercially viable sensor for detection of chosen antigens in liquid samples. The investigations within this research programme did not involve solid sample testing. Similar work gave rise to sensors for the detection of Myelin Basic Protein and Prostate Specific Antigen (PSA).

The concept of impedance increase or decrease upon exposure to antigens has been discussed within this work on a number of occasions. All specific binding is thought to give rise to decreasing impedance while non-specific binding persistently gives rise to impedance increases. Larger molecules, however, such as Myelin basic protein and the chelated form of ciprofloxacin have been shown to cause impedance increases. We conclude that larger or somewhat modified molecules may possess an insulating effect that can predominate the changes in impedance upon binding, thus increasing impedances are observed in the mentioned cases above.

Suggestions for future work

A number of antigen/antibody pairs have been investigated for the effects of their binding effects on impedance changes. While changes in impedance were obvious, there is not yet a definitive answer to why we observe an increase or decrease of impedance under different conditions. It has been shown that polyclonal IgG responses and those obtained for non purified antibodies displayed an increase in impedance upon increasing antigen concentrations. However, purified antibodies generally displayed impedance decreases with increasing antigen concentrations with the exception of ciprofloxacin in milk, which is not found as a free antigen but rather in chelation complexes. Future work from this research could focus on explaining the variations described above from a biochemist's point of view in order to better understand both the variations in responses (impedance increase or decrease) and the effects of the binding event on the impedance of the system.

With the range of commercially available antibodies and the overwhelming amount of target antigens, this research could be further extended into analysing more

antigen/antibody pairs for medical, environmental and biodefence purposes. While the current range analysed by this work and previous works is indeed large, it is possible to further extend our knowledge of impedimetric sensor capabilities for more important target antigens.

References

Adhikari, B. & Majumdar, S., 2004. Polymers in sensor applications, *Progress in Polymer Science*, **29**, 699-766

Alocilja, E. & Radke, S., 2003. Market analysis of biosensors for food safety. *Biosensors and Bioelectronics,***18**, 841-846

Anzai, J., Hoshi, T., Lee, S. & Osa, T., 1993. Use of the avidin-biotin system for immobilization of an enzyme on the electrode surface, *Sensors and Actuators*, **13-14 (B)**, 73-75

Anzai, J., Kobayashi, Y., Suzuki, Y., Takeshita, H., Chen, Q., Osa, T., Hoshi, T. & Du, X., 1998. Enzyme sensors prepared by layer-by-layer deposition of enzymes on a platinum electrode through avidin–biotin interaction, *Sensors and Actuators B*, 52, 3-9

Anzai, J., Kobayashi, Y., Suzuki, Y., Takshita, H., Chen, Q., Osa, T., Hoshi, T. & Du, X., 1998. Enzyme sensors prepared by layer-by-layer deposition of enzymes on a platinum electrode through avidin-biotin interaction, *Sensors and Actuators*, **52 (B)**, 3-9

Aus, G., Abbou, C. C., Bolla, M., Heidenreich, A., Schmid, H. P., van Poppel, H., Wolff, J. & Zattoni, F., 2005. EAU Guidelines on Prostate Cancer, *European Urology*, **48**, 546-551

Baeumner, B. J., Leonard, J. & Montagna, R. A., 2004. A rapid biosensor for viable *B. anthracis* spores, *Analytical and Bioanalytical Chemistry*, **380** (1), 15–23

Bakker & Meyerhoff, 2000. Ionophore-based membrane electrodes: new analytical concepts and non-classical response mechanisms, *Analytica Chimica Acta*, **416**, 121-137

Ball, **P.,** 2000. Quinolone generations: natural history or natural selection? *Journal of Antimicrobial Chemotherapy*, **46**, 17-24

Bartlett, P. N. & Birkin, P. R., 1993. The application of conducting polymers in biosensors, *Synthetic Metals*, **61**, 15-21

Barton, A. C., Collyer, S. D., Davis, F., Garifallou, G. Z., Tsekenis, G., Tully, E., O'kennedy, R., Gibson, T., Millner, P. A. & Higson, S. P. J., 2009. Labeless AC impedimetric antibody-based sensors with pg ml−1 sensitivities for point-of-care biomedical applications, *Biosensors and Bioelectronics*, **24**, 1090-1095

Barton, A. C., Collyer, S. D., Davis, F., Gornall, D. D., Law, K. A., Lawrence, C. D. L., Mills, D. W., Myler, S., Pritchard, J. A., Thompson, M. & Higson, S. P. J., 2004. Sonochemically fabricated microelectrode arrays for biosensors offering widespread applicability: Part I, *Biosensors and Bioelectronics*, **20**, 328-337

Barton, A. C., Davis, F. & Higson, S. P. J., 2008. Labeless immunosensor assay for prostate specific antigen with picogram per milliliter limits of detection based upon an ac impedance protocol. *Analytical Chemistry*, **80 (16)**, 6198-6205

Batt, A. L., Bruce, I. B. & Aga, D. S., 2006. Evaluating the vulnerability of surface waters to antibiotic contamination from varying wastewater treatment plant discharges, *Environmental Pollution*, **142,** 295-302

Bender, S. & Sadik, O. A., 1998. Direct Electrochemical Immunosensor for Polychlorinated Biphenyls, *Environmental Science and Technology*, **32**, 788-797

Berson, S. A. & Yallow, R. S., 1959. Quantitave aspects of the reaction between insulin and insulin-binding antibody, *Journal of Clinical Investigations*, ***38***, 1996-2016

Bilitewski, **U.,** 2006. Protein-sensing assay formats and devices, *Analytica Chmica Acta*, **538**, 232-247

Bishai, **W.,** 2002. Current Issues on Resistance, Treatment Guidelines, and the Appropriate Use of Fluoroquinolones for Respiratory Tract Infections. *Clinical Therapeutics*, **24**, 838-850

Blondeau, J. M., 2004. Fluoroquinolones: Mechanism of Action, Classification, and Development of Resistance, *Survey of Ophthalmology*, **49**, 73-78

Bogialli, S., D'Ascenzo, G., Di Corcia, A., Lagana, A. & Nicolardi, S., 2008. A simple and rapid assay based on hot water extraction and liquid chromatography–tandem mass spectrometry for monitoring quinolone residues in bovine milk, *Food Chemistry*, **108**, 354-360

Bucknall, S., Silverlight, J., Coldham, N., Thorne, L., Jackman, R., 2006. Antibodies to the quinolones and fluoroquinolones for the development of generic and specific immunoassays for detection of these residues in animal products *Food Additives and Contaminants*, **20**, 221-228.

Bunde, L. R., Jarvi, E. R. & Rosentreter. J. J., 1998. Piezoelectric quartz crystal biosensors, *Talanta*, **46**, 1223-1246

Cai H., Xu C., He P. & Fang Y., 2001. Colloid Au-enhanced DNA immobilization for the electrochemical detection of sequence-specific DNA, Journal of Electroanalytical Chemistry, **510**, 78– 85.

Cao, L. M., Lin, H., Mirsky, V. M., 2007. Surface plasmon resonance biosensor for enrofloxacin based on deoxyribonucleic acid, *Analytica Chimica Acta*, **589**, 1-5

Cass A.E.G., Francis D.G., Hill H.A.O., Aston W.J., Higgins I.J., Plotkin E.V., Scott L.D.L. and Turner A.P.F., 1984. Ferrocene-mediated enzyme electrode for amperometric determination of glucose *Analytical Chemistry,* **56**, 667-671

Chun, J. & Chodosh J., 2006. Controversy in Heart Failure Management: Digoxin Use in the Elderly. *Journal of the Americam Medical Directors Association*, **7**, 581-586

Clark L.C., Jnr., 1956. Monitoring and control of blood and tissue O2 tensions. *Trans. American Society of Artificial Internal Organs 2*, **1956**, 41

Clark, L. C. & Lyons, C., 1962. Electrode systems for continuous monitoring in cardiovascular surgery**,** *Annals Of The New York Academy Of Sciences,* **102***,* 29-45

Clemens A.H., Chang P.H. & Myers R.W., 1976. Development of an automatic system of insulin infusion controlled by blood sugar, its system for the determination of glucose and control algorithms, *Proc. Journes Ann. de Diabtologie de l'Hotel-Dieu*, Paris, 269-278

Cooney, C.L., Weaver, J.C., Tannebaum, S.R., Faller, S.R., Shields, D.V. & Jahnke, M., 1974. *Enzyme Engineering*, E.K. Pye and L.B. Wingard Jnr., **2**, 411-417. Plenum, New York

Cooper, J. C. & Hall, E. A. H., 1992. Electrpochemical response of an enzyme-loaded polyaniline film, *Biosensors and Bioelectornics*, **7**, 473-485

Dakshinamurti, K., Bhullar, R. P., Scoot, A., Rector, E. S., Delespesse, G. & Sehon, A. H., 1986. Production and characterization of a monoclonal antibody to biotin, *The Biochemical Journal,* **237(2)***,* 477-482

Daly, D. J., O'Sullivan, C. K. & Guibault, G. G., 2000. The use of electrochemically grown polymers on metallized electrodes to reduce electrode fouling in biological matrices, *Biochemical Society Transactions*, **28**, 89-93

Davis F., Hughes, M. A., Cossins, A. R., Higson S. P. J., 2007. Single gene differentiation by DNA-modified carbon electrodes using an AC impedimetric approach, *Analytical Chemistry,* **79**, 1153-1157.

Davis, F., Nabok, A. V. & Higson, S. P. J., 2005.Species differentiation by DNA-modified carbon electrodes using an ac impedimetric approach, *Biosensors and Bioelectronics*, **20 (8)**, 1531-1538

Davis, G., 1986. Advances in the Biomedical Sensor Technology: A Review of the 1985 Patent Literature, *Biosensors*, **2**, 101-124

Davis, J., Vaughan, D.H. & Cardosi, M.F., 1995**.** Elements of Biosensor Construction. *Enzyme and Microbial Technology*, **17**, 1030-1035.

Dawson, A. & Buckley, N., 2007. Poisonous Substances: Digoxin, *Medicine*, **35**, 613-614

Degefa, T. H. & Kwak, J., 2008. Electrochemical impedance sensing of DNA at PNA self assembled monolayer, *Journal of Electroanalytical Chemistry*, **612**, 37-41

Deisingh A. K. & Badrie, N., 2005. Detection approaches for genetically modified organisms in food, *Food Research International*, **38**, 639-649

Ding, S. J., Chang, B. W., Wu, C. C., Lai, M. F. & Chang, H. C., 2005. Electrochemical evaluation of avidin–biotin interaction on self-assembled gold electrodes, *Electrochimica Acta*, **50**, 3660-3666

Divis C., 1975. Remarques sur l'oxydation de l'éthanol par une electrode micro-bienned' acetobacter zylinum, *Annals of Microbiology,* **126** , 175-186

Duan, J. and Yuan, Z., 2001. Development of an Indirect Competitive ELISA for Ciprofloxacin Residues in Food Animal Edible Tissues, *Journal of Agricultural Food Chemistry*, **49**, 1087-1089

Dumoulin, M. & Dobson, C. M., 2004. Probing the origins, diagnosis and treatment of amyloid diseases using antibodies**,** *Biochimie,* **86 (9-10)***,* 589-600

Eberl, L., Schulze, R., Ammendola, A., Geisenberger, O., Earhart, R., Steinberg, C., Molin, S., Amann, R., 1997. Use of green fluorescent protein as a marker for ecological studies of activated sludge communities. *FEMS Microbioly Letters*, 149, 77– 83

ELISHA Annex, 2003. Electronic Immuno-Interfaces and Surface Nanobiotechnology: A Heterodoxical Approach. Sixth framework programme priority [3]: Nano-technologies and nano-sciences, knowledge-based multifunctional materials, and new production processes and devices-'NMP'

Errampalli, D., Leung, K., Cassidy, M. B. & Kost, M., 1999. Applications of the green fluorescent protein as a molecular marker in environmental microorganisms, *Journal of Microbiological Methods*, **35**, 187-199

Falagas, M. E., Bliziotis, I. A. & Rafailidis, P. I., 2007. Do high doses of quinolones decrease the emergence of antibacterial resistance? A systematic review of data from comparative clinical trials, *Journal of Infection*, **55**, 97-105

Farace, G., Lillie, G., Hianik, T., Payne, P. & Vadgama, P., 2002. Reagentless bioaenaing uaing electrochemical impedance spectroscopy, *Bioelectrochemistry*, **55**, 1-3

Fernandez, L. & Carrero, H., 2005. Electrochemical evaluation of ferrocene carboxylic acids confined on surfactant–clay modified glassy carbon electrodes: oxidation of ascorbic acid and uric acid, *Electrochimica Acta*, **50**, 1233-1240

Fernandez-Sanchez, C., Mcneil, C. J. & Rawson, K., 2005. Electrochemical impedance spectroscopy studies of polymer degradation: application to biosensor development, *Trends in Analytical Chemistry*, **24 (1)**, 37-48

Gardner J. W. and Bartlett, P. N., 1995. Application of conducting polymer technology in Microsystems, *Sensors and Actuators A*, **51**, 57-66

Garifallou, G. Z., Tsekenis, G., Davis, F., Higson, S. P. J., Millner, P. A., Pinacho, D. G., Sanchez-Baeza, F., Marco, M. P., Girona, J. & Gibson, T. D., 2007. Labeless Immunosensor Assay for Fluoroquinolone Antibiotics Based Upon an AC Impedance Protocol, *Analytical Letters*, **40**, 1412-1422

Gendrel, D., Chalumeau, M., Moulin, F. & Raymond, J., 2003. Fluoroquinolones in paediatrics: a risk for the patient or for the community? *The Lancet Infectious Diseases*, **3**, 537-546

Genies, E. M., Penneau, J. F., Lapkowski, M. and Boyle, A., 1989. Electropolymerisation reaction mechanism of para-aminodiphenylamine, *Journal of Electroanalytical Chemistry*, **269**, 63-75

Gerard, M., Caubey, A. & Malhotra, B. D., 2002, Application of conducting polymers to biosensors, *Biosensors and Bioelectronics*, **17**, 345-359

Goldstein, I., Levy, T., Galili, D., Ovadia, H., Yirmiya, R., Rosen, H. & Lichtstein, D., 2006. Involvement of Na^+, K^+-ATPase and Endogenous Digitalis-

Like Compounds in Depressive Disorders, *Journal of Biological Psychiatry*, **60**, 491-499

Gooding, J. J., 2006. Biosensor technology for detecting biological warfare agents: Recent progress and future trends, *Analytica Chimica Acta*, **539**, 137-151

Grant, S., Davis, F., Law, K. A., Barton, A. C., Collyer, S. D., Higson, S. P. J. & Gibson, T. D., 2005. Label-free and reversible immunosensor based upon an ac impedance interrogation protocol, *Analytica Chimica Acta*, **537**, 163-168

Grant, S., Davis, F., Pritchard, J. A., Law, K. A., Higson, S. P. J. & Gibson, T. D., 2003. Labeless and reversible immunosensor assay based upon an electrochemical current-transient protocol, Analytica Chimica Acta, **495**, 21-32

Guan J., Miao, Y. & Zhang, Q., 2004. Impedimetric Biosensors, *Journal of Bioscience and Bioengineering*, **97 (4)**, 219-226

Guerrieri, A., De Benedetto, G. E., Palmisano, F. & Zambonin, P. G., 1998, Electrosynthesized non-conducting polymers as permselective membranes in amperometric enzyme electrodes: a glucose biosensor based on a co-crosslinked glucose oxidase/overoxidized polypyrrole bilayer, *Biosensors and Bioelectornics*, **13 (1)**, 103-112

Guilbault, G. G., 1976**.** Handbook of Enzymatic Methods of Analysis, Marcel. Dekker, New York, NY

Guilbault, G. G. & Montalvo, J. J., 1969. Urea specific enzyme electrode, *Journal of the American Chemical Society,* **91**, 2164-2569

Guimard, N. K., Gomez, N. & Schmidt, C. E., 2007. Conducting polymers in biomedical engineering, *Progress in Polymer Science*, **32**, 876-921

Hahn, S., Mergenthaler, S., Zimmermann, B. & Holzgreve, W., 2005. Nucleic acid based sensors: The desires of the user, *Bioelectrochemistry*, **67**, 151-154

Halamek, J., Makowe, A., Knosche, K., Skladal, P. & Scheller, F. W., 2005. Piezoelectric affinity sensors for cocaine and cholinesterase inhibitors. *Talanta*, **65 (2)**, 337-342

Hartmann, A., Golet, E. M., Gartiser, S., Alder, A. C., Koller, T. & Widmer, R. M., 1999. Primary DNA Damage But Not Mutagenicity Correlates with Ciprofloxacin Concentrations in German Hospital Wastewaters, *Archives of Environmental Contamination and Toxicology*, **36,** 115-119

Hassouan, M., Ballesteros, O., Vilchez, J., Zafra, A., Navalon, A., 2007. Simple Multiresidue Determination of Fluoroquinolones in Bovine Milk by Liquid Chromatography with Fluorescence Detection, *Analytical Letters*, **40**, 779-791.

Hervás Pérez, J. P., López-Cabarcos, E. & López-Ruiz, B., 2006. The application of methacrylate-based polymers to enzyme biosensors, *Biomolecular Engineering*, **23**, 233-245

Higson, S.P.J., 2003. *In Analytical Chemistry*. Oxford University Press, 286–288.

Hollman, A., 1996. Digoxin comes from Digitalis lanata, *British Medical Journal*, 312, 912

Ionescu , R. E., Jaffrezic-Renault , N., Bouffier , L., Gondran, C., Cosnier, C., Pinacho, D. G., Marcoc, M. P., Sanchez-Baeza, F., Healy, T. & Martelet, C., 2007. Impedimetric immunosensor for the specific label free detection of ciprofloxacin antibiotic, *Biosensors and Bioelectronics*, **23**, 549-555

IUPAC, 1997. Compendium of Chemical Terminology, 2nd edition. (the "Gold Book"). Compiled by A. D. McNaught and A.Wilkinson. Blackwell Scientific Publications, Oxford

Janata, J., 1985. An Immunoelectrode, *Journal of The American Chemical Society*, **97**, 2914-2916

Jianrong, C., Yuqing, M., Nongyue, H., Xiaohua W. & Sijiao, L., 2004. Nanotechnology and biosensors, *Biotechnology Advances*, **22**, 505-518

John, R., Spencer, M., Wallace, G. G. & Smyth, M. R., 1999. Development of a polypyrrole-based human serum albumin sensor, *Analytica Chimica Acta*, **249**, 381-385

Jung, S., Honergger, A. & Pluckthun, 1999**.** A selection for improved protein stability by phage display**,** *Journal of Molecular Biology*, **294**, 163-180

Katz, E. & Willner, I., 2003. Probing Biomolecular Interactions at Conductive and Semiconductive Surfaces by Impedance Spectroscopy: Routes to Impedimetric Immunosensors, DNA-Sensors, and Enzyme Biosensors, *Electroanalysis*, **15***,* 913-947

Killard, A. J., Deasy, B., O'Kennedy, R. & Smyth, M. R., 1995. Antibodies: production, functions and applications in biosensors, *Trends in Analytical Chemistry*, **14 (6)**, 257-265

Kissinger, P. T., 2005. Biosensors- A perspective, *Biosensors and Bioelectronics, **20***, 2512-2516

Korri-Youssoufi, H., Richard, C. & Yassar, A., 2001. A new method for the immobilisation of antibodies in conducting polymers, *Materials Science and Engineering*, **15 (C)**, 307-310

Law, K. A. & Higson, S. P. J., 2005. Sonochemically fabricated acetylcholinesterase micro-electrode arrays within a flow injection analyser for the determination of organophosphate pesticides, *Biosensors and Bioelectronics*, **20**, 1914-1924

Law, K. A., Derrick, J. P. & Higson, S. P. J., 2003. Initial investigations into the ultrasonic lysis of microbial cells for the release of adenosine triphosphate, *Analytical Biochemistry*, **317**, 366-367

Lazcka , O., Del Campo, F. J. & Munoz, F. X., 2007. Pathogen detection: A perspective of traditional methods and biosensors. *Biosensors and Bioelectronics*, **22**, 1205-1217

Lei, Y., Chen, W. & Mulchandani, A., 2006. Microbial biosensors, *Analytica Chimica Acta*, **568**, 200-210

Leonard, P., Hearty, S., Brennan, J., Dunne, L., Quinn, J., Chakraborty, T. & O'Kenndey R., 2003. Advances in biosensors for detection of pathogens in food and water, *Enzyme and Microbial Technology***, 32,** 3-13

Licitra, C.M., Brooks, R.G. & Sieger, B.E., 1987. Clinical efficacy and levels of ciprofloxacin in tissue in patients with soft tissue infection. *Journal of Antimicrobial Agents and Chemotherapy*, 31, 805–807

Liedberg. B., Nylander, C. & Lundstrom. I.,1983. Surface plasmon resonance for gas detection and biosensing, *Sensors and Actuators*, **4**, 299-304

Lower, S. K., 1994. *Electrochemsitry: a chem1 Supplement Text*, Simon Fraser University

Lubbers D.W. & Opitz N. Z., 1975. Naturforsch*, Bioscience*, **30c**, 532-533

Luppa, P. B., Sokoll, L. J. & Chan D. W., 2001. Immunosensors-principles and applications to clinical chemistry, *Clinica Chimica Acta*, **314**,1–26

Martinez , M., McDermott, P. & Walker, R., 2006. Pharmacology of the fluoroquinolones: A perspective for the use in domestic animals, *The Veterinary Journal*, **172**, 10-28

Martinusz K., Czirók E. and Inzelt G., 1994. Studies of the formation and redox transformation of poly(o-phenylenediamine) films using a quartz crystal microbalance, *Journal of Electroanalytical chemistry,* **379***,* 437-444

Maxwell D., Taylor M. J. & Nie S., 2001. Self-assembled nanoparticle probes for recognition and detection of biomolecules, *Journal of American Chemical Society*, **124**, 9606– 12

Meadows, 1996. Recent developments with biosensing technology and applications in the Pharmaceutical Inustry, *Advanced Drug Delivery Reviews*, **21**, 179-189

Mello, L. D. & Kubota L. T., 2002. Review of the use of biosensors as anhalytical tools in the food and drink industries, *Food Chemistry*, **77**, 237-256

Miller, W. G. & Anderson, F. P., 1989. Antibody properties for chemically reversible biosensor applications, *Analytica Chimica Acta*, **227**, 135-143

Mirsky, V. M., Riepl, M. & Wolfbeis. O. S., 1997. Capacitive monitoring of protein immobilization and antigen-antobody reactions on monomolecular alkylthiol films on gold electrodes, *Biosensors & Bioelectronics*, **12**, 977-989

Mohanty, S. P., 2001. Biosensors: A Survey Report, Department of Computer Science and Engineering, University of South Florida

Monk, P. M. S., 2001. Fundamentals of Electroanalytical Chemistry, *Analytical Techniques in the Sciences*, Ando, D. J., John Wiley and Sons Ltd

Mosbach, K. & Danielsson, 1974. An enzyme thermistor, *Biochimica et Biophysica Acta*, **364**, 140-145

Myler, S., Davis F., Collyer, S. D. & Higson, S. P. J., 2004. Sonochemically fabricated microelectrode arrays for biosensors—part II Modification with a polysiloxane coating, *Biosensors and Bioelectronics*, **20,** 408-412

Myler, S., Eaton, S., Higson, S.P.J., 1997. Poly(*o*-phenylenediamine) ultrathin polymer-film composite membranes for enzyme electrodes. *Analytica Chimica Acta*, **357**, 55–61.

NBPDP:*Antibiotic Resistance-An Urgent Problem*, 2002. Fluroquinoline Antibiotics: The need for reductions in ciprofloxacin consumption, New Brunswick Prescription Drug Program, *Clinical and Benefit Status Summary*

Newman, J. & Turner, A. P. F., 2005. Home blood glucose biosensors: a commercial perspective. *Biosensors and Bioelectronics*, 20, 2435–2453

Ouerghi, O., Touhami, T., Jaffrezic-Renault, N., Martelet, C., Ouada, H. B. & Cosnier, S., 2002. Impedimetric immunosensor using avidin-biotin for antibody immobilisation, *Bioelectrochemistry*, **56**, 131-133

Patterson, G.H., Knobel, S.M., Sharif, W.D., Kain, S.R. & Piston, D. W., 1997. Use of the Green Fluorescent Protein and its mutants in quantitative fluorescence microscopy, *Journal of Biophysiology*, **73 (5)**, 2782-2790

Pejcic, B. & De Marco, R., 2006. Impedance spectroscopy: Over 35 years of electrochemical sensor optimization, *Electrochimica Acta*, **51**, 6217-6229

Pinacho, D. G., Sanchez-Baeza, F., Marco, M. P., paper in preparation

Pinachoa, D. G., Gorgy, B., Cosnier, S., Marcoa, M. P. & Sánchez-Baeza, F. J., 2008. Electrogeneration of polymer films functionalized by fluoroquinolone models for the development of antibiotic immunosensor, *ITBM-RBM*, Article in press

Pritchard, J., Law, K., Vakurov, A., Millner, P. & Higson, S. P. J., 2004. Sonochemically fabricated enzyme microelectrode arrays for the environmental monitoring of pesticides. *Biosensors and Bioelectronics,* **20,** 765-772

Purohit, H. J., 2003. Biosensors as molecular tools for use in bioremediation, *Journal of Cleaner Production*, **11**, 293-301

Ramanathan, K. & Danielson, B., 2001. Principles and applications of thermal biosensors, *Biosensors & Bioelectronics*, **16**, 417-423

Rodriguez-Diaz, R. C., Fernandez-Romero, J. M., Aguilar-Caballos, M. P., Gomez-Hens, A., 2006. Determination of Fluoroquinolones in Milk Samples by Postcolumn Derivatization Liquid Chromatography with Luminescence Detection, *Journal of Agricultural and Food Chemistry*, **54 (26)**, 9670-9676

Sadik, O. A. & Wallace, G. G., 1993. Pulsed amperometric detection of proteins using antibody containing conducting polymers, *Analytica Chimica Acta*, **279**, 209-212

Safarik, I. & Safarikova, M., 1999. Use of magnetic techniques for the isolation of cells, *Journal of Chromatography*, **722**, 33-53

Sargent, A. & Sadik, O. A., 1999. Monitoring antibody–antigen reactions at conducting polymer-based immunosensors using impedance spectroscopy, *Electrochimica Acta*, **44**, 4667-4675

Sasaki, K., Kaya, A., Yano, J., Kitani, A. & Kunai. A., 1986. Growth mechanism in the electropolymerisation of aniline and *p*-aminodiphenylamine. *Journal of Electroanalytical Chemistry*, **215**, 401-407

Saxena, V. & Malhotra, B. D., 2003. Prospects of conducting polymers in molecular electronics, Current Applied Physics, 3, 293-305

Scheper, T. H., Hilmer, J. M., Lammers, F., Miiller. C. & Reinecke. M., 1996. Biosnesors in bioprocess monitoring, *Journal of Chromatography*, **725**, 3-12

Shichiri M., Kawamori R., Yamaski R., Hakai Y. and Abe H., 1982. Wearable Artificial Endocrine Pancreas with Needle-Type Glucose Sensor, *The Lancet ii*, 1129-1131

Smith, R. G., D'Souza, N. & Nicklin, S., 2008. A review of biosensors and biologically-inspired systems for explosives detection. *Analyst*, **133**, 571-584

Torriero, A. J. A., Ruiz-Diaz, J. J. J., Salinas, E., Marchevsky, E. J., Sanz, M. I. & Raba, J., 2006. Enzymatic rotating biosensor for ciprofloxacin determination, *Talanta*, **69**, 691-699

Tsekenis, G., Garifallou, G. Z., Davis, F., Millner, P. A.,Gibson, T. D., and Higson, S. P. J., 2008. Label-less Immunosensor Assay for Myelin Basic Protein Based upon an ac Impedance Protocol, *Analytical Chemistry*, **80,** 2058-2062

Tully, E., Higson, S. P. J. & O'Kennedy, R., 2008, The development of a 'labeless' immunosensor for the detection of *Listeria monocytogenes* cell surface protein, Internalin B, *Biosensors and Bioelectronics*, **23**, 906-912

Turner, A. P., Karube, I. & Wilson, G., 1986. Biosensors: fundamentals and applications. Oxford Science Publications, Oxford

Upadhyay, S. K., Kumar, P., Arora, V., 2006. Complexes of quinolone drugs norfloxacin and ciprofloxacin with alkaline earth metal perchlorates *Journal of Structural Chemistry*, **47**, 1078-1083

Updike, S.J. & Hicks, J.P., 1967. Enzyme electrode, *Nature*, **214**, 986-988

van der Voort, D., McNeil, C. A., Renneberg, R., Korf, J., Hermens, W. T. & Glatz, J. F. C., 2005. Biosensors: basic features and application for fatty acid-binding protein, an early plasma marker of myocardial injury, *Sensors and Actuators*, **105 (B)**, 50-59

Voelkl, K. P., Opitz, N., and Lubbers, D. W., 1980. Continuous measurement of concentrations of alcohol using a fluorescence-photometric enzymatic method. *Fres. Z. Anal. Chem.* **301**, 162–163

Wallace, G. G., Smyth, M. & Zhao, H., 1999. Conducting electroactive polymer-based biosensors, *Trends in Analytical Chemistry*, **18**, 245-251

Wang, J., 2006. Electrochemical biosensors: Towards point-of-care cancer diagnostics, *Biosensors & Bioelectronics*, **21**, 1887-1892

Wang, L. & Song, S., 2005. Digoxin may reduce the mortality rates in patients with congestive heart failure, *Medical Hypotheses*, **64**, 124-126

Yuqing, M., Jianrong, C. & Xiaohua, W., 2004. Using electropolymerized non-conducting polymers to develop enzyme amperometric biosensors, *Trends in Biotechnology,* **22 (5)**, 227-231

Websites

1) www.cartage.org.lb/en/themes/Sciences/Chemistry/Electrochemis/Electrochemical/ElectrodeKinetics/ElectrodeKinetics.htm

2) www.cheng.cam.ac.uk/research/groups/electrochem/teaching.html

3) www.strategyr.com

4) www.abbottdiabetescare.com

Appendix 1

Published work

Analytical Letters, 40: 1412–1422, 2007

ISSN 0003-2719 print/1532-236X online
DOI: 10.1080/00032710701327070

Taylor & Francis
Taylor & Francis Group

IMMUNOLOGY

Labeless Immunosensor Assay for Fluoroquinolone Antibiotics Based Upon an AC Impedance Protocol

G.-Z. Garifallou, G. Tsekenis, F. Davis, and S. P. J. Higson
Cranfield Health, Cranfield University, Silsoe, Bedfordshire

P. A. Millner
University of Leeds, Leeds

D. G. Pinacho, F. Sanchez-Baeza, and M.-P. Marco
Institute of Chemical and Environmental Research (IIQAB-CSIC), Jorge Girona, Barcelona, Spain

T. D. Gibson
T and D Technology, Wakefield, West Yorkshire

Abstract: This paper describes the construction of a labeless immunosensor for the antibiotic ciprofloxacin and its interrogation using an AC impedance protocol. Commercial screen-printed carbon electrodes were used as the basis for the sensor. Polyaniline was electrodeposited onto the sensors and then utilized to immobilize a biotinylated antibody for ciprofloxacin using classical avidin-biotin interactions.

Electrodes containing the antibodies were exposed to solutions of antigen and interrogated using an AC impedance protocol. The faradaic component of the impedance of

Received 20 January 2007; accepted 27 February 2007

This work has been supported by the Ministry of Science and Technology (Spain) (Contract numbers AGL2005-07700-C06-01 and NAN2004-09195-C04-04) and by the European Community Framework VI NMP2-CT-2003-505485, "ELISHA" contract. The AMR group is a consolidated Grup de Recerca de la Generalitat de Catalunya and has support from the Departament d'Universitats, Recerca i Societat de la Informació la Generalitat de Catalunya (expedient 2005SGR 00207). DG has a FPI fellowship from the Spanish Ministry of Education.

Address correspondence to S. P. J. Higson, Cranfield Health, Cranfield University, Silsoe, Bedfordshire MK45 4DT. E-mail: s.p.j.higson@scranfield.ac.uk

the electrodes was found to increase with increasing concentration of antigen. Control samples containing a non-specific IgG antibody were also studied and calibration curves obtained by subtraction of the responses for specific and non-specific antibody-based sensors, thereby eliminating the effects of non-specific adsorption of antigen.

Keywords: Fluoroquinolone, ciprofloxacin, AC impedance, immunosensor, polyaniline

INTRODUCTION

The principle of immunoassays was established in 1959 by Yalow and Berson (Yalow and Berson, 1959). Their work developed the widely used radio-immunoassay to examine the properties of insulin-binding antibodies in human serum, using samples obtained from subjects that had been treated with insulin.

Following the newly developed immunoassay technique, the concept of a biosensor was pioneered by Clark and Lyons in 1962 (Clark and Lyons, 1962). The original methodology was to immobilize enzymes on the surface of electrochemical sensors-assuming that this would enhance the ability of a sensor to detect specific analytes. This idea has remained virtually unchanged since this original design, however, technological advances have allowed for the expansion of this field of science.

The incorporation of antibodies into conducting polymer films was first reported in 1991 (John et al. 1991). Anti-human serum albumin (anti-HSA) was incorporated into a polypyrrole film, which was galvanostatically polymerized onto a platinum wire substrate. When grown in the absence of a counterion, a poor polymeric film, both in appearance and electrochemical properties was formed, suggesting that the presence of a counterion was necessary for the polymerization process to be successful. Amino acid analysis of the polymer using a leucine marker showed that approximately 0.1% w/v (0.2 μg) of the antibody was incorporated into the matrix. When the pyrrole anti-HSA electrode was exposed to 50 μg ml^{-1} HSA for 10 min, a new reduction peak was observed at a potential of approximately +600 mV versus Ag/AgCl. This peak increased in magnitude after a further 30 min in the same solution and it was suggested this could be due to an antibody/antigen interaction with the polymer. Further work by the same group gave rise to reports of a reversible real-time immunosensor (John et al. 1991). Other early work utilized a pulsed amperometric detection technique for other analytes, including *p*-cresol (Barnett et al. 1994), thaumatin (Sadik et al. 1994), and polychlorinated biphenyls (Bender and Sadik 1994). Since this work there has been a huge increase in the development of electrochemical immunosensors as detailed in several recent reviews (Cosnier 2005; Diaz-Gonzalez et al. 2005; Rodriguez-Mozaz et al. 2006).

Antibody-antigen interactions are by their very nature complex and the reproducible response characteristics of immunosensors requires that the

affinity reaction occurring is minimally perturbed by the fabrication procedure. We have previously shown that up to 2–3 μg antibodies for BSA and digoxin may be successfully incorporated into conducting polymer films by entrapment in a growing polypyrrole film with no detrimental effect to antibody activity (Grant et al. 2003). Electrochemical interrogation of these films demonstrated selective interactions with the target antigens. Further work utilized an AC impedance protocol (Grant et al. 2005) as the method of interrogation for these films and led to the development of immunosensors for digoxin and bovine serum albumin.

The quinolones are a family of broad-spectrum antibiotics with the majority of quinolones in clinical use being fluoroquinolones, which have a fluoro group attached to the central ring system. They are widely used within adult patients because of excellent tissue penetration which makes them extremely effective against bacteria that grow intracellularly such as salmonella (Gendrei et al. 2003). One of these groups is ciprofloxacin (Fig. 1) which is a broad-spectrum antibiotic active against many bacteria including anthrax (Torriero et al. 2006). Many of these fluoroquinolones are added to farm animal feed since they can lead to greater and more rapid weight gain. Unfortunately the effect of this is thought to have enabled the rise of resistant species of bacteria (Gendrei et al. 2003).

The monitoring of fluoroquinolones within both food and the environment is important since these antibiotics have potential health and environmental damaging effects. Ciprofloxacin concentrations in hospital wastewaters were monitored and correlations with DNA damaging effects made (Hartmann et al. 1999). Levels of ciprofloxacin in hospital outflow water between 0.7–124.5 ng ml^{-1} were measured using high performance liquid chromatography (HPLC) (Hartmann et al. 1999) and shown to display genotoxicity at levels as low as 5.2 ng ml^{-1}. Similar work (Batt et al. 2006) measured wastewater ciprofloxacin using liquid chromatography/mass spectrometry/mass spectrometry (LC/MS/MS) and found levels between 0.031–5.6 ng ml^{-1} (even after treatment) with a limit of detection of 0.030 ng ml^{-1}. Levels *in vivo* have also been widely studied with the therapeutic ranges typically being between 0.57–2.30 μg ml^{-1} in serum and 1.26–4.03 μg g^{-1} in tissue (Licitra et al. 1987).

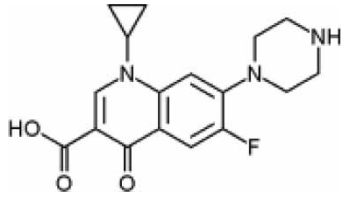

Figure 1. Structure of ciprofloxacin.

A recent publication (Torriero et al. 2006) details the use of a horseradish peroxidase based biosensor for the detection of ciprofloxacin due to its inhibition of the oxidation of catechol, however other piperazine based compounds could potentially interfere with this determination. Linear responses were obtained between 0.02–65 μM with the limit of detection being 0.4 nM. We have within this work developed a labeless immunosensor for ciprofloxacin as a typical fluoroquinolone. The sensor utilizes screen-printed carbon electrodes, modified by deposition of first, a conducting polymer (polyaniline) which is then modified with biotinylating reagent. Complexion of the immobilized biotin with avidin allows the further binding of biotinylated antibodies via standard avidin-biotin interactions (Fig. 2). The resultant electrodes are capable of detecting low levels of the antigen-ciprofloxacin. Control electrodes containing non-specific IgG have also been fabricated and allow the subtraction out of unspecific interactions.

EXPERIMENTAL

Sodium dihydrogen orthophosphate, disodium hydrogen orthophosphate, sodium chloride, and hydrochloric acid, were obtained from BDH (Poole, Dorset). Potassium chloride was obtained from Fisher Scientific UK Ltd, (Loughborough). Aniline, polyclonal IgG from human serum, the biotinylation kit (part no. BK101), biotin 3-sulfo-*N*-hydroxysuccinimide, avidin, bovine serum albumin (BSA), potassium ferrocyanide, and potassium ferricyanide were obtained from Sigma-Aldrich, (Gillingham, Dorset). All water used was obtained from a Purelab UHQ Deioniser (Elga, High Wycombe). Commercial screen-printed carbon electrodes (Fig. 3) containing carbon working and counter electrodes and an Ag/AgCl reference electrode were obtained from Parlex Corp Ltd, Isle of Wight. The surface area of the working electrode was 0.2178 cm^2.

Phosphate Buffered Saline (PBS) at pH 7.4 stock solution was prepared containing 0.14 mol l^{-1} NaH_2PO_4, 0.52 mol l^{-1} Na_2HPO_4, and 0.0051 mol l^{-1} NaCl. Aniline buffer (pH 1–2) was prepared containing 0.5 mol l^{-1} KCl, 0.3 mol l^{-1} HCl, and 0.2 mol l^{-1} aniline.

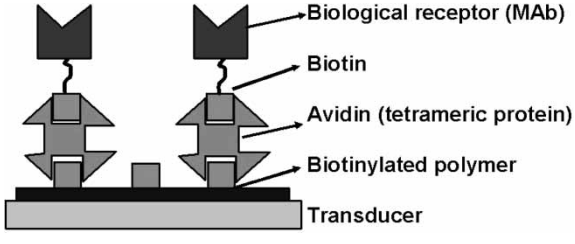

Figure 2. Schematic of antibody modified electrodes.

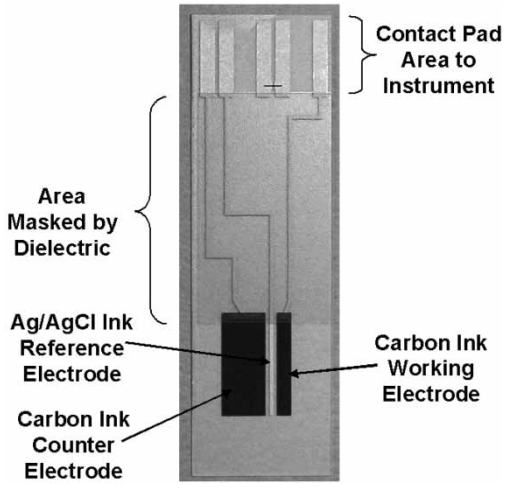

Figure 3. Screen-printed carbon electrodes used within this work.

Polyclonal antiserum (As 171) was raised against 1-(3mercaptopropyl)-6-fluoro-7-(piperanicyl)-1,4-dihydro-4-oxo-quinoline-3-carboxylic acid coupled to HCH. The preparation of the immunogen and of the antibodies will be described elsewhere (Pinacho et al. 2007).

For antibody biotinylation the procedure outlined in the BK101 kit was followed (see manufacturer's instructions for details). Biotinylated antibodies were kept frozen in aliquots of 200-μl at a concentration of 1 mg ml^{-1} until required.

Cyclic voltammetry (Sycopel Potentiometer, Sycopel Scientific, Tyne & Wear) was utilized to deposit polyaniline films on the carbon electrodes. Screen-printed carbon electrodes were placed in aniline buffer and cycled from −200 mV to +800 mV versus Ag/AgCl for approximately 20 cycles (occasionally this was varied slightly to ensure that the same amount of polyaniline was deposited on each electrode. Deposition was terminated at +800 mV to ensure the polyaniline remained in its conducting form. After deposition, electrodes were rinsed in water.

Initially 30 μl of biotin-sulfo-NHS (10 mg ml^{-1} in water) was placed on the polymer coated working electrode surface for 24 h. The sensors were rinsed with copious water and 30 μl of avidin (10 μg ml^{-1} in water) placed on the working electrode for 1 h followed by rinsing in water. Then 30 μl biotinylated antibody (1 mg ml^{-1} in water, 1 hour) was added followed by rinsing. Finally, non-specific interactions were blocked by BSA (10^{-6} M in PBS, 1 hour); the sensors are ready to use at this point, however, if opted, can be stored in PBS at 4°C for no longer than 24 h.

AC impedance measurements were performed using an ACM Auto AC DSP frequency response analyser. Antigen solutions for AC impedance

were prepared by diluting the required concentration of antigen in 30 ml of PBS pH 7.4. A range of concentrations were utilized, since genotoxicity is noted at levels above 5.2 ng ml^{-1}; we set our minimum level at 1 ng ml^{-1} with an upper limit of 10 μg ml^{-1}, which covers the therapeutic/clinical range. However other work within our group suggests detection limits of about 10 pg ml^{-1}. The sensors were first interrogated without antigen addition. Following this, each sensor was exposed to the required antigen concentration for 30 min, rinsed well with deionized water and then subjected to impedance interrogation. Potassium ferrocyanide (10 mM) and potassium ferricyanide (10 mM) in PBS buffer were utilized as a redox couple for impedimetric measurements. Three electrodes were used for each measurement. A frequency range from 10 kHz to 1 Hz was measured, with peak amplitude of 5 mV and a DC offset of +400 mV against Ag/AgCl.

RESULTS AND DISCUSSION

Deposition of Polyaniline

The voltammograms for the deposition of polyaniline/DNA are depicted in Fig. 4 and imply a steady in situ formation of polymer at the electrode surface. As the number of scans increases, peaks appear between +350–400 mV versus Ag/AgCl corresponding to the oxidation and reduction of surface bound polyaniline. The increase in current from scan

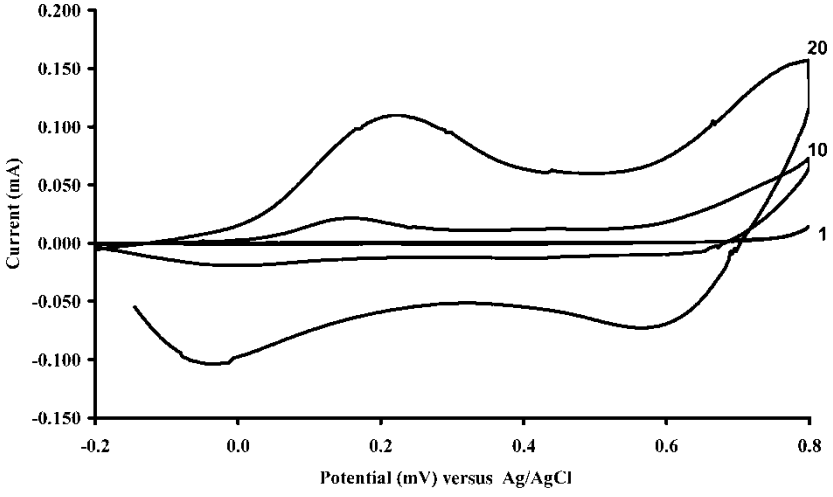

Figure 4. Deposition of conducting polyaniline films by cyclic voltammetry, curves shown after 1, 10, and 20 cycles.

10 to 20 is due to the increase in polyaniline thickness and coverage of the electrode.

Impedance Profiles of the Electrodes

A series of Nyquist curves were obtained for the sensors after exposure to various levels of ciprofloxacin in PBS (Fig. 5a). As can be seen, there is a

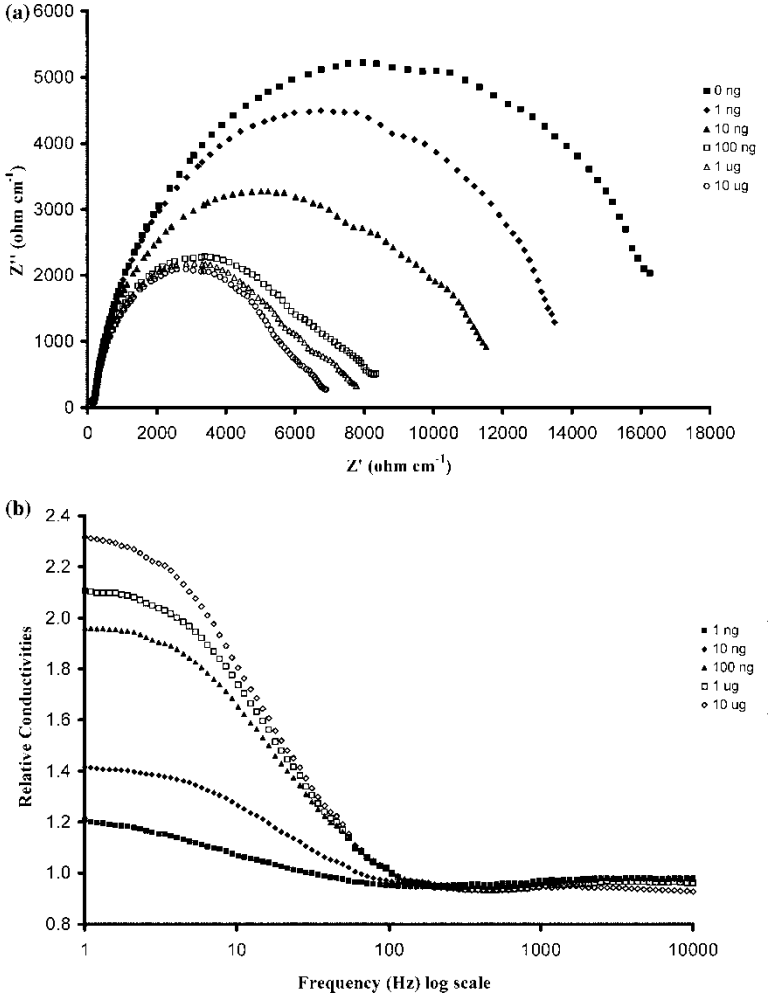

Figure 5. Nyquist plots of a typical antibody modified electrode exposed to various concentrations of antigen.

steady decrease in the impedance of the electrodes with increasing antigen concentration. The relative conductivities of the system, which are obtained by dividing the impedance for each frequency with no antigen present—by the impedance (at the same frequency) for each antigen concentration, are shown in Fig. 5b. As can be seen, we see much larger increases in conductivity at the lower frequencies. Therefore, it was decided that changes in impedance at 1 Hz would be used as a measurement of antigen binding.

The impedance spectra consists of two components, the real (Z') component where the impedance in phase with the AC potential waveform is measured and the imaginary (Z'') where the impedance is 180° out of phase. It is important to differentiate between the individual components of the total impedance of the cell so that the capacitive and Faradaic components of the composite impedimetric response may be identified and quantified. Previous work by our group showed that while both the imaginary and real components increased, the increase in the real component dominated the total increase in the impedance (Grant et al. 2005). Although in this case, changes in both real and imaginary components are visible and again the real component is the major component of total impedance, perhaps more importantly it was also found that the real component offers far greater reproducibility in comparison to the imaginary contribution.

Figures 6a shows the percentage decrease in Z' across a range of antigen concentrations. As can be seen, there is a steady decrease in impedance as antigen concentration increases up to a concentration of about 100 ng ml^{-1}, above which concentration there is a tend towards a plateau, possibly indicating saturation of the specific binding sites. It is possible that any further changes in impedance beyond this level could simply be due to non-specific interactions. Between a concentration range of 1–100 ng ml^{-1}, there is a near linear correlation of the impedance change with the $\log_{10}$ of concentration ($R^2 = 0.96$).

Non-specific interactions could potentially interfere with immunosensor performance. This could be addressed by utilization of a second sensor containing either no antibodies—or alternatively a non-specific antibody. Therefore an identical set of immunosensors were fabricated utilizing a non-specific IgG antibody in place of the specific ciprofloxacin antibody. Results for these electrodes were obtained in exactly the same way and the calibration plot is shown (Fig. 6b). As can be seen, there is a much lower response for the non-specific antibody, showing that although there are non-specific interactions, between the ranges of 1–100 ng ml^{-1}, they comprise a minor component of the detected response. Figure 6c shows the subtracted responses (6a–6b) and again this demonstrates linearity between the response and the $\log_{10}$ of ciprofloxacin concentration between 1–100 ng ml^{-1} ($R^2 = 0.96$).

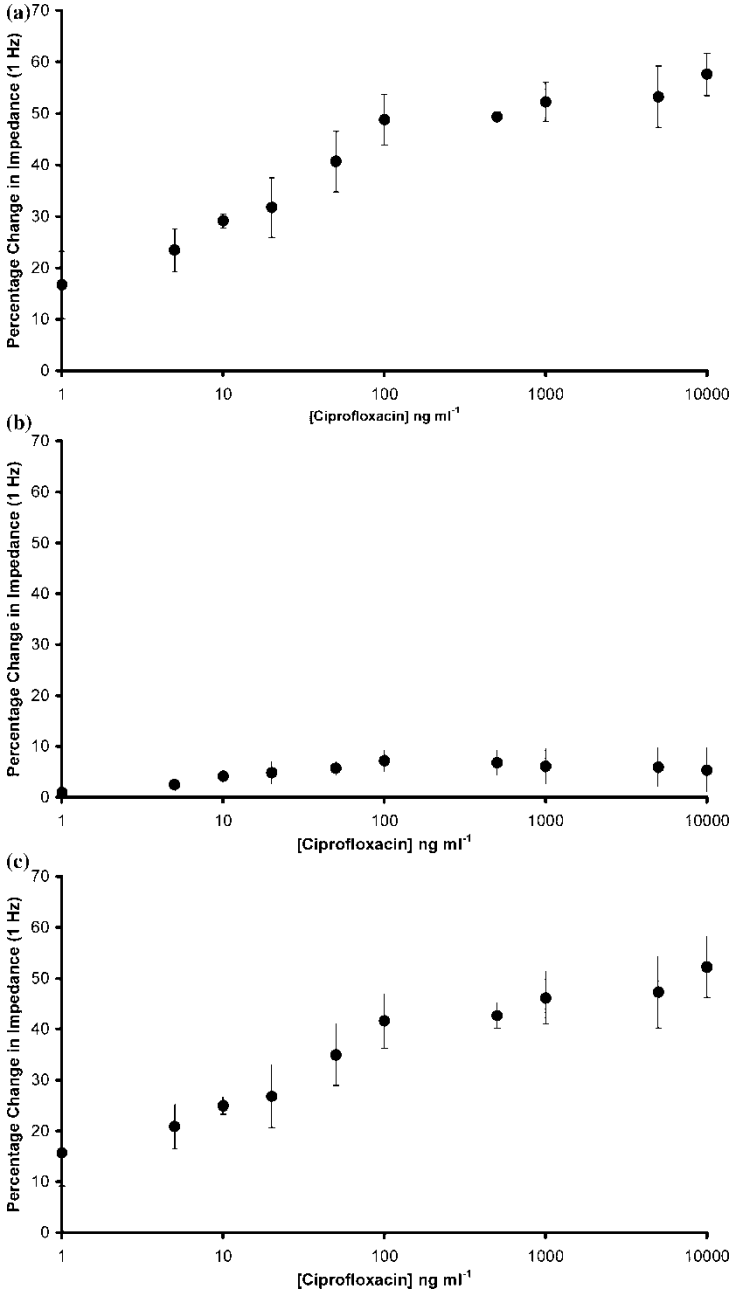

Figure 6. Calibration curves for (a) anti-ciprofloxacin modified electrodes (b) IgG modified electrodes (c) corrected calibration curves (curve a−curve b). All data points are averages of three electrodes; error bars give a measure of the reproducibility of the system.

CONCLUSIONS

We have demonstrated the construction of an immunosensor for the antibiotic ciprofloxacin using a combination of screen-printed electrodes coated with conducting polyaniline and an immobilized polyclonal antibody. Interrogation of the electrodes by AC impedance demonstrated the detection of the antigen. Linear correlation of the impedance change with the $\log_{10}$ of concentration ($R^2 = 0.96$) was observed between concentrations of 1–100 ng ml^{-1}.

REFERENCES

Barnett, D., Laing, D.G., Skopec, S., Sadik, O.A., and Wallace, G.G. 1994. Determination of *p*-cresol (and other phenolics) using a conducting polymer-based electro-immunological sensing system. *Anal. Lett.*, 27: 2417–2429.

Batt, A.L., Bruce, I.B., and Aga, D.S. 2006. Evaluating the vulnerability of surface waters to antibiotic contamination from varying wastewater treatment plant discharges. *Environ. Poll.*, 142: 295–302.

Bender, S. and Sadik, O.A. 1998. Direct electrochemical immunosensor for polychlorinated biphenyls. *Environ. Sci. Tech.*, 32: 788–797.

Clark, L.C. and Lyons, I.R. 1962. Electrode systems for continuous monitoring in cardiovascular surgery. *Ann New York Academy Sci.*, 102: 29.

Cosnier, S. 2005. Affinity biosensors based on electropolymerized films. *Electroanalysis*, 17: 1701–1715.

Diaz-Gonzalez, M., Gonzalez-Garcia, M.B., and Costa-Garcia, A. 2005. Recent advances in electrochemical enzyme immunoassays. *Electroanalysis*, 17: 1901–1918.

Grant, S., Davis, F., Pritchard, J.A., Law, K.A., Higson, S.P.J., and Gibson, T.D. 2003. Labeless and reversible immunosensor assay based upon an electrochemical current-transient protocol. *Anal. Chim. Acta.*, 495: 21–32.

Grant, S., Davis, F., Law, K.A., Barton, A.C., Collyer, S.D., Higson, S.P.J., and Gibson, T.D. 2005. A reagentless immunosensor for the detection of bsa at platinum electrodes by an ac impedance protocol. *Anal. Chim. Acta.*, 537: 163–168.

Gendrei, D., Chalumeau, M., Moulin, F., and Raymond, J. 2003. Fluoroquinolones in paediatrics: A risk for the patient or for the community. *Lancet Inf. Dis.*, 3: 537–546.

Hartmann, A., Golet, E.M., Gartiser, S., Alder, A.C., Koller, T., and Widmer, R.M. 1999. Primary DNA damage but not mutagenicity correlates with ciprofloxacin concentrations in German hospital wastewaters. *Ach. Environ. Contam. Toxicol.*, 115–119.

John, R., Spencer, M., Wallace, G.G., and Smyth, M.R. 1991. Development of a polypyrrole-based human serum albumin sensor. *Anal. Chim. Acta.*, 249: 381–385.

Licitra, C.M., Brooks, R.G., and Sieger, B.E. 1987. Clinical efficacy and levels of ciprofloxacin in tissue in patients with soft tissue infection. *Antimicrob. Agents Chemother.*, 31: 805–807.

Pinacho, D.G., Sanchez-Baeza, F., and Marco, M.P. 2007. Development of a class selective indirect competitive enzyme-linked immunosorbent assay (ELISA) for detection of fluoroquinolone antibiotics, in preparation .

Rodriguez-Mozaz, S., de Alda, M.J.L., and Barcelo, D. 2006. Biosensors as useful tools for environmental analysis and monitoring. *Anal. Bioanal. Chem.*, 386: 1025–1041.

Sadik, O.A., John, M.J., Wallace, G.G., Barnett, D., Clarke, C., and Laing, D.G. 1994. Pulsed amperometric detection of thaumatin using antibody-containing poly(pyrrole) electrodes. *Analyst.*, 119: 1997–2000.

Torriero, A.A.J., Ruiz-Dıaz, J.J.J., Salinas, E., Marchevsky, E.J., Sanz, M.I., and Raba, J. 2006. Enzymatic rotating biosensor for ciprofloxacin determination. *Talanta*, 69: 691–699.

Yalow, R.S. and Berson, S.A. 1959. Assay of plasma insulin in human subjects by immunological methods. *Nature*, 184: 1648–1649.

Anal. Chem. **2008,** *80,* 9233–9239

Detection of Fluoroquinolone Antibiotics in Milk via a Labeless Immunoassay Based upon an Alternating Current Impedance Protocol

Georgios Tsekenis,[†] Goulielmos-Zois Garifallou,[†] Frank Davis,[†] Paul A. Millner,[‡] Daniel G. Pinacho,[§] Francisco Sanchez-Baeza,[§] M.-Pilar Marco,[§] Tim D. Gibson,[||] and Séamus P. J. Higson*,[†]

Cranfield Health, Cranfield University, Silsoe, Bedfordshire, MK45 4DT, U.K., School of Biochemistry and Molecular Biology, University of Leeds, Leeds, LS2 9JT, U.K., Applied Molecular Receptors Group (AMRg), CSIC, CIBER of Bioengineering, Biomaterials and Nanomedicine, Jorge Girona 18-26, 08034-Barcelona, Spain, and T and D Technology Ltd., Wakefield, West Yorkshire, WF3 4AA, U.K.

This paper describes the construction of a labeless immunosensor for the antibiotic ciprofloxacin in milk and its interrogation using an ac impedance protocol. Commercial screen-printed carbon electrodes were used as the basis for the sensor. Polyaniline was electrodeposited onto the sensors and then utilized to immobilize a biotinylated antibody for ciprofloxacin using classical avidin−biotin interactions. Antibody loaded electrodes were exposed to solutions of antigen in milk and interrogated using an ac impedance protocol. The faradaic component of the impedance of the electrodes was found to increase with increasing concentration of antigen. Control samples containing a nonspecific IgG antibody were also studied but were found to display large nonspecific responses, probably due to the antibody binding some of the large number of components found in milk. Control sensors could, however, be fabricated using antibodies specific for species not found in milk. Calibration curves could be obtained by subtraction of the responses for specific and control antibody-based sensors, thereby eliminating the effects of nonspecific adsorption of antigen. Sensors exposed to ciprofloxacin in milk gave increases in impedance whereas ciprofloxacin in phosphate buffer led to decreases, indicating the possibility of developing sensors which can both detect and differentiate between free and chelated antigen.

The principle of immunoassays was first established by Yalow and Berson[1] in 1959 and led to the development of the widely used radioimmunoassay technique, initially to determine insulin-binding antibodies in human serum, using samples obtained from subjects that had been treated with insulin. Independently within unconnected work, Clark and Lyons[2] in 1962 developed the concept of a biosensor. The original methodology involved immobilizing enzymes on the surface of electrochemical sensors so as to exploit the selectivity of enzymes for analytical purposes. Although the field has undergone continual technological developments over the last 40 years, the basic idea has remained virtually unchanged since the original design.

The incorporation of antibodies into conducting polymer films was first reported[3] in 1991. Polypyrrole films were galvanostatically polymerized onto a platinum wire substrate. When grown in the absence of a counterion, a poor polymeric film (both in appearance and electrochemical properties) was formed, suggesting that the presence of a counterion was necessary for the polymerization process to be successful. Antihuman serum albumin (anti-HSA) could be incorporated into the film; amino acid analysis of the resulting polymer using a leucine marker determined that approximately 0.1% w/w (0.2 μg) of the antibody was incorporated into the matrix. Exposure of the pyrrole anti-HSA electrode to a 50 μg mL^{-1} HSA solution for 10 min led to the formation of a new reduction peak at a potential of approximately +600 mV versus Ag/AgCl. This peak increased in magnitude after a further 30 min in the same solution, suggesting that this could be due to an antibody/antigen interaction with the polymer. Further work by the same group gave rise to reports of a reversible real-time immunosensor.[3] Other early work utilized a pulsed amperometric detection technique for other analytes, including *p*-cresol,[4] thaumatin,[5] and polychlorinated biphenyls.[6] Since this early work there has been burgeoning interest in the development of electrochemical immunosensors, as detailed in several recent reviews.[7−9]

* Corresponding author. Fax (+44) 01525 863433, e-mail s.p.j.higson@cranfield.ac.uk.

[†] Cranfield University.

[‡] University of Leeds.

[§] Applied Molecular Receptors Group (AMRg), CSIC, CIBER of Bioengineering, Biomaterials and Nanomedicine.

[||] T and D Technology Ltd.

(1) Yalow, R. S.; Berson, S. A *Nature* **1959**, *184*, 1648–1649.

(2) Clark, L. C.; Lyons, I. R. *Ann. N. Y. Acad. Sci.* **1962**, *102*, 29.

(3) John, R.; Spencer, M.; Wallace, G. G.; Smyth, M. R. *Anal. Chim. Acta* **1991**, *249*, 381–385.

(4) Barnett, D.; Laing, D. G.; Skopec, S.; Sadik, O. A.; Wallace, G. G. *Anal. Lett.* **1994**, *27*, 2417.

(5) Sadik, O. A.; John, M. J.; Wallace, G. G.; Barnett, D.; Clarke, C.; Laing, D. G. *Analyst* **1994**, *119*, 1997–2000.

(6) Bender, S.; Sadik, O. A. *Environ. Sci. Technol.* **1998**, *32*, 788–797.

(7) Rodriguez-Mozaz, S.; de Alda, M. J. L.; Barcelo, D. *Anal. Bioanal. Chem.* **2006**, *386*, 1025–1041.

(8) Diaz-Gonzalez, M.; Gonzalez-Garcia, M. B.; Costa-Garcia, A. *Electroanalysis* **2005**, *17*, 1901–1918.

(9) Cosnier, S. *Electroanalysis* **2005**, *17*, 1701–1715.

10.1021/ac8014752 CCC: $40.75 © 2008 American Chemical Society
Published on Web 10/28/2008

Antibody−antigen interactions are by their very nature complex, and it follows that the affinity reaction must be only minimally perturbed by the fabrication procedure to allow the immunosensors to display reproducible response characteristics. Previously within our group we have shown that up to 2−3 μg of antibodies for BSA and digoxin may be successfully incorporated into conducting polymer films by entrapment in a growing polypyrrole film with no detrimental effect to antibody activity.[10] Electrochemical interrogation of these films demonstrated selective interactions with the target antigens. Further work utilized an ac impedance protocol[11] as the method of interrogation for these films, and led to the development of immunosensors for digoxin and bovine serum albumin. Later work by our group studied approaches for immobilization of antibodies onto polyaniline-coated screen-printed carbon electrodes utilizing a classical avidin−biotin chemistry. This enabled the construction of immunosensors for the fluoroquinolone antibody ciprofloxacin[12] in buffer solutions. We have also demonstrated selective immunosensors for myelin basic protein,[13] prostate specific antigen,[14] and the stroke marker proteins neuron specific enolase[15] and S-100 [β].[16]

Fluoroquinolones are members of the quinolone family of broad-spectrum antibiotics and comprise the majority of quinolones in clinical use, the name fluoroquinolone deriving from the fact they have a fluoro group attached to the central ring system. Antibiotics of this type have excellent tissue penetration which makes them extremely effective against bacteria that grow intracellularly such as salmonella, and this has led to their widespread use within adult patients.[17] One antibiotic within this group is ciprofloxacin (Figure S1, Supporting Information) which is a broad-spectrum antibiotic active against many bacteria including anthrax.[18] Many of these fluoroquinolones are added to farm animal feed since they can lead to greater and more rapid weight gain. Unfortunately this is also thought to have contributed to the rise of antibiotic resistant species of bacteria.[17]

The monitoring of fluoroquinolones within both food and the environment is important since these antibiotics have potential health related and environmental damaging effects. Ciprofloxacin concentrations in hospital wastewater were monitored and correlations with DNA damaging effects made.[19] HPLC techniques have been utilized to measure levels of ciprofloxacin in hospital outflow water[19] and found levels between 0.7−124.5 ng mL^{-1}, as well as displaying genotoxicity at levels as low as 5.2 ng mL^{-1}. Similar work utilized LC/MS/MS methods[20] and found wastewater ciprofloxacin levels between 0.031−5.6 ng mL^{-1} (even after treatment) with a limit of detection of 0.030 ng mL^{-1}. Levels in vivo have also been widely studied with the therapeutic ranges typically being between 0.57−2.30 μg mL^{-1} in serum and 1.26−4.03 μg g^{-1} in tissue.[21]

A horseradish peroxidase-based biosensor[18] has been developed for the detection of ciprofloxacin due to its inhibition of the oxidation of catechol. Linear responses were obtained between 0.02−65 μM with the limit of detection being 0.4 nM; however, other piperazine-based compounds could potentially interfere with this determination. We have within earlier work developed a labeless immunosensor for ciprofloxacin as a typical fluoroquinolone which utilizes screen-printed carbon electrodes modified by deposition of first, a conducting polymer (polyaniline) which is then functionalized with a biotinylating reagent.[12] Complexation of the immobilized biotin with neutravidin allows the further binding of biotinylated antibodies via standard avidin−biotin interactions (Figure S2, Supporting Information). The resultant electrodes are capable of detecting low levels of the ciprofloxacinin antigen dissolved in phosphate buffer.[12] For an immunosensor to be of practical use, however, it must be capable of the analysis of the substrate within a wide range of matrixes. Since fluoroquinonolones are widely used within the animal industry, it was decided to investigate whether ciprofloxacin could be detected in milk. The European Union has set a maximum residue limit of 100 ng mL^{-1} for enrofloxacin plus ciprofloxacin in milk.[22] Previous studies have utilized techniques such as HPLC to detect various fluoroquinolone antibodies in bovine milk[22] with a detection limit of 3 ng mL^{-1} for ciprofloxacin and LC with luminescence detection[23] to measure ciprofloxacin in milk with a linear range of 8−3500 ng mL^{-1} and a detection limit of 3 ng mL^{-1}. A number of ELISA-based tests[24,25] have also been developed to detect fluoroquinolones in milk with detection limits of several nanograms per milliliter. Recent work has also described the construction of a DNA-based sensor which when combined with a surface plasmon resonance method allows quantification of enrofloxacin between 3−20 μg mL^{-1} in milk.[26] An immunosensor for ciprofloxacin based on polypyrrole films combined with an ac impedance technique[27] has also been described with sensitivities as low as 10 pg mL^{-1}.

EXPERIMENTAL SECTION

Sodium dihydrogen orthophosphate, disodium hydrogen orthophosphate, sodium chloride, hydrochloric acid, were obtained from BDH (Poole, Dorset, U.K.). Potassium chloride was obtained from Fisher Scientific UK Ltd., Loughborough, U.K.. Aniline,

(10) Grant, S.; Davis, F.; Pritchard, J. A.; Law, K. A.; Higson, S. P. J.; Gibson, T. D. *Anal. Chim. Acta* **2003**, *495*, 21–32.
(11) Grant, S.; Davis, F.; Law, K. A.; Barton, A. C.; Collyer, S. D.; Higson, S. P. J.; Gibson, T. D. *Anal. Chim. Acta* **2005**, *537*, 163–168.
(12) Garifallou, G.-Z.; Tsekenis, G.; Davis, F.; Millner, P. A.; Pinacho, D. G.; Sanchez-Baeza, F.; Marco, M.-P.; Gibson, T. D.; Higson, S. P. J. *Anal. Lett.* **2007**, *40*, 1412–1442.
(13) Tsekenis, G.; Garifallou, G. Z.; Davis, F.; Millner, P. A.; Gibson, T. D.; Higson, S. P. J. *Anal. Chem.* **2008**, *80*, 2058–2062.
(14) Barton, A. C.; Davis, F.; Higson, S. P. J. *Anal. Chem.* **2008**, *80*, 6198–6205.
(15) Barton, A. C.; Davis, F.; Higson, S. P. J. *Anal. Chem.*, submitted.
(16) Barton A. C., Ph.D. Thesis, Cranfield University, Silsoe, 2008.
(17) Gendrei, D.; Chalumeau, M.; Moulin, F.; Raymond, J. *Lancet Inf. Dis.* **2003**, *3*, 537–546.
(18) Torriero, A. A. J.; Ruiz-Dıaz, J. J. J.; Salinas, E.; Marchevsky, E. J.; Sanz, M. I.; Raba, J. *Talanta* **2006**, *69*, 691–699.
(19) Hartmann, A.; Golet, E. M.; Gartiser, S.; Alder, A. C.; Koller, T.; Widmer, R. M. *Arch. Environ. Contam. Toxicol.* **1999**, 115–119.
(20) Batt, A. L.; Bruce, I. B.; Aga, D. S. *Environ. Pollut.* **2006**, *142*, 295–302.
(21) Licitra, C. M.; Brooks, R. G.; Sieger, B. E. *Antimicrob. Agents Chemother.* **1987**, *31*, 805–807.
(22) Hassouan, M.; Ballesteros, O.; Vilchez, J.; Zafra, A.; Navalon, A. *Anal. Lett.* **2007**, 779–791.
(23) Rodriguez-Diaz, R. C.; Fernandez-Romero, J. M.; Aguilar-Caballos, M. P.; Gomez-Hens, A. *J. Agric. Food Chem.* **2006**, 9670–9676.
(24) Bucknall, S.; Silverlight, J.; Coldham, N.; Thorne, L.; Jackman, R. *Food Addit. Contam.* **2006**, *20*, 221–228.
(25) Duan, J.; Yuan, Z. H. *J. Agric. Food Chem.* **2001**, *49*, 1087–1089.
(26) Cao, L. M.; Lin, H.; Mirsky, V. M. *Anal. Chim. Acta* **2007**, *589*, 1–5.
(27) Ionescu, R. E.; Jaffrezic-Renault, N.; Bouffier, L.; Gondran, C.; Cosnier, S.; Pinacho, D. G.; Marco, M. P.; Sanchez-Baeza, F. J.; Healy, T.; Martelet, C. *Biosens. Bioelectron.* **2007**, *23*, 549–555.

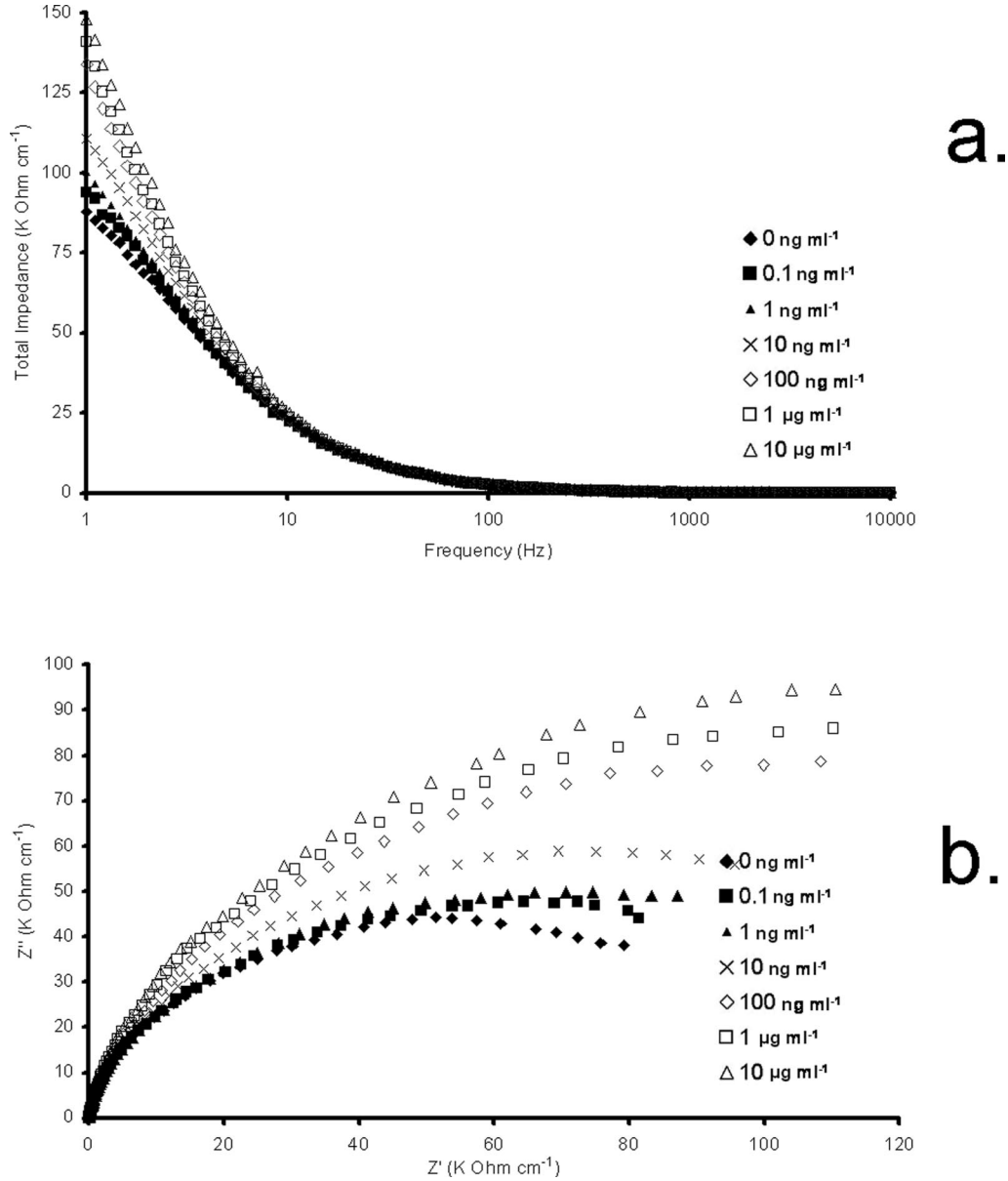

Figure 1. (a) Bode and (b) Nyquist plots of a typical ciprofloxacin-specific antibody modified electrode exposed to ciprofloxacin.

polyclonal IgG (rabbit), the biotinylation kit (part no. BK101), biotin 3-sulfo-*N*-hydroxysuccinimide, avidin, and bovine serum albumin (BSA) were obtained from Sigma-Aldrich, Gillingham, Dorset, U.K. Ciprofloxacin hydrochloride was purchased from UQUIFA (Barcelona, Spain). All water used was obtained from a Purelab UHQ Deioniser (Elga, High Wycombe, U.K.). Commercial screen-printed carbon electrodes identical to those used in previous work (Figure S3, Supporting Information) containing carbon working and counter electrodes and an Ag/AgCl reference electrode were obtained from Microarray Ltd., Manchester, U.K. The surface area of the working electrode was 0.2178 cm^2. Semiskimmed bovine milk was purchased from a local supermarket.

Phosphate Buffered Saline (PBS) stock solution (pH 7.4) was prepared containing 0.14 mol L^{-1} NaH_2PO_4, 0.52 mol L^{-1} Na_2HPO_4, and 0.0051 mol L^{-1} NaCl. Aniline buffer (pH 1−2) was prepared containing 0.5 mol L^{-1} KCl, 0.3 mol L^{-1} HCl, and 0.2 mol L^{-1} aniline.

Polyclonal antiserum (As 171) was a gift from AMRg and was raised (in rabbit) against 1-(3- mercaptopropyl)-6-fluoro-7-(piperanicyl)-1,4-dihydro-4-oxo-quinoline-3-carboxylic acid coupled to horseshoe crab hemicyanin. The preparation of the immunogen and of the antibodies has been described elsewhere.[36] The antibody was supplied in raw serum. Monoclonal antibody to prostate specific antigen (PSA 30 mAb, isotype IgG1, product number 323-01) with sodium azide preservative was supplied by Canag Diagnostics, Ltd. (Gothenburg, Sweden).

For antibody biotinylation, the procedure outlined in the BK101 kit was followed (see manufacturer's instructions for details). Biotinylated antibodies were kept frozen in aliquots of 200 μL at a concentration of 1 mg mL^{-1} until required.

Cyclic voltammetry (Sycopel Potentiometer, Sycopel Scientific, Tyne and Wear, U.K.) was utilized to deposit polyaniline films on the carbon electrodes. Screen-printed carbon electrodes were placed in aniline buffer and cycled from −200 to +800 mV versus Ag/AgCl for approximately 20 cycles (occasionally this was varied

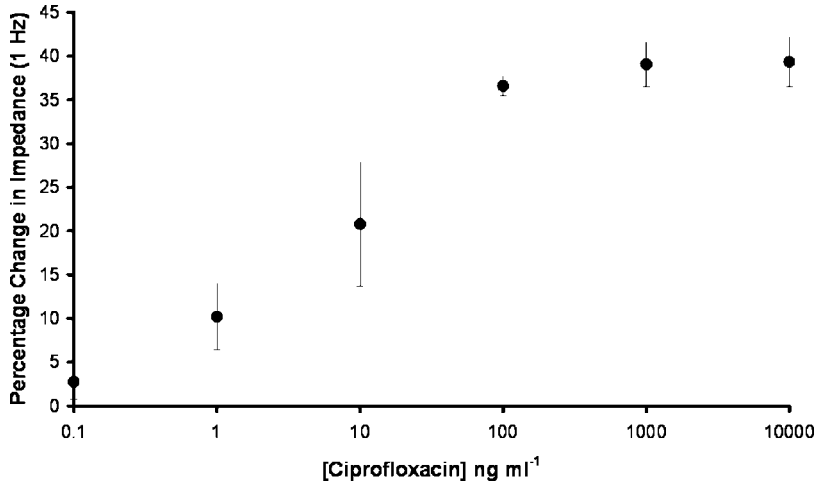

Figure 2. Calibration curve for anticiprofloxacin modified electrodes.

slightly to ensure the same quantity of polyaniline was deposited on each electrode). Deposition was terminated at +800 mV to ensure the polyaniline remained in its conducting form. After deposition, electrodes were rinsed in water.

A volume of 30 μL of biotin-sulfo-NHS (10 mg mL^{-1} in water) was placed on the polymer-coated working electrode surface for 24 h. The sensors were rinsed with copious water, and 30 μL of avidin (10 μg mL^{-1} in water) was placed on the working electrode for 1 h followed by rinsing in water. Then 30 μL of biotinylated antibody (1 mg mL^{-1} in water) was added followed by rinsing. Finally, nonspecific interactions were blocked by BSA (10^{-6} M in PBS); the sensors may be used at this point, however, if opted, can be stored in PBS at 4 °C for up to 24 h or dry at 4 °C for several weeks.[14−16]

Alternating current impedance measurements were performed using an ACM Auto AC DSP frequency response analyzer. Antigen solutions were prepared by initially dissolving ciprofloxacin in PBS, then diluting to the required concentration of antigen in 30 mL of milk. A range of concentrations was utilized; we set our minimum level at 0.1 ng mL^{-1} with an upper limit of 10 μg mL^{-1}. The sensors were first interrogated without antigen addition. Following this, each sensor was exposed to the required antigen concentration for 30 min, rinsed well with deionized water, and then subjected to impedance interrogation in fresh milk. Three electrodes were used for each measurement. A frequency range from 10 kHz to 1 Hz was measured, with a peak amplitude of 5 mV and a dc offset of +400 mV against Ag/AgCl.

RESULTS AND DISCUSSION

Deposition of Polyaniline. The voltammograms for the deposition of polyaniline were as found in earlier work[12,13] and imply a steady in situ formation of polymer at the electrode surface. As the number of scans increases, peaks appear between +350 and 400 mV vs Ag/AgCl corresponding to the oxidation and reduction of surface bound polyaniline, with the current passed increasing with the number of scans due to the increase in polyaniline thickness and coverage of the electrode.

Impedance Profiles of the Electrodes. A series of Bode (Figure 1a) and Nyquist curves (Figure 1b) were obtained for the sensors after exposure to various levels of ciprofloxacin in milk. As can be seen, there is a steady increase in the impedance of the electrodes with increasing antigen concentration. This was unexpected since our work on ciprofloxacin in phosphate buffer (containing 10 mM ferri/ferrocyanide) clearly demonstrates that binding of the antigen leads to a drop in impedance. As can be seen, we see much larger increases in impedance at the lower frequencies. Therefore it was decided that changes in impedance at 1 Hz would be used as a measurement of antigen binding.

The Nyquist plots display the two components of the impedance spectra: the real (Z') component where the impedance in phase with the ac potential waveform is measured and the imaginary (Z'') where the measured impedance is 180° out of phase. Both of the individual components contribute to the total impedance of the cell. However it is important to differentiate between these so that the individual components of the composite impedimetric response may be identified and quantified.

In this system, the Z' (real) component of the impedance can be seen to steadily increase with decreasing frequency. In the baseline plot, the Z'' (imaginary) component increases to a maximum value before falling as the frequency approaches 1 Hz. Similar behavior appears to occur as antigen binding increases except that for the higher concentrations of ciprofloxacin the maximum value is beyond our frequency range. This type of impedance spectrum is indicative of a surface-modified electrode system where the electron transfer is slow and the impedance is controlled by the interfacial electron transfer.[28]

In previous pieces of work within our group we have demonstrated that although both the imaginary and real components increase, the increase in the real component dominates the total increase in the impedance.[11−13] Although in this case and in previous work,[11−13] changes in both real and imaginary components are visible, once again the real component is the major component of total impedance and perhaps more importantly we have repeatedly found that the real component offers far greater reproducibility in comparison to the imaginary contribution.

Figure 2 shows the percentage increase in Z' (measured at 1 Hz) across a range of antigen concentrations. As can be seen, there is a steady increase in the real component of impedance as antigen concentration increases up to a concentration of about 100 ng mL^{-1}, above which concentration there is a tendency

(28) Katz, E.; Willner, I. *Electroanalysis* **2003**, *15*, 913–947.

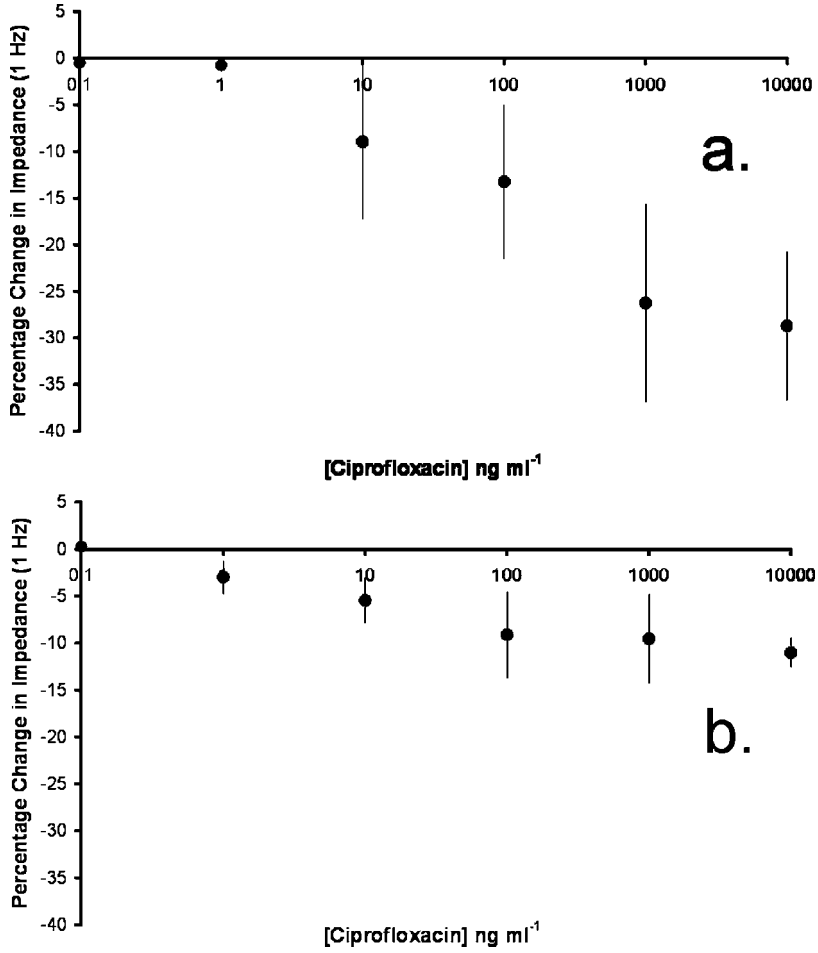

Figure 3. Control calibration curves for (a) IgG modified electrodes and (b) PSA modified electrodes.

toward a plateau, possibly indicating saturation of the specific binding sites. It is possible that any further changes in impedance beyond this level could simply be due to nonspecific interactions. Between a concentration range of 1−100 ng mL^{-1}, there is a near linear correlation of the impedance change with the $\log_{10}$ of concentration ($R^2 = 0.96$).

Nonspecific interactions could potentially interfere with immunosensor performance. We have previously described the utilization of control electrodes containing a nonspecific IgG antibody.[11−13] These permit the subtraction of unspecific interactions from the specific binding response and also may help to increase the stability and reliability of these sensors when applied to complex mixtures such as milk, other foodstuffs, or clinical samples. Therefore an identical set of immunosensors were fabricated utilizing a nonspecific IgG antibody in place of the specific ciprofloxacin antibody. The commercial IgG sample was taken from the same species as the specific antibody was raised (rabbit) in order to make the match as relevent as possible. Results for these electrodes were obtained in exactly the same way, and the calibration plot is shown (Figure 3a). As can be seen, there is a very high decrease in impedance for the nonspecific antibody. However further experiments showed that these results are a function of the time of exposure rather than ciprofloxacin concentration, i.e., a repeat of the experiment where the electrodes were exposed just to milk without antigen gave an identical plot. A possible explanation for this is that since milk is such a complex mixture of components and IgG is a mixture of different antibodies, some of the antibodies will specifically bind to certain species in milk.

In order to test this theory, another set of control electrodes were utilized, where instead of nonspecific IgG antibody, a specific antibody for an antigen not normally found in milk was utilized. Figure 3b shows the results upon exposure to ciprofloxacin in milk for electrodes fabricated using a specific antibody for prostate specific antigen (PSA), used in earlier work.[14] Results for these electrodes showed that although there are nonspecific interactions, between the ranges of 0.1−100 ng mL^{-1}, they comprise a minor component of the detected response and in fact lead to a drop rather than a gain in impedance, as was found within our earlier work on ciprofloxacin in PBS.[12] Although PSA has been found in human milk,[29] the median levels were well below 1 ng mL^{-1} and also as all readings are referenced to electrodes after exposure to bovine milk containing zero ciprofloxacin, any effect to due binding of "bovine PSA" would cancel out. Also our previous work has shown antibodies can differentiate between similar compounds from different species, for example, they can differentiate between bovine and human serum albumin.[30]

(29) Yu, H.; Diamandis, E. P. *Clin. Chem.* **1995**, *41*, 54–58.
(30) Barton, A. C.; Collyer, S. D.; Davis F.; Garifallou G.-Z.; Tsekenis G.; Tully, E.; O'Kennedy, R.; Gibson T. D.; Millner P. A.; Higson S. P. J. *Biosens. Bioelectron.*, in press.

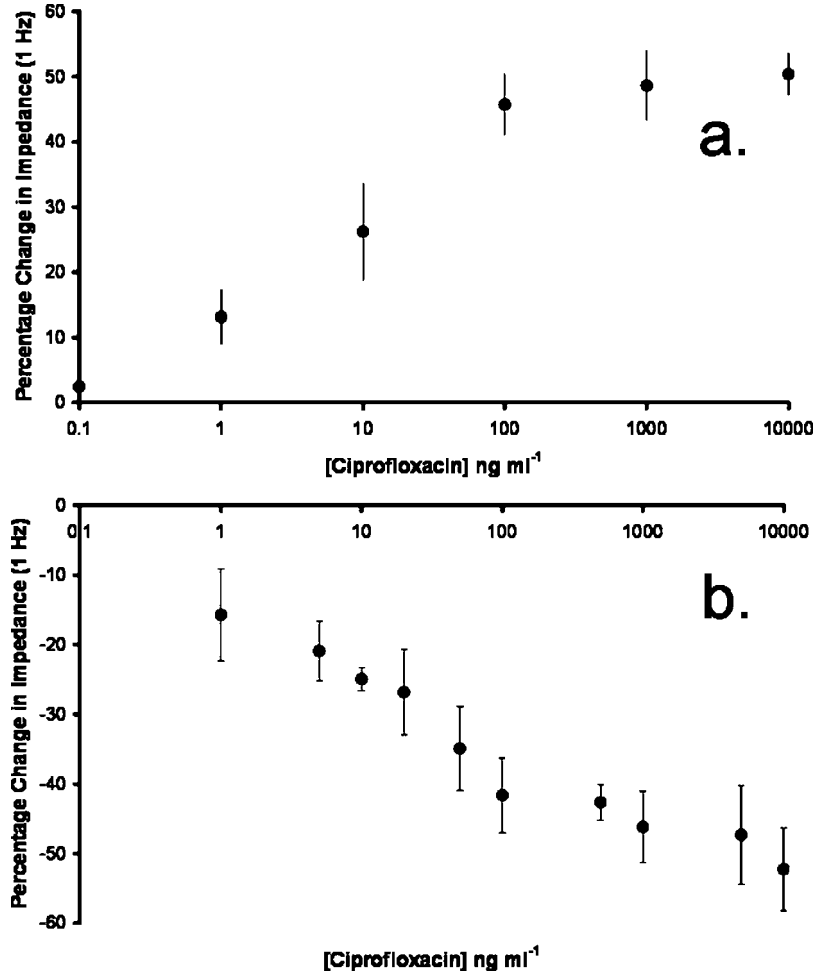

Figure 4. (a) Corrected calibration curve for anticiprofloxacin modified electrodes in milk (Figure 2 − Figure 3b) and (b) for comparison purposes the calibration curve for ciprofloxacin in phosphate buffer previously reported.[12] All data points are means of three electrodes; error bars give a measure of the reproducibility of the system.

Figure 4a shows the subtracted responses (Figure 3a − Figure 2). As can be seen this demonstrates linearity between the response and the $\log_{10}$ of ciprofloxacin concentration between 0.1−100 ng mL^{-1} ($R^2 = 0.98$). Above 100 ng mL^{-1}, the receptors appear to be saturated. Figure 4b displays our earlier results for ciprofloxacin in PBS (containing 10 mM ferri/ferrocaynide)[12] overlaid over those for milk. As can be seen, the results are very similar in that they give linear ranges with very similar gradients in the region 0−100 ng mL^{-1} and above 100 ng mL^{-1} appear to be saturated. However they are of opposite nature; adsorption of ciprofloxacin from milk gives an increase in Z' whereas from PBS a decrease is observed. One potential explanation for this is that in milk a different ciprofloxacin species is being adsorbed. It has been reported that in the presence of calcium ions, many fluoroquinolone antibiotics, including ciprofloxacin, readily form calcium chelate complexes.[31,32] These complexes are usually dimeric in nature with two ciprofloxacin units complexed to a single calcium ion.[31] Binding of ciprofloxacin in either its free or chelated form over similar concentration ranges is occurring, as shown by responses compared to control samples, with the great structural differences between the free and complexed forms of the antigen leading to different effects on the ac impedance results. The effects of adsorption of various moieties on the ac impedance behavior is highly complex and not well understood. For example in previous work by our group on DNA-based sensors, adsorption of cDNA stands has been shown to lead to drops in the ac impedance of our electrodes whereas adsorption of noncDNA leads to an increase.[33,34] Unfortunately control experiments where calcium ions were added to PBS were not possible since addition of calcium to the buffer cause immediate precipitation of calcium phosphates.

These results are of interest since they show that it may be possible to differentiate between complexed and free ciprofloxacin. Ongoing work is attempting to determine whether the complexed and uncomplexed forms can be differentiated. This is of interest since complexed form of ciprofloxacin is inactive, for example, the FDA recommends that ciprofloxacin is not taken with dairy products, calcium fortified juices, or calcium containing antacids[35] since they may lower adsorption of the drug.

(31) Upadhyay, S. K.; Kumar, P.; Arora, V. *J. Struct. Chem.* **2006**, *47*, 1078–1083.
(32) Toyoguchi, T.; Ebihara, M.; Ojima, F.; Hosoya, J.; Nakagawa, Y. *Biol. Pharm. Bull.* **2005**, *28*, 841–844.
(33) Davis, F.; Nabok, A. V.; Higson, S. P. J. *Biosens. Bioelectron.* **2004**, *20*, 1531–1538.
(34) Davis, F.; Hughes, M. A.; Cossins, A. R.; Higson, S. P. J. *Anal. Chem.* **2007**, *79*, 1153–1157.

CONCLUSIONS

We have demonstrated the construction of an immunosensor for the antibiotic ciprofloxacin using a combination of screen-printed electrodes coated with conducting polyaniline and immobilized antibodies. The electrodes were then exposed to solutions of the antigen in milk. Interrogation of the electrodes by ac impedance demonstrated the detection of the antigen. Linear increases of the impedance change with the $\log_{10}$ of concentration ($R^2 = 0.98$) was observed between concentrations of 0.1−100 ng mL^{-1}. The sensor not only bound the antigen from PBS or milk but the ac response was dependent on the matrix the ciprofloxacin was adsorbed from, possibly due to formation of a dimeric calcium chelated form of the antibiotic in milk. This is especially of interest, since free and chelated ciprofloxacin have very different adsorption characteristics when ingested.

(35) http://www.fda.gov/cder/foi/label/2002/19537s41lbl.pdf.
(36) Adrian, J.; Pinacho, D. G.; Granier, B.; Diserens, J. M.; Sánchez-Baeza, F.; Marco, M. P. *Anal. Bioanal. Chem.* **2008**, *391*, 1703–1712.

ACKNOWLEDGMENT

This work has been supported by the Ministry of Science and Technology (Spain) (Contract Numbers AGL2005-07700-C06-01 and NAN2004-09195-C04-04) and by the European Community Framework VI NMP2-CT-2003-505485, "ELISHA" Contract. The AMR group is a consolidated Grup de Recerca de la Generalitat de Catalunya and has support from the Departament d'Universitats, Recerca i Societat de la Informació la Generalitat de Catalunya (Expedient 2005SGR 00207). D.G. has a fellowship from the Fundación EROSKI.

SUPPORTING INFORMATION AVAILABLE

Additional information as noted in text. This material is available free of charge via the Internet at http://pubs.acs.org.

Received for review July 15, 2008. Accepted October 7, 2008.

AC8014752

Anal. Chem. **2008,** *80,* 2058−2062

Label-less Immunosensor Assay for Myelin Basic Protein Based upon an ac Impedance Protocol

Georgios Tsekenis,[†] Goulielmos-Zois Garifallou,[†] Frank Davis,[†] Paul A. Millner,[‡] Tim D. Gibson,[§] and Séamus P. J. Higson*,[†]

Cranfield Health, Cranfield University, Silsoe, Beds, MK45 4DT, U.K., Biosensors and Biocatalysis Group, Research Institute of Membrane and Systems Biology, Garstang Building, University of Leeds, Leeds, LS2 9JT, U.K., and ELISHA Systems Limited, Sigma House, Burlow Road, Buxton, SK17 9JB, U.K.

This paper describes the development and characterization of a label-less immunosensor for myelin basic protein (MBP) and its interrogation using an ac impedance protocol. Commercial screen-printed carbon electrodes were used as the basis for the sensor. Polyaniline was electrodeposited onto the sensors, and this modified surface then utilized to immobilize a biotinylated antibody for MBP using a classical avidin−biotin approach. Electrodes containing the antibodies were exposed to solutions of MBP and interrogated using an ac impedance protocol. The real component of the impedance of the electrodes was found to increase with increasing concentration of antigen. Control samples containing a nonspecific IgG antibody were also studied, and calibration curves were obtained by subtraction of the responses for specific and nonspecific antibody-based sensors, thereby accounting for and eliminating the effects of nonspecific adsorption of MBP. A logarithmic relationship between the concentration of MBP in buffer solutions and the impedimetric response was observed.

The principle of immunoassays was first established by Yalow and Berson[1] in 1959. Their work led to the development of the widely used radioimmunoassay to examine the properties of insulin-binding antibodies in human serum, using samples obtained from subjects that had been treated with insulin.

Independently within unconnected work, the concept of a biosensor was pioneered by Clark and Lyons[2] in 1962. The original methodology involved immobilizing enzymes on the surface of electrochemical sensors so as to exploit the selectivity of enzymes for analytical purposes. This idea has remained virtually unchanged since the original design, although the field has undergone continual technological developments over the last 40 years.

The incorporation of antibodies into conducting polymer films was first reported[3] in 1991. Antihuman serum albumin (anti-HSA) was incorporated into a polypyrrole film, which was galvanostatically polymerized onto a platinum wire substrate. When grown in the absence of a counterion, a poor polymeric film (both in appearance and electrochemical properties) was formed, suggesting that the presence of a counterion was necessary for the polymerization process to be successful. Amino acid analysis of the polymer using a leucine marker showed that approximately 0.1% w/v (0.2 μg) of the antibody was incorporated into the matrix. When the pyrrole anti-HSA electrode was exposed to 50 μg mL^{-1} HSA for 10 min, a new reduction peak was observed at a potential of approximately +600 mV versus Ag/AgCl. This peak increased in magnitude after a further 30 min in the same solution—and it was suggested this could be due to an antibody/antigen interaction with the polymer. Further work by the same group gave rise to reports of a reversible real-time immunosensor.[3] Other early work utilized a pulsed amperometric detection technique for other analytes, including *p*-cresol,[4] thaumatin,[5] and polychlorinated biphenyls.[6] Since this early work there has been burgeoning interest in the development of electrochemical immunosensors—as detailed in several recent reviews.[7−9]

Antibody−antigen interactions are by their very nature complex, and the reproducible response characteristics of immunosensors requires that the affinity reaction is minimally perturbed by the fabrication procedure. We have previously shown that up to 2−3 μg of antibodies for bovine serum albumin and digoxin may be successfully incorporated into conducting polymer films by entrapment in a growing polypyrrole film with no detrimental effect to antibody activity.[10] Electrochemical interrogation of these films demonstrated selective interactions with the target antigens. Further work utilized an ac impedance protocol[11] as the method of interrogation for these films—and led to the development of immunosensors for digoxin and bovine serum albumin. Later work

* Corresponding author. Fax: (+44) 01525 863433. E-mail: s.p.j.higson@cranfield.ac.uk.

† Cranfield University.

‡ University of Leeds.

§ ELISHA Systems Ltd.

(1) Yalow, R. S.; Berson, S. A. *Nature* **1959**, *184*, 1648−1649.

(2) Clark, L.C.; Lyons, I. R. *Ann. N.Y. Acad. Sci.* **1962**, *102*, 29.

(3) John, R.; Spencer, M.; Wallace, G. G.; Smyth, M. R. *Anal. Chim. Acta* **1999**, *249*, 381−385.

(4) Barnett, D.; Laing, D. G.; Skopec, S.; Sadik, O. A.; Wallace, G. G. *Anal. Lett.* **1994**, *27*, 2417.

(5) Sadik, O. A.; John, M. J.; Wallace, G. G.; Barnett, D.; Clarke, C.; Laing, D. G. *Analyst* **1994**, *119*, 1997−2000.

(6) Bender, S.; Sadik, O. A. *Environ. Sci. Technol.* **1998**, *32*, 788−797.

(7) Rodriguez-Mozaz, S.; de Alda, M. J. L.; Barcelo, D. *Anal. Bioanal. Chem.* **2006**, *386*, 1025−1041.

(8) Diaz-Gonzalez, M.; Gonzalez-Garcia, M. B.; Costa-Garcia, A. *Electroanalysis* **2005**, *17*, 1901−1918.

(9) Cosnier, S. *Electroanalysis* **2005**, *17*, 1701−1715.

(10) Grant, S.; Davis, F.; Pritchard, J. A.; Law, K. A.; Higson, S. P. J.; Gibson, T. D. *Anal. Chim. Acta* **2003**, *495*, 21−32.

(11) Grant, S.; Davis, F.; Law, K. A.; Barton, A. C.; Collyer, S. D.; Higson, S. P. J.; Gibson, T. D. *Anal. Chim. Acta* **2003**, *537*, 163−168.

10.1021/ac702070e CCC: $40.75
Published on Web 02/09/2008

by our group studied approaches for immobilization of antibodies onto polyaniline-coated screen-printed carbon electrodes utilizing a classical avidin−biotin chemistry. This enabled the construction of immunosensors for the fluoroquinolone antibody ciprofloxacin.[12]

Myelin is a complex membrane which forms a sheath around axons in vertebrate species.[13] It is the most abundant membrane structure within the vertebrate nervous system, allowing the fast conduction of nerve impulses through the nerve fibers[14] due to its high resistance and low capacitance. Myelin basic protein (MBP) is a cytoplasmic protein important in the process of myelination of nerves in the central nervous system since it comprises the bulk of the main line of compact myelin[13] and up to 30% of the protein content of myelin overall.[14]

A demyelinating disease is any disease of the nervous system in which the myelin sheath of neurons becomes damaged. This impairs the conduction of signals in the affected nerves, causing impairment in sensation, movement, cognition, or other functions, depending on which nerves are involved. Multiple sclerosis (MS), which is a chronic and inflammatory disease of the central nervous system, is an example of a demyelinating disease. Multiple sclerosis affects neurons within the brain and spinal cord that are involved with sensory and motor control functions. The name multiple sclerosis is derived from the multiple scars (or scleroses) that can be observed on the myelin sheaths. At the time of writing MS does not have a cure, although several treatments are available that may slow the appearance of new symptoms.

Multiple sclerosis is currently often diagnosed following occurrence of a number of indicative symptoms. Magnetic resonance imaging (MRI) may be used to evaluate patients who display these symptoms. MRI is capable of imaging areas where demyelination is occurring, with lesions caused by demyelination showing up as bright areas on the scan. Cerebrospinal fluid can also be utilized in the diagnosis of MS, and the presence of immunoglobins can be detected in the majority of MS sufferers. It should be noted, however, that other conditions can also lead to the presence of these species.[15]

Other demyelinating diseases include transverse myelitis, Guillain−Barré syndrome, and progressive multifocal leukoencephalopathy. There are various identified potential causes of demyelination, including autoimmune reactions,[16] infectious agents,[17] genetic conditions,[18] and also exposure to compounds such as carbamate pesticides.[19]

The presence of antibodies against myelin proteins such as MBP can be a predictor of MS.[20] Clinical studies of 103 patients suffering from MS demonstrated that the presence of antibodies

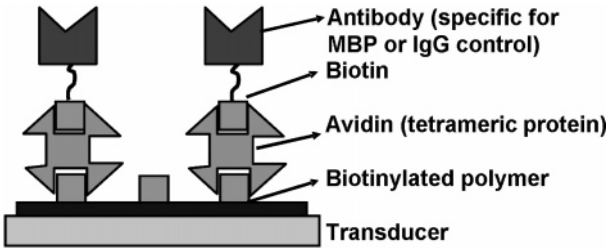

Figure 1. Schematic of antibody-modified electrodes showing the assembly of avidin and biotinylated electrodes and binding of biotinylated antibody.

for MBP and myelin oligodendrocyte glycoprotein within serum could be correlated with a greatly increased level of relapse compared to patients without these antibodies. Other demyelinating conditions also lead to elevated levels of MBP in cerebrospinal fluid,[21,22] for example, in cases of closed head trauma[23] or acquired immunodeficiency syndrome (AIDS) dementia complex (ADC).[24] A significant correlation has also been determined between the clinical stage of the childhood-onset cerebral form of adrenoleukodystrophy and cerebrospinal fluid MBP levels.[25] MBP levels between 4 and 8 ng L^{-1} in cerebrospinal fluid may indicate a chronic breakdown of myelin or recovery from an acute episode. MBP levels greater than 9 ng mL^{-1} indicate that active demyelination may be occurring. Normally there should be less than 4 ng mL^{-1} of MBP in the cerebral spinal fluid.

Increased MBP levels can also occur as a result of a stroke. A stroke, also known as cerebrovascular accident (CVA), is an acute neurological injury in which blood supply to a part of the brain is interrupted. Strokes involve a sudden loss of neuronal function due to arterial or even venous disturbance in cerebral perfusion. The part of the brain with disturbed perfusion no longer receives an adequate supply of oxygen. This initiates the ischemic cascade which causes brain cells to die or be seriously damaged, impairing local brain function. An indirect result of stroke is an active breakdown of myelin or demyelination, and therefore, the levels of MBP in cerebral spinal fluid (CSF) can act as markers for stroke.

Commercial ELISA tests exist for MBP; Diagnostic Systems Laboratories (Texas), for example, manufactures an ELISA which can measure levels of MBP in cerebrospinal fluid in 4 h.

We have within this work developed a label-less immunosensor for MBP. The sensor utilizes screen-printed carbon electrodes and is modified first by deposition of a conducting polymer (polyaniline) and thence biotinylating reagent. Complexion of the immobilized biotin with avidin allows the further binding of biotinylated antibodies via standard avidin−biotin interactions as described earlier[12] and as shown schematically in Figure 1. The resultant electrodes are capable of detecting the antigen within

(12) Garifallou, G.-Z.; Tsekenis, G.; Davis, F.; Millner, P. A.; Pinacho, D. G.; Sanchez-Baeza, F.; Marco, M.-P.; Gibson, T. D.; Higson, S. P. J. *Anal. Lett.* **2007**, *40*, 1412−1442.
(13) Arroyo, E. G.; Scherer, S. S. *Cell Biol.* **2000**, *113*, 1−18.
(14) Baumann, N.; Pham-Dinh, D. *Physiol. Rev.* **2001**, *81*, 871−927.
(15) Rudick, R. A.; Whitaker, J. N. In *Neurology/Neurosurgery Update*; Scheinberg, P., Ed.; CPEC: Princeton, NJ, 1987; Vol. 7.
(16) Ercolini, A. M.; Miller, S. D. *J. Immunol.* **2006**, *176*, 3293−3298.
(17) Wingerchuk, D. M. *Neurol. Res.* **2006**, *28*, 341−347.
(18) Kilfoyle, D. H.; Dyck, P. J.; Wu, Y.; Litchy, W. J.; Klein, D. M.; Dyck, P. J. B.; Kumar, N.; Cunningham, J. M.; Klein, C. J. *J. Neurol., Neurosurg. Psychiatry* **2006**, *77*, 963−966.
(19) Santinelli, R.; Tolone, C.; D'Avanzo, A.; del Giudice, E. M.; Perrone, L.; D'Avanzo, M. *Clin. Toxic.* **2006**, *44*, 327−328.
(20) Berger, T.; Rubner, P.; Schautzer, F.; Egg, R.; Ulmer, H.; Mayringer, I.; Dilitz, E.; Deisenhammer, F.; Reindl, M. *N. Engl. J. Med.* **2003**, *349*, 139−45.
(21) Manzo, L.; Artigas, F.; Martinez, E.; Mutti, A.; Bergamaschi, E.; Nicotera, P.; Tonini, M.; Candura, S. M.; Ray, D. E.; Costa, L. G. *Hum. Exp. Toxicol.* **1996**, *15*, S20−S35.
(22) Lamers, K. J. B.; Vos, P.; Verbeek, M. M.; Rosmalen, F.; Van Geel, W. J. A.; Van Engelen, B. G. M. *Brain Res. Bull.* **2003**, *61*, 261−264.
(23) Mukherjee, A.; Vogt, R. F.; Linthicum, D. S. *Clin. Biochem.* **1985**, *18*, 304−307.
(24) Liuzzi, G. M.; Mastroianni, C. M.; Vullo, V.; Jirillo, E.; Delia, S.; Riccio, P. *J. Neuroimmunol.* **1992**, *36*, 251−254.
(25) Phillips, J. P.; Lockman, L. A.; Shapiro, E. G.; Blazar, B. R.; Loes, D. J.; Moser, H. W.; Krivit, W. *Pediatr. Neurol.* **1994**, *10*, 289−294.

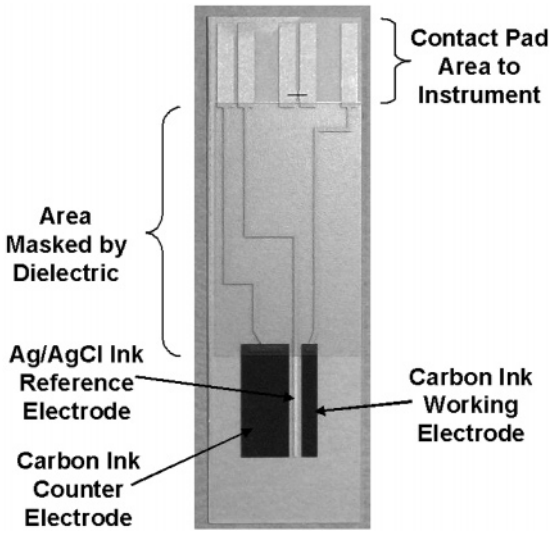

Figure 2. Screen-printed carbon electrodes used within this work.

the required physiological range. Control electrodes containing nonspecific IgG have also been fabricated to measure the effects of nonspecific binding and permit the subtraction of these unspecific interactions from the response toward specific binding of MBP. This approach helps to increase the stability and reliability of these sensors when applied to clinical samples.

EXPERIMENTAL SECTION

Sodium dihydrogen orthophosphate, disodium hydrogen orthophosphate, sodium chloride, and hydrochloric acid were obtained from BDH (Poole, Dorset, U.K.). Potassium chloride was obtained from Fisher Scientific U.K. Ltd., Loughborough, U.K. Aniline, MBP (from mouse, M2941), myelin basic protein antibody (monoclonal anti-MBP from rat, M9434), polyclonal IgG (from mouse, I5381), the biotinylation kit (part no. BK101), biotin 3-sulfo-*N*-hydroxysuccinimide, neutravidin, bovine serum albumin (BSA), potassium ferrocyanide, and potassium ferricyanide were obtained from Sigma-Aldrich, Gillingham, Dorset, U.K. All water used was obtained from a Purelab UHQ Deionizer (Elga, High Wycombe, U.K.). Commercial screen-printed carbon electrodes (Figure 2) containing carbon working and counter electrodes and a Ag/AgCl reference electrode were obtained from Microarray Ltd., Manchester, U.K. The surface area of the working electrode was 0.2178 cm^2.

Phosphate-buffered saline (PBS), pH 7.4 stock solution was prepared containing 0.14 mol L^{-1} NaH_2PO_4, 0.52 mol L^{-1} Na_2HPO_4, and 0.0051 mol L^{-1} NaCl. Aniline buffer, pH 1−2, was prepared containing 0.5 mol L^{-1} KCl, 0.3 mol L^{-1} HCl, and 0.2 mol L^{-1} aniline.

For antibody biotinylation, the procedure outlined in the BK101 kit was followed (see manufacturers instructions for details). Biotinylated antibodies were kept frozen in aliquots of 200 μL at a concentration of 1 mg mL^{-1} until required.

Cyclic voltammetry (Sycopel potentiometer, Sycopel Scientific, Tyne & Wear, U.K.) was utilized to deposit polyaniline films on the carbon electrodes. Screen-printed carbon electrodes were placed in aniline buffer and cycled from −200 to +800 mV versus Ag/AgCl for approximately 20 cycles, (the number of cycles could be varied to ensure the same quantity of polyaniline was deposited on each electrode). Deposition was terminated at +800 mV to ensure the polyaniline remained in its conducting form. Following deposition the polymer-coated electrodes were rinsed in water.

A volume of 30 μL of biotin−sulfo−NHS (10 mg mL^{-1} in water) was placed on the polymer-coated working electrode surface for 24 h. The sensors were rinsed with copious water and 30 μL of avidin (10 μg mL^{-1} in water) placed on the working electrode for 1 h—followed by further rinsing in water. Then 30 μL of biotinylated antibody (1 mg mL^{-1} in water) was added followed by rinsing. Finally, nonspecific interactions were blocked by BSA (10^{-6} M in PBS); the sensors are ready to use at this point; however, if opted, they can be stored in PBS at 4 °C up to 24 h.

The ac impedance measurements were performed using an ACM auto ac DSP frequency response analyzer (ACM Instruments, Grange over Sands, UK). Antigen solutions for ac impedance were prepared by diluting the required concentration of antigen in 30 mL of PBS, pH 7.4. A range of concentrations were utilized; since levels should be less than 4 ng mL^{-1} for a healthy individual, we set our minimum level at 1 ng mL^{-1} with an upper limit of 1 μg mL^{-1}, so as to cover the clinical range.

The sensors were first interrogated without antigen addition. Following this, each sensor was exposed to the required antigen concentration for 30 min, rinsed well with deionized water, and then subjected to impedance interrogation. Potassium ferrocyanide (10 mM) and potassium ferricyanide (10 mM) in PBS buffer were utilized as a redox couple for impedimetric measurements. Three electrodes were used for each measurement. A frequency range from 10 kHz to 1 Hz was measured, with a peak amplitude of 5 mV and a dc offset of +400 mV against Ag/AgCl.

RESULTS AND DISCUSSION

Deposition of Polyaniline. The voltammograms for the deposition of polyaniline onto the screen-printed carbon electrodes[12] are depicted in Figure 3 and imply a steady in situ formation of polymer at the electrode surface. As the number of scans increases, voltammetric peaks are seen between +350 and 400 mV versus Ag/AgCl, corresponding to the oxidation and reduction of surface bound polyaniline. The increase in current from scan 10 to 20 is due to the increase in polyaniline thickness and coverage of the electrode.[11]

Impedance Profiles of the Electrodes. A series of Nyquist curves were obtained for the sensors after exposure to various levels of MBP in PBS (Figure 4a). As can be seen, there is a steady decrease in the impedance of the electrodes with increasing antigen concentration. The relative impedances of the system for various antigen concentrations can be obtained by dividing the impedance for each frequency when a given concentration of antigen has been applied by the impedance (at the same frequency) for the sensor exposed to zero antigen concentration; these are shown in Figure 4b. This figure clearly shows that the impedance of the electrodes steadily increases with the concentration of MBP. Myelin basic protein is a mixture of epitopes with molecular weights of 14−21 kDa.[14] However the commercial antibody recognizes the peptide strand between amino acids 36 and 50 which is common to all the epitopes. The increases in impedance are most probably due to binding of the protein to the surface, since the protein molecules are likely to be insulating in nature. As can be seen, much larger increases in impedance are observed at the lower frequencies, which again indicates

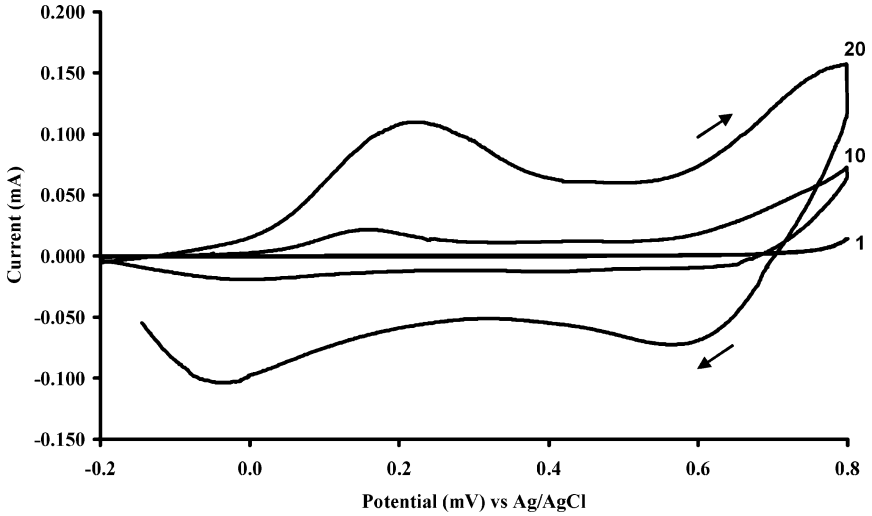

Figure 3. Deposition of conducting polyaniline films by cyclic voltammetry between −0.2 and +0.8 V at 50 mV s^{-1}; current transients are shown for the 1st, 10th, and 20th cycles.

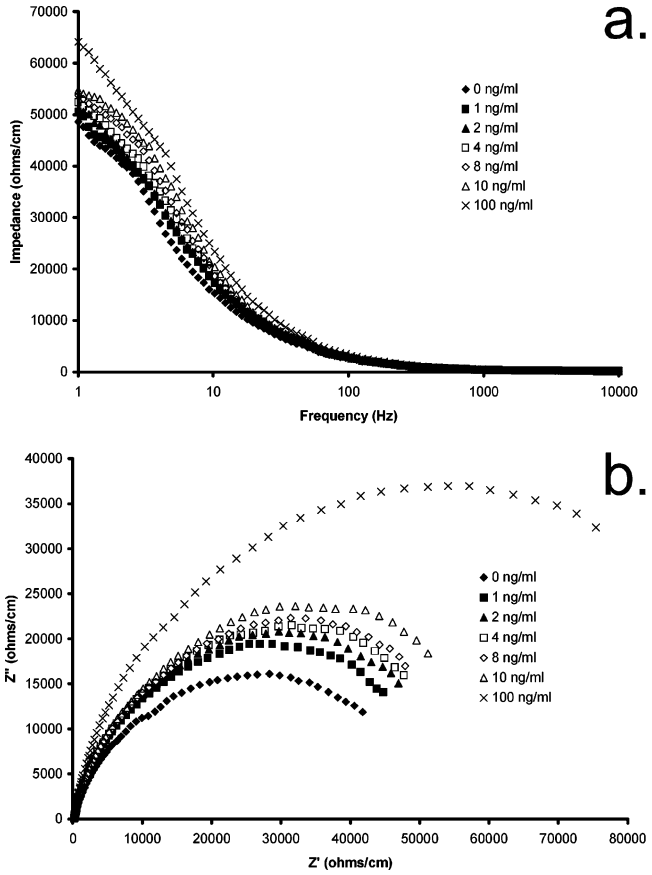

Figure 4. (a) Bode and (b) Nyquist plots of a typical specific anti-MBP-modified electrode exposed to various concentrations of antigen (MBP); for brevity not all concentrations are shown, but just for 0, 1, 2, 4, 8, 10, and 100 ng mL^{-1}.

deposition of insulating material. Therefore, it was decided that changes in impedance at 1 Hz would be used as a measurement of antigen binding.

The impedance spectra consists of two components: the real (Z') component, where the impedance in phase with the ac potential waveform is measured, and the imaginary (Z''), where the impedance is 180° out of phase. It is important to differentiate between the individual components of the total impedance of the cell. Previous work by our group showed that while both the imaginary and real components increase, the increase in the real component dominated the total increase in the impedance.[11,12] Although in this case changes in both real and imaginary components are visible and again the real component is the major component of the total impedance, it was also found (perhaps more importantly) that the real component offers far greater reproducibility in comparison to the imaginary contribution.[11,12]

Figure 5a shows the percentage increase in Z' across a range of antigen concentrations. As can be seen, there is a steady increase in impedance as antigen concentration increases toward a concentration of about 100 ng mL^{-1}. Levels higher than 100 ng mL^{-1} do not appear to lead to even higher impedances, but rather tend toward a plateau, Figure 5a. This possibly indicates saturation of the specific binding sites. Any further changes in impedance beyond this level are likely to be due to nonspecific interactions.

Nonspecific interactions have the potential to interfere with immunosensor performance, leading to erroneously elevated results. This could be addressed by utilization of a second sensor containing either no antibodies or, alternatively, by exploitation of a nonspecific antibody. For this reason an identical set of immunosensors were fabricated utilizing a nonspecific IgG antibody in place of the specific MBP antibody. The nonspecific antibody was a commercial polyclonal IgG antibody, from the same species (mouse) as the specific MBP antibody. This was biotinylated using an identical protocol and then incorporated into the sensor using identical conditions, buffers, concentrations, etc. as utilized for the specific antibody electrodes. Whereas specific binding of MBP will only occur when the anti-MBP antibody is present, electrodes fabricated using a nonspecific antibody should undergo the same nonspecific binding events as those fabricated using specific antibodies. It therefore follows that utilization of both types of electrodes followed by simple subtraction of nonspecific electrode response from those of the specific electrodes should allow the nonspecific responses to be cancelled out.

Results for the nonspecific IgG electrodes were obtained in exactly the same manner as for the specific electrodes, and the calibration plot for these measurements is shown within Figure 5b. As can clearly be seen, there is a much lower response for

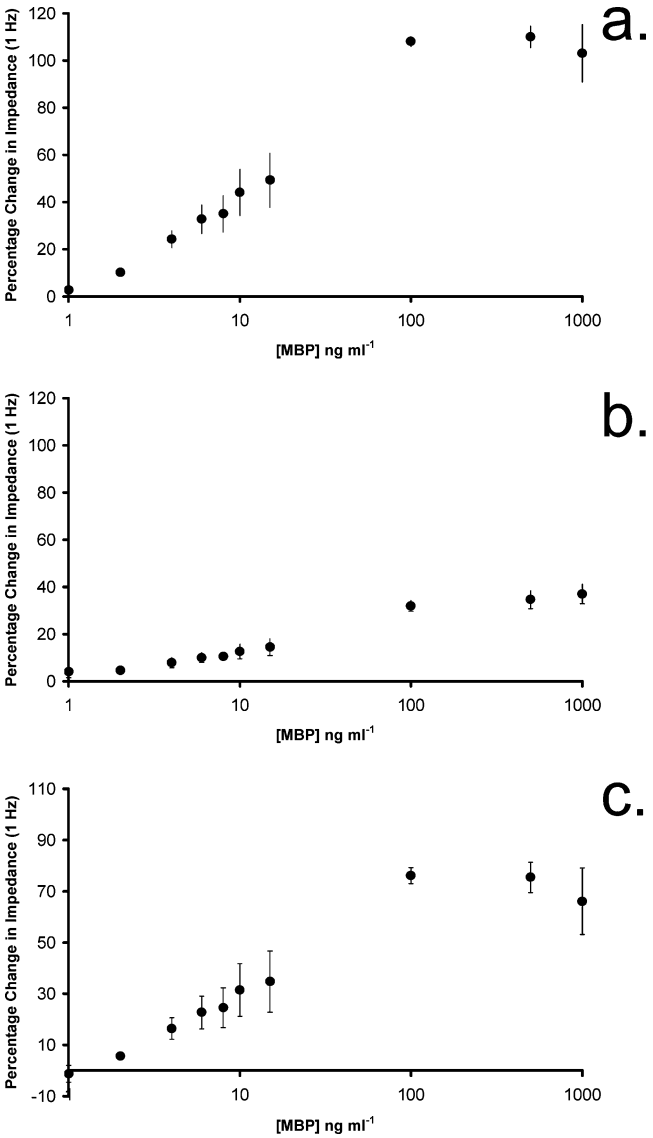

Figure 5. Calibration curves showing the increase in the real component of impedance at 1 Hz for (a) specific anti-MBP-modified electrodes exposed to varying concentrations of antigen (MBP), (b) IgG-modified electrodes exposed to antigen under identical conditions, and (c) corrected calibration curves where the nonspecific response has been subtracted from the specific response (curve a − curve b). All data points are means for the responses of three electrodes; error bars give a measure of the reproducibility of the system.

the nonspecific antibody, showing that although there are nonspecific interactions, between the concentration ranges of 1−100 ng mL^{-1}, they comprise a minor component of the detected response.

Once the nonspecific responses have been subtracted (Figure 5a − Figure 5b), a corrected plot (Figure 5c) shows the calibration curve for the corrected sensor response. Between a concentration range of 1−100 ng mL^{-1}, there is a near linear correlation of the corrected impedance change with the log of concentration (R^2 = 0.976). Between the lower range of 1−15 ng mL^{-1}, the correlation of the impedance change with the log of concentration is further improved (R^2 = 0.990). The limit of detection of this system was found to be approximately 1 ng mL^{-1}, based on a multiple of 3× the standard deviation of the baseline samples—and combined with the good linear response, indicates that we have developed a sensor with good performance within the required range of detection for MBP.

As yet we have not attempted to either reverse the antibody−antigen binding process or remove the antibody and replace it with fresh protein. In view of the low potential unit cost of the electrodes it would be simpler just to use sensors as single-use devices. However, for this to be feasible there must be both good sensor-to-sensor and batch-to-batch reproducibility. We have found that repeated runs on the same electrode give reproducible results with RSDs < 2%. We have also determined the electrode-to-electrode reproducibility of responses to have RSDs < 5% variability in a series of trials.

CONCLUSIONS

We have demonstrated the construction of an immunosensor for the MBP using a combination of screen-printed electrodes coated with conducting polyaniline and an immobilized polyclonal antibody. Interrogation of the electrodes by ac impedance demonstrated the detection of the antigen. Linear correlation of the impedance change with the log of concentration (R^2 = 0.977) was observed between concentrations of 1−100 ng mL^{-1}. A similar logarithmic relationship was observed in our earlier work with ciprofloxacin immunosensors.[12]

Further work utilizing samples of cerebrospinal fluid with various levels of MBP will be undertaken, and it is expected that the use of a dual-antibody (specific and nonspecific) electrode system should allow subtraction of any nonspecific binding events to allow the detection of MBP levels in "real" samples. These studies will be reported in a future publication.

One major drawback associated with immunosensors is the strength of the antibody/antigen binding which can render the interaction essentially irreversible. This would lead to the sensor rapidly becoming saturated upon multiple usage, a process which would be very difficult to reverse by simple washing. The use of inexpensive screen-printed electrodes as a template for these sensors will allow for the production of simple and, more importantly, inexpensive single-use immunosensors, thereby eliminating the need for washing and reuse of sensors.

Commercialization of this research is proceeding through a new spin-out company ELISHA Systems Ltd., which is in the process of developing a range of label-less immunosensors for a number of different antigens.

ACKNOWLEDGMENT

This work, including funding for G.T., G.-Z.G., and F.D., has been supported by the European Community Framework VI NMP2-CT-2003-505485, "ELISHA" contract.

Received for review October 8, 2007. Accepted December 21, 2007.

AC702070E

Biosensors and Bioelectronics 24 (2009) 1090–1095

Contents lists available at ScienceDirect

Biosensors and Bioelectronics

journal homepage: www.elsevier.com/locate/bios

Labeless AC impedimetric antibody-based sensors with pg ml^{-1} sensitivities for point-of-care biomedical applications

Andrew C. Barton[a], Stuart D. Collyer[a], Frank Davis[a], Goulielmos-Zois Garifallou[a], Georgios Tsekenis[a], Elizabeth Tully[b], Richard O'Kennedy[b], Tim Gibson[c], Paul A. Millner[c], Séamus P.J. Higson[a,*]

[a] *Cranfield Health, Cranfield University, Silsoe, Beds MK45 4DT, UK*
[b] *School of Biotechnology, Dublin City University, Dublin 9, Eire*
[c] *Biosensors & Bioelectronics Group, Research Institute of Membrane & Systems Biology, Garstang Building, University of Leeds, Leeds, LS2 9JT, UK*

ARTICLE INFO

Article history:
Received 4 March 2008
Received in revised form 16 April 2008
Accepted 4 June 2008
Available online 11 June 2008

Keywords:
AC impedance
Immunosensor
Polyaniline
Microelectrode
BSA
Digoxin

ABSTRACT

This paper describes the development and characterisation of labeless immunosensors for (a) the cardiac drug digoxin and (b) bovine serum albumin (BSA). Commercial screen-printed carbon electrodes were used as the basis for the sensors. Two methods were used to immobilise antibodies at the electrode surface. Aniline was electropolymerised onto these electrodes to form a thin planar film of conductive polyaniline; the polyaniline film was then utilised as a substrate to immobilise biotinylated anti-digoxin using a classical avidin-biotin affinity approach. As an alternative approach, poly(1,2-diaminobenzene) was electrodeposited onto the carbon electrodes and this modified surface was then sonochemically ablated to form an array of micropores. A second electropolymerisation step was then used to co-deposit conductive polyaniline along with antibodies for BSA within these pores to produce a microarray of polyaniline protrusions with diameters of several μm, containing entrapped anti-BSA.

The resulting antibody grafted electrodes were interrogated using an AC impedance protocol before and following exposure to digoxin or BSA solutions, along with control samples containing a non-specific IgG antibody. The impedance characteristics of both types of electrode were changed by increasing concentrations of antigen up to a saturation level. Calibration curves were obtained by subtraction of the non-specific response from the specific response, thereby eliminating the effects of non-specific adsorption of antigen. Both the use of microelectrode arrays and affinity binding protocols showed large enhancements in sensitivity over planar electrodes containing entrapped antibodies and gave similar sensitivities to our other published work using affinity-based planar electrodes. Detection limits were in the order of 0.1 ng ml^{-1} for digoxin and 1.5 ng ml^{-1} for BSA.

1. Introduction

The principle of immunoassays was first established in 1959 (Yalow and Berson, 1959) and their work led to the development of the widely used radioimmunoassay to determine insulin-binding antibodies in human serum, using samples obtained from subjects that had been treated with insulin. Later, within unconnected work (Clark and Lyons, 1962), the concept of a biosensor was pioneered. These workers exploited the selectivity of enzymes for analytical purposes via a methodology which involved immobilising enzymes on the surface of electrochemical sensors and measuring the oxygen consumption by the glucose oxidase enzymatically catalysed oxidation of glucose. This basic idea has remained virtually unchanged since the original design, although the field has undergone continual technological developments over the last 40 years.

The incorporation of antibodies into conducting polymer films was first reported (John et al., 1991) in 1991. Pyrrole was galvanostatically polymerised onto a platinum wire substrate from a solution which contained anti-human serum albumin (anti-HSA). The antibody was incorporated into the polypyrrole film and the polypyrrole anti-HSA electrode found to give a specific electrochemical response to HSA. Since this is early work, there has been burgeoning interest in the development of electrochemical immunosensors — as detailed in several recent reviews (Rodriguez-Mozaz et al., 2006; Diaz-Gonzalez et al., 2005; Cosnier, 2005).

Antibody–antigen interactions are complex by their very nature and it is thought necessary that the affinity reaction be minimally perturbed by the fabrication procedure to give reproducible

* Corresponding author. Fax: +44 1234 758370.
E-mail address: s.p.j.higson@cranfield.ac.uk (S.P.J. Higson).

0956-5663/$ – see front matter © 2008 Published by Elsevier B.V.
doi:10.1016/j.bios.2008.06.001

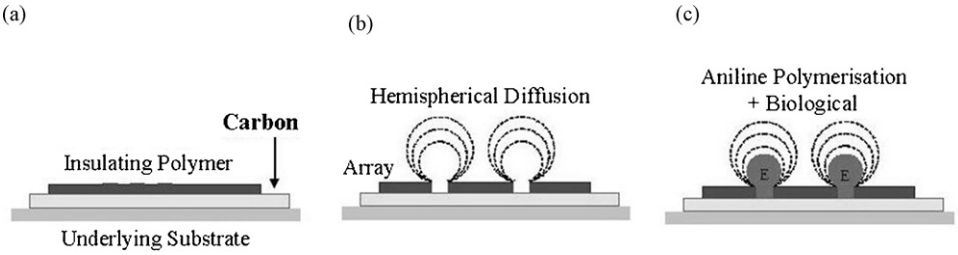

Fig. 1. Formation of polyaniline microarrays: (a) deposition of insulating layer, (b) sonochemical formation of pores and (c) polymerisation of aniline.

response characteristics. We have previously shown that up to 2–3 μg antibodies for BSA and digoxin may be successfully incorporated into conducting polymer films by entrapment in a growing polypyrrole film with no detrimental effect to antibody activity (Grant et al., 2003). Electrochemical interrogation of these films demonstrated selective interactions with the target antigens. Further work utilised an AC impedance protocol (Grant et al., 2005) as the method of interrogation for these films and led to the development of immunosensors for digoxin and bovine serum albumin. Later work by our group utilised polyaniline coated screen-printed planar carbon electrodes as substrates for immobilisation of antibodies utilising the classical avidin-biotin interaction. This enabled the construction of immunosensors for the fluoroquinolone antibody ciprofloxacin (Garifallou et al., 2007) and myelin basic protein—a marker for conditions such as stroke and multiple sclerosis (Tsekenis et al., 2008).

Our group has also pioneered the development of sonochemically fabricated microarrays of conductive polymers (Higson, 1996), the schematic for the formation of which is shown within Fig. 1. Poly(1,2-diaminobenzene) can be electrodeposited on a variety of conductive surfaces to form an insulating layer[15]. We have utilised commercial screen-printed three electrode strips as the basis for these sensors. The working electrodes are initially coated with a thin film (50–70 nm thickness) of an insulating polymer formed by the electrochemical deposition of 1,2-diaminobenzene (Myler et al., 1997). An advantage of this process is that it is self-limiting, making it highly reproducible. Sonochemical ablation is then used to ablate or "drill" holes in this insulating material with diameters of 0.1 to several microns and a density of up to 120,000 pores cm^{-2}. We have used these micropore arrays for the detection of aqueous chlorine (Davis et al., 2007). The arrays may be used as substrates for further electropolymerisation reactions, generating arrays of conducting polyaniline protrusions, consisting of just the polymer or alternatively containing entrapped biological species (Barton et al., 2004). Previous work within our group has utilised these microarrays containing entrapped enzymes for the amperometric detection of glucose (Barton et al., 2004; Myler et al., 2004), alcohol (Myler et al., 2005). and a range of organophosphate pesticides (Pritchard et al., 2004; Law and Higson, 2005) with extreme sensitivity (10^{-17} M).

One difficulty often encountered when using sensors for practical analytical applications is that the species being detected can in some situations be present only at very low concentration while being contained within a complex biological system such as blood. This means that any sensor must display high sensitivities and also low non-specific adsorption of possible foulants or interferents. As can be seen from previous work using enzymes, use of microelectrodes rather than planar electrodes can lead to extremely high sensitivities (Pritchard et al., 2004; Law and Higson, 2005). Attempts therefore were made within this study to determine whether the use of microelectrodes rather than planar electrodes within immunosensors similar to those previously reported (Grant et al., 2003, 2005) would lead to sensitivity enhancements. Microelectrode arrays containing entrapped anti-BSA were constructed and their performance compared with our previous work on planar, entrapped sensors.

A disadvantage associated with the entrapment method used within much of our previous work for antibody immobilisation is that the antigen will often be too bulky to diffuse through the polymer matrix and so only antibodies located at the surface of the polymer film or microelectrode — and suitably orientated, will be available for antigen binding. Other work comparing monolayers of randomly and specifically orientated antibody fragments (Bonroy et al., 2006) showed that immunosensor responses typically double when the fragment is specifically orientated.

Digoxin (Supplementary data, Fig. S2) is a cardiac drug, widely used in the treatment of various heart conditions such as atrial fibrillation and atrial flutter, with a narrow therapeutic range of 0.8–2.0 ng ml^{-1} (Terra et al., 1999). Previous work by our group demonstrated the construction of an immunosensor for digoxin, however, these sensors were only capable of detecting the antigen in the mg–μg ml^{-1} ranges (Grant et al., 2003). The anti-digoxin antibodies used in this early study were entrapped within a planar, electropolymerised film. We therefore within this work also compare results obtained using an affinity method to graft antibodies to the surface of the film with those obtained previously by entrapment (Grant et al., 2003) in an attempt to improve sensitivity.

The focus of this paper is not just to describe the development of particular sensors — but rather to compare the behaviour of sensors fabricated using a variety of methods, namely our earlier work on entrapment in planar polymer films with affinity grafted planar films and also entrapment of the antibodies within conductive polymer protrusions. As will be demonstrated, both methods lead to an enhancement in sensitivity.

2. Experimental

2.1. Materials and equipment

Sodium dihydrogen orthophosphate, disodium hydrogen orthophosphate, sodium chloride and hydrochloric acid were obtained from BDH (Poole, Dorset, UK). Aniline, polyclonal human anti-IgG (AIgG), biotin 3-sulfo-N-hydroxysuccinimide, the biotinylation kit (part no. BK101), neutravidin, human serum albumin (HSA), BSA, anti-bovine serum albumin (ABSA, developed in rabbit), digoxin, anti-digoxin (developed in rabbit-whole antiserum), sodium acetate, acetic acid, sodium perchlorate, potassium ferrocyanide and potassium ferricyanide were obtained from Sigma–Aldrich, Gillingham, Dorset, UK. All water used was obtained from a Purelab UHQ Deioniser (Elga, High Wycombe, UK). Commercial screen-printed carbon electrodes (Supplementary data, Fig. S1) containing carbon working and counter electrodes and an Ag/AgCl reference electrode were obtained from Microarray Ltd., Manchester, UK. The surface area of the working electrode

was 0.2178 cm^2. AC impedance measurements were performed using an ACM auto AC DSP frequency response analyser (ACM Instruments, Grange-over-Sands, UK). Cyclic voltammetry was performed using a Sycopel potentiometer (Sycopel Scientific, Tyne & Wear, UK) to electrodeposit polyaniline.

Aniline buffer (pH 1–2) was prepared containing 0.5 mol l^{-1} KCl, 0.3 mol l^{-1} HCl and 0.2 mol l^{-1} aniline. Phosphate buffer (PBS, pH 7.4) was prepared comprising 52.8 mmol l^{-1} disodium hydrogen orthophosphate 12-hydrate, 13 mmol l^{-1} sodium dihydrogen orthophosphate 1-hydrate and 5.1 mmol l^{-1} sodium chloride. Acetate buffer (pH 4.0) was prepared comprising 0.4 mol l^{-1} sodium acetate, 0.4 mol l^{-1} acetic acid and 0.4 mol l^{-1} sodium perchlorate.

The anti-digoxin was supplied as a solution in whole antiserum and was purified using a 5 ml protein G-column (Pharmacia). IgG fraction was eluted using glycine buffer (pH 2.7) and dialyzed overnight. For antibody biotinylation, the procedure outlined in the BK101 kit was followed (see manufacturers instructions for details). The biotinylated anti-digoxin was very dilute (0.01 mg ml^{-1}) and was concentrated using a Centriprep centrifugal filter unit (Millipore, Hertfordshire, UK) fitted with an ultracel YM-30 membrane containing glycerol, to prevent drying. This procedure also ensured the removal of sodium azide from the antibody solution. The procedure involved three subsequent centrifugations in a cold room (4 °C), each for 20 min at 30,000 rpm; the final concentration was 0.5 mg ml^{-1}. Biotinylated antibodies were kept frozen in aliquots of 200 μl until required.

2.2. Formation of microarrays

Sonochemically fabricated microarrays were constructed as previously described (Barton et al., 2004). To deposit the insulating layer, a 5 mmol l^{-1} solution of 1,2-diaminobenzene in pH 7.4 phosphate buffer was utilised. Prior to the immersion of the carbon electrode, the monomer solution used was thoroughly purged with N_2 for 20 min in a sealed cell to provide an oxygen free atmosphere. An initial 1 s blast of ultrasound was also applied to a submerged electrode to displace air bubbles trapped at the surface of the electrodes. Homogenous insulation of a planar carbon electrode was achieved by sequentially scanning the working electrode potential from 0 mV to +1000 mV (vs. Ag/AgCl) and back to the starting potential at a scan rate of 50 mV s^{-1} for 20 sweeps.

Sonication experiments were performed using a custom built 2 kW, 25 kHz ultrasound tank with internal dimensions of 750 mm × 750 mm × 600 mm (working volume 750 mm × 750 mm × 500 mm) (Ultrawave Ltd., Cardiff, UK). Ultrasound was applied at a frequency of 25 kHz for 10 s duration.

2.3. Incorporation of antibody within microarrays via electrochemical deposition

A 0.2 M aniline hydrochloride solution was prepared in a pH 4.0 acetate buffer. The solution pH fell to approximately 2.6 upon addition of monomer. Monoclonal antibody receptor was incorporated into the buffered monomer solution prior to polymerisation at a resultant concentration of 0.5 mg ml^{-1}. The pH of the monomer solution increases upon addition of antibody, this was monitored to ensure the pH remained below 4.0 so that the conductive protonated 'emeraldine' form of polyaniline was deposited at the working electrode. Electrochemical deposition of the polyaniline was performed by sequentially cycling the working electrode potential from −200 mV to +800 mV (vs. Ag/AgCl) and back to the starting potential at a scan rate of 50 mV s^{-1}. A linear sweep from −200 to +800 mV (50 mV s^{-1}) was performed at the end of cyclic voltammetry to leave the polyaniline in its protonated emeraldine salt form. This led to formation of polyaniline protrusions containing entrapped antibodies as previously described (Barton et al., 2004; Law and Higson, 2005).

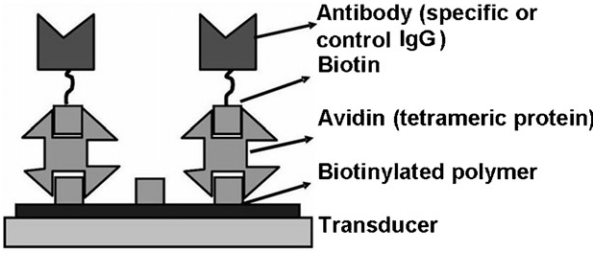

Fig. 2. Schematic of the affinity binding procedure used to immoblise anti-digoxin.

2.4. Construction of planar antibody electrodes via an affinity protocol

Anti-digoxin was immobilised at the surface of planar electrodes by the methods previously described (Garifallou et al., 2007; Tsekenis et al., 2008) and the immunosensor structure is shown schematically in Fig. 2. The potentiodynamic electrodeposition of polyaniline from aniline buffer, pH 1–2 into the microelectrode array was achieved electrochemically as described for the microarrays.

30 μl of biotin-sulfo-NHS (10 mg ml^{-1} in water) was placed on the working electrode surface for 24 h. The sensors were rinsed with copious water and 30 μl of neutravidin (10 μg ml^{-1} in water) placed on the working electrode for 1 h followed by further rinsing in water. 30 μl biotinylated anti-digoxin (0.5 mg ml^{-1} in water, 1 h) was then added followed by rinsing. Finally, non-specific interactions were blocked by HSA (10^{-6} mol l^{-1} in PBS, 1 h).

2.5. Determination of antigen concentration

AC impedance measurements were performed using an ACM auto AC DSP frequency response analyser. Following immobilisation of antibody, impedance analyses were performed from 1 Hz to 10,000 Hz (±5 mV amplitude perturbation) in pH 7.4 phosphate buffer, i.e. containing no antigen, as a baseline trace. This buffer solution did, however, contain a 50:50 mixture of $[Fe(CN)_6]^{3-/4-}$, at a concentration of 10 mmol l^{-1} as redox mediator so as to perform faradaic impedance spectroscopy. The potential of the electrochemical cell is offset to the formal potential of the redox probe (+0.12 V vs. Ag/AgCl identified via cyclic voltammetry). Following the recording of a baseline spectral trace (0 ng ml^{-1} antigen), the same sensor is used for all concentrations and exposed for 30 min time periods to the increasing concentrations of antigen in phosphate buffered test solution.

After each 30 min exposure to a known concentration, the sensor was thoroughly flushed with 50 ml of pH 7.4 phosphate buffer (containing $[KFe(CN)_6]^{3-/4-}$ and no antigen) to remove any non-specifically adsorbed matter before AC impedance spectra were recorded in the phosphate buffered test solution (containing $[KFe(CN)_6]^{3-/4-}$ and no antigen). This sensor was then exposed to an increasing antigen concentration and the process repeated for the full range of applied antigen concentrations under investigation. Traces recorded may then be compared to the baseline trace. Immunosensors were also tested where the electrode was exposed to a diminishing series of antigen concentrations i.e. starting with the highest and gave similar results (Garifallou, 2008).

The electrode assemblies were found to be very stable, for example a sensor placed in pH 7.4 phosphate buffer (containing

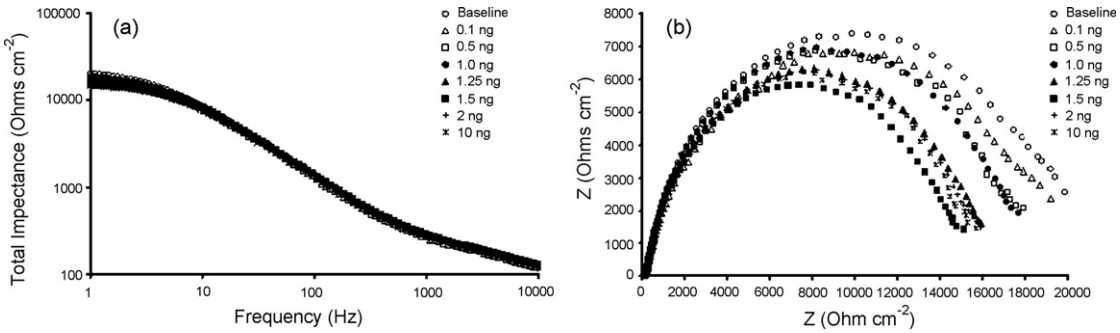

Fig. 3. (a) Bode and (b) Nyquist plots of a typical specific anti-digoxin modified electrode exposed to various concentrations in the range 0–10.0 ng ml^{-1} of digoxin in PBS.

$[KFe(CN)_6]^{3-/4-}$ showed no change in the AC impedance curves even after 90 min equillibration (Tsekenis, 2008).

3. Results and discussion

3.1. Impedance results for planar, affinity immobilised anti-digoxin electrodes

Fig. 3 shows the (a) Bode and (b) Nyquist curves obtained for a planar polyaniline/anti-digoxin modified, carbon electrode exposed to various concentrations in the range of 0–10 ng ml^{-1} of antigen. The Nyquist curve (Fig. 3b) demonstrates that the Z' (real) component of the impedance increases steadily with decreasing frequency whereas the Z'' (imaginary) component increases to a maximum value (at frequencies in the range 5–10 Hz) before falling as the frequency approaches 1 Hz. This type of impedance spectrum is indicative of a surface-modified electrode system where the electron transfer is slow and the impedance is controlled by the interfacial electron transfer (Katz and Willner, 2003).

As can be seen, there is a steady decrease in impedance as antigen concentration increases towards a concentration of about 1.5 ng ml^{-1}. Levels of 2 ng ml^{-1} and 10 ng ml^{-1} did not lead to even lower impedances, but rather tend towards a plateau, indicating saturation of the specific binding sites. Any further changes in impedance beyond 1.5 ng ml^{-1} are likely to be due to non-specific interactions. The corresponding Bode plots (Fig. 3a) also show a decrease in the total impedance as the digoxin levels increase. This indicates that the binding of digoxin is facilitating electron transfer between the electrode and the redox probe. Since the therapeutic range is 0.8–2.0 ng ml^{-1} (Terra et al., 1999) this indicates that these sensors will be sufficiently sensitive and in fact there may be a need to undertake some dilution of the sample. However the range of these sensors is unfortunately rather small, which may preclude their use in real situations. What is of interest though is the much higher sensitivity compared to digoxin sensors fabricated by entrapment, indicating that controlled immobilisation does lead to enhanced sensitivity.

The impedance spectra consists of two components, the real (Z') component where the impedance in phase with the AC potential waveform is measured and the imaginary (Z'') where the impedance is 180° out of phase. Previous work by our group has demonstrated that in these type of systems, the increase in the real component dominated the total increase in the impedance and perhaps more importantly the real component offers far greater reproducibility in comparison to the imaginary contribution (Garifallou et al., 2007; Tsekenis et al., 2008).

Our previous work demonstrated that the sensors of this type gave the largest relative changes at the lower frequencies (Garifallou et al., 2007, Tsekenis et al., 2008). Calibration curves could be drawn (Fig. 4a) showing the percentage decrease in Z' at 1 Hz across a range of antigen concentrations. Again these show a relationship between antigen concentration and the decrease in Z'.

Non-specific interactions have the potential to either exaggerate or mask specific interactions. Whereas specific binding of antigens will only occur when their antibodies is present, electrodes fabricated using a non-specific antibody should undergo the same non-specific binding events as those fabricated using specific antibodies. The calibration curve showing the percentage decrease in Z' at 1 Hz is shown for sensors fabricated using an identical protocol except that the specific antibody is replaced by a non-specific IgG antibody (Fig. 4b). As can clearly be seen, there is a much lower response for the non-specific antibody, showing that although there are non-specific interactions, between the concentration ranges of 0–2 ng ml^{-1}, they comprise a minor component of the detected response.

Once the non-specific responses have been subtracted, a corrected plot (Fig. 4c) shows the calibration curve for the corrected sensor response. Between a concentration range of 0–1.5 ng ml^{-1}, there is a clear correlation of the corrected impedance change with

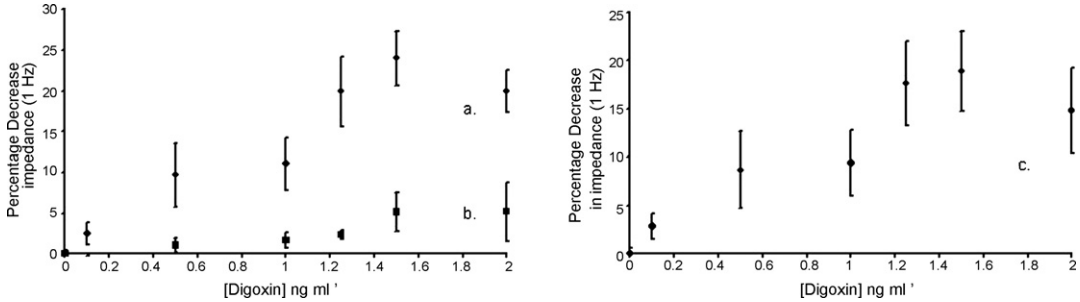

Fig. 4. Calibration curves showing the decrease in the real component of impedance (in the range 0–2.0 ng ml^{-1} digoxin) at 1 Hz for: (a) specific anti-digoxin modified electrodes exposed to varying concentrations of antigen, (b) IgG modified electrodes exposed to antigen under identical conditions and (c) corrected calibration curves where the non-specific response has been subtracted from the specific response (curve a minus curve b). All data points are means for the responses of three electrodes; error bars give a measure of the reproducibility of the system.

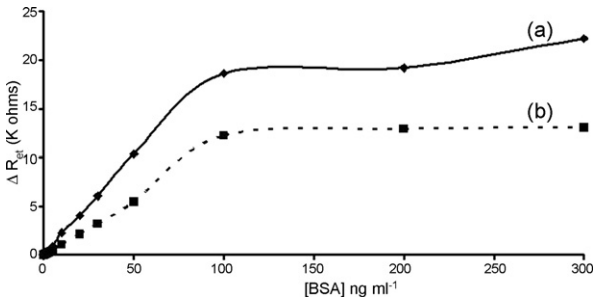

Fig. 5. Calibration plot showing changes in electron transfer resistance vs. BSA concentration: (a) entrapped ABSA (0–300 ng ml^{-1}) and (b) entrapped anti-IgG (0–300 ng ml^{-1}).

the concentration. The limit of detection, calculated as 3× the standard deviation of the baseline sample of this system (Analytical Methods Committee, 1987) is approximately 0.1 ng ml^{-1}. Our previous system using entrapment of digoxin within a polymer film combined with pulsed waveform detection (Grant et al., 2003) was only capable of resolving digoxin at levels higher than 50 μg ml^{-1}, so as can be seen the combination of an AC interrogation protocol and an affinity-based immobilisation procedure leads to at least a two orders of magnitude increase in sensitivity. The responses for 10 ng ml^{-1} digoxin (not shown in plots) were indistinguishable from those at 2 ng ml^{-1}.

3.2. Impedance results for entrapment immobilised anti-BSA microelectrodes

Impedance traces for polyaniline microelectrode sensors containing entrapped ABSA were obtained as for the anti-digoxin-based electrodes. These were very similar in appearance to those obtained for previous electrodes, again indicating a electrochemical system where the electron transfer is slow and the impedance is controlled by the interfacial electron transfer (Katz and Willner, 2003). Rather than just studying the change in Z' at 1 Hz, it was decided to undergo a more detailed investigation of the electrochemical system. A computer fitting of the experimental data to a theoretical model, represented by a simple equivalent circuit, may be performed by the software accompanying the frequency response analyser. In this case, the interface is modelled by an equivalent circuit (Supplementary data, Fig. S3), also called a Randles circuit (Randles, 1947), consisting of a double-layer capacitor in parallel with a polarization resistor (also known as a charge transfer resistor with certain constraints) and a Warburg impedance, connected in series with a resistor that measures the resistance of the electrolyte solution. For a more thorough evaluation of the data obtained, the changes in the Nyquist curves may be translated into electron transfer resistance changes to provide a clear and consistent format.

The relative electron transfer resistance changes from the baseline response at each concentration of BSA for a typical electrode modified with ABSA are plotted in Fig. 5a. The electron transfer resistance increases with increasing BSA concentration and demonstrates that an entrapped ABSA immunosensor gave a linear response to the analyte from 0 ng ml^{-1} to 100 ng ml^{-1} ABSA.

The insulation of the modified electrode upon formation of stable antibody–antigen immunocomplexes hinders the electron transfer kinetics of the redox probe resulting in the increase of electron transfer resistance. The electron transfer resistance increases with increasing antigen concentration for both types of electrode. The limit of detection (three times the standard deviation of the baseline value) of the entrapped ABSA immunosensor is 1 ng ml^{-1}. There is negligible change from 100 ng ml^{-1} to 300 ng ml^{-1} suggesting that the immunosensor approaches saturation.

Non-specific interactions have the potential to interfere with immunosensor performance, leading to erroneously elevated results. For this reason, identical sets of immunosensors were fabricated by both methods utilising a non-specific IgG antibody in place of the specific ABSA antibody. Results for these electrodes were obtained in exactly the same manner as for the specific electrodes. From the Nyquist plots for these systems (not shown), it could be seen that while binding of BSA to the non-specific immunosensors occurs, the responses are smaller than for ABSA modified sensors. A calibration plot for this system can also be drawn (Fig. 5b) and shows a linear-type non-specific response is observed for the affinity-based anti-IgG immunosensor from 1 to 100 ng ml^{-1} BSA with a plateau above this concentration. Upon comparison of Fig. 5a with Fig. 5b, it is apparent that approximately 50% of the ABSA-affinity immobilised sensor response encountered is, in fact, non-specific. This is most likely due to the fact that BSA is a protein with a high affinity for surfaces and no blocking reagents have been utilised for these electrodes.

To obtain a calibration profile, in terms of 'corrected' electron transfer resistance change for an ABSA immunosensor, accounting for any non-specific responses, the non-specific response was subtracted from the specific response over the entire analytical concentration range. In total 10 ABSA-immobilised sensors of each type and 10 corresponding anti-IgG-immobilised sensors were interrogated over their active concentration range, to allow an assessment of the reproducibility of the responses for this system. Results are presented in Fig. 6. The error bars are the standard deviations obtained for the 10 matched sensor pairs from the mean 'corrected' values.

From Fig. 6 a linear response was observed for the immunosensors from 0 to 100 ng ml^{-1} BSA. Fig. 6 (inset) shows an expanded view from 0 to 10 ng ml^{-1} BSA and shows linear behaviour with $R^2 > 0.99$. At concentrations above 100 ng ml^{-1}, the sensor becomes saturated. From the standard deviations obtained, we can say that discrimination of BSA antigen analyte is possible at 5 ng ml^{-1}. The limit of detection of the ABSA immunosensor is 1.5 ng ml^{-1} BSA and is calculated from 3× the standard deviation of the baseline response and extrapolated from the line of best-fit according to IUPAC guidelines (Analytical Methods Committee, 1987). Previous work (Grant et al., 2003, 2005) allowed detection of BSA at levels as low as 10 μg ml^{-1}. As can be seen the use of polyaniline microelectrodes has greatly increased sensitivity, although in this instance there is a problem with high non-specific responses.

3.3. Stability of the BSA immunosensors and regeneration studies

Although a long-term sensor stability test was not performed, a batch of 18 sensor pairs was assessed from storage in dry state, at 4 °C, for a period of 12 weeks. Again an identical experimental protocol was employed for electrochemical impedance interrogation and the 'corrected' electron transfer change was the analysis method for response recovery.

Every 2 weeks a set of three matched sensor pairings was removed from storage and interrogated over the full BSA antigen analyte concentration range from 1 to 300 ng ml^{-1}. After 2 weeks no loss of sensor response occurred but after 4 weeks there was a 10% loss in response and further steady decreases until after 10 weeks storage only 10% of the original response was detected.

Some of our previous work demonstrated that acid washing of some immunosensors led to their regeneration (Barton, 2007). Attempts were made so see whether it was possible to regenerate the sensors by acid washing. 5 ABSA-immobilised sensors and 5 matched non-specific AIgG-immobilised sensors are exposed to

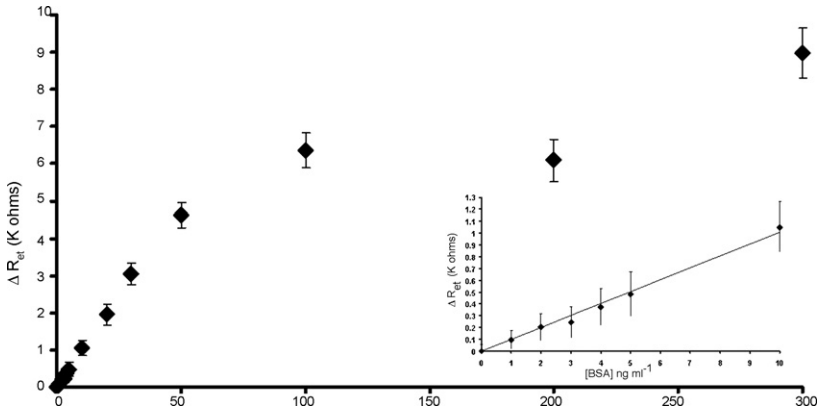

Fig. 6. Corrected calibration curves where the non specific response has been subtracted from the specific response (0–300 ng ml^{-1}) (inset) corrected calibration plot (0–10 ng ml^{-1}).

the full interrogation procedure prior to reversibility investigations. In order to split the antibody–antigen complex and to regenerate the sensors, 0.1 M HCl acidic buffer (pH 2.3) was applied for three separate 1 min time periods. In between each acidic buffer exposure, pH 7.4 PBS was used to rinse the sensor surface. Finally the sensors were rinsed with 50 ml PBS to produce PSA-free sensors which could then be used for fresh analysis. Unfortunately in all cases the washing removed all activity. An identical baseline response could be achieved which suggests that the sensor surface integrity remains, yet the antigen recognition and binding capabilities of the receptor antibodies are severely damaged by the treatments.

4. Conclusions

Our work verifies several fabrication techniques and an AC experimental interrogation protocol as a viable approach towards the labeless sensing of BSA and digoxin. Affinity-based sensors where anti-digoxin is immobilised on planar electrodes using avidin–biotin interactions have been shown to display much higher sensitivities (by two orders of magnitude, capable of detection of ng ml^{-1} levels of antigen) than sensors developed in earlier work utilising entrapment within planar conductive polymer electrodes as the method of immobilisation. Low non-specific binding of these electrodes was also observed. However the range of these electrodes was very limited which could preclude their use in real analyses.

Similarly sensors developed where ABSA is entrapped in conductive polymer microelectrodes rather than planar polymer films have been studied. The microelectrode array sensors were three orders of magnitude more sensitive, again allowing detection of ng ml^{-1} levels of antigen. These types of sensors however displayed higher non-specific binding. However BSA is a protein noted for its high binding ability to surfaces and future sensors for other analytes will include a BSA blocking step to reduce non-specific interactions.

The next step involved combining these two methods in an attempt to enhance the sensitivity levels even further. Sensors have been developed involving a multi-step procedure. Initially conductive polyaniline microarrays were constructed. The polyaniline was then modified with biotinylating reagents and biotinylated antibodies immoblised by the affinity procedures described above. Finally the sensors are blocked with HSA. Ongoing work has demonstrated the construction of sensors for prostate specific antigen, neuron specific enolase and the stroke marker protein S-100[β]. These immunosensors have been shown capable of quantifying antigens at levels as low as 1 pg ml^{-1}, these will be the subject of a further series of publications to be submitted for publication shortly and will be described in detail at the 10th World Congress in Biosensors, Shanghai, May 14th–18th 2008.

Acknowledgements

This work, including funding for ACB, G-ZG, GT and FD, has been supported by the European Community QLRT-2001-02583 (SMILE) and NMP2-CT-2003-505485, (ELISHA) Framework VI contracts.

Appendix A. Supplementary data

Supplementary data associated with this article can be found, in the online version, at doi:10.1016/j.bios.2008.06.001.

References

Analytical Methods Committee, 1987. Analyst 112, 199–204.
Barton, A.C., Collyer, S.D., Davis, F., Gornall, D.D., Law, K.A., Lawrence, E.C.D., Mills, D.W., Myler, S., Pritchard, J.A., Thompson, M., Higson, S.P.J., 2004. Biosens. Bioelectron. 20, 328–337.
Barton, A.C., 2007. PhD Thesis. Cranfield University.
Bonroy, K., Frederix, F., Reekmans, G., Dewolf, E., De Palma, R., Borghs, G., Declerck, P., Goddeeris, B., 2006. J. Immunol. Methods. 312, 167–181.
Clark, L.C., Lyons, I.R., 1962. Ann. NY Acad. Sci. 102, 29–45.
Cosnier, S., 2005. Electroanalysis 17, 1701–1715.
Davis, F., Collyer, S.D., Gornall, D.D., Law, K.A., Mills, D.W., Higson, S.P.J., 2007. Chim. Oggi/Chemistry Today 25, 28–31.
Diaz-Gonzalez, M., Gonzalez-Garcia, M.B., Costa-Garci, A., 2005. Electroanalysis 17, 1901–1918.
Garifallou, G.-Z., Tsekenis, G., Davis, F., Higson, S.P.J., Millner, P.A., Pinacho, D.G., Sanchez-Baeza, F., Marco, M.-P., Gibson, T.D., 2007. Anal. Lett. 40, 1412–1442.
Garifallou, G.-Z., 2008. PhD Thesis. Cranfield University.
Grant, S., Davis, F., Pritchard, J.A., Law, K.A., Higson, S.P.J., Gibson, T.D., 2003. Anal. Chim. Acta. 495, 21–32.
Grant, S., Davis, F., Law, K.A., Barton, A.C., Collyer, S.D., Higson, S.P.J., Gibson, T.D., 2005. Anal. Chim. Acta. 537, 163–168.
Higson, S.P.J., 1996. 'Sensor', International Patent: PCT/GB96/0092.
John, R., Spencer, M., Wallace, G.G., Smyth, M.R., 1991. Anal. Chim. Acta. 249, 381–385.
Katz, E., Willner, I., 2003. Electroanalysis 15, 913–947.
Law, K.A., Higson, S.P.J., 2005. Biosens. Bioelectron. 21, 1914–1924.
Myler, S., Eaton, S., Higson, S.P.J., 1997. Anal. Chim. Acta. 357, 55–61.
Myler, S., Davis, F., Collyer, S.D., Higson, S.P.J., 2004. Biosens. Bioelectron. 20, 408–412.
Myler, S., Davis, F., Collyer, S.D., Gornall, D.D., Higson, S.P.J., 2005. Biosens. Bioelectron. 21, 666–671.
Pritchard, J.A., Law, K.A., Vakurov, A., Millner, P.A., Higson, S.P.J., 2004. Biosens. Bioelectron. 20, 765–772.
Randles, J.E.B., 1947. Discuss. Faraday Soc. 1, 11–19.
Rodriguez-Mozaz, S., de Alda, M.J.L., Barcelo, D., 2006. Anal. Bioanal. Chem. 386, 1025–1041.
Terra, S.G., Washam, J.B., Dunham, G.D., Gattis, W.A., 1999. Pharmacotherapy 19 (10), 1123–1126.
Tsekenis, G., Garifallou, G.Z., Davis, F., Millner, P.A., Gibson, T.D., Higson, S.P.J., 2008. Anal. Chem. 20, 2058–2062.
Tsekenis, G., 2008. PhD Thesis. Cranfield University.
Yalow, R.S., Berson, S.A., 1959. Nature 184, 1648–1649.